

**SOIL LIQUEFACTION HAZARD ASSESSMENT ALONG
SHORELINE OF PENINSULAR MALAYSIA**

HUZAIFA BIN HASHIM

**FACULTY OF ENGINEERING
UNIVERSITY OF MALAYA
KUALA LUMPUR**

2017

**SOIL LIQUEFACTION HAZARD ASSESSMENT
ALONG SHORELINE OF PENINSULAR MALAYSIA**

HUZAIFA BIN HASHIM

**THESIS SUBMITTED IN FULFILMENT OF THE
REQUIREMENTS FOR THE DEGREE OF DOCTOR OF
PHILOSOPHY**

**FACULTY OF ENGINEERING
UNIVERSITY OF MALAYA
KUALA LUMPUR**

2017

UNIVERSITY OF MALAYA
ORIGINAL LITERARY WORK DECLARATION

Name of Candidate: HUZAIFA BIN HASHIM

Matric No: KHA110047

Name of Degree: DOCTOR OF PHILOSOPHY

Title of Project Paper/Research Report/Dissertation/Thesis ("this Work"):

SOIL LIQUEFACTION HAZARD ASSESSMENT ALONG SHORELINE OF
PENINSULAR MALAYSIA

Field of Study: GEOTECHNICAL ENGINEERING

I do solemnly and sincerely declare that:

- (1) I am the sole author/writer of this Work;
- (2) This Work is original;
- (3) Any use of any work in which copyright exists was done by way of fair dealing and for permitted purposes and any excerpt or extract from, or reference to or reproduction of any copyright work has been disclosed expressly and sufficiently and the title of the Work and its authorship have been acknowledged in this Work;
- (4) I do not have any actual knowledge nor do I ought reasonably to know that the making of this work constitutes an infringement of any copyright work;
- (5) I hereby assign all and every rights in the copyright to this Work to the University of Malaya ("UM"), who henceforth shall be owner of the copyright in this Work and that any reproduction or use in any form or by any means whatsoever is prohibited without the written consent of UM having been first had and obtained;
- (6) I am fully aware that if in the course of making this Work I have infringed any copyright whether intentionally or otherwise, I may be subject to legal action or any other action as may be determined by UM.

Candidate's Signature

Date: 17/08/17

Subscribed and solemnly declared before,

Witness's Signature

Date:

Name:

Designation:

ABSTRACT

The thesis provides a complete liquefaction potential hazard study for shoreline of 1972 km covering 40 shoreline districts of 11 major states of Peninsular Malaysia. Two main aspects are considered in defining soil liquefaction study which consists of regional geotechnical settings and regional seismicity information. 4 interrelating approaches are introduced in study; soil liquefaction screening, cyclic triaxial testing, earthquake study and liquefaction hazard mapping. In this study, governing factors contributing to soil liquefaction hazard were selected and adapted in soil liquefaction screening in highlighting soil liquefaction potential areas. The cyclic loading was applied on sand and clay samples to establish the shear modulus reduction curves and damping ratio curves that represents regional soil performance for seismic response. Probabilistic seismic hazard analysis (PSHA), spectrum matching procedure (SMP) and site response analysis (SRA) was adapted in seismic study in generating ground motion of studied sites. Soil liquefaction assessment approach based on Simplified Procedure was used in developing the hazard map for shoreline of Peninsular Malaysia. A mitigation chart is also introduced in the study as a precursory measure in promoting safe built environment in the region. Findings revealed that shoreline area consist of vulnerable conditions to soil liquefaction hazard. The ground motion generated presents high amplification factor on the east coast region of Peninsular Malaysia specifically in the state of Terengganu and Kelantan. In general, the hazard map produced indicates that shoreline areas are vulnerable to soil liquefaction hazard. This soil liquefaction study will contribute towards promoting preparedness and enhanced awareness in the changing environment in today's context.

ABSTRAK

Tesis ini merangkumi kajian menyeluruh mengenai potensi pencecairan tanah di sepanjang pantai yang berukuran 1972 km meliputi 40 daerah pantai dalam 11 negeri di Semenanjung Malaysia. Kajian ini terbahagi kepada 2 aspek penting iaitu keadaan geoteknik dan juga keadaan seismik kawasan kajian. 4 kaedah yang berkait dalam kajian ini adalah penapisan kawasan pencecairan tanah, ujian kitaran 3-paksi, kajian gempa bumi dan peta bahaya pencecairan tanah. Di dalam kajian ini, faktor-faktor penyumbang kepada pencecairan tanah telah dipilih dan diterapkan kedalam penapisan kawasan pencecairan tanah untuk mengenal pasti kawasan yang berpotensi kepada bahaya pencecairan tanah. Beban kitaran yang dikenakan ke atas sampel tanah pasir dan tanah liat telah menghasilkan beberapa parameter tanah untuk mengkaji prestasi tanah terhadap beban yang dikenakan. Analisa kebarangkalian bahaya seismik (PSHA), prosedur persamaan spektrum (SMP) dan analisa tindakbalas lapangan (SRA) telah digunakan untuk menjana ciri-ciri gempa di kawasan kajian. Analisis pencecairan menggunakan kaedah mudah telah diterapkan dalam kajian untuk menghasilkan peta bahaya pencecairan tanah di sepanjang pantai Semenanjung Malaysia. Carta mitigasi juga telah dihasilkan untuk tujuan langkah berjaga-jaga ke arah pembangunan yang lebih selamat di rantau ini. Hasil kajian mendapati kawasan-kawasan yang berpotensi terhadap bahaya pencecairan tanah. Ciri-ciri gempa bumi yang dihasilkan adalah kritikal di negeri Terengganu dan negeri Kelantan. Secara amnya, peta yang dihasilkan menunjukkan kawasan kajian mempunyai potensi terhadap bahaya pencecairan tanah. Kajian pencecairan tanah ini merupakan penyumbang kepada langkah-langkah berjaga-jaga dan peningkatan kesedaran terhadap bahaya-bahaya alam di persekitaran.

ACKNOWLEDGEMENTS

All praise is due to الله we praise Him and seek His aid and forgiveness. Furthermore, we seek refuge in الله from our souls' and actions' evil. Whomsoever الله guides there is none to misguide, and whomsoever الله misguide there is none to guide. I bear witness there is none worthy of worship except الله and that محمد (ﷺ) is His slave and messenger.

Secondly I would like to thank my family, especially Wan Samsiah binti Wan Latif and Hashim bin Abdul Razak for the continuous comfort, warmth and hospitality throughout my days.

In preparing this thesis, I was in contact with academicians, and practitioners. They have contributed towards my understanding on study. In particular, I wish to express my sincere appreciation to my supervisor, Dr. Meldi Suhatri, for the encouragement, guidance, critics and friendship. I am also thankful to Prof. Ir. Dato' Dr. Roslan bin Hashim and Dr Hendriyawan for the guidance, advices and motivation. Without their continued support and interest, this thesis would not have been the same as presented here.

I am also indebted to University of Malaya (UM) for providing the research facilities. Staff at the Engineering Faculty also deserves special thanks for their assistance. I also like to extend my thanks to Ministry of Education Malaysia, Jabatan Kerja Raya (JKR) and Kumpulan IKRAM Sdn. Bhd. My fellow postgraduate combats should also be recognized for their support at various occasions. Their views and tips are useful indeed. Lastly the reviewers for all the motivation and encouragement. Unfortunately, it is not possible to list all of them in this limited space.

Huzaifa bin Hashim

TABLE OF CONTENTS

Abstract	iii
Abstrak	iv
Acknowledgements	v
Table of Contents	vi
List of Figures	x
List of Tables.....	xvii
List of Symbols and Abbreviations.....	xix
CHAPTER 1: INTRODUCTION.....	1
1.1 Soil Liquefaction Hazard	2
1.2 Aim of Study	3
1.3 Problem Statement.....	3
1.4 Objectives of Study.....	4
1.5 Scope of Work	4
CHAPTER 2: LITERATURE REVIEW.....	5
2.1 Historical Liquefaction Events	6
2.2 Soil Liquefaction Susceptibility	11
2.2.1 Soil Liquefaction Susceptibility	12
2.2.2 Groundwater Table	14
2.2.3 Soil Type	14
2.2.4 Particle Size Gradation	17
2.2.5 Malaysia's Context in Soil Liquefaction Hazard	18
2.3 Regional Data Collection.....	21
2.3.1 Regional Geological Content	21

2.3.2	Regional Seismicity and Ground Motion	24
2.3.3	Regional Hydrogeological	28
2.3.4	Regional and Neighboring Hazard Map	30
2.3.5	Regional Seismic Hazard Analysis	33
2.4	Liquefaction Hazard Assessment	37
2.4.1	The Padang Earthquake 2009	37
2.4.2	The Tohoku Earthquake 2011	39
2.4.3	The Christchurch Earthquake 2010 – 2011	43
2.5	Literature Review Summary	45
CHAPTER 3: METHODOLOGY		46
3.1	Soil Liquefaction Screening	46
3.1.1	Studied location	47
3.1.2	Database of Soil Collection	48
3.1.3	Site Investigation Report	50
3.1.4	SI Report, Soil Sampling, SPT-N correction	51
3.1.5	Illustrations, Chart and Tabulated Information	51
3.2	Cyclic Triaxial Testing	53
3.2.1	Laboratory Testing Program	53
3.2.2	Materials	61
3.2.3	Controlled Parameters and Parameters Obtained from Dynamic Cyclic Triaxial Tests	63
3.3	Earthquake Study	64
3.3.1	Probabilistic Seismic Hazard Analysis (PSHA)	64
3.3.2	Spectral Matching Procedure (SMP)	69
3.3.3	Site Response Analysis (SRA)	71
3.4	Liquefaction Hazard Mapping	75

3.4.1	Simplified Procedure by Seed and Idriss	76
3.4.2	Soil Strength Measurement from SPT.....	82
3.4.3	Soil Liquefaction Method Adapted in Study.....	87
3.4.4	Liquefaction Factor of Safety	91
3.4.5	Addressing Liquefaction Severity	91
CHAPTER 4: RESULTS AND DISCUSSIONS		93
4.1	Soil Liquefaction Screening	93
4.1.1	Perlis	93
4.1.2	Kedah.....	97
4.1.3	Penang	102
4.1.4	Perak	107
4.1.5	Selangor.....	110
4.1.6	Negeri Sembilan	114
4.1.7	Melaka	118
4.1.8	Johor	122
4.1.9	Pahang	128
4.1.10	Terengganu	132
4.1.11	Kelantan.....	136
4.1.12	Susceptibility of Soil at Study Location.....	140
4.1.13	Summary	147
4.2	Cyclic Triaxial Test	149
4.2.1	Soil Liquefaction Observation.....	149
4.2.2	Stress-Strain Behavior	152
4.2.3	Shear Modulus Reduction and Damping Ratio Curves.....	153
4.2.4	Summary	155
4.3	Earthquake Study.....	156

4.3.1	Probabilistic Seismic Hazard Assessment (PSHA).....	156
4.3.1.1	Generation and Simulation of Synthetic Ground Motion	156
4.3.1.2	De-Aggregation Hazard	161
4.3.1.3	Scaled Spectrum	167
4.3.2	Generation and Simulation of Synthetic Ground Motion	169
4.3.3	Microzonation Line (Amplification Factor).....	176
4.3.4	Comparative Study of Recent Findings to Previous Works.....	184
4.3.5	Summary	185
4.4	Liquefaction Hazard Assessment and Mapping	187
4.4.1	Graphical Illustration of Liquefaction Zones	187
4.4.2	Liquefaction Hazard Map.....	195
4.4.3	Mitigation Zoning.....	196
4.4.4	Summary	200
CHAPTER 5: CONCLUSION AND RECOMMENDATION		201
5.1	Conclusions	201
5.2	Recommendation for Future Work.....	202
5.3	Implication and Application of Study	202
References		203
List of Publications and Papers Presented		213

LIST OF FIGURES

Figure 1.1: Normal condition at site	2
Figure 1.2: Soil liquefaction condition at site	2
Figure 2.1: Side by side damage in Japan and New Zealand due to liquefaction (Aydan et al., 2012; Tokimatsu et al., 2012; Wilkinson et al., 2013)	10
Figure 2.2: Liquefaction plot (Tsuchida, 1970).	17
Figure 2.3: The National Physical Plan (Bhuiyan et al., 2013).....	19
Figure 2.4: Malaysia Tourism Master Plan (Marzuki, 2010)	20
Figure 2.5: 8th edition of Peninsular Malaysia geological map (Hutchison, 1989)	22
Figure 2.6: Recent Peninsular Malaysia geological map (Tate et al., 2008)	23
Figure 2.7: Plate boundaries of earth (DeMets et al., 2010).	24
Figure 2.8: Earthquakes catalog (Adnan et al., 2006).....	25
Figure 2.9: Seismotectonic map of Peninsular Malaysia (Ngah et al., 1996).....	27
Figure 2.10: Open arrows show velocities of neighboring plates (Gao et al., 2011).....	28
Figure 2.11: Hydrogeological map of Peninsular Malaysia (Chong & Pfeiffer, 1975) ..	29
Figure 2.12: Hazard map of Thailand (Ornthammarath et al., 2011)	30
Figure 2.13: Co-seismic deformation model (Vigny et al., 2005)	32
Figure 2.14: Hazard map of Malaysia (Petersen et al., 2004).....	33
Figure 2.15: De-aggregation in Kuala Lumpur (Petersen et al., 2004).....	34
Figure 2.16: PGA contour map 10% PE in 50 years (Irsyam et al., 2008)	35
Figure 2.17: Deaggregation hazard and scaled response spectra (Irsyam et al., 2008) ..	35
Figure 2.18: Seismic maps of Thailand and adjacent areas (Pailoplee et al., 2010).....	36
Figure 2.19: Grain size distribution plot (Muntohar, 2014).....	38
Figure 2.20: Soil Liquefaction in Padang (Hakam & Suhelmidawati, 2013)	38
Figure 2.21: Grain size distribution plot (Hakam & Suhelmidawati, 2013).....	38

Figure 2.22: Grain size distribution plot (Unjoh et al., 2012).....	40
Figure 2.23: Grain size distribution plot (Tsukamoto et al., 2012).....	40
Figure 2.24: Liquefaction affected site (Tsukamoto et al., 2012).....	41
Figure 2.25: Erupted ground due to soil liquefaction (Tsukamoto et al., 2012).....	42
Figure 2.26: Soil profile of the studied area (Tsukamoto et al., 2012)	42
Figure 2.27: A map highlighting soil details (Wotherspoon et al., 2015).....	43
Figure 2.28: Grain size distribution plot (Green et al., 2013).....	44
Figure 2.29: Soil profile observation on liquefy site (Green et al., 2013)	44
Figure 2.30: Site investigation on liquefy site (Green et al., 2013)	44
Figure 3.1: Main process in soil liquefaction screening	46
Figure 3.2: Distribution of studied borehole along shoreline	47
Figure 3.3: Typical borelog properties from SI report.....	50
Figure 3.4: Set-up of the cyclic triaxial test	53
Figure 3.5: Actuator on test system	54
Figure 3.6: Power up electronics at the base of system	54
Figure 3.7: Dynamic control system (bottom) and pneumatic controller (top)	54
Figure 3.8: Standard controller for backpressure.....	55
Figure 3.9: PC system with pre-installed software	56
Figure 3.10: Object/Hardware window.....	57
Figure 3.11: Triaxial cell installed on the main load frame	58
Figure 3.12: Sample preparation on the base plate of the load frame.....	60
Figure 3.13: Soil samples used in lab works.....	61
Figure 3.14: Particle size distribution of sands	62
Figure 3.15: Fault source model.....	67

Figure 3.16: Logic Tree used in the analysis (Megathrust)	68
Figure 3.17: Logic Tree used in the analysis (Benioff)	69
Figure 3.18: 1-D layered soil deposit system (Bardet & Tobita, 2001).....	74
Figure 3.19: General terminology in SRA (Bardet & Tobita, 2001)	74
Figure 3.20: SPT-Based empirical method (Seed & Idriss, 1971) adapted in study	75
Figure 3.21: Early liquefaction chart by (Seed, 1976)	77
Figure 3.22: Revised liquefaction chart by Youd and Idriss (2001).....	78
Figure 3.23: Sketch of common approach in Simplified Procedure	80
Figure 3.24: Equivalent cycles versus earthquake magnitude (Seed, 1976).....	81
Figure 3.25: Stress reduction factor versus depth (Andrus & Stokoe II, 2000).....	82
Figure 3.26: Magnitude Scaling Factor versus magnitude.....	83
Figure 3.27: Correction factor σ'_o (Seed et al., 1983)	86
Figure 3.28: Correction factor for σ'_o (Liao & Whitman, 1986).....	87
Figure 3.29: Typical borehole information in Kelantan district	88
Figure 3.30: $CRR_{7.5}$ using different approach	90
Figure 3.31: Factor of safety using different approach	90
Figure 4.1: Kuala Perlis beach front	93
Figure 4.2: Perlis state map and study location	95
Figure 4.3: Grain size distribution plot in liquefaction margin of Perlis	95
Figure 4.4: Soil layer composition of Perlis shoreline.....	96
Figure 4.5: Distribution of SPT-N blow counts of Perlis shoreline.....	96
Figure 4.6: Distribution of SPT-N blow counts of Perlis shoreline.....	97
Figure 4.7: Kedah state map and study location	98
Figure 4.8: Grain size distribution plot in liquefaction margin of Kedah.....	99

Figure 4.9: Soil layer composition of Langkawi Island shoreline	100
Figure 4.10: Distribution of SPT-N blow count of Langkawi Island shoreline.....	100
Figure 4.11: Soil layer composition of Kedah (Mainland) shoreline.....	101
Figure 4.12: Distribution of SPT-N blow count of Kedah (Mainland) shoreline	101
Figure 4.13: Seberang Perai beach front overlooking Penang Island	102
Figure 4.14: Penang state map and study location.....	103
Figure 4.15: Grain size distribution plot in liquefaction margin of Penang.....	104
Figure 4.16: Soil layer composition of Penang (Island) shoreline.....	105
Figure 4.17: Distribution of SPT-N blow count of Penang (Island) shoreline	105
Figure 4.18: Soil layer composition of Penang (Mainland) shoreline	106
Figure 4.19: Distribution of SPT-N blow count of Penang (Mainland) shoreline.....	106
Figure 4.20: Teluk Rubiah located in Manjung district, Perak	107
Figure 4.21: Perak state map and study location.....	108
Figure 4.22: Grain size distribution plot in liquefaction margin of Perak	109
Figure 4.23: Soil layer composition of Perak shoreline.....	109
Figure 4.24: Distribution of SPT-N blow count of Perak shoreline	110
Figure 4.25: A small fishing village Sabak Bernam, Selangor	111
Figure 4.26: Selangor state map and study location	111
Figure 4.27: Grain size distribution plot in liquefaction margin of Selangor	112
Figure 4.28: Soil layer composition of Selangor shoreline.....	113
Figure 4.29: Distribution of SPT-N blow count of Selangor shoreline	113
Figure 4.30: Port city in Port Dickson, Negeri Sembilan	114
Figure 4.31: Port city in Port Dickson, Negeri Sembilan	115
Figure 4.32: Grain size distribution plot in liquefaction margin of Negeri Sembilan ..	116

Figure 4.33: Soil layer composition of Negeri Sembilan shoreline	117
Figure 4.34: Distribution of SPT-N blow count of Negeri Sembilan shoreline.....	117
Figure 4.35: Melaka city overlooking south direction	118
Figure 4.36: Melaka city overlooking north direction	118
Figure 4.37: Melaka state map and study location.....	119
Figure 4.38: Grain size distribution plot in liquefaction margin of Melaka	120
Figure 4.39: Soil layer composition of Melaka shoreline	121
Figure 4.40: Distribution of SPT-N blow count of Melaka shoreline.....	121
Figure 4.41: Johor Bahru city overlooking Singapore	122
Figure 4.42: Johor state map and study location.....	123
Figure 4.43: Grain size distribution plot in liquefaction margin of West Johor	124
Figure 4.44: Grain size distribution plot in liquefaction margin of East Johor.....	124
Figure 4.45: Soil layer composition of West Johor shoreline	125
Figure 4.46: Distribution of SPT-N blow count of West Johor shoreline	126
Figure 4.47: Soil layer composition of East Johor shoreline	127
Figure 4.48: Distribution of SPT-N blow count of East Johor shoreline.....	127
Figure 4.49: Pantai Cherating located in Kuantan district, Pahang	128
Figure 4.50: Pahang state map and study location.....	130
Figure 4.51: Grain size distribution plot in liquefaction margin of Pahang.....	130
Figure 4.52: Soil layer composition of Pahang shoreline	131
Figure 4.53: Distribution of SPT-N blow count of Pahang shoreline.....	131
Figure 4.54: Northern coastal area of Terengganu state	132
Figure 4.55: Terengganu state map and study location.....	133
Figure 4.56: Grain size distribution plot in liquefaction margin of Terengganu	134

Figure 4.57: Soil layer composition of Terengganu shoreline	135
Figure 4.58: Distribution of SPT-N blow count of Terengganu shoreline	135
Figure 4.59: Pantai Cahaya Bulan, Tumpat district (northern area)	136
Figure 4.60: Pantai Irama, Bachok district (southern area)	137
Figure 4.61: Kelantan state map and study location	137
Figure 4.62: Grain size distribution plot in liquefaction margin of Kelantan	138
Figure 4.63: Soil layer composition of Kelantan shoreline.....	139
Figure 4.64: Distribution of SPT-N blow count of Kelantan shoreline	139
Figure 4.65: Ground water table location for west coast areas	145
Figure 4.66: Ground water table location for east coast areas	146
Figure 4.67: Plot of deviator stress vs number of cycle of load application (sand)	150
Figure 4.68: Plot of axial strain vs number of cycle (sand)	150
Figure 4.69: Plot of pore pressure vs number of cycle (sand)	150
Figure 4.70: Plot of axial displacement vs number of cycle (sand)	150
Figure 4.71: Plot of axial strain vs number of cycle (clay)	151
Figure 4.72: Plot of pore pressure vs number of cycle (clay)	151
Figure 4.73: Plot of axial displacement vs number of cycle (clay).....	151
Figure 4.74: Stress-strain behavior of sand subjected to controlled loading	152
Figure 4.75: Stress-strain behavior of clay subjected to controlled loading	152
Figure 4.76: Shear modulus reduction curve for sand	153
Figure 4.77: Shear modulus reduction curve for clay	153
Figure 4.78: Damping ratio curve for sand	154
Figure 4.79: Damping ratio curve for clay	154
Figure 4.80: Typical probabilistic hazard at west coast areas for PGA	159

Figure 4.81: Typical probabilistic hazard at east coast areas for PGA	161
Figure 4.82: De-aggregation hazard of 500 year return period for west coast	165
Figure 4.83: De-aggregation hazard of 500 year return period for east coast	166
Figure 4.84: Bedrock spectrum with 500 year return period of hazard	168
Figure 4.85: Bedrock spectrum with 2500 year return period of hazard	168
Figure 4.86: Simulation from bedrock (PGA) to surface (PSA) of west coast region..	173
Figure 4.87: Simulation from bedrock (PGA) to surface (PSA) of east coast region...	175
Figure 4.88: Microzonation line of 11 states in Peninsular Malaysia.....	183
Figure 4.89: Liquefaction layer of Perlis	187
Figure 4.90: Liquefaction layer of Langkawi	188
Figure 4.91: Liquefaction layer of Kedah	188
Figure 4.92: Liquefaction layer of Penang Island	189
Figure 4.93: Liquefaction layer of Seberang Perai	189
Figure 4.94: Liquefaction layer of Perak	190
Figure 4.95: Liquefaction layer of Selangor	190
Figure 4.96: Liquefaction layer of Negeri Sembilan	191
Figure 4.97: Liquefaction layer of Melaka	191
Figure 4.98: Liquefaction layer of West Johor	192
Figure 4.99: Liquefaction layer of East Johor.....	192
Figure 4.100: Liquefaction layer of Pahang.....	193
Figure 4.101: Liquefaction layer of Terengganu	194
Figure 4.102: Liquefaction layer of Kelantan	194
Figure 4.103: Liquefaction hazard map of shoreline areas of Peninsular Malaysia	196

LIST OF TABLES

Table 2.1: Summary of topic in literature review	5
Table 2.2: Records of liquefaction cases during earthquake.....	9
Table 2.3: Earthquake magnitude scales (McGuire, 2004).....	13
Table 2.4: Approximate correlations between seismic indicator (Day, 2002).....	13
Table 2.5: Susceptibility of coastal soil (Boulanger & Idriss, 2008).....	14
Table 2.6: Main criteria for a cohesive soil to liquefy (Wang, 1979).....	15
Table 2.7: Liquefaction susceptibility of silty soils (Andrews & Martin, 2000)	16
Table 2.8: Soil classification system in general (Holtz & Kovacs, 1981)	16
Table 2.9: Earthquake events in Bukit Tinggi area (Shuib, 2009).....	26
Table 3.1: Summary of data collection	48
Table 3.2: Detail summary of data collection	49
Table 3.3: Engineering properties of soil	62
Table 3.4: Controlled parameters for cyclic triaxial testing.....	63
Table 3.5: Properties of selected earthquake records for SMP of study	71
Table 3.6: Field test SPT-N corrections (Soils et al., 1997)	84
Table 4.1: General information of shoreline areas.....	142
Table 4.2: The susceptibility of soil at studied area.....	143
Table 4.3: Decision making process for soil liquefaction screening	144
Table 4.4: The deaggregation hazard of 500 year return period for 11 states	167
Table 4.5: Amplification factor of 11 studied states for 500 years return period	175
Table 4.6: Comparative study of PGA for 500 years return period.....	185
Table 4.7: Input for score	198
Table 4.8: Output 1 for the shoreline zoning and soil liquefaction category	198

Table 4.9: Output 2 for the severity level, action and mitigation	198
Table 4.10: Liquefaction zone for 40 shoreline districts of Peninsular Malaysia.....	199

LIST OF SYMBOLS AND ABBREVIATIONS

a_{\max}	:	Maximum peak ground acceleration
BMG	:	Indonesian Meteorology Agency
ζ	:	Damping Ratio
ρ	:	Density
ISC	:	International Seismological Center
m_b	:	Body-wave magnitude (short period)
m_B	:	Body wave magnitude (long period)
M_e	:	Energy magnitude
M_L	:	Local magnitude
M_s	:	Surface wave
M_w	:	Moment magnitude
MMD	:	Malaysian Meteorological Department
PGA	:	Peak ground acceleration
PSHA	:	Probabilistic seismic hazard analysis
SI	:	Site investigation
τ	:	Shear stress
G	:	Shear Modulus
SMP	:	Spectral matching procedure
SPT	:	Standard penetration test
SRA	:	Site response analysis
γ	:	Unit weight

CHAPTER 1: INTRODUCTION

Natural hazard related to the instability of saturated soil due to strong ground motion commonly termed as soil liquefaction have significant impact on built environment. The human mind is limited to a degree in which its capability is only able to adapt to the changing environment and improve to a certain extend. Hence common practice in geotechnical earthquake engineering involves assessment of the impacts by disaster and quantifying them to make an analytical solution in which assumptions are based upon to prepare for worse scenario.

In general, the process involves investigation and identification of the source mechanism of an earthquake, the extraction of basic soil parameters using geotechnical testing and laboratory works, determining the performance of regional soil samples under cyclic loading, quantifying ground motion waves which propagates through different medium of soil layers, and provide hazard indicator using specific variables to develop hazard map in which indicates different levels of vulnerability of a studied area to a potential seismic threat.

The geotechnical earthquake engineers carry responsibility in providing optimized, near-sufficient and appropriate information on design earthquake for structural engineers in assisting them in designing earthquake resistance structures. Lessons from the past earthquake event is a sign, a guide and essential tool to learn in which it provide us with a way we could improve the built environment around us and enhanced preparedness in the future.

1.1 Soil Liquefaction Hazard

Earthquake induced liquefaction event throughout the world have presented us with different pattern of damage effect in which soil conditions at site are very close related to the intensity of ground motion. Figure 1.1 presents normal condition at site. Under normal condition in soil liquefaction context, the structures and facilities are supported by areas of flat, low lying land with groundwater table near the surface. Figure 1.2 below shows another sketch of a condition during earthquake disaster related to soil liquefaction hazard. The main contribution factors are vulnerable soil deposits, groundwater table and large ground motion.

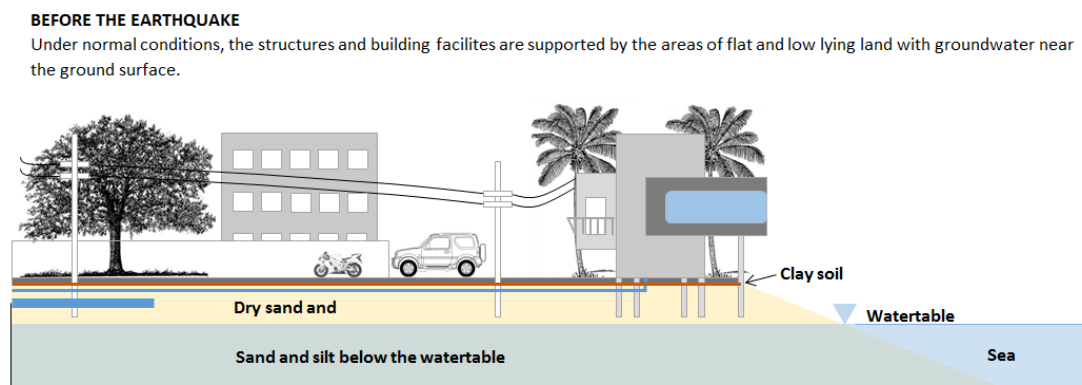


Figure 1.1: Normal condition at site

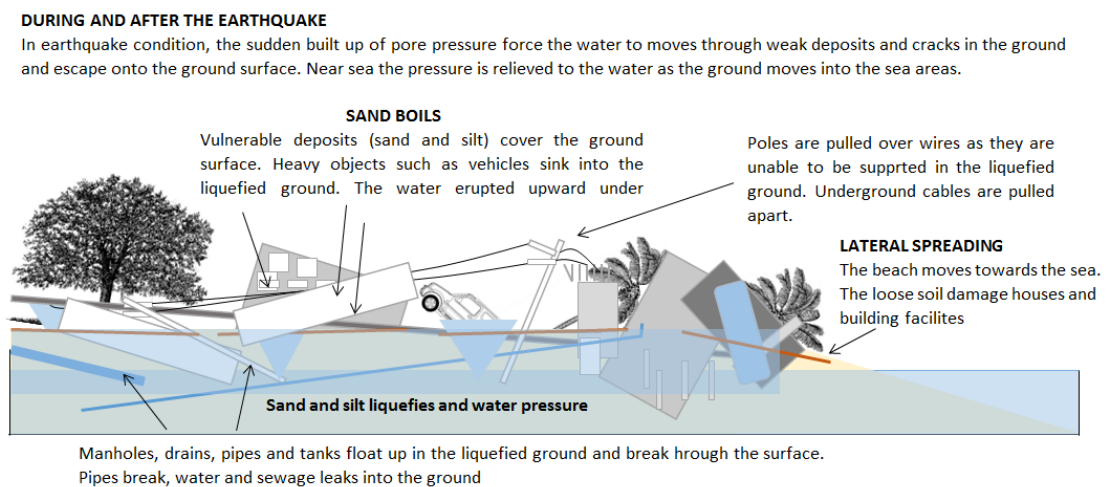


Figure 1.2: Soil liquefaction condition at site

1.2 Aim of Study

The aim of study is to provide reader from different background with adequate information and solution to soil liquefaction hazard. Past events as major contribution in the development of study provide fundamental in the overall process of assessing soil liquefaction hazard. Hence by conducting investigation on selected location allows access in the hidden information of the regional ground setting.

1.3 Problem Statement

In the context of development in Peninsular Malaysia, the management and modification of natural environment into built environment are increasing every year. The land use planning includes projects such as residential, coastal road, port cities and iconic structures to cater increasing population by providing basic needs and facilities. Most of the existing built environment does not take into account of any seismic loading in the design as natural disaster such as earthquake are not a priority or a major issue in the country. Missing information on regional earthquake is likely to be a major disadvantage in the sense towards promoting safe and quality built environment. The damage effect from such event in neighboring country has presented increase resources in handling maintenance and repair on assets and facilities after shock event. Many parties may lose trust which could result in decreasing revenues and profits. Moreover it further affects the construction quality reputation besides risking public safety. Therefore prior to the problem statement the questions arise as follows:

1. Is Peninsular Malaysia vulnerable towards soil liquefaction hazard?
2. How severe is the impact if soil liquefaction occurs in the region?
3. What is the solution if a development is to be taken placed in a liquefied site?

1.4 Objectives of Study

A total of 4 objectives are as follows:

- i. To assess soil liquefaction potential hazard along the shoreline area of Peninsular Malaysia.
- ii. To established geotechnical properties and performance of regional soil (sand and clay) under cyclic loading for seismic local site response
- iii. To generate synthetic ground motions using probabilistic seismic hazard analysis (PSHA), spectrum matching procedure (SMP) and site response analysis (SRA) for site study.
- iv. To develop soil liquefaction hazard map and mitigation chart for shoreline of Peninsular Malaysia.

1.5 Scope of Work

The study focuses on the following:

- i. Shoreline areas of 40 shoreline district in Peninsular Malaysia.
- ii. A nonlinear approach with one dimensional wave propagation method is adapted in the earthquake study.
- iii. The ground motion design covers design peak ground acceleration for 500 years return period.
- iv. The liquefaction analysis is conducted using soil penetration test (SPT) data.

CHAPTER 2: LITERATURE REVIEW

In recent years, severe liquefaction during earthquake event has been reported in number of countries such as Indonesia, Japan and New Zealand. The definition and awareness of soil liquefaction becomes a major concern in Peninsular Malaysia especially with rapidly increasing number of high-rise buildings and important structures such as ports and power station being constructed on reclaimed land which is likely prone to liquefy during intense shaking. 4 main topics are reviewed as presented Table 2.1 which covers the compilation of various documentations around the world on soil liquefaction during earthquake event and how it is assessed. This chapter includes findings on the first liquefaction event ever recorded until the current time.

Table 2.1: Summary of topic in literature review

Heading	Topic	Discussions
2.1	Records of liquefaction event	<ul style="list-style-type: none">• Early and current case of liquefaction around the world• Photos of damage
2.2	Liquefaction susceptibility	<ul style="list-style-type: none">• Factors concerning liquefaction susceptibility• Malaysia's context on soil liquefaction
2.3	Regional data collection	<ul style="list-style-type: none">• Geological Content• Seismicity and Ground Motion• Hydrogeological• Hazard Map• Seismic Hazard Analysis
2.4	Liquefaction Assessment	<ul style="list-style-type: none">• The Padang Earthquake 2009• The Tohoku Earthquake 2011• The Christchurch 2011 – 2011• Similar Damage in Local Settings

2.1 Historical Liquefaction Events

A compilation of soil liquefaction cases during earthquake event is presented in Table 2.2. Each of the reference summarizes the detail properties of the earthquake event and the liquefaction damage which triggered during the event, beginning year 1811 in New Madrid, Missouri USA compiled by (Liu & Li, 2001) to the recent Christchurch earthquake in 2011 documented by (Cubrinovski & Robinson, 2016). Selected reports compiled in Table 2.2 present a clear image of catastrophic events mainly the damage on built environment. A key note learned from the early events documented to the current event which takes place in remote areas is that structures were not designed or engineered to cater unforeseen incident but they are just built extensively. The variety of magnitude and peak ground acceleration (PGA) in Table 2.2 contributes solely to the liquefaction damage along with different soil profile. In Taiwan liquefaction site assessment on soil profile was found to be high sand concentration and the location of ground water table ranged 0.5 meter to 5 meter below surface (Wang & Guldman, 2016). Moreover, the potential liquefiable properties demonstrate performance of the site in the earthquake which resulted in settlement and sand boiling phenomenon that is related to soil liquefaction (Kawamura & Chen, 2013).

A different approach by reported coseismic coastal uplift and subsidence associated with the 2010 Maule earthquake (Melnick et al., 2012). Photos on field view of coseismic displacement presented by in the study produced systematic quantification using sessile intertidal organisms to highlight difference between pre- and post-earthquake event. A continuous assessment is well presented in Japan literatures ranging from newspaper report, research article and technical papers on soil liquefaction event. Referring to the 1964 Niigata earthquake in Japan, other nearby continent experienced almost the same disaster (Bhattacharya et al., 2014; Isobe et al., 2014; Kang et al., 2014; Kramer et al., 2016; Xu et al., 2013). Access of soil profile in most of the Japan

literatures was found to be highly sand concentrated. Reports shows newly reclaimed land shows severe damage compared to existing land in the same earthquake location. The sand is also vulnerable to scouring effect when water table rises and flooding takes place resulting in liquefaction-induced damage (Tokimatsu et al., 2012).

In other part of the continent, a soil liquefaction report observed in Christchurch with the continuous earthquake triggered 3 times in 2011. A compilation of borehole from literatures was found to be in accordance to liquefaction main contributing factors which is highly dense concentrated loose soil, water table near ground surface and increase amplitude of seismic wave (Bouziou & O'Rourke, 2017; Bray et al., 2016, 2017; Bretherton, 2017; Cubrinovski & Robinson, 2016; MacAskill & Guthrie, 2017; Maurer et al., 2015; Wotherspoon et al., 2015). The liquefaction damage effect in New Zealand since its first appearance related to build environments is ground settlement, lateral spreading and uplifts (Cubrinovski & Robinson, 2016). The 3 effect listed contributes to damage such as tilting and turnover of high rise structure, broken underground pipelines, expose of structure's foundation and underground storage tanks, skewed railway and roadways, uplift of underground sewerage system, sand boils, sinking structures, abutment failure of a bridge and the damage of telecommunication poles and tower.

Soil liquefaction is also observed in Southeast Asia region (Hatmoko & Suryadharma, 2015). The recorded event in 2004 by presents soil liquefaction in Banda Aceh and Meulaboh which damage embankments adjacent to bridge abutments. The event destroys most of the path way for quick evacuation for the people. Another event in 2009 during earthquake event in Padang, Indonesia, soil liquefaction tends to worsen the tremor effect by continuous damage to houses, water facilities and road ways. Numerous sand boils were observed prior to the disastrous event at roadway, river bank

and play grounds. Furthermore, based on laboratory testing the soil sample at site satisfy the criteria of liquefaction susceptibility of more than 65% of fine-sand grain (Hakam & Suhelmidawati, 2013). Other significant and similar soil liquefaction event is also observed in Turkey (Akçal et al., 2015) and Canada(Robertson et al., 2000). A collection of photos on soil liquefaction damage on structures and environments is presented in Figure 2.1 which indicates the same damage type in two different earthquakes prone location in Japan and New Zealand.

Table 2.2: Records of liquefaction cases during earthquake

Location	Year	M*	PGA (g)	Damage*	Reference
Alaska	1964	9.2	0.18	B, Br, R, Rw	Hansen (1965) McCulloch and Bonilla (1970) Youd and Bartlett (1989)
Niigata	1964	7.6	0.15	B, Br, R	Ohsaki (1966) Kawakami and Asada (1966) Kawasumi (1968)
Miyagi	1978	7.7	0.44	B, R	Iwasaki and Tokida (1980)
Kobe	1995	7.3	0.80	B, Br, R, P, Rw	Sonoda and Kobayashi (1997) Pollitz and Sacks (1997) Chang (2000) Chang and Nojima (2001) Menoni (2001)
Chi-Chi	1999	7.3	1.01	B, Br, R	Tsai and Hashash (2008)
Indonesia	2009	7.6	0.40	B, Br, R	Hakam and Suhelmidawati (2013)
Chile	2010	8.8	0.94	B, Br, R, P, Rw, D	Yasuda et al. (2010) Huang and Yu (2013)
Christchurch	2010	7.1	1.26	B, Br, R, Rw	Orense et al. (2011)
Christchurch	2011	6.3	2.20	B, Br, R, Rw	Villemure et al. (2012)
Tokyo	2011	9.0	2.70	B, Br, R, P, Rw	Huang and Yu (2013)
M* = Earthquake Magnitude Damage* = Buildings, Br = Bridges, R = Routes, P = Ports, Rw = Railways, D = Dams					

Japan	Damage	New Zealand
	Large ground settlement	
	Lateral ground spreading	
	Tilted building	
	Uplift manhole	
	Expose pile foundation	
	Boiled sand at location	

Figure 2.1: Side by side damage in Japan and New Zealand due to liquefaction (Aydan et al., 2012; Tokimatsu et al., 2012; Wilkinson et al., 2013)

2.2 Soil Liquefaction Susceptibility

In order to understand unforeseen hazard at local site, preliminary assessment of available data is crucial in meeting the actual condition at site. Field observations and studies in literatures conducted on damage in the previous topic resulted in the investigation of several factors that may have caused the sudden and large-scale disaster phenomenon. From the past to recent information listed in Table 2.2, it can be concluded that the governing factors are mainly the ground motion characteristics from an earthquake point of view and the type of soil at site from the geological aspect. 4 selected factors that govern liquefaction from literatures listed in Table 2.2 are as follows;

1. Earthquake intensity and duration
2. Groundwater table at site
3. Soil type and soil composition
4. Particle size distribution of soil deposits

For each of the factors mentioned, the findings from Malaysia's context are discussed in providing evidence on the importance of this research for shoreline areas of Peninsular Malaysia. Two official maps are presented. The geological map and hydrogeological map showing the soil distribution in Peninsular Malaysia and measured ground water table. As from the seismological aspect, a map of recent earthquakes is presented. Having both the geological and seismological information of local soil at hand, the data collection process presents informative approach in assessing the vulnerability study of local ground performance in the shoreline areas of Peninsular Malaysia.

2.2.1 Soil Liquefaction Susceptibility

Earthquake event can be measured as acceleration and duration of shaking. In the event of earthquake, the ground motion will generate movement of the soil particles and develop excess pore water pressures leading to unstable soil condition and complicated water path. Soil type which is highly susceptible to liquefaction tends to lose its strength and as seismicity energy dissipates into the soil there will be increase in pore water pressure which controls the amplification of wave through soil layer which affect the intensity and duration of triggering effect (Davis & Berrill, 1996).

It can be summarized from previous study listed in Table 2.2 that as the seismicity energy increase, the intensity of liquefaction is increased. From observed literatures in this study, the range of earthquake magnitude that triggers liquefaction ranges from 6.3 to 9.2 magnitude and the peak ground acceleration ranges from as low as 0.15 g to as high as 2.7 g. As for measuring the size of earthquake, seismologist have proposed scales which is used in almost in any earthquakes event reported or measured. The variety of earthquake magnitude scales are summarized in Table 2.3 (McGuire, 2004).

Approximate correlations between local magnitude M_L , peak ground acceleration (a_{max}), duration of shaking, and earthquake intensity using modified Mercalli level of damage near vicinity of fault rupture is presented in Table 2.4 summarized by (Day, 2002). From Table 2.3 and Table 2.4, it can be concluded that with increase intensity and duration of earthquake will increase potential of liquefaction hazard. Moreover higher magnitude result in increase in peak ground acceleration and the duration of ground shaking.

Table 2.3: Earthquake magnitude scales (McGuire, 2004)

Designation	Symbol
Local magnitude	M_L
Body-wave magnitude (short period)	m_b
Body wave magnitude (long period)	m_B
Surface wave	M_s
Energy magnitude	M_e
Moment magnitude	M_w

Table 2.4: Approximate correlations between seismic indicator (Day, 2002).

Local magnitude M_L	Typical peak ground acceleration a_{max} near the vicinity of the fault rupture	Typical duration of ground shaking near the vicinity of fault rupture	Modified Mercalli intensity level near the vicinity of the fault rupture
≤ 2	-	-	I-II
3	-	-	III
4	-	-	IV-V
5	0.09g	2s	VI-VII
6	0.22g	12s	VII-VIII
7	0.37g	24s	IX-X
≥ 8	$> 0.50g$	$> 34s$	XI-XII

2.2.2 Groundwater Table

Based on observation on literatures the liquefaction phenomenon occurred at sites where groundwater table is near the surface. The site could be a bay area, reclaimed land (Tokimatsu et al., 2012) and also few saturated loose deposits areas far from sea reported in New Zealand by (Brackley, 2012). Most of the areas significantly affected by liquefaction induced damage coincide with low lying land where the ground surface is near the ground water table. In contrast, sites which are of higher elevation where the ground surface is higher than the groundwater table is less affected by liquefaction hazard (Van Ballegooy et al., 2014).

2.2.3 Soil Type

Terminologically, soil type which is vulnerable to liquefaction is saturated, cohesionless loose granular deposits (Liyanapathirana & Poulos, 2004; Thevanayagam & Martin, 2002). A table of susceptibility of soil deposits to liquefaction during ground motion at coastal zone is presented in Table 2.5.

Table 2.5: Susceptibility of coastal soil (Boulanger & Idriss, 2008).

Type of deposit	Distribution of cohesion less sediments in deposit	Likelihood that cohesion less sediments, when saturated, would be susceptible to liquefaction			
		<500 years	Holocene	Pleistocene	Pre-Pleistocene
Delta	Widespread	Very high	High	Low	Very low
Estuarine	Locally variable	High	Moderate	Low	Very low
Beach –high wave energy	Widespread	Moderate	Low	Very low	Very low
Beach –low wave energy	Widespread	High	Moderate	Low	Very low
Lagoonal	Locally variable	High	Moderate	Low	Very low
Foreshore	Locally variable	High	Moderate	Low	Very low

Although clean and silty sand are found in almost all of the liquefaction records reported in this study, it does not limit the liquefaction susceptibility to other broader range of soil types. For this study the discussion on variety type of soil are simplified into 4 types of soil which is gravel, sand, silty and clay. A research conducted on liquefaction susceptibility of cohesive soil such as clay needs to agree with 4 main criteria as presented and compiled by (Chávez et al., 2017) in order for liquefaction to take place. Table 2.6 presents main criteria for a cohesive soil to liquefy.

Table 2.6: Main criteria for a cohesive soil to liquefy (Wang, 1979)

Criteria	
Clay fraction (finer than 0.0005 mm)	$\leq 15\%$
Liquid limit, LL	$< 35\%$
Natural water content	$\geq 0.90LL$
Liquidity index	≤ 0.75

In addition other cohesive soil such as silty soil is also observed in recent study. A recent susceptibility liquefaction study on silty soil conducted by Andrews and Martin (2000) and Thevanayagam and Martin (2002) shows evidence that silty soils are also vulnerable to liquefaction. A summary of the liquefaction susceptibility of silty soils study result is presented in Table 2.7. As a result liquefaction occurs not limited to sand but also in silty and clay soil if it meets the criteria in research literature mentioned. A figure of grain size distribution according to variety of soil classification standard is presented in Table 2.8 which can be useful in identifying the type of soil which is vulnerable to liquefaction phenomenon.

Table 2.7: Liquefaction susceptibility of silty soils (Andrews & Martin, 2000)

Clay content	Liquid Limit <32	Liquid Limit ≥ 32
Clay content < 10%	Susceptible	Further Studies Required (Considering plastic non-clay sized grains – such as Mica)
Clay content $\geq 10\%$	Further Studies Required (Considering non-plastic clay sized grains – such as mine and quarry tailings)	Non susceptible

Table 2.8: Soil classification system in general (Holtz & Kovacs, 1981)

Classification System*	Soil Group			
USC	Gravel	Sand	Fines (silt and clay)	
	75 – 4.75	4.75 – 0.075	< 0.075	
AASHTO	Gravel	Sand	Silt	Clay
	75 - 2	2 – 0.05	0.05 – 0.002	< 0.002
MIT	Gravel	Sand	Silt	Clay
	>2	2 – 0.06	0.06 – 0.002	< 0.002
ASTM	Gravel	Sand	Silt	Clay
	>4.75	4.75 – 0.075	0.075 – 0.002	< 0.002
USDA	Gravel	Sand	Silt	Clay
	75 - 2	2 – 0.05	0.05 – 0.002	< 0.002

* USC - *Unified Soil Classification*,
AASHTO - *The American Association of State Highway and Transportation Officials*,
MIT - *Massachusetts Institute of Technology*,
ASTM - *American Society for Testing and Materials*,
USDA - *United States Department of Agriculture*

2.2.4 Particle Size Gradation

Cubrinovski and Robinson (2016) reported that soil in uniform gradation is highly susceptible to liquefaction. On the other hand, well-graded soil are found to be more stable to liquefaction hazard because during earthquake, small particles and big particles collides and filling of voids occurs which resulting in very small pore water pressure being generated making a stable arrangement of soil to liquefaction hazard (Day, 2002). A report by Tsuchida (1970) adapted in Koester and Tsuchida (1988) illustrates a grain size distribution for soil which are liquefiable and non-liquefiable (Figure 2.2). The boundary developed in the chart is a summarization of results conducted using sieve analysis performed on samples of alluvial and diluvial soils. The soil sample is known to have liquefied and not liquefy during earthquakes in Japan. In accordance to this chart, a sieve analysis could be an initial observation whether a soil sample obtained from field is likely to liquefy or not by means of comparative study of soil sample.

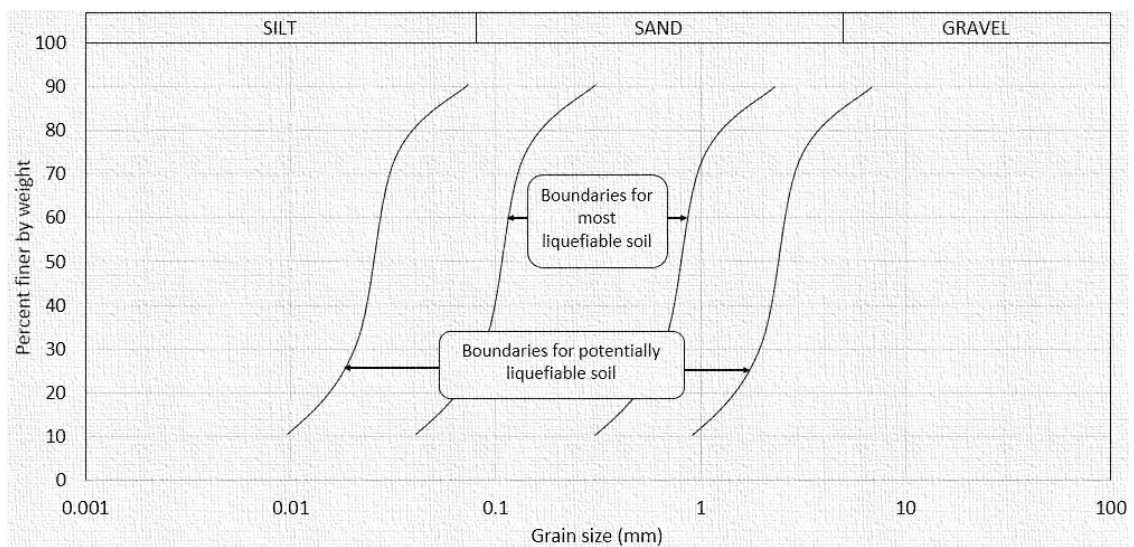


Figure 2.2: Liquefaction plot (Tsuchida, 1970).

2.2.5 Malaysia's Context in Soil Liquefaction Hazard

Tremors felt in Malaysia have been significantly increasing resulted in the demand of safer building design environment. An observation and lesson learned on soil liquefaction in the neighboring countries and throughout the world have resulted in critical thinking and new perspective for Malaysia. Impacts on the human safety, built environment and the socio-economy are the main concern in soil liquefaction. Hence a step in venturing in an understanding on this disaster could be a main discussion in today's time in Malaysia prior to the physical development plan (Marzuki, 2010).

Figure 2.3 presents The National Physical Plan in the Ninth Malaysia Plan. The development observed in figure is the planning of coastal road which connects the main attraction. The high population in each state is also highlighted as a turning point from rural areas to developed areas as presented in Figure 2.4 on the Malaysia Tourism Master Plan by Marzuki (2010). Awareness among the citizen and the government needs to be improved in understanding the natural surroundings. A unique cycle is seen in this matter whereby an impact on other country are being considered and taken as lesson here due to the effect that triggers the country. A preparation in minimizing the effect could be a challenge for Malaysia especially in the building construction industry. The research may lead to a finding in preparing for soil liquefaction hazard in the near future.

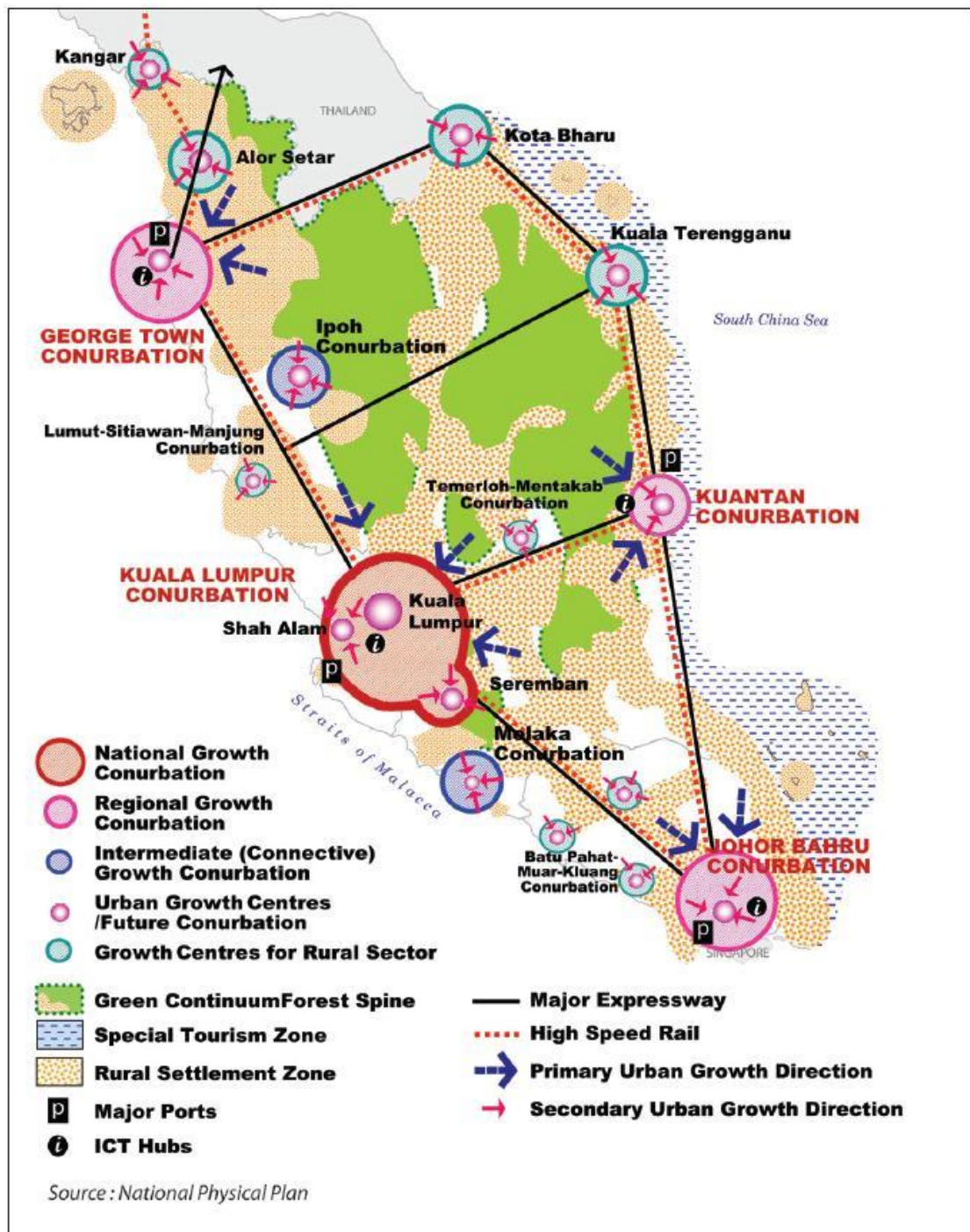


Figure 2.3: The National Physical Plan (Bhuiyan et al., 2013)

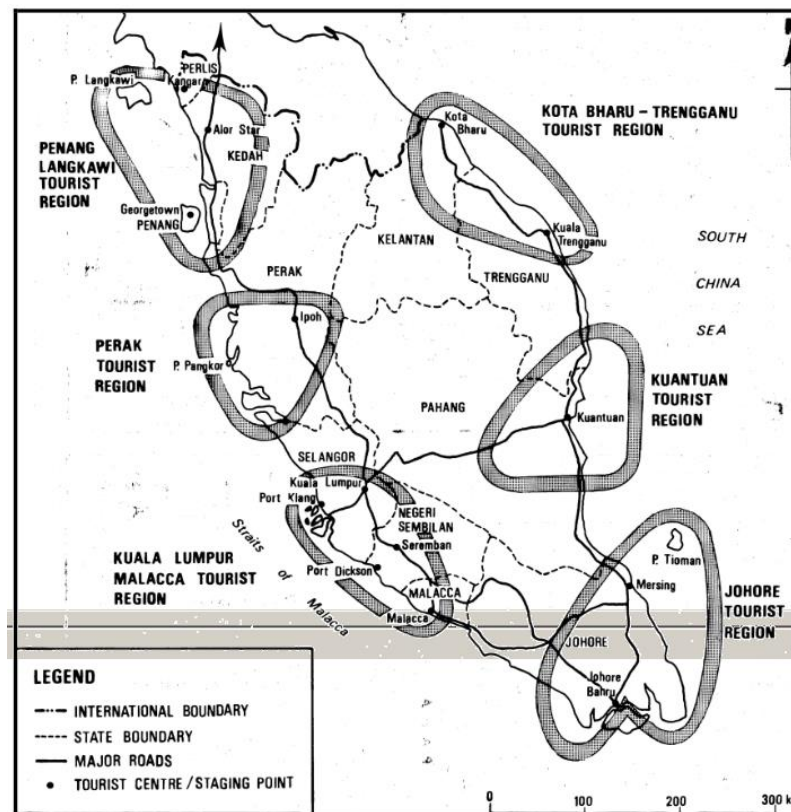


Figure 2.4: Malaysia Tourism Master Plan (Marzuki, 2010)

Proposed guidelines from study in adapting to a location which may be triggered by soil liquefaction can be summarized into 3 main procedures which begin with preliminary study which includes site visit, photo visuals, data collection and screening. Each of the data will undergo screening and evaluation process in achieving a reliable decision on the subject matter. The second process takes into account of detail study on the geological and seismological content. Field testing such logging, boring, sampling and testing are carried out to extract the soil details and parameters. Soil sample is taken to the laboratory for assessment in static and dynamic aspect. Last procedure is to conduct liquefaction analysis. The result will indicate a decision making process (building construction context) which may involve the owner, engineer and contractor to decide whether the location is a suitable place to be developed. In following the guidelines, one may benefit from this study in many aspect; public safety, building performance, repair and maintenance and future investment.

2.3 Regional Data Collection

The assessment on soil liquefaction is inclusive of the geological and the seismological environment. Two main environments are being considered in this study for observation and evaluation which will later be discussed in the later chapter. The sub topic below will be presenting on the Malaysia's geological and seismological environment obtained from available sources. Each of the data provided will be discussed on the relevancy and significant on conducting this research.

2.3.1 Regional Geological Content

An 8th revised edition of geological map of Peninsular Malaysia was produced in 1985 indicating the type of soil distribution (Harun, 2002). Figure 2.5 presents the early version of the geological map. Few years later, a revised version of the map is reprinted in 2004 presented in Figure 2.6 which indicates few changes of geological content from the color and details output. It is found on the map that the coastal zone which stretches approximately 2068 km are found to be concentrated with marine and continental deposits; clay, sand and peat with minor gravel. Basalt of early Pleistocene age is observed in Kuantan, Pahang area. Also the beaches can be categorized into two types which are muddy and sandy beaches. Sandy beaches are found mostly in the east of Peninsular Malaysia running north along Kelantan shoreline and all the way south to eastern Johor while the muddy beaches are found concentrated in the western part of Peninsular Malaysia (Malaysia, 2007). From the map a clear summarization is that, the shoreline area fulfilled one of the main governing factors of soil type which is vulnerable to liquefaction. Further investigation is needed to find the soil particle size and other related parameters in the liquefaction studies for initial screening of the site in this research.



2.3.2 Regional Seismicity and Ground Motion

A view of the earth plate boundaries is presented in Figure 2.7 (DeMets et al., 2010). The plates which are connected in the surrounding area of Malaysia are consisted of Eurasia, India, Australia, Philippines Sea and Yangtze. Peninsular Malaysia sits on Sundaland plate which is reported to be a stable tectonic plate ranging from low to moderate seismic activity level and also being considered a low seismicity and strain rates. Having referred to as a low seismicity country, large earthquake generally produced by neighboring country is reported to have triggered quite a number of areas in Peninsular Malaysia since 1976 recorded by the Malaysian Meteorological Department (MMD), Malaysia.

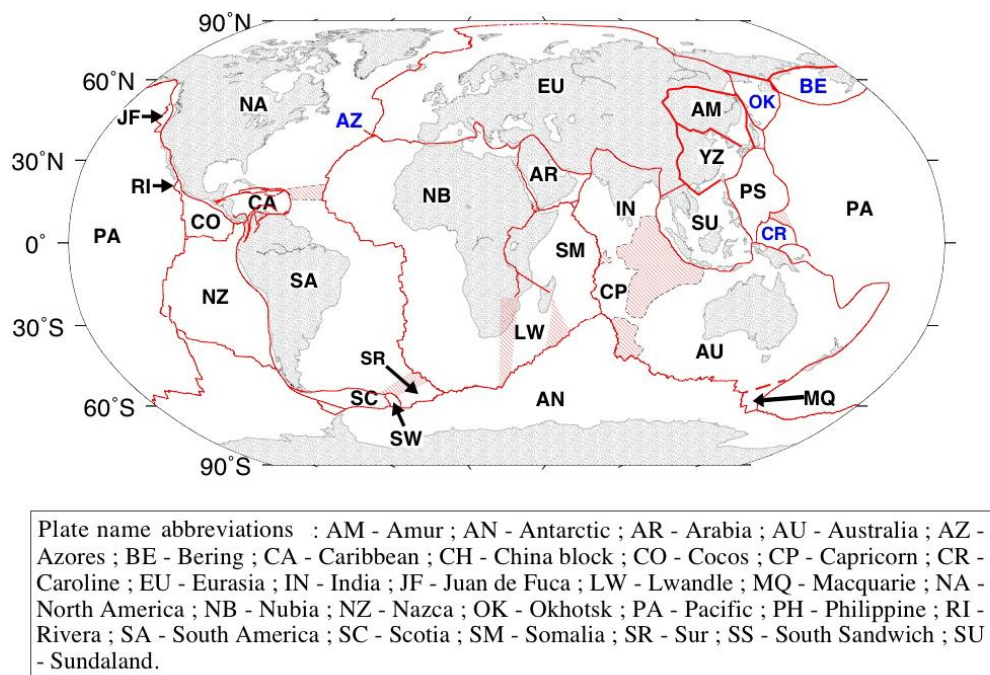


Figure 2.7: Plate boundaries of earth (DeMets et al., 2010).

The seismic network in the region consists of 17 seismological stations throughout the nation along with 10 strong motion stations located in the city center. This study compiles data on the historical earthquake recorded around Peninsular Malaysia from 1

May 1900 until the 31 December 2009. Figure 2.8 presents the historical earthquake recorded around Peninsular Malaysia. The map shows 7359 locations of earthquake epicenters scattered with different variable parameters on the magnitude of earthquake (the bigger dot the bigger magnitude) and the depth of earthquake (yellow dot indicate depth of 0 – 50 km, blue dot indicate depth of 50 – 100 km and red dot indicate depth of 100 – 200 km).

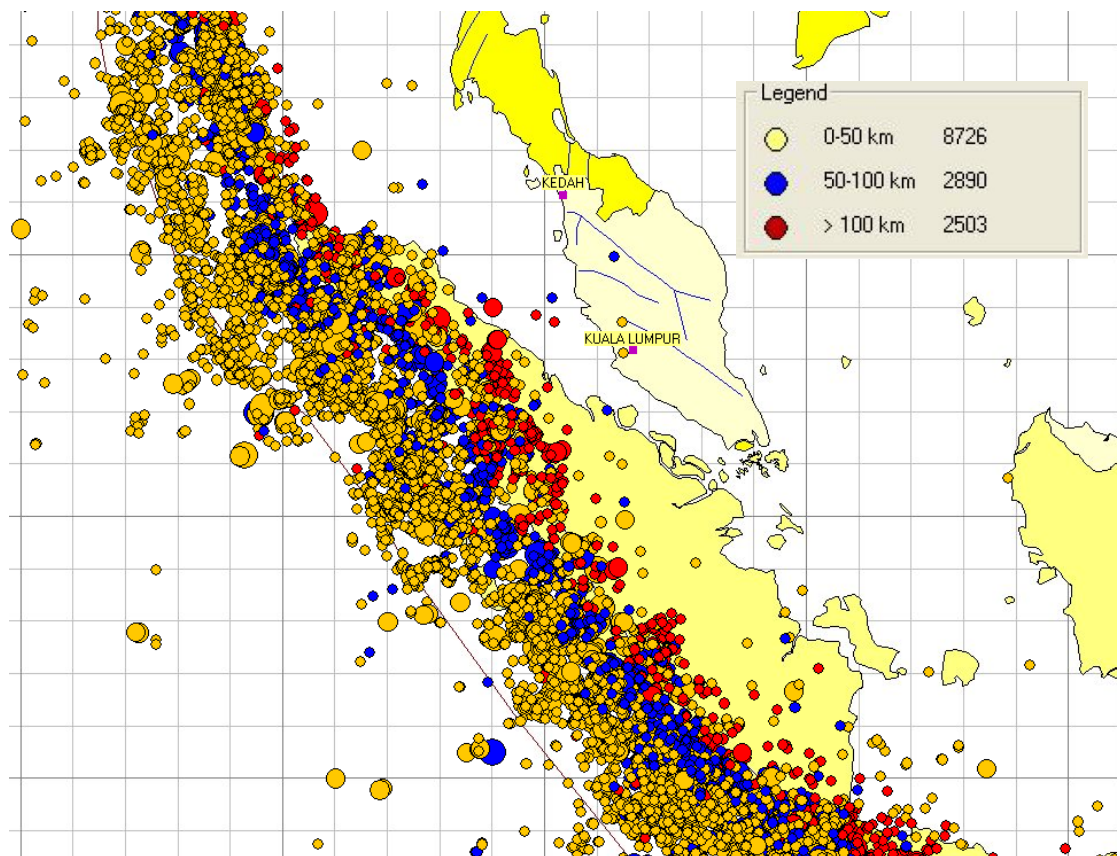


Figure 2.8: Earthquakes catalog (Adnan et al., 2006)

Buildings in Peninsular Malaysia have been experiencing ground motion from earthquake ranging 300 – 600 km distance from two main sources namely the Sumatra subduction fault and Sumatra fault (Balendra & Li, 2008; Petersen et al., 2004). Local fault are also reported to have contribute to tremors in Peninsular Malaysia(Ghani et al., 2008; Lat & Ibrahim, 2009; Nabilah & Balendra, 2012).Shuib (2009) reported tremors

in Bukit Tinggi area along the Selangor and Pahang Boundary are emerging from Bukit Tinggi fault. A series of earthquake event is presented in Table 2.9 which occurs in the Bukit Tinggi area.

Table 2.9: Earthquake events in Bukit Tinggi area (Shuib, 2009).

Date	Time (MST)	Latitude	Longitude	Magnitude (Mw)	Depth (km)
30/11/2007	10.13 am	3.36°N	101.80°E	3.5	2.3
30/11/2007	10.42 am	3.34°N	101.80°E	2.8	<10
30/11/2007	8.42 pm	3.31°N	101.84°E	3.2	6.7
4/12/2007	6.12 pm	3.40°N	101.80°E	3.0	<10
5/12/2007	3.57 am	3.37°N	101.81°E	3.3	<10
6/12/2007	11.23 pm	3.36°N	101.81°E	2.7	<10
9/12/2007	8.55 pm	3.33°N	101.82°E	3.5	4.9
12/12/2007	6.01 pm	3.48°N	101.76°E	3.2	<10
31/12/2007	5.19 pm	3.32°N	101.81°E	2.5	<10
10/01/2008	9.26 pm	3.17°N	101.61°E	1.7	1.2
10/01/2008	11.38 pm	3.39°N	101.80°E	2.5	3.0
13/01/2008	10.24 am	3.30°N	101.90°E	2.9	<10
13/01/2008	6.18 pm	3.30°N	101.80°E	2.5	<10
13/01/2008	11.59 pm	3.40°N	101.86°E	1.9	3.0
14/01/2008	11.45 pm	3.42°N	101.79°E	3.4	<10
15/01/2008	6.24 am	3.63°N	101.24°E	2.9	<10
15/01/2008	12.41 pm	3.35°N	101.77°E	2.5	<10
10/01/2008	11.38 pm	3.39°N	101.73°E	3.0	<10
15/03/2008	8.50 am	3.30°N	101.70°E	3.3	<10
15/03/2008	7.35 am	3.50°N	101.80°E	1.8	<10
15/03/2008	7.16 am	3.30°N	101.70°E	2.8	<10
27/03/2008	9.46 am	3.80°N	102.40°E	3.0	<10
25/05/2008	9.36 am	3.31°N	101.65°E	3.0	<10

A seismotectonic map of Peninsular Malaysia in Figure 2.9 mentioned in (Ngah et al., 1996) indicate 4 local faults mainly Bukit Tinggi fault, KL fault, Lebir fault, Baubak fault and Bentong suture. All of which is considered insignificant to any ground tremors and few highlighted as active seismic source. Figure 2.10 presents the seismotectonic map of Peninsular Malaysia. There are about 70 tremors of $M_w > 7.0$ occurring from 1977 to 2007 in the South Asian region, those of which being felt in the Peninsular Malaysia region. The local settings are bordered to the west and to the south by seismically active Sunda-Banda Volcanic Arc which moves at 6-8 cm/yr and to the east by the Philippines-Pacific Plate which moves at 11 cm year.

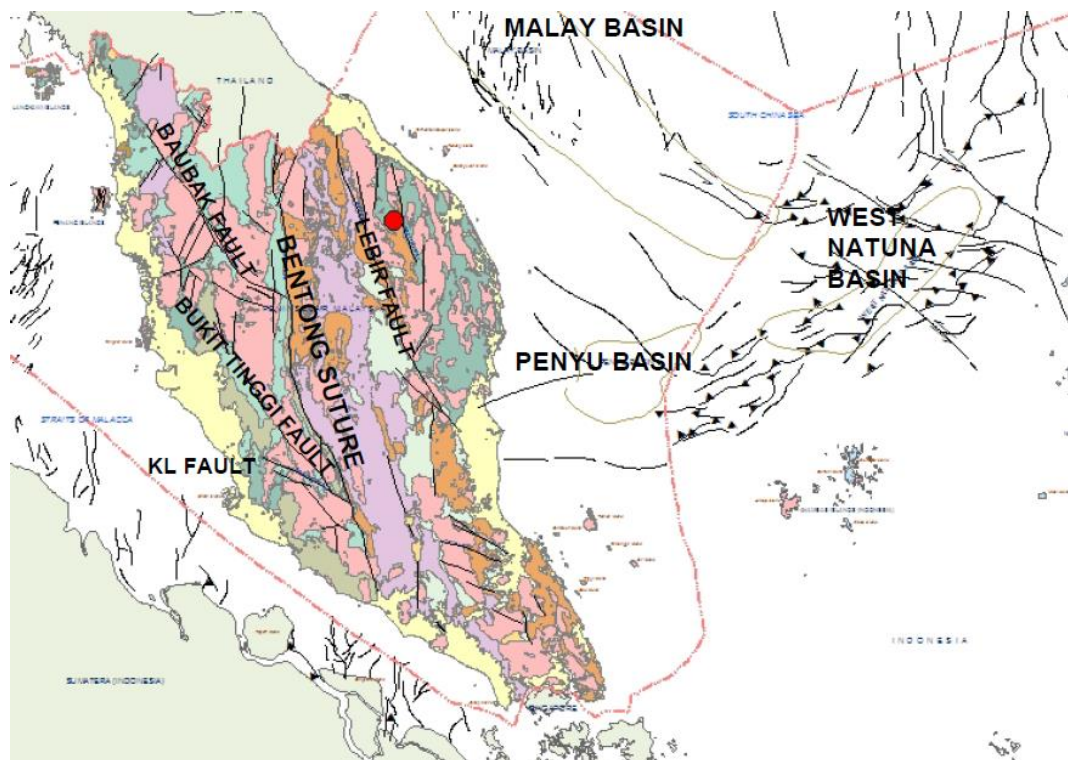


Figure 2.9: Seismotectonic map of Peninsular Malaysia (Ngah et al., 1996)

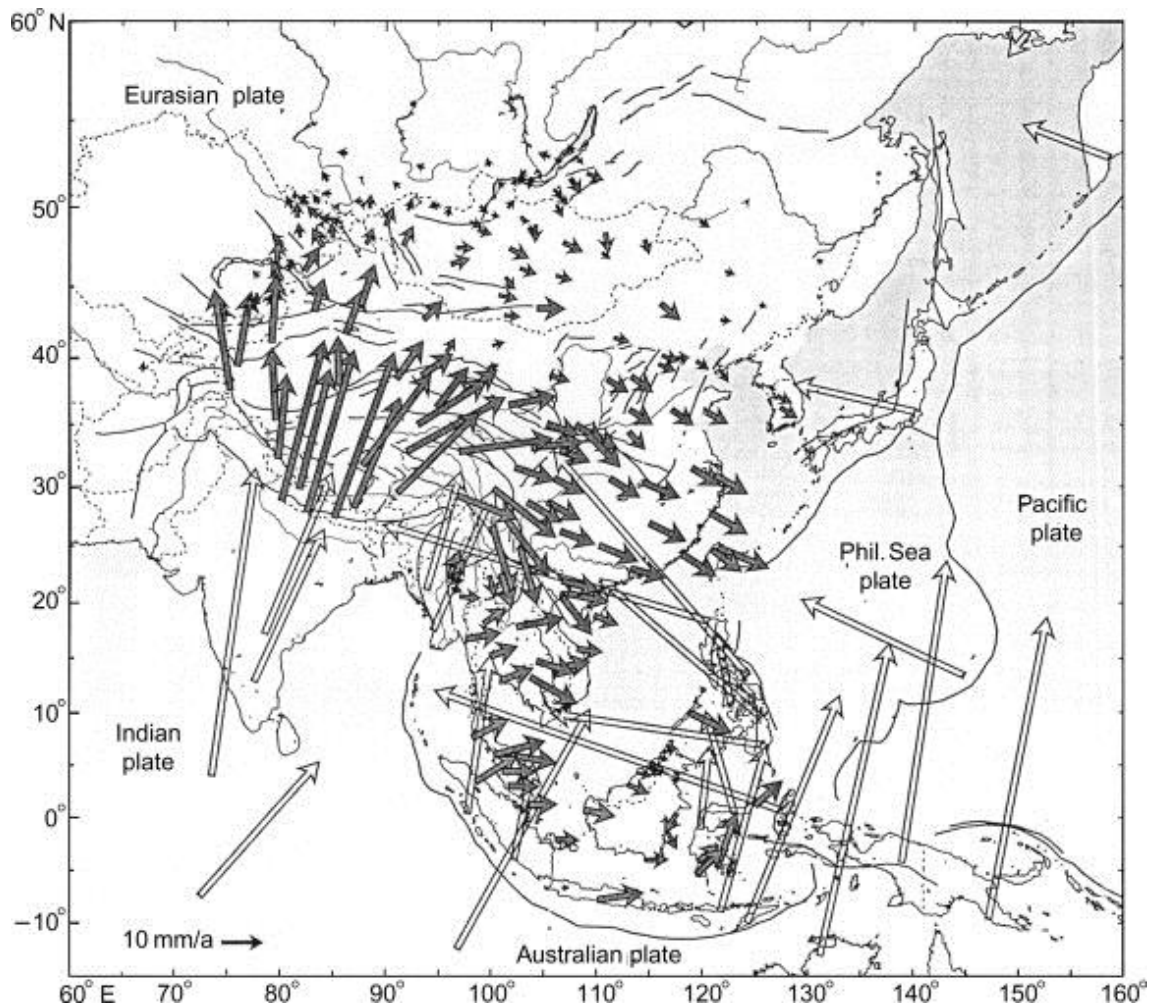


Figure 2.10: Open arrows show velocities of neighboring plates (Gao et al., 2011)

2.3.3 Regional Hydrogeological

Another important aspect which is highlighted is the hydrogeological setting of Peninsular Malaysia. Figure 2.11 presents the simplified hydrogeological map of Peninsular Malaysia mentioned in Chong and Pfeiffer (1975) . By observing the map, a high concentration of alluvial aquifers (sand and gravel) located on the shoreline areas is an indication of liquefaction susceptibility in the areas. Extensive distribution of aquifers along the shoreline areas is very important for the study.

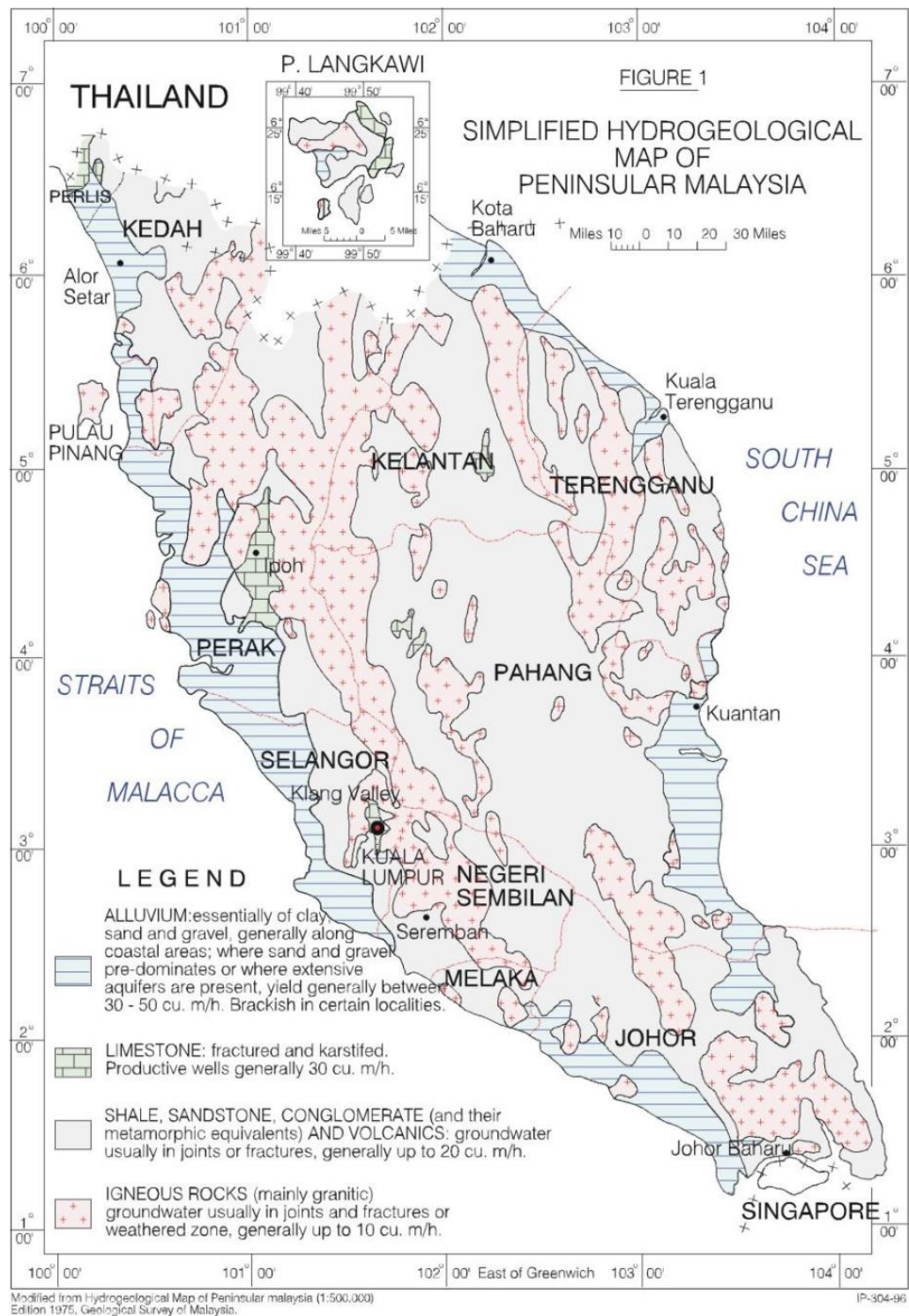


Figure 2.11: Hydrogeological map of Peninsular Malaysia (Chong & Pfeiffer, 1975)

2.3.4 Regional and Neighboring Hazard Map

The initiation of seismic hazard study are conducted by referring to available literatures including neighboring countries by incorporating secondary data obtained from government and local authorities. A report by U.S Geological Survey (USGS) highlighted interest in the local seismicity settings presented after the 26 December, 2004 Sumatran earthquake measuring 9.2. The objectives mainly concentrate in developing seismic hazard maps as a guideline for reaching out seismic information to the public and policy makers corresponding to seismic hazard matters and mitigation of related risk. A team from Universiti Teknologi Malaysia consists of earthquake hazard and building code expertise has initially presented seismic study of the local settings to be implemented in the building code. The study is expanded with a series of workshops with USGS experts in the matter. Figure 2.12 presents hazard map cases of neighboring Malaysia, Thailand which will be a reference in generating seismicity of local surface ground motion.

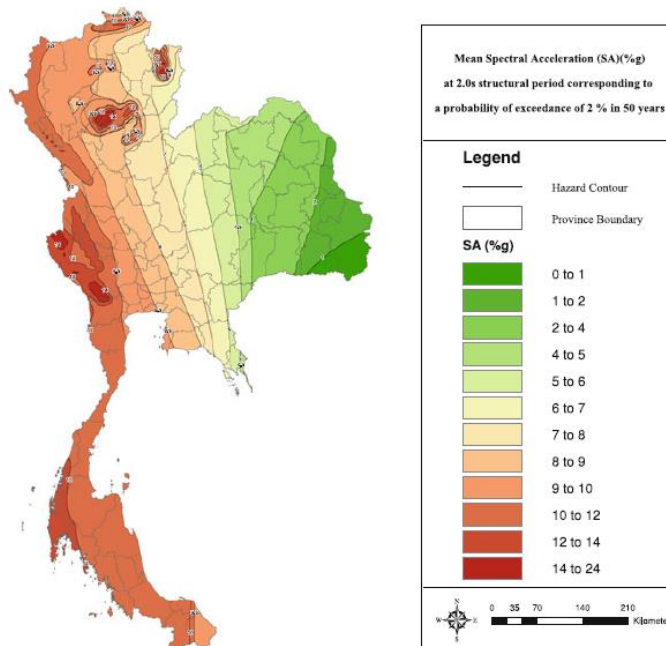


Figure 2.12: Hazard map of Thailand (Ornthammarath et al., 2011)

The study of regional seismic study has been emphasized since the 26 December 2004 Sumatra-Andaman megathrust earthquake. The continuing subduction process along the Sumatra trench has been highlighted in many reports concerning the effect in regional settings (Balendra & Li, 2008). Many of which incorporate significant findings using available methodology applied in high intensity earthquake region. The crustal deformation caused by the earthquake has been studied extensively in Southeast Asia using GPS measurements. Figure 2.13 presents the findings from of co-seismic displacement field derived from GPS observation. The study reports large co-seismic displacement of 17 cm on Langkawi Island, Malaysia which is situated more than 400 km away from the epicenter.

The study also reported potential triggering of earthquake on surrounding faults due to the stress transfer which provide crucial information related to earthquake mechanism and on possible follow on scenarios for the Peninsular Malaysia. A motivation from the local expertise and government officials enhanced more study to be developed in the regional seismic study context in adjusting to the uncertainties in the environment today. In venturing more on the seismic study, a revised national annex on earthquake properties of the region is in progress at the recent time along with platform offered in higher education level on seismicity study being planned to educate the young minds in learning more about the earthquake (Ramli & Adnan, 2004).

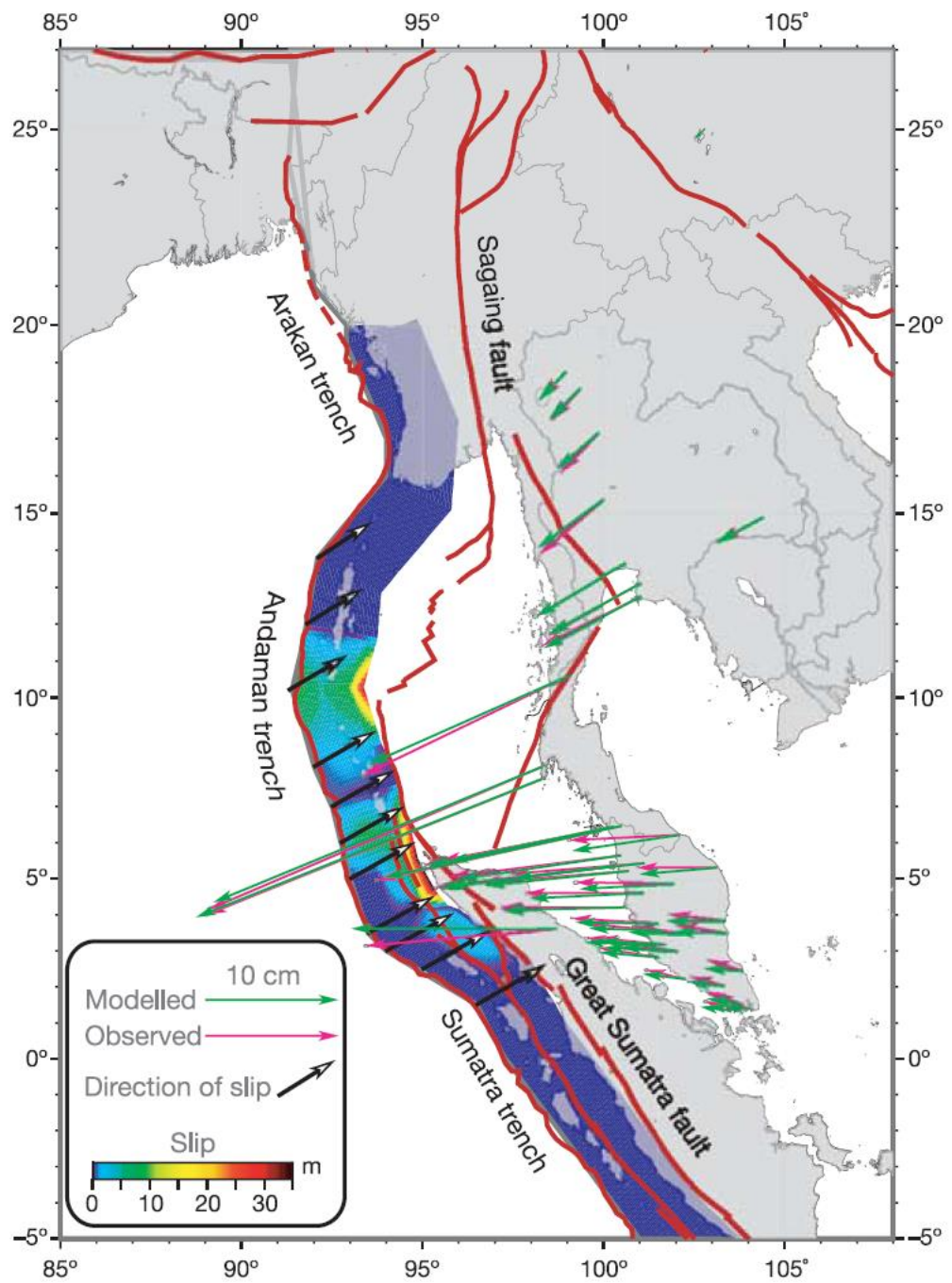


Figure 2.13: Co-seismic deformation model (Vigny et al., 2005)

2.3.5 Regional Seismic Hazard Analysis

Probabilistic approach in the development of seismic hazard analysis is commonly used in evaluating the earthquake probability of a study location. A study conducted by (Petersen et al., 2004) resulted in the development of earthquake source models and attenuation functions of 2% and 10% probability of exceedance in 50 years for rock site conditions earthquake design for Sumatra, Indonesia and across the Southern Malaysian Peninsula. Figure 2.14 presents hazard map for southern Malaysian peninsula at 10% probability of exceedance in 50 years on rock site conditions. The regional hazard of the study presents a relatively high level across the Sumatran region. In contrast a low to moderate level is observed across Malaysia.

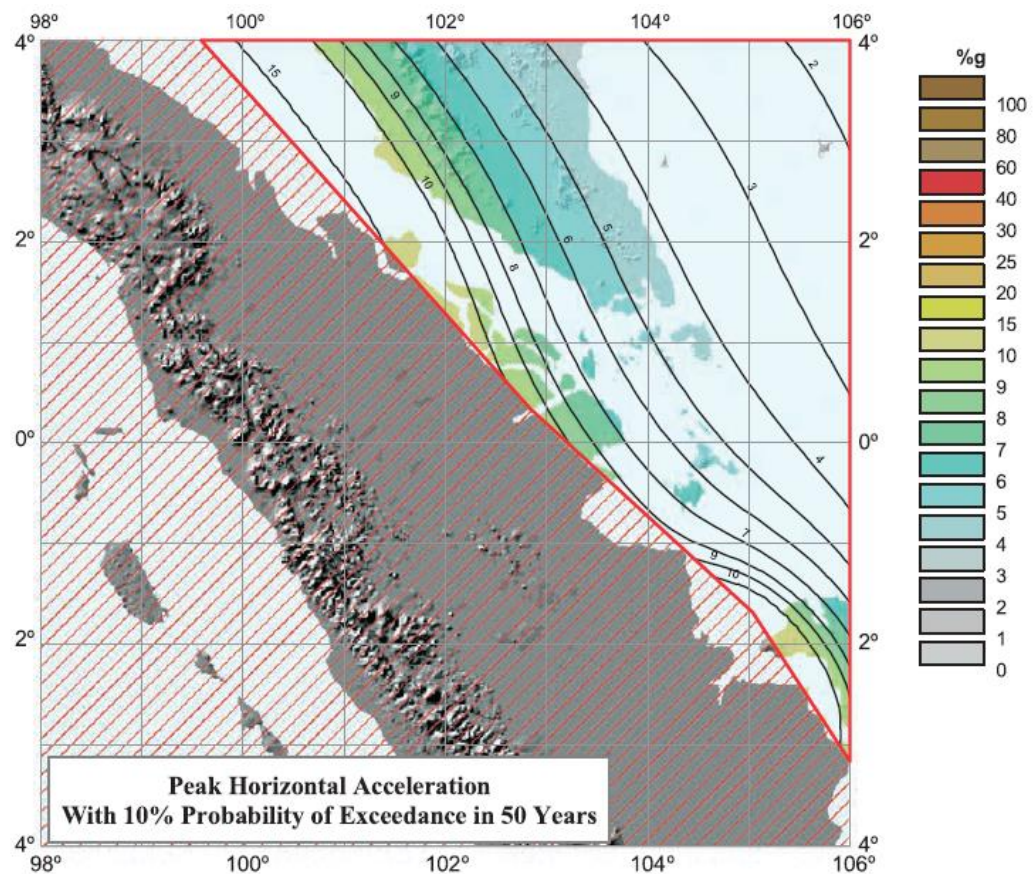


Figure 2.14: Hazard map of Malaysia (Petersen et al., 2004)

Figure 2.15 presents the de-aggregation hazard as a function of magnitude and distance at a site in Kuala Lumpur, Malaysia. However the analysis did not consider amplification of soils or basin response which can increase the ground motion and significant consideration in site-specific analysis. As a summary, the result obtained from the study is limited to a certain degree that refinement in the seismographic registration is needed in better estimate of seismic hazard. In addition the earthquake originating from the local settings also needs to be considered in the earthquake hazard model.

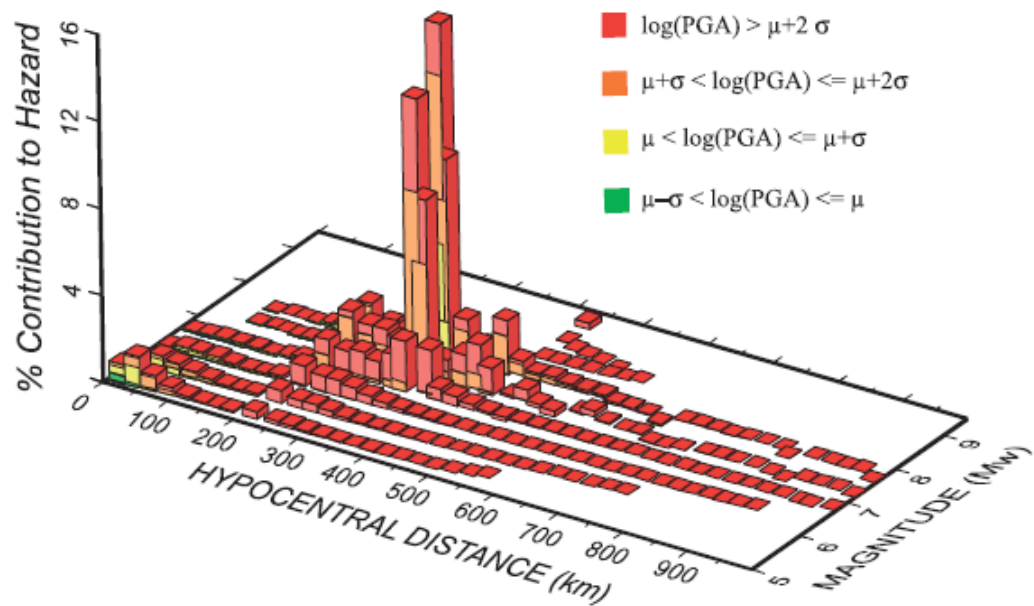


Figure 2.15: De-aggregation in Kuala Lumpur (Petersen et al., 2004)

A similar approach is presented by on the seismic hazard analysis for Jakarta City, Indonesia. Figure 2.16 and Figure 2.17 present the peak ground acceleration contour map 10% PE in 50 years and the deaggregation hazard and scaled response spectra at bedrock. The result presents a significant finding when compared to the existing regional seismic design code which does not consider parameters used in the PHSA.

The higher values of seismic characteristics from study denote that the existing seismic design code needs revision in adapting to the recent earthquake characteristics and analysis approach. Although the development of result were based on nonlinear response of a regional soil deposit, the study is limited to Jakarta city as the risk are observed higher compared to other cities in Indonesia.

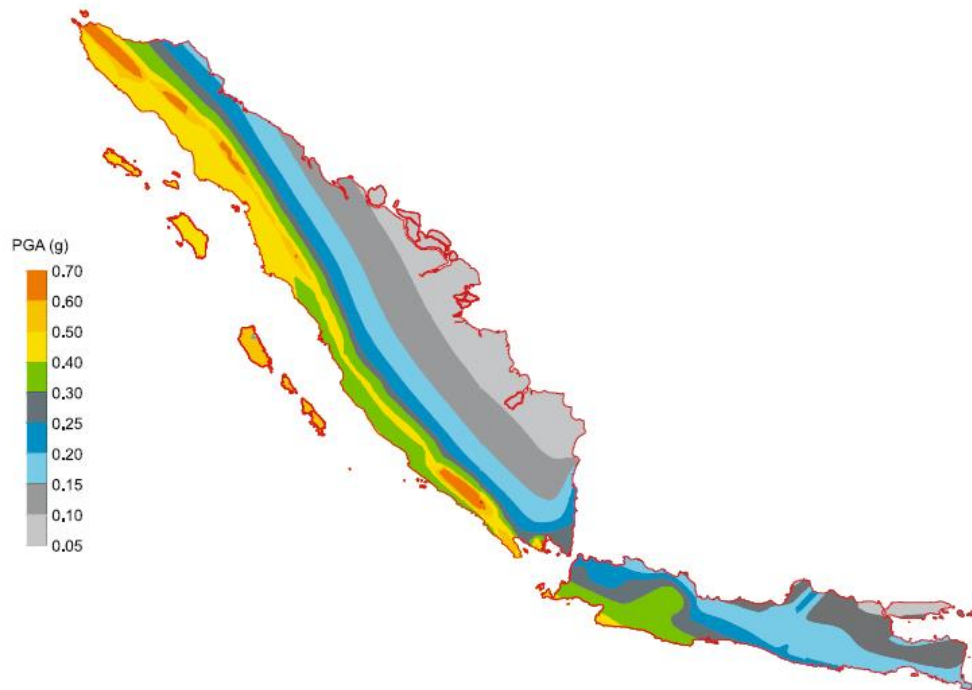


Figure 2.16: PGA contour map 10% PE in 50 years (Irsyam et al., 2008)

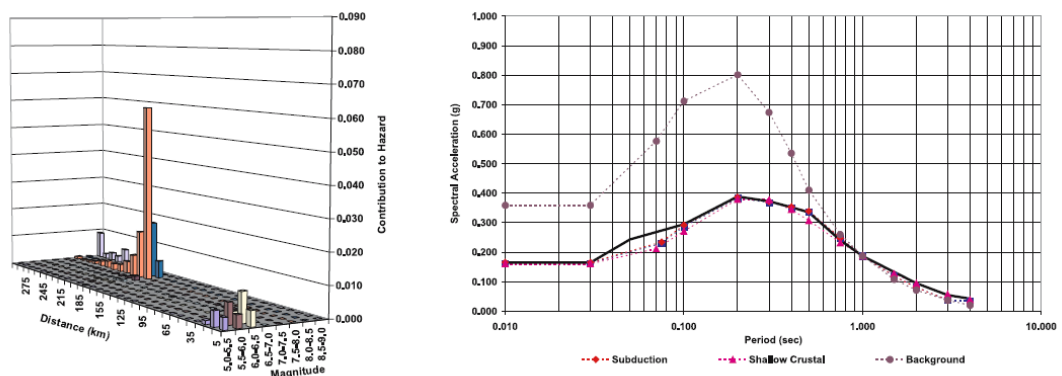


Figure 2.17: Deaggregation hazard and scaled response spectra (Irsyam et al., 2008)

A seismic hazard analysis is also developed for Thailand. Figure 2.18 presents the seismic maps of Thailand and adjacent areas. The earthquake catalog covers 1963-2007 seismic records. The resulted maps present ground motion of 0.4g to 1.0g in the northern and western Thailand and 0.0g to 0.4g in other part of the study areas. The findings can be improved with the consideration of recent earthquake in the Malaysia region. A unique finding from different researchers is defined as the approach and source model adapted varies from one researcher to the other.

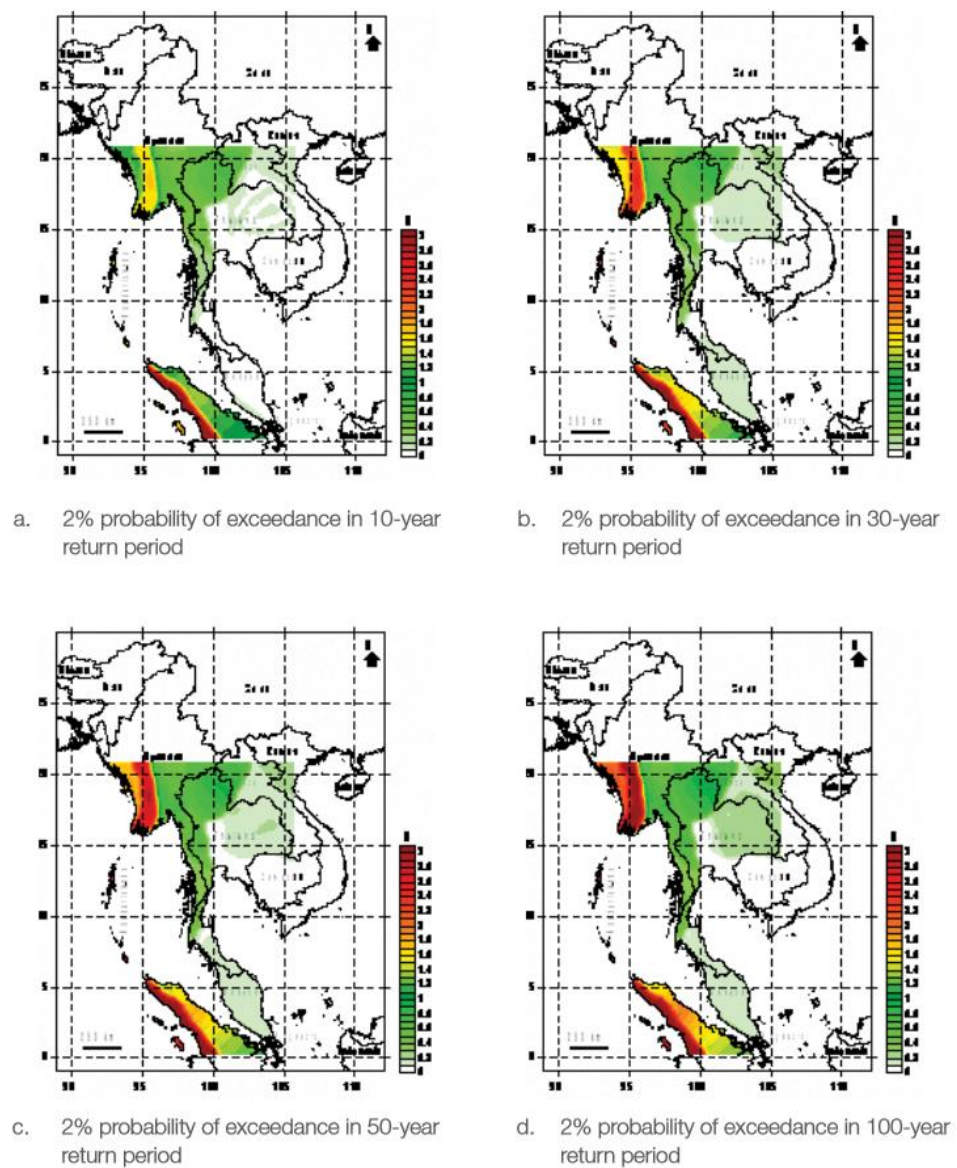


Figure 2.18: Seismic maps of Thailand and adjacent areas (Pailoplee et al., 2010)

2.4 Liquefaction Hazard Assessment

The initiation of soil liquefaction screening and assessment are conducted based on available literatures on recent soil liquefaction cases using secondary data obtained from government and local authorities. The findings highlight key points which could be an indicator and motivation of further studies of soil liquefaction in shoreline areas of Peninsular Malaysia. 3 main literatures are discussed and compared for the extraction of input and process of study.

2.4.1 The Padang Earthquake 2009

Padang is located in the west region of Sumatra, Indonesia. A major shock measuring a magnitude of Mw 7.6 occurred in 30th of September 2009 left extensive damage to buildings, houses, public facilities and roadways. According to Grundy (2010) a total of 1150 people were killed and 1200 people were injured. Soil liquefaction was observed at various locations in which is identified by numerous sand boils right after the earthquake. Soil samples from affected site were collected and examined in the laboratory to determine the soil grain size distributions. It was found that most of the soil satisfies the criteria of liquefaction susceptibility when plotted in the limit curve in Figure 2.19. A map was also introduced in Figure 2.20 in presenting the identified location of soil liquefaction in Padang area. The plotted map shows affected areas are likely to be concentrated along riverbeds and beaches in which there is high possibility of saturated deposits exist in the areas. Prior to the findings, laboratory was conducted on the soil sample and CPT was conducted to further analyze the effected site. Figure 2.21 shows the grain size distribution plot of the study in which is similar to the findings by (Grundy, 2010) mentioned previously. As a conclusion the area was further analyzed using soil liquefaction analysis and result shows high potential in soil liquefaction hazard.

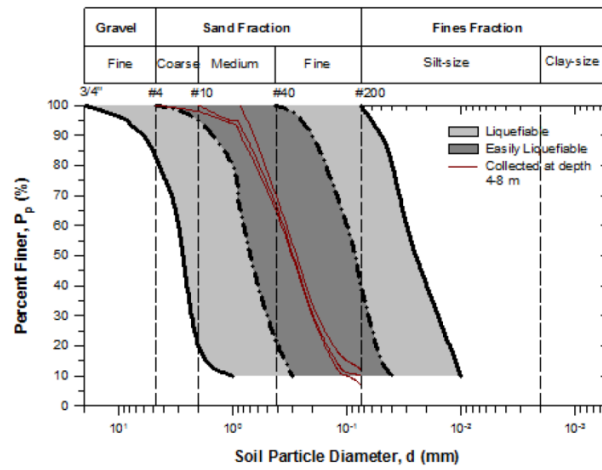


Figure 2.19: Grain size distribution plot (Muntohar, 2014)

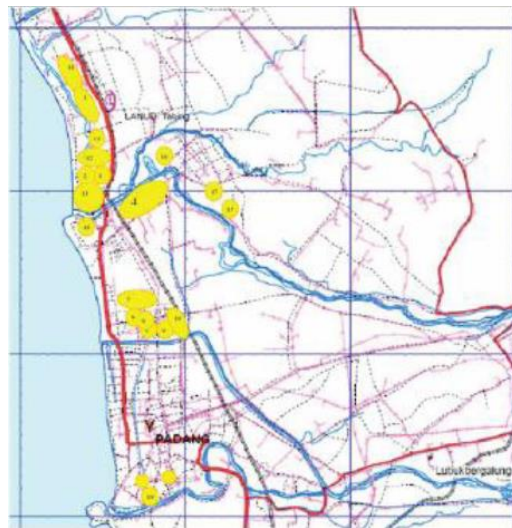


Figure 2.20: Soil Liquefaction in Padang (Hakam & Suhelmidawati, 2013)

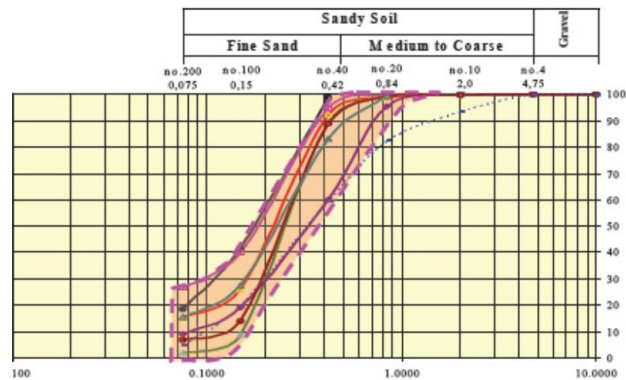


Figure 2.21: Grain size distribution plot (Hakam & Suhelmidawati, 2013)

2.4.2 The Tohoku Earthquake 2011

Japan have been known to have experiencing a number of large earthquake scenarios which have demonstrated massive damage by turning the land upside down as documented by Kawakami and Asada (1966) and Yoshida and Kudo (2000) during the ‘Niigata Earthquake’ in 1964. The continuous natural hazard occurrence in Japan has contributed to the revolution in the engineering practice and mindset in the people on the aspect. Many significant researchers have made it possible to expand the knowledge on theory and technology prior to the observation from the surroundings. In 2011, earthquake with a magnitude of 9 have produced soil liquefaction in wide area from the Tohoku district to the Kanto district in which produce serious ground failure. An observation study conducted by Yamaguchi et al. (2012) and Ashford et al. (2011) presents detail investigation on soil liquefaction occurrence in the Kanto district and Tohoku district. Various sizes of sand boils are observed in farm land, river dikes and flood channels mainly consisted of sand and silty clay. A reclamation site was also observed to have extensive damage to the buildings and facilities. Remedial measures reported to have adapted in airport runaway by infiltration sodification and X-jet grouting method have made it possible for excavation and hospitality. Another observation made presents a massive area of reclaimed site affected by soil liquefaction during the same Tohoku Earthquake in 2011. The report documented widespread of liquefaction in Tokyo Bay. The site involves reclaimed land, fill areas and site having young alluvium. Moreover the main findings by Bhattacharya et al. (2014) is that the liquefaction hazard is dependent on the age of fill material, type of fill material and the type of ground improvement carried out. Figure 2.22 and Figure 2.23 presents the grain size distribution plot from sieve analysis on soil sample of various affected liquefaction site conducted by Unjoh et al. (2012) and Tsukamoto et al. (2012).

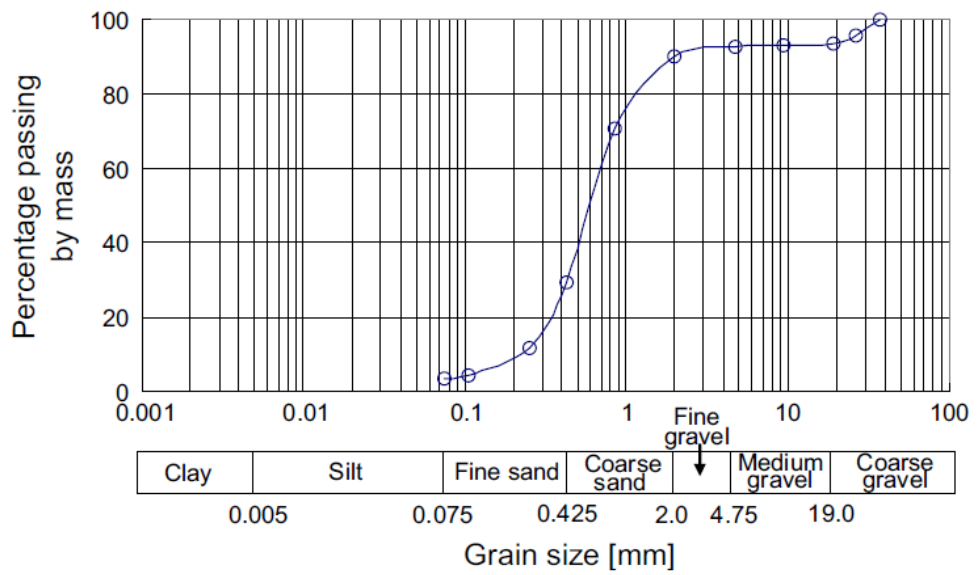


Figure 2.22: Grain size distribution plot (Unjoh et al., 2012)

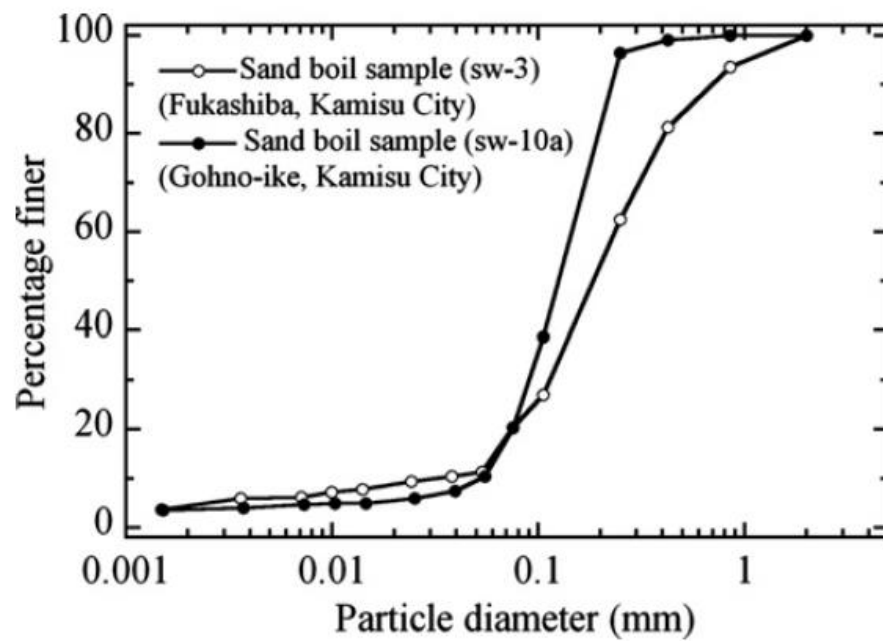


Figure 2.23: Grain size distribution plot (Tsukamoto et al., 2012)

The map of liquefaction site in Figure 2.24 by Tsukamoto et al. (2012) highlight the widespread of soil liquefaction on areas of reclamation. The hazard is situated near public facilities and important structures which is the port area. Figure 2.25 presents a photo on the erupted ground due to the hazard. Prior to the findings from this study, proper ground improvement method need to be implemented at liquefy site for future reference. Hence the initial pre-assessment study is much important in an area with no available information on the ground profile and performance of the local site. Figure 2.26 summarized the soil profile in which liquefies soil deposits is highlighted in the affected areas.

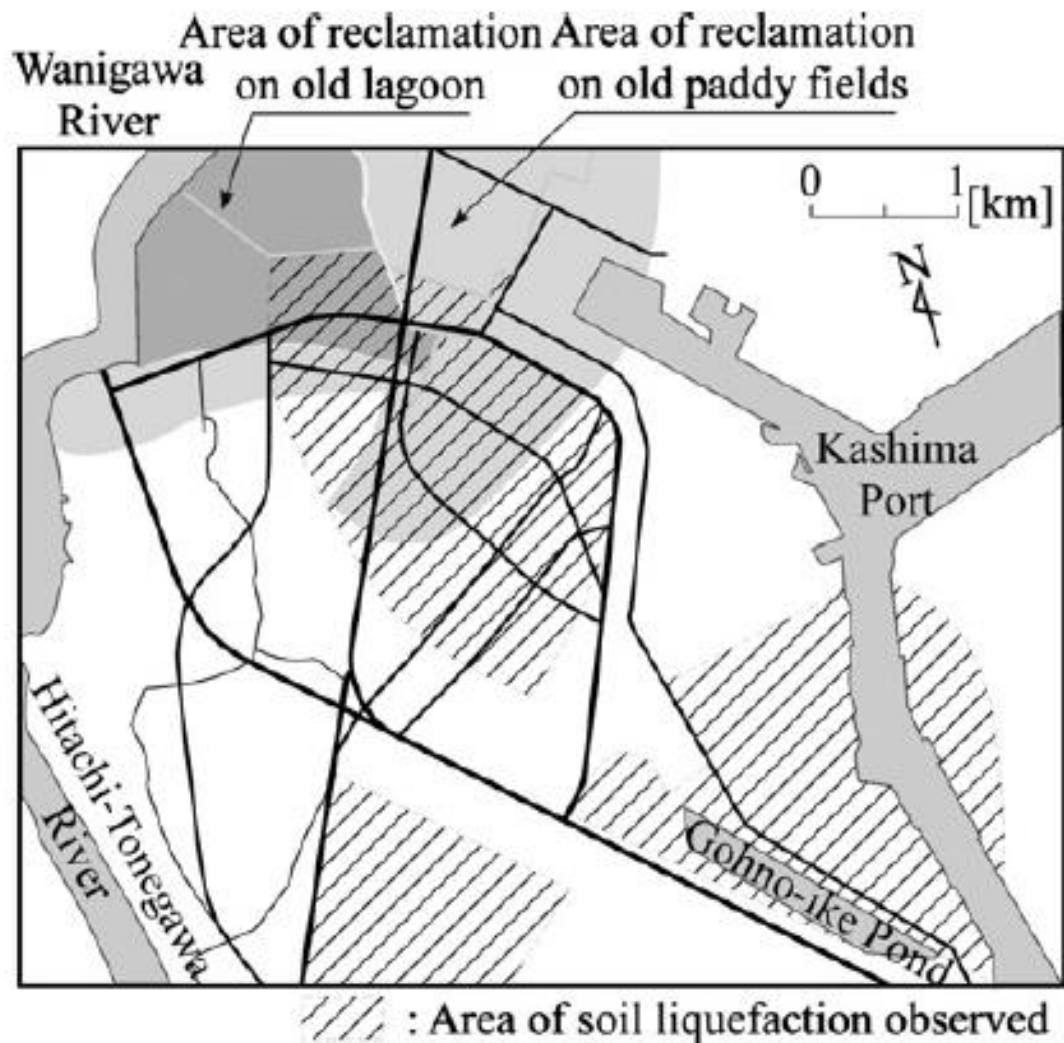


Figure 2.24: Liquefaction affected site (Tsukamoto et al., 2012)



Figure 2.25: Erupted ground due to soil liquefaction (Tsukamoto et al., 2012)

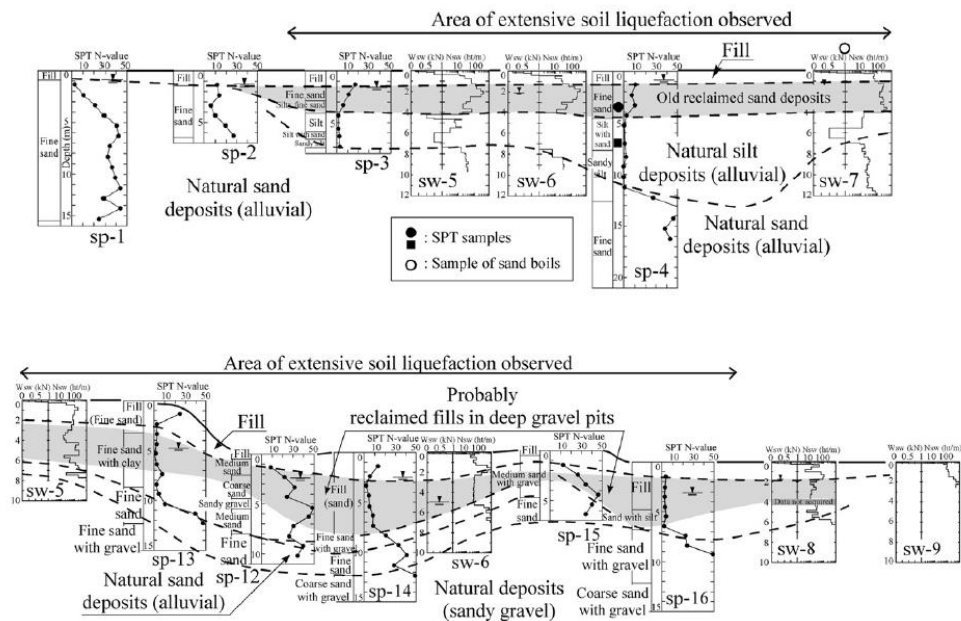


Figure 2.26: Soil profile of the studied area (Tsukamoto et al., 2012)

2.4.3 The Christchurch Earthquake 2010 – 2011

A series of continuous tremors in early September 2010 to early June 2011 have witnessed a severe event which left the city paralyzed. The magnitude ranging from 6.0 to 7.2 is followed by aftershock recording significant impact in the history of natural hazard in New Zealand. Soil liquefaction widespread in extreme populated area left almost half the structures in the city center destroyed. An investigation carried out by Wotherspoon et al. (2012) highlighted loose deposits of silts and sands in many of the affected site which is a reclaimed site and old river channels which have been diverted away (Figure 2.27). Figure 2.28 presents the grain size distribution plot reported by (Green et al., 2013) . Most of the soil deposits resting on liquefy areas falls within the boundary of liquefied soil of which explains the widespread of the hazard. Soil profile investigation also presents a variety of potential soil that have played important role in reacting with ground tremors leaving instability to ground condition which is dangerous to underground facilities or structures lies in or above it. Figure 2.29 shows the soil profile plot of studied area based on Figure 2.30 of the excavation site of liquefy area.

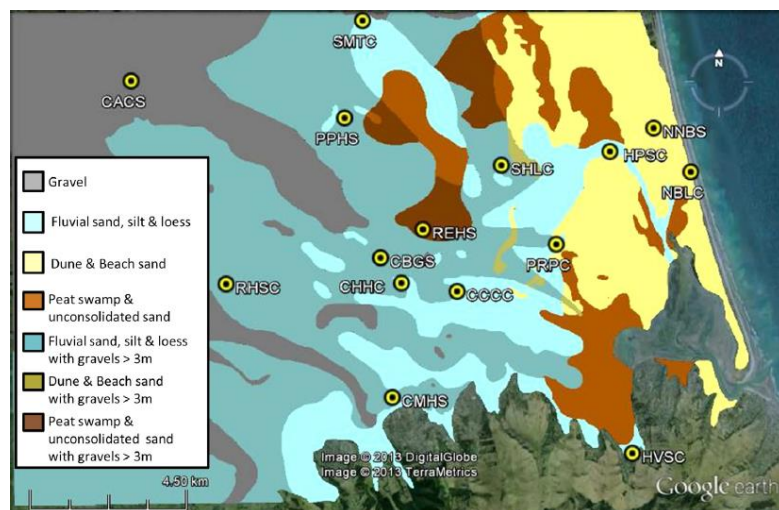


Figure 2.27: A map highlighting soil details (Wotherspoon et al., 2015)

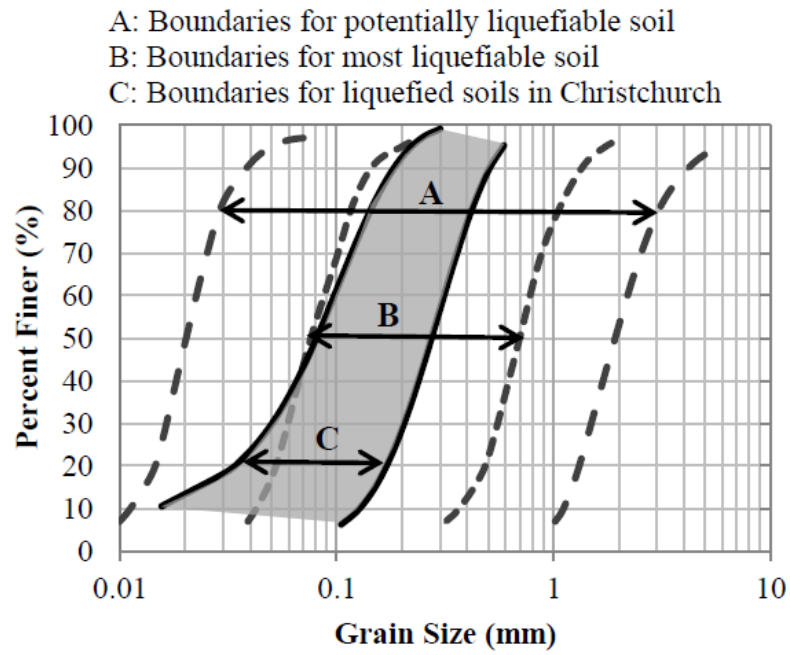


Figure 2.28: Grain size distribution plot (Green et al., 2013)

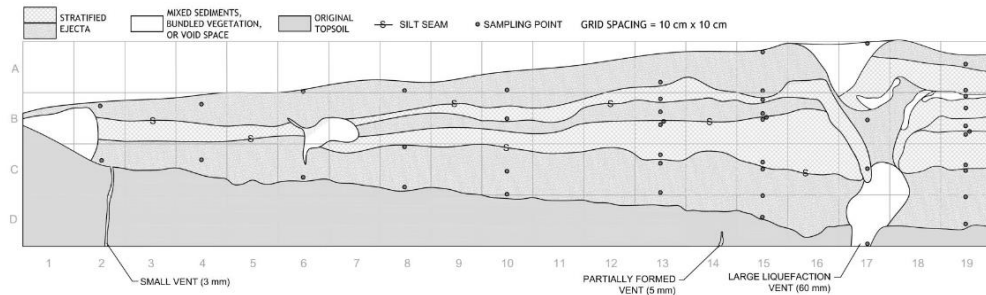


Figure 2.29: Soil profile observation on liquefy site (Green et al., 2013)

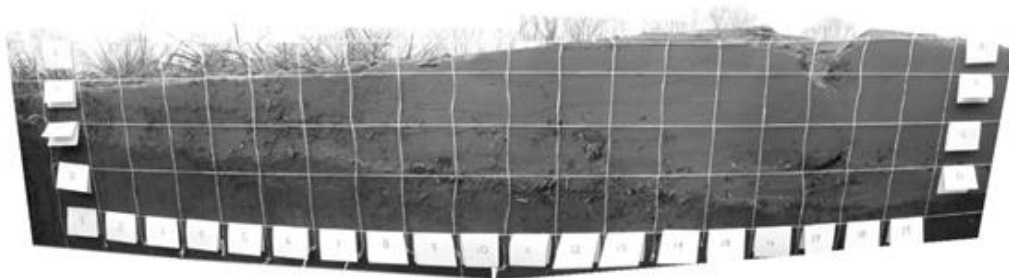


Figure 2.30: Site investigation on liquefy site (Green et al., 2013)

2.5 Literature Review Summary

Main observation which is highlighted in all of the literatures mentioned was the damage scenarios in previous events, the liquefaction susceptibility, regional geological and seismological content towards hazard and general liquefaction assessment throughout the world. There are very few studies conducted hence resulted in limited resources and information for the development of liquefaction hazard study in Peninsular Malaysia. Significant contribution from soil investigation is the soil properties ranging from depth, type and basic parameters from geotechnical testing of soil deposits. Hence field test such as the standard penetration testing, cone penetration test, shear wave test or seismic refraction test is crucial in conducting the preliminary study of soil liquefaction on the shoreline areas of Peninsular Malaysia. Photographs of studied site is also important in finding different aspect of environment definition such as population type, facilities and structures, socio-economy and area size in developing further study of the main research.

CHAPTER 3: METHODOLOGY

This section includes 4 main methodologies which are continuously interrelates to one another in developing the thesis structure as presented in Table 1.2 in Chapter 1.

3.1 Soil Liquefaction Screening

Data collection was conducted prior to site visit. Secondary data is the main source of the study input. Hence SI (site investigation) report contributed most in study. A first approach in quantifying hazard and risk assessment is based on quantitative approach based on soil liquefaction susceptibility. The aim is to estimate the potential of hazard at studied site. An easy way of looking into the study is by collections of available data within the study scope and evaluation being made result in indication as an output in a form of graphical illustrations, chart and tabulated findings. Figure 3.1 presents the process in soil liquefaction screening. Based on the basic principal of soil liquefaction susceptibility, parameters which are being observed are basically the soil properties for the first 20 meters depth and location of ground water table (Arion et al., 2015).

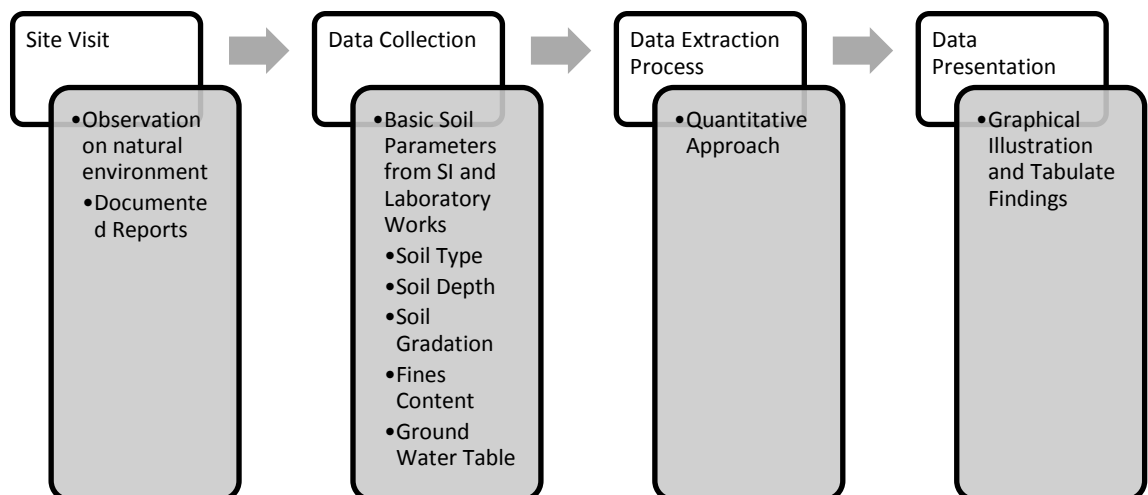


Figure 3.1: Main process in soil liquefaction screening

3.1.1 Studied location

The study location covers approximately 1972 km stretch of coastal line which includes 11 states in the Peninsular Malaysia. Figure 3.2 presents map of Peninsular Malaysia with distribution of studied boreholes (red symbol) along shoreline. The distribution of studied borehole location is site specific hence updating of data will be a continuous process in developing updated soil liquefaction hazard map. In this study the uncertainties in natural environment in most part of the shoreline which are inaccessible due to natural formation is merged using spatial analysis in presenting the findings of this study.

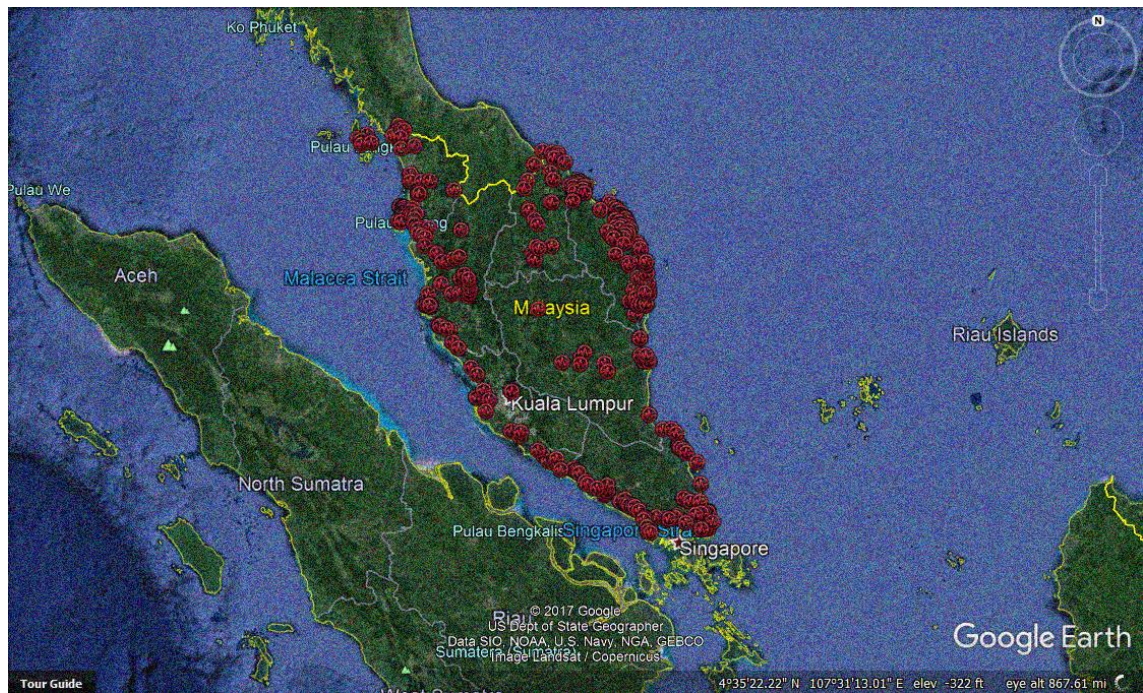


Figure 3.2: Distribution of studied borehole along shoreline

3.1.2 Database of Soil Collection

Borehole exploration soil investigation was promoted through the collection of SI report based on SPT. The availability of data within the study location significantly increases the database of project for wider coverage of information on local grounds. A quick summary of database detail is presented in Table 3.1 and Table 3.2. 11 states containing 40 shoreline districts are identified for soil liquefaction screening. Database of research contains a total of 325 number of location with 2074 number of borehole. The SI report is of 1987 to 2014 projects consists of coastal roads, schools, service apartments, clinics, residential units and bridges. Each state and shoreline district is given a codename based on the car plate number for easy referencing in later process of study.

Table 3.1: Summary of data collection

Peninsular Malaysia	State	State Label	No. Location	No. Borehole
	Perlis	R	8	86
	Kedah	K	17	104
	Pulau Pinang	P	31	178
	Perak	A	42	210
	Selangor	B	13	79
	Negeri Sembilan	N	2	20
	Melaka	M	8	27
	Johor	J	71	384
	Pahang	C	12	103
	Terengganu	T	95	546
	Kelantan	D	26	341
	Total	11	325	2074

Table 3.2: Detail summary of data collection

Peninsular Malaysia	State	State Label	Shoreline District	Shoreline Distance (km)	Shoreline District Label
	Perlis	R	Perlis	20	R1
	Kedah	K	Langkawi	148	K1
			Kubang Pasu		K2
			Kota Setar		K3
			Yan		K4
			Kuala Muda		K5
	Penang	P	Penang Island	152	P1
			Seberang Perai		P2
	Perak	A	Kerian	230	A1
			Larut, Matang & Selama		A2
			Manjung		A3
			Hilir Perak		A4
	Selangor	B	Sabak Bernam	213	B1
			Kuala Selangor		B2
			Klang		B3
			Kuala Langat		B4
			Sepang		B5
	Negeri Sembilan	N	Port Dickson	58	N1
	Melaka	M	Alor Gajah	73	M1
			Melaka Tengah		M2
			Jasin		M3
	Johor	J	Muar	492	J1
			Batu Pahat		J2
			Pontian		J3
			Johor Bahru		J4
			Kota Tinggi		J5
			Mersing		J6
	Pahang	C	Kuantan	271	C1
			Pekan		C2
			Rompin		C3
	Terengganu	T	Besut	244	T1
			Setiu		T2
			Kuala Terengganu		T3
			Marang		T4
			Dungun		T5
			Kemaman		T6
	Kelantan	D	Tumpat	71	T7
			Kota Bharu		T8
			Bachok		T9
			Pasir Puteh		T10
	Total	11	40	1972	40

3.1.3 Site Investigation Report

Soil data recorded with SPT sampler at different depths and geologic layers provide important information for studying local site effects. The soil data compiled in a log report consists of geotechnical information on the subsoil conditions which is generally required for the purpose of design and construction works. It comprises of field and laboratory data. The field investigation includes the drilling works, undisturbed samplings and standard penetration test, whereas, the laboratory testing performed on undisturbed samples to obtained basic soil parameters. Laboratory tests which includes the moisture content test, bulk and dry density determination tests, unconsolidated undrained triaxial compression test and consolidation undrained triaxial test are carried out for the evaluation of shear strength, compressibility characteristics and classification of soil properties. A summary of soil strata is presented as the main output of the report along with boreholes location plan and site photographs. Figure 3.3 presents typical borehole log report from SI report.

DEPTH (meter)	DESCRIPTION OF SOIL, COLOUR CONSISTENCY, RELATIVE DENSITY GRAIN SIZE, TEXTURE ETC.	SAMPLE								N Blows	R/r %	REMARKS
		DEPTH (meter)	No. (Cls.)	Field Test								
				75 mm	75 mm	75 mm	75 mm	75 mm	75 mm			
0.00	Light brown CLAY.	0.00-	-	-	-	-	-	-	-	-	-	Top Soil
1.00	Medium dense brownish red clayey GRAVEL of high plasticity and with some sand.	1.50- 1.95	D1 GCH	2	3	3	4	3	4	14	70	
2.50	Very stiff reddish brown sandy CLAY of intermediate plasticity and with a little gravel.	3.00- 3.45	D2 CIS	2	2	5	7	9	6	27	75	
4.00	Hard yellowish brown sandy CLAY of intermediate plasticity and with traces of gravel.	4.50- 4.925	D3 CIS	2	5	10	15	12	13 50	50 275mm	85	
6.00	Hard brown sandy CLAY of intermediate plasticity and with traces of gravel.	6.00- 6.40	D4 CIS	3	4	11	12	15	12 25	50 250mm	90	

Figure 3.3: Typical borelog properties from SI report

3.1.4 SI Report, Soil Sampling, SPT-N correction

The SI report collected presents information of the ground according to B.S 1377: Part 9: 1990, “Determination of the penetration resistance using split-barrel sampler”, using a self-tripping hammer of 63.5 ± 0.5 kg weight of designated design. Soil samples were taken in the form of undisturbed or disturbed but representative when drilling. The disturbed samples are used for laboratory classification tests. The samples were sealed in polythene bags before sending to laboratory for further investigation whereas the undisturbed samples were collected by applying hydraulic thrust on thin wall sampling tubes of 60 mm diameter for very soft cohesive soils. The sampling tubes are later secured with wax to maintain water content. All the samples were placed in cushioned boxes and transported to laboratory to ensure minimum disturbance.

The SPT-N value is subjected to a large number of variables that affect the results. SPT-N values are standardized to $N_{(1)60}$ values in reducing the significant variability. Therefore correction factors are adapted study regardless of the equipment used at site. The approach is to ensure SPT-N data used is close representation of the actual subsurface condition.

3.1.5 Illustrations, Chart and Tabulated Information

3 illustrations are developed for the soil liquefaction screening. Each shoreline district is presented with soil composition, SPT-N distribution and ground water table (GWT) location. The soil composition consists of 4 soil types; clay, silt, sand and gravel. The SPT-N distribution on the other hand presents the stiffness of each layer. The harder the layer denotes by the higher value of SPT-N blow counts. Lastly is the GWT location which presents the zone of saturation (dry and wet zone). All the 3 illustrations are made possible using linear stratigraphy correlation method to represent the governing factor of soil liquefaction; ground water table and loose deposits.

The vulnerability of soil is further analyzed using liquefaction margin. The liquefaction margin is developed by Tsuchida (1970) in the form of particle size distribution curve. The liquefaction margin defined 2 level of liquefaction potential which is high possibility of liquefaction and possibility of liquefaction.

The tabulated information consist of general information of shoreline areas, the susceptibility of soil at studied areas and decision making process for soil liquefaction screening. The general information highlights type of beach, district areas, district population and economy. The second tabulated information highlight governing factors of soil liquefaction hazard (soil type, depth of deposits, soil grading, GWT and fine content). The last presentation of tabulated information is the remarks on liquefaction evaluation. The significant aspect of land usage and also the level of seismic hazard is adapted for the decision making process whether the shoreline district needs further analysis in soil liquefaction hazard.

3.2 Cyclic Triaxial Testing

This section will be describing on the test instruments and materials used for testing program. The cyclic triaxial cell is working in the same way as the static triaxial cell with the advantage of applying any kind of load sequence to the test sample.

3.2.1 Laboratory Testing Program

In general the test system consists of both electrical and mechanical parts. Figure 3.4 presents the set-up of the cyclic triaxial test consists of a cyclic triaxial cell which could sample up to 100 mm diameter and 200 mm height. It has a dynamic upgrade which is a linear bearing that holds the triaxial ram laterally stiff and reduces the friction during dynamic testing. The main load frame of the triaxial system has an actuator (Figure 3.5) installed on the top which is responsible for moving and controlling the system operation converting energy into motion. The base part of the triaxial system holds electronics which power up the system (Figure 3.6). A dynamic control system (DCS) is a 16-bit high speed data acquisition which is a 5 kHz high speed control capable up to 5 Hz for the system (Figure 3.7). The system also comes with a standard controller for the backpressure and pneumatic controller for the cell pressure (Figure 3.8).



Figure 3.4: Set-up of the cyclic triaxial test



Figure 3.5: Actuator on test system



Figure 3.6: Power up electronics at the base of system



Figure 3.7: Dynamic control system (bottom) and pneumatic controller (top)



Figure 3.8: Standard controller for backpressure

The connection of system is by using 25 pin to 25 pin, male to female cable for the analog signal between the DCS box and the triaxial load frame and 9 pin to 9 pin, male to female digital cable. Both cables are connected to the back of the load frame. A normal IEC connector and large blue sleeve connector type is used to power up the DCS box and the load frame respectively. Both power supplies run from 110-115V or 220-240V. The DCS is connected to a PC system using USB cable. Specific software, GDSLAB and HASP dongle file is pre-installed in the PC system in order to run a test (Figure 3.9). Transducers device for converting physical quantity into an electrical signal are connected to the DCS by respective channels on the DCS. Channel 0 on the DCS is for the load cell because it has an input range of ± 30 mV. Channel 1 and Channel 2 both have an input range of ± 200 mV specifically designed for pressure transducers. Channel 3 has an input range of ± 10 V, specifically for output of the pneumatic pressure controller which is connected with a 3-pin to 5-pin connector. The 3 pin goes into the front of the pneumatic pressure controller and the 5 pin goes into the 10 v channel, Channel 3. The measuring of displacement is by using the high accuracy integrated displacement encoder built in the actuator.

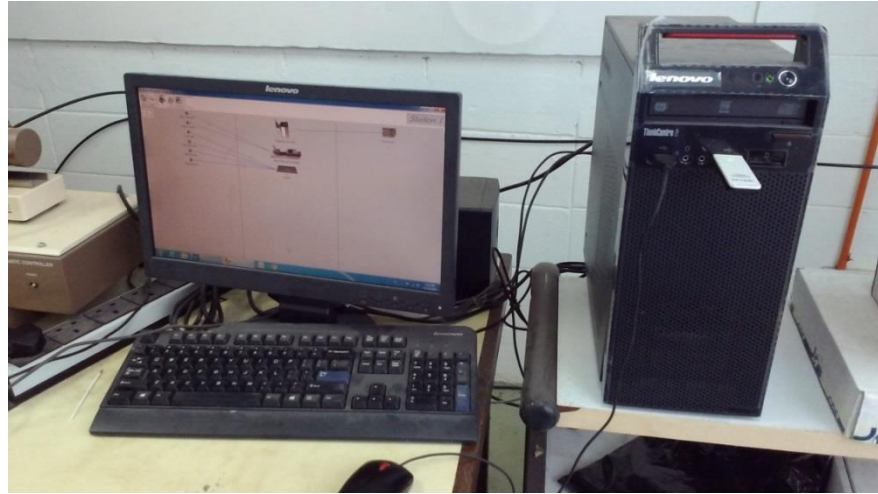


Figure 3.9: PC system with pre-installed software

A specific software known as GDSLAB is the main communication between the cyclic triaxial system and the end user. The first step after running the GDSLAB is to create a station from the control window and save it with a .ini extension suitable for the test. Next is to highlight the Object/Hardware Display tab. A new window (Figure 3.10) will eventually popped out and the DCS figure is highlighted. The DCS is configured using this control panel with 4 different tab. On the 'System tab', the respective DCS is selected using the serial number in the selection tab. A system message indicating successful connection is mentioned whenever the main load frame is turn on. The next setting is on the 'Control' tab which needs to follow two main procedures namely set platen position and move platen. The set platen position allows the actuator ram to be set to a particular height, relative to its full stroke. For example when the value is set to 50, the platen will be positioned in the center of its stroke. The full stroke of the system is 100 mm so it will move to 50 mm. The nominal stroke is 100 mm so first it needs to detect and calculate exactly what the full stroke is. If set position is highlighted, the platten will go to the top of its stroke and then it will track down to the bottom of its stroke, finally calculate the full stroke compared to its limit and then move to a position 50% between those limits. The position of ram and stroke details is important for the

test. The preferable value is 50 for the test is selected. On the move platen section, a unique control of platen position can be defined by the user giving a simple movement for the control of actuator position. The third tab is the 'DIO Status' which presents the important information for diagnosis purposes of the system. The final tab on the DSC control panel is the 'RT Graphs' which indicates changes in the specimen during testing in the form of graph presentation. The channels on the DCS can be selected and is limited to 2 graphs per viewing.

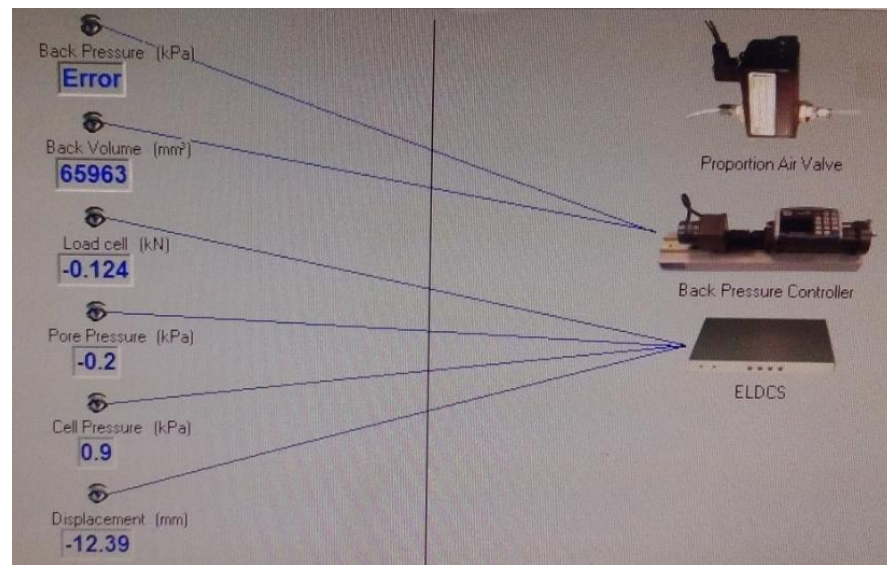


Figure 3.10: Object/Hardware window

The transducers can also be found in the Object/Hardware window. The first transducer which is the load cell is highlighted and a tab will eventually popped out presenting 3 main tab. 'Detail' tab presents the status of transducers. The 'Advanced' tab shows a more detail technical information on the device which can be configured accordingly such as calibration values and safety limits settings. The last tab is the 'Calibration' which allows the settings for sensitivity configuration. The next transducer is the displacement device. The option for general setting similar to the load cell is presented in the control menu and can be adjusted accordingly. Having both the

transducers setup, a sanity check is conducted to check that all the system are working accordingly. By taking out the entire submersible load cell out of the triaxial cell and apply pressure on the load cell by the body weight and observed the pressure value in the measurement control panel. The value need to be the same with the pressure applied by the body weight. The second sanity check in on the encoder device. The displacement setting is measured using a ruler and check accordingly with the value setup in the PC. Finally, having all the system in order, the dynamic test is conducted by installing the triaxial cell in the main load frame (Figure 3.11).



Figure 3.11: Triaxial cell installed on the main load frame

By having the triaxial cell in place and positioned in the main load frame, the cell pressure line is connected from the pneumatic controller to the triaxial cell. The 8 mm air line connector is connected on the top of the triaxial cell in preventing water from entering the bottom of cell through the air pressure controller. The final hydraulic connector is the backpressure tube which connects the standard controller for backpressure to the base of triaxial cell. Before connecting the backpressure tube, air is flushed out of the backpressure tube before making a connection. The final part of the setup within the load frame is to clamp the cell down to the base using the adjustable clamping bars. The bars are to ensure the triaxial cell to be in the frame throughout the dynamic loading test.

The first test is to run the saturation test followed by consolidation test and lastly the dynamic test. Three main items are needed in the dynamic test which is the load on the sample, cell pressure and backpressure. At the very beginning of dynamic test, the sample is docked to be in contact with the load cell by setting a load target from the 'Load Control' panel of the Object/Hardware Display. After docking process, a starting position test is configured by cell pressure is set constant at 100 kPa. The backpressure is set slightly higher and the ramp load cell value is set at 1 kN at 4 minute. By observing the graph in the GDSLAB, the load cell value is 1 kN and the cell pressure is 100 kPa. The starting position process is paused and the deflection reading is set at 'zero' so that the test is easier with a datum of 'zero' as a starting point. The next process is to add another test on dynamic loading displacement control. For starters, the test is configured at frequency of 1 Hz, datum at existing datum which is zero, amplitude of ± 2 mm. The cell pressure is set to 100 kPa. On the next step of the test configuration, backpressure is set again. Cycles are set to 10. Point per cycle is the data points we can acquire throughout the cycle. After starting the test, real time graphs can be observed in the software. There are two option available for dynamic cyclic test

namely the displacement control test and the load control test in which is differ by the estimation of stiffness for the load control. The high stiffness value indicates stiff sample and the system are able to accommodate the loadings for the sample tested. Unlike a soft sample whereby the stiffness is low, hence the system is more aggressive in term of the loading to achieve the desired loading. Figure 3.12 presents the Sample preparation on the base plate of the load frame.

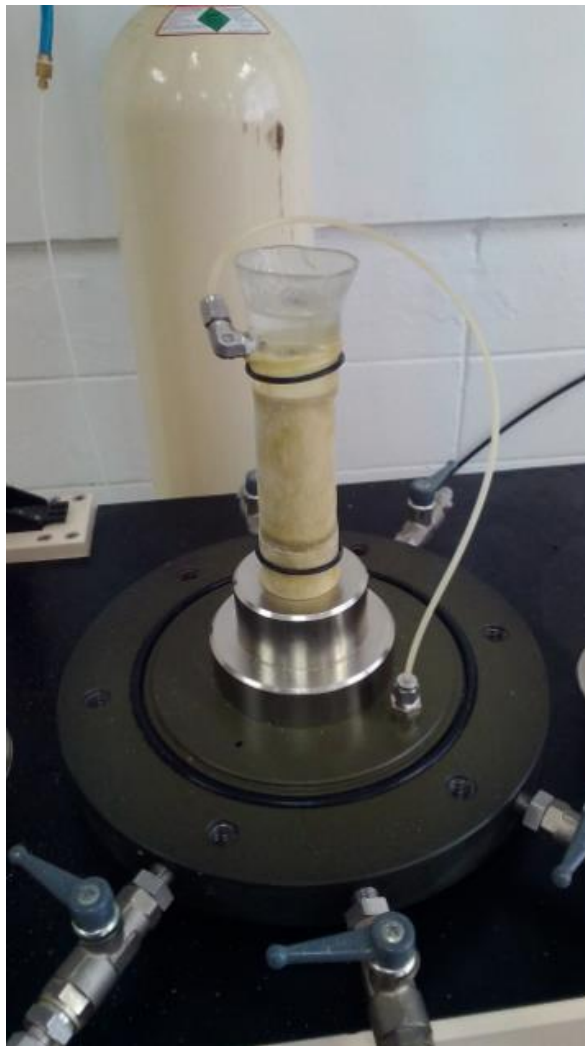


Figure 3.12: Sample preparation on the base plate of the load frame

3.2.2 Materials

Two (2) type of soil sample was used in the performed tests. The soil sample is of sand and clay. The sand obtained from Pahang state which represents the east coast of Peninsular Malaysia whereas the clay obtained from Johor state which represents the west coast of Peninsular Malaysia. Both are located on the shoreline area and the depth of which the sample are taken are within 1 meter from the beach surface. Figure 3.13 presents the clay sample taken from clayey type beach and the sand taken from the sandy type beach. The laboratory works was carried out in limited time frame of 5 days in Universiti Teknologi Malaysia (UTM) Skudai, managed to utilize 2 samples of clay and 5 samples of sand. The best presentation of each soil type in term of proper end result is chosen for further study.

Although the study covered approximately 1972 km shoreline and the properties of soil varies with different site, the laboratory works is limited to Pahang and Johor areas only.



Figure 3.13: Soil samples used in lab works

The engineering properties and particle size distribution of sands are presented in Table 3.3 and Figure 3.14 respectively.

Table 3.3: Engineering properties of soil

Engineering parameters	Sand	Clay
D_{10} (mm)	0.34	-
D_{30} (mm)	0.36	-
D_{50} (mm)	0.41	-
D_{60} (mm)	0.45	-
C_u	1.32	-
C_c	0.85	-
0.075 mm < Particle sizes < 2.36 mm (%)	2	0
Particle sizes < 0.075 mm	0	100
Density, γ (g/cm ³)	1.48	1.12
Specific Gravity, G_s	2.70	2.57
Void ratio, e_{max}	0.85	1.90
Natural Moisture Content (%)	13.49	37.52
Bulk Density (Mg/m ³)	1.457	1.469
Dry Density (Mg/m ³)	1.300	0.885
Degree of Saturation	91.542	89.064
Liquid Limit (%)	-	37
Plastic Limit (%)	-	18
Plastic Index	-	19

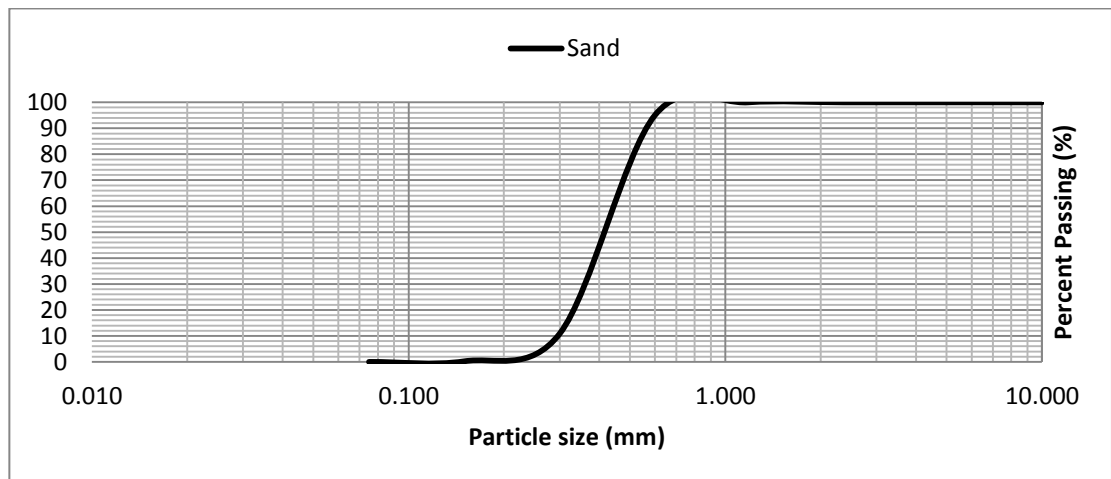


Figure 3.14: Particle size distribution of sands

3.2.3 Controlled Parameters and Parameters Obtained from Dynamic Cyclic Triaxial Tests

Table 3.4 summarizes the controlled parameters for the cyclic triaxial testing conducted in this study.

Table 3.4: Controlled parameters for cyclic triaxial testing

Controlled parameters	Value	
	Sand	Clay
Loading Frequency (Hz)	0.5, 1 and 2	1
Amplitude	0.1, 0.5	
Stiffness Estimate	1	
Number of Cycles	40, 400	
Cell Pressure for consolidation (kPa)	450	210
Back Pressure for consolidation (kPa)	350	200
Confining pressure (kPa)	400	300
Diameter (mm)	38	
Height (mm)	76	
Type of Cyclic Loading	2-way	
Mass (g)	145	97

There are many aspects of the dynamic cyclic response of soils that can be investigated (Kaya & Erken, 2015; Kumar et al., 2017). As for this study the aim is to determine the modulus and damping properties of soils (Srbulov, 2014).

3.3 Earthquake Study

The earthquake study is inclusive of Probabilistic Seismic Hazard Analysis (PSHA), Spectral Matching Procedure (SMP) and the Site Response Analysis (SRA).

3.3.1 Probabilistic Seismic Hazard Analysis (PSHA)

The total probability theorem introduced by McGuire (1976) in PSHA was based on the probability concept originally by Cornell (1968) and takes basic form as follows, $P[I \geq$

$$i] = \iint_{rm} P[I \geq i | m \text{ and } r] f_M(m) \cdot f_R(r) dm dr \quad [3-1]$$

The source of these parameters for [3-1] as follows:

f_M = density function of magnitude, f_R = density function of hypocenter distance

$P[I \geq i | M \text{ and } R]$ = conditional probability of random intensity, I exceeding value i at the site for a given earthquake magnitude M and hypocenter distance R

The assumptions made in (3-1) is that the earthquake magnitude, M and the hypocenter distance, R is a continuous independent random variable. As for calculating set of the source zones, I in the common form as follows:

$$\ln I = C_1 + C_2 M + C_3 \ln R + C_4 R + \epsilon \quad [3-2]$$

$$\epsilon \approx N(0, \sigma_1^2) \quad [3-3]$$

Equation [3-2] and [3-3] can be modified into

$$P[I \geq i | m \text{ and } r] = \phi^* \left(\frac{\ln i - \ln I(m, r)}{\sigma_I} \right) \quad [3-4]$$

The source of these parameters for [3-2], [3-3] and [3-4] as follows:

R = distance measured to the earthquake rupture

C_1, C_2, C_3 and C_4 = earthquake rupture

σ_1^2 = constants, independent of M and R

ϕ^* = normal complementary cumulative distribution function

$\ln I(m,r)$ = value of $\ln I$ obtain from equation [3-2] and [3-3] by setting $\varepsilon = 0$

In equation [3-1], the distribution of magnitude is generally assumed to be doubly truncated exponential as follows:

$$f_M(m) = k_i(-\beta_i(m - M_{oi})), M_{oi} < m < M_{maxi} \quad [3-5]$$

Youngs and Coppersmith (1985) introduced the characteristics model as an alternative to the exponential magnitude distribution by the equation:

$$f_M(m) = k_i' \exp(-\beta(m - M_{oi})) \quad M_{oi} \leq m \leq M_{maxi}^{1/2} \quad [3-6]$$

$$f_M(m) = k_i' \exp(-\beta(M_{maxi} - 3/2) - M_{oi}) \quad M_{maxi}^{1/2} \leq m \leq M_{maxi} \quad [3-7]$$

The source of these parameters for [3-5], [3-6] and [3-7] as follows:

$k_i = (1 - \exp(\beta_i(m - M_{oi})))^{-1}$ = normalizing constant

k_i' = normalizing constant for [3-6] and [3-7] integrated to 1

M_{oi} = threshold magnitude, M_{maxi} = largest magnitude in the source

As for the distance, the distribution is obtained by the dimensions of the source and its distance and orientation relative to the site. The distribution of distance depends on the magnitude when the ruptured is assumed in the calculation of distance. Two aspects are being considered in the calculation of distance which is the finite dimensions of rupture and the dependence of rupture size on earthquake magnitude. The detail location (depth and horizontal) of earthquake rupture are assumed to be uniformly distributed. The rupture length can be calculated as follows:

$$\log_{10}(\text{rupture length}) = \log L_R = AL + BL + \delta \quad [3-8]$$

$$\delta \approx N(0, SIGL^2)$$

[3-9]

The source of these parameters for [3-8] and [3-9] as follows:

L_R = fault/rupture length, W_R = fault/rupture width

AL , BL and $SIGL$ = define the rupture length as a function of magnitude m according to [3-8] where the rupture length (horizontal) is measured in kilometers and σ has a standard deviation $SIGL$.

δ = the width of the characteristic portion for the characteristic magnitude model

The horizontal and vertical locations of the rupture are decoupled for a simpler calculation presentation. By adapting to this simple modification, the rupture length at a depth is different from L_R , where L_R represents measured rupture length at surface in the case whereby the rupture extends between two segments of a dipping fault. The differences are small due to the slight changes of strike of the fault between segments. In general the fault sources are characterized into three definitions for distance R as presented in Figure 3.15:

- R_0 = the shortest distance to the rupture
- R_1 = based on the shortest distance to the horizontal projection of the rupture
- R_2 = based on the shortest distance to the surface expression of the rupture

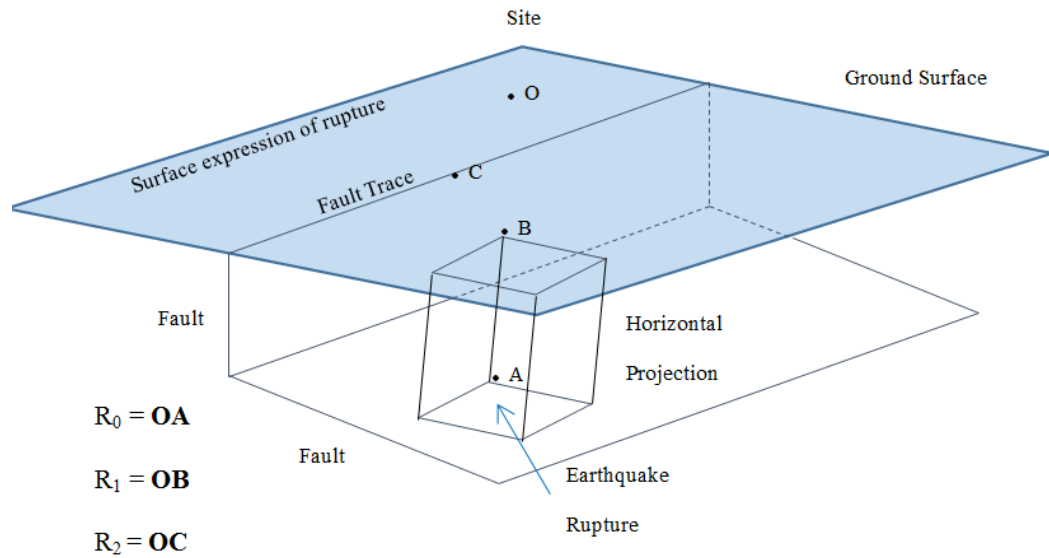


Figure 3.15: Fault source model

By modifying [3-1], a representative of seismic hazard sequence calculations for fault sources are as follow:

$$P[I \geq i] = \int f_M(m) \int f_{LR}(1) \int P[I \geq i : m, r]. f_{R;M,LR}(r, m, l) dr. dl. dm \quad [3-10]$$

Gutenberg and Richter (1956), introduced a linear relationship between earthquake magnitudes and the frequency at which they occur at a particular site namely the frequency distribution equation (FMD) as follows;

$$\log_{10} N(M) = a - b M \quad [3-11]$$

The source of these parameters for [3-11] as follows:

$N(M)$ = number of events greater than or equal to magnitude M , M = earthquake magnitude, b = slope which related the log of the frequency to the event magnitude, a = constant characteristics of the source area examined.

Another aspect in the analysis are relationship between the annual total probability of earthquakes with the intensity, $I \geq i$ at a particular site (Baker & Jayaram, 2008). The probability of each source is summed as follows;

$$N_A = \sum_{i=1}^N N_1(M \geq m_0)_1 > P [I \geq i] \quad [3-12]$$

The source of these parameters for [3-12] as follows:

N_A = total annual earthquake occurrence with intensity $I \geq i$ from all sources, $P[I \geq i]$ = the risk of single event with intensity $I > I$ for one seismic source, $N_1 [M \geq m_0]$ = the annual earthquake occurrence with magnitude $M > m$ for one source zone

The uncertainties in model parameters are cater by applying the logic tree approach and using multiple attenuation equations in highlighting the uncertainty in the ground motion calculations. The logic tree (Kulkarni et al., 1984; Youngs & Coppersmith, 1985) are introduced in study to allow uncertainty in selection of models for recurrence models, recurrence rates, attenuation functions and minimum magnitudes. Figure 3.16 and Figure 3.17 presents the logic tree used in analysis for Megathrust and Benioff respectively. The logic tree features various weights assigned to recurrence models and attenuation equations.

Recurrence/Subduction Model			Magnitude Uncertainty		Attenuation Function	
Interface Trace		Kijiko and Sellevol (1989)				
		0.33				
		Weichert (1980)				
		0.33				
		Least Square				
		0.33				
			Mmax + 0.20			
			Max		Young et al., (1997)	
					0.5	
			Mmax - 0.20		Atkinson and Boore (2003)	
					0.5	

Figure 3.16: Logic Tree used in the analysis (Megathrust)

$$\gamma(f) = 1.178f^{-0.93} \quad [3-14]$$

The source of these parameters for [3-13] and [3-14] as follows:

$f_j(t)$ = set of adjustment functions

t_j = time of the peak response of the j^{th} oscillator under the action of the j^{th} wavelet

ω'_j = frequency

γ_j = frequency dependent coefficient used to adjust the duration of the adjustment function

Δt_j = difference between the time of peak response t_j and the reference origin of the wavelet

The selection of initial time series for SMP are based on earthquake magnitude, style-of-faulting, directivity condition, site condition, peak ground acceleration, hypocentral distance and earthquake mechanism. The earthquake records for study are selected based on the de-aggregation hazard result from PSHA for each state. The magnitude ranges 6.5M to 9M with distance of 152 km to 520 km. The Pacific Earthquake Engineering Research Center (PEER) and the Consortium of Organizations for Strong-Motion Observation Systems (COSMOS) provide various recording of ground motion. Table 3.4 presents the properties of the selected records for SMP of the study.

Table 3.5: Properties of selected earthquake records for SMP of study

Earthquake	Date	Station	M _w	Latitude	Longitude	Depth (km)	Site Condition
Kobe, Japan	1995	Tottori, Shin-Osaka, Osaka, Okayama, Mzh, Hikari, Fukuyama,	6.9	34.5948	135.0121	18	Rock
Victoria, Mexico	1980	Chihuahua	6.4	32.1850	-115.0760	11	Rock
Imperial Valley, California	1995	Compuertas	6.5	32.6435	-115.3088	10	Rock
Kuril Islands, Japan	2013	Betsukai	7.2	46.2210	150.7880	110	Rock
Auckland Islands, New Zealand	2007	Dunedin Kings High School	7.4	-49.2710	164.1150	10	Rock
SW Haast, New Zealand	1925	Westport	5.7	-43.9400	169.0100	55	Rock

3.3.3 Site Response Analysis (SRA)

The simulation of wave propagation from the bedrock to the surface in study is analyzed by using one-dimensional (1-D) site response analysis based on nonlinear approach (Bardet & Tobita, 2001). An assumption is being made whereby the shear wave's propagates vertically in 1-D layered system. Each layer is assumed to be in similar soil properties throughout the horizontal direction, infinite horizontal distance and restricted only to horizontal motion from bedrock. The 1-D layered soil deposit system and its spatial discretization is illustrated in Figure 3.18. General terms in the analysis are illustrated in Figure 3.19. The term free surface motion means the motion at the surface of soil layer whereas the bedrock motion is the motion at the base of the soil layer. Another term is the rock outcropping motion which define motion at where the

bedrock is exposed on the surface level. The main equation and algorithm in relation to Figure 3.18 and Figure 3.19 is as follows:

$$\rho \frac{\delta^2 d}{\delta t^2} + \eta \frac{\delta d}{\delta t} = \frac{\delta \tau}{\delta z} \quad [3-15]$$

$$\tau = 0 \text{ at } z = 0 \text{ and } \tau = \tau_B \text{ at } z = H \quad [3-16]$$

The step by step algorithm start with the initialization for each layer is as follows:

$$n = 1, v_{i,n} = 0, a_{i,n} = 0, d_{i,n} = 0, \tau_{i,n} = 0, \gamma_{i,n} = 0, i = 1, \dots, N \text{ and } V_{I,0} = 0, a_{I,0} = 0$$

Next step is to calculate the strain, strain increment and stress (i=1, ..., N-1)

$$\gamma_{i,n} = \frac{d_{i+1,n} - d_{i,n}}{\Delta z_i} \quad [3-17]$$

$$\Delta \gamma_{i,n} = \gamma_{i,n} - \gamma_{i,n-1} \quad [3-18]$$

$$\tau_{i,n} = IM(\tau_{i,n-1}, \Delta \gamma_{i,n}) \quad [3-19]$$

The velocity input from prescribed acceleration $a_{I,n}$ and predicted velocity as follows:

$$V_{I,n} = V_{I,n-1} + 1/2 (a_{I,n} + a_{I,n-1}) \Delta t \quad [3-20]$$

At node N (bottom)

$$v_{N,n+1} = \frac{v_{N,n}(\Delta z_{N-1} - v_s \Delta t) + 4v_s V_{I,n} \Delta t - 2\tau_{N-1,n} \frac{\Delta t}{\rho_N}}{\Delta z_{N-1} - v_s \Delta t} \quad [3-21]$$

At node $i = 2, \dots, N-1$

$$v_{i,n+1} = v_{i,n} + 2 \frac{\tau_{i,n} - \tau_{i-1,n} \Delta t}{\Delta z_i + \Delta z_{i-1} \rho_N} \quad [3-22]$$

At node 1 (surface)

$$v_{1,n+1} = v_{1,n} + 2 \frac{\tau_{1,n} \Delta t}{\Delta z_1 \rho_N} \quad [3-23]$$

Next is to calculate the displacement, velocity and acceleration ($i=1, \dots, N$)

$$d_{i,n+1} = d_{i,n} + v_{i,n+1} \Delta t \quad [3-24]$$

$$v_{i,n} = 1/2 (v_{i,n+1} + v_{i,n}) \quad [3-25]$$

$$a_{i,n} = 1/\Delta t (v_{i,n+1} - v_{i,n}) \quad [3-26]$$

Finally for the next $n, n+1$, the step is repeated from [3-17] to [3-26] again

The source of these parameters for [3-15] and [3-26] as follows:

ρ = unit mass of soil, d = horizontal displacement, z = depth, t = time, τ = shear stress, η = mass-proportional damping coefficient

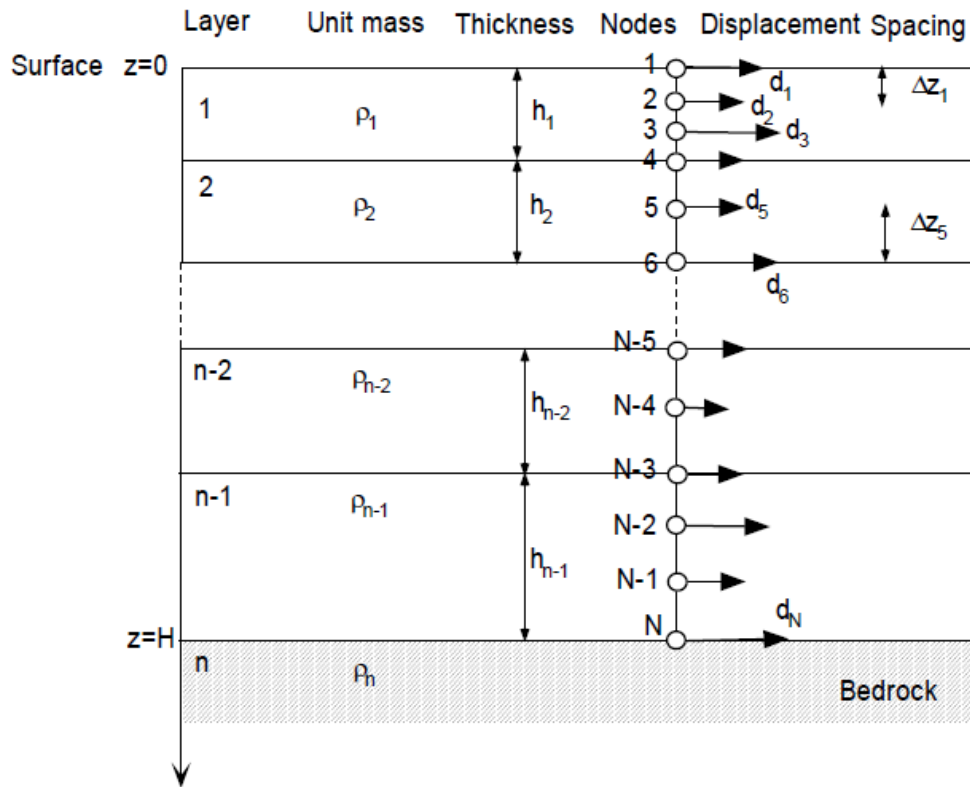


Figure 3.18: 1-D layered soil deposit system (Bardet & Tobita, 2001)

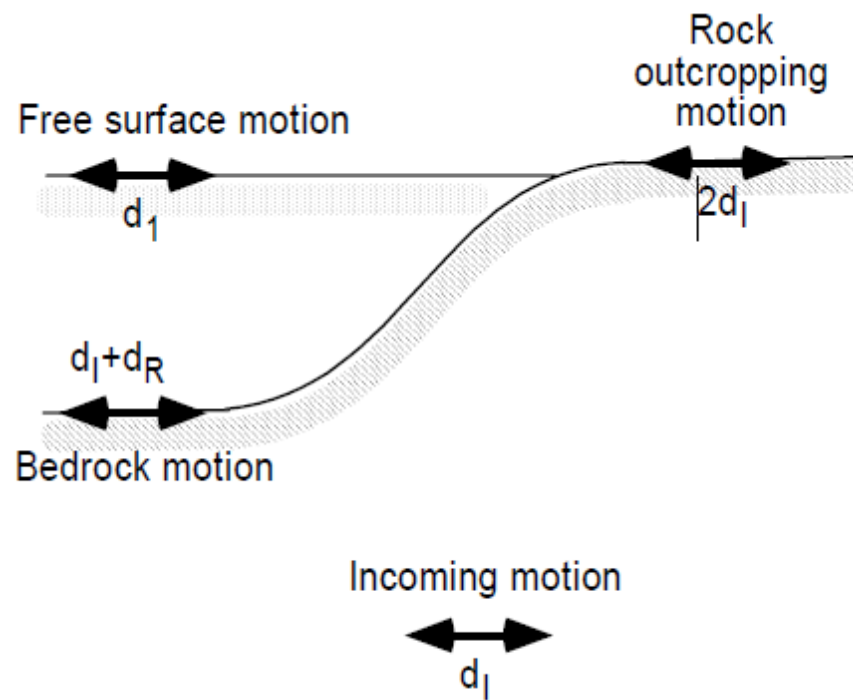


Figure 3.19: General terminology in SRA (Bardet & Tobita, 2001)

3.4 Liquefaction Hazard Mapping

Figure 3.20 presents the simple methodology presentation in the form of flowchart which is adapted in this study. A total of 10 significant steps are selected for the main soil liquefaction analysis. Each of the parameters involved and development of formulation in the analysis is discussed in detail in this chapter.

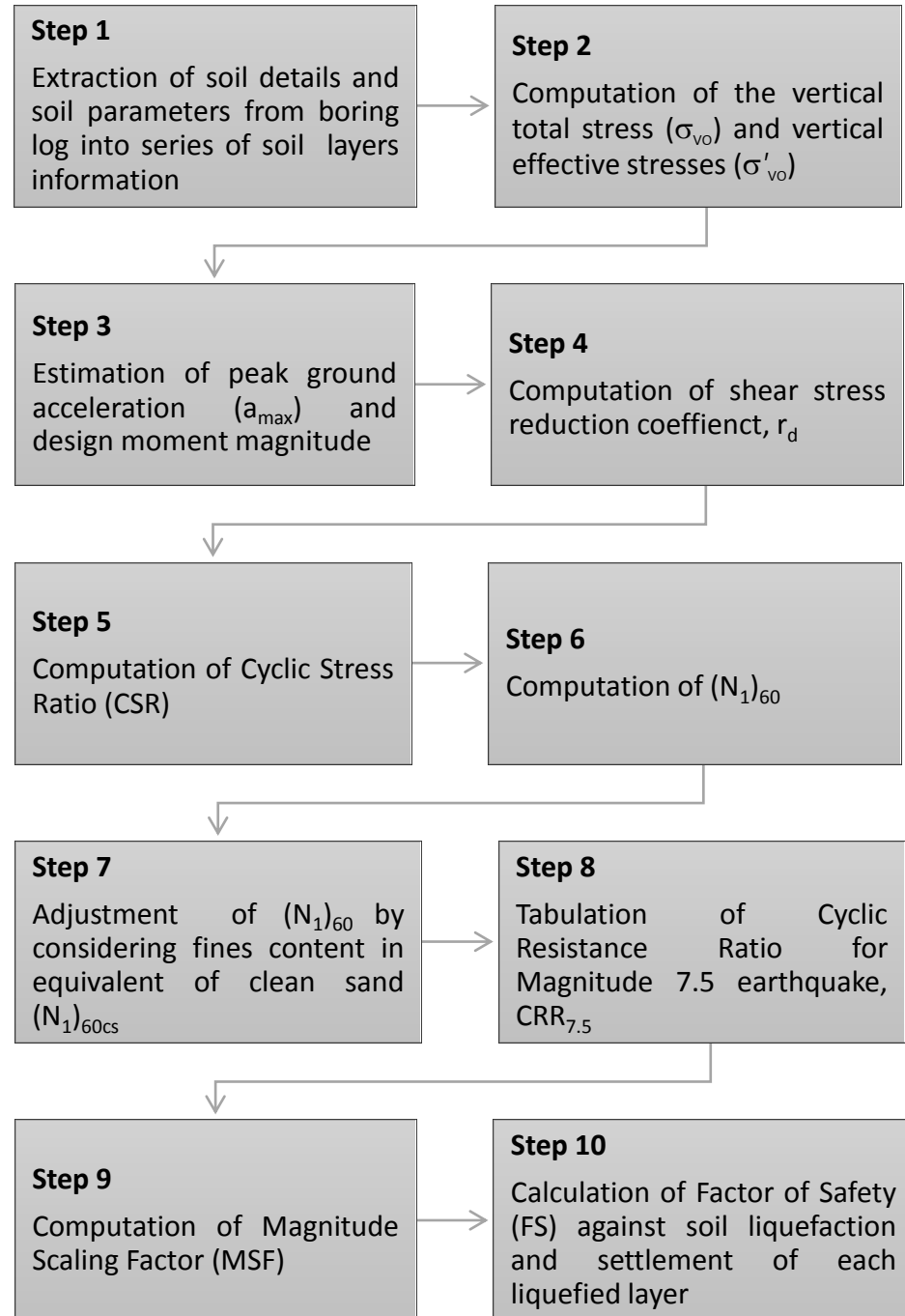


Figure 3.20: SPT-Based empirical method (Seed & Idriss, 1971) adapted in study

Soil liquefaction and its effects can be defined using state of the art (SOA) and state of practice (SOP) method. The SOA discussed earlier is mainly produce from laboratory measurements and correlations of basic soil parameters resulting in a very big amount of data, a number of significant models, information on mechanism behind soil liquefaction and a simulation of ground shaking by intense cyclic loading. In SOA, the sand properties obtained from laboratory measurements are correlated to void ratio or relative density. In contrast, the SOP are developed based on earthquake case histories using empirical indicator which is based on field charts and correlations produced from field measurement test. The common field measurement tests are from penetration resistance, SPT or CPT. There are also literatures reporting field measurements based on shear wave velocity but the literature discussion is mainly focusing on SPT. In this section the theory behind SOP is presented and discussed in meeting the output that will be developed for this study on liquefaction hazard assessment.

3.4.1 Simplified Procedure by Seed and Idriss

The evaluation of soil liquefaction resistance of soil deposits has been developed throughout the years with many approaches being consistently being introduced and revised. Since the first soil liquefaction incident occurred in which motivates researches and engineers studying the causes and factors contribute to this natural disaster result in quantifying the parameters from earthquake loading and soil resistance. An evaluation procedure based on field SPT measurement originally developed by Seed and Idriss (1971) commonly known as Simplified Procedure becomes the standard of practice in North America and in many other countries. The charts in this procedure are developed by using standard penetration resistance of the sand and vertical overburden pressure of each blowcount, $(N1)_{60}$. The $(N1)_{60}$ is originally refering to $N1$ in Seed (1976) .The data are then calibrated with actual case histories during ground tremors. The procedure is revised, modified, improved and updated prior to recent case histories specifically on

soil liquefaction. The early version of the chart is presented in Figure 3.21. The chart is later modified in a workshop (Youd & Idriss, 2001) and is presented in Figure 3.22. The magnitude of earthquake in which the chart is developed is 7.5 and need to further modified in analysis which will be discussed in the next heading.

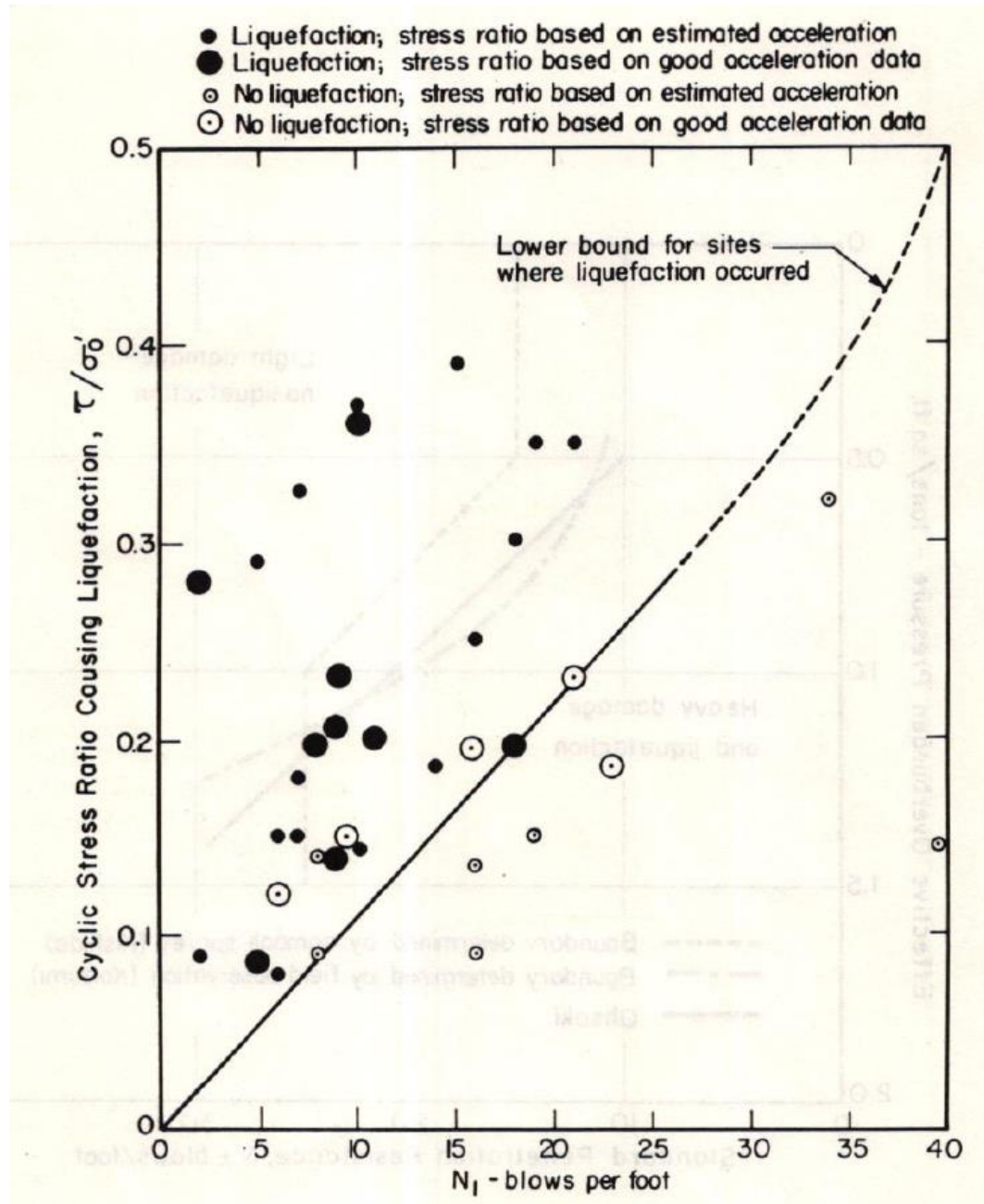


Figure 3.21: Early liquefaction chart by (Seed, 1976)

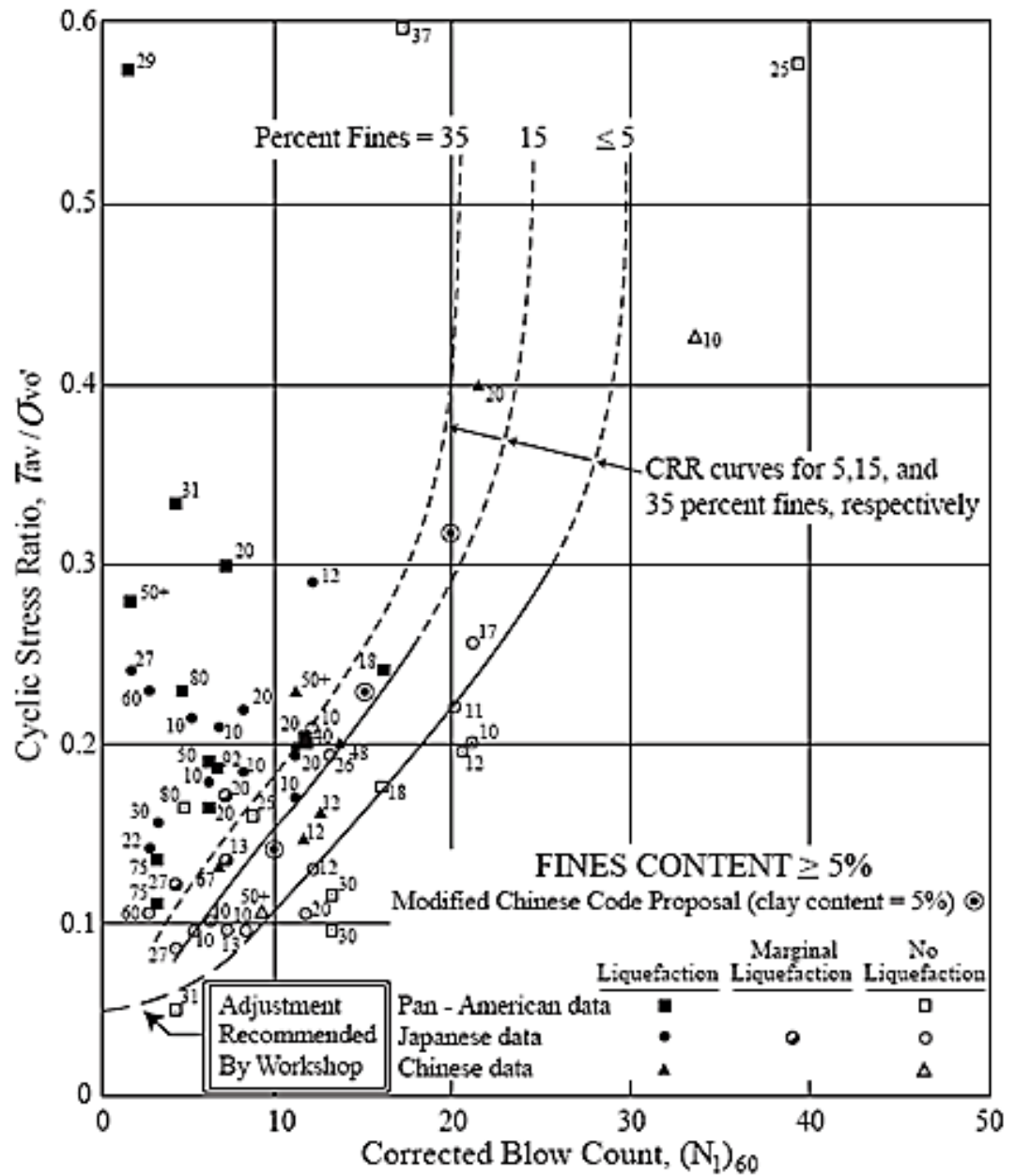


Figure 3.22: Revised liquefaction chart by Youd and Idriss (2001)

Similar charts are also developed from other field measurement such as the CPT and shear wave velocity which uses the same background approach and share the same properties. During earthquakes occurrence these charts have indicate good correlation which makes it a good prediction tool for soil liquefaction study. Prior to the findings Idriss and Boulanger (2008) and Youd and Idriss (2001) have defined seismic

liquefaction evaluation on saturated sand sites. Figure 3.23 presents sketch of common approach in Seed and Idriss Simplified Procedure which produced the deterministic chart in Figure 3.21 and Figure 3.22. The features from the chart is summarized as follows:

1. The chart is related to an earthquake case of moment magnitude, $M_w = 7.5$. A conversion factor is needed in corresponding to other magnitudes through Magnitude Scalling Factor (MSF).
2. The chart contains Cyclic Resistance Ratio (CRR) curve versus a normalized soil liquefaction resistance parameter which separates liquefaction zones and non-liquefaction zones. CRR introduced in the procedure represent limiting conditions to liquefaction occurrence.
3. Data points were plotted from calculation of Cyclis Stress Ratio (CSR) based on actual soil liquefaction cases and the CRR curve is adjusted accordingly to cover the data points.
4. For future liquefaction evaluation, CSR is first calculated using design earthquake parameters. Then, new points are plotted in the chart. In general, data points which is plotted above the CRR curve, liquefaction is predicted, whereas if the data points is plotted below, the site is safe from liquefaction. Hence, CSR represents the earthquake loading and CRR is the soil resistance against earthquake loading. Thus when $CSR > CRR$, soil liquefaction is likely to occur.

The main equation of the procedure is the calculation of CSR regardless of whether it is historic or future assessment of site.

$$CSR = \frac{\tau_c}{\sigma'_{vo}} = \frac{0.65\tau_{max}}{\sigma'_{vo}} = \frac{0.65a_{max} \sigma_{vo} r_d}{(g) \sigma'_{vo}} \quad [3-27]$$

The source of these measurements for [3-27] as follows:

a_{max} = maximum horizontal acceleration at the ground surface, τ_{max} = maximum horizontal shear stress in the liquefiable layer, σ_{vo} = total vertical normal stress before the earthquake, σ'_{vo} = effective vertical normal stress before the earthquake, r_d = stress reduction coefficient ($r_d = 1$ at surface and $r_d < 1$ below ground surface or can be obtained from Figure 3.24)

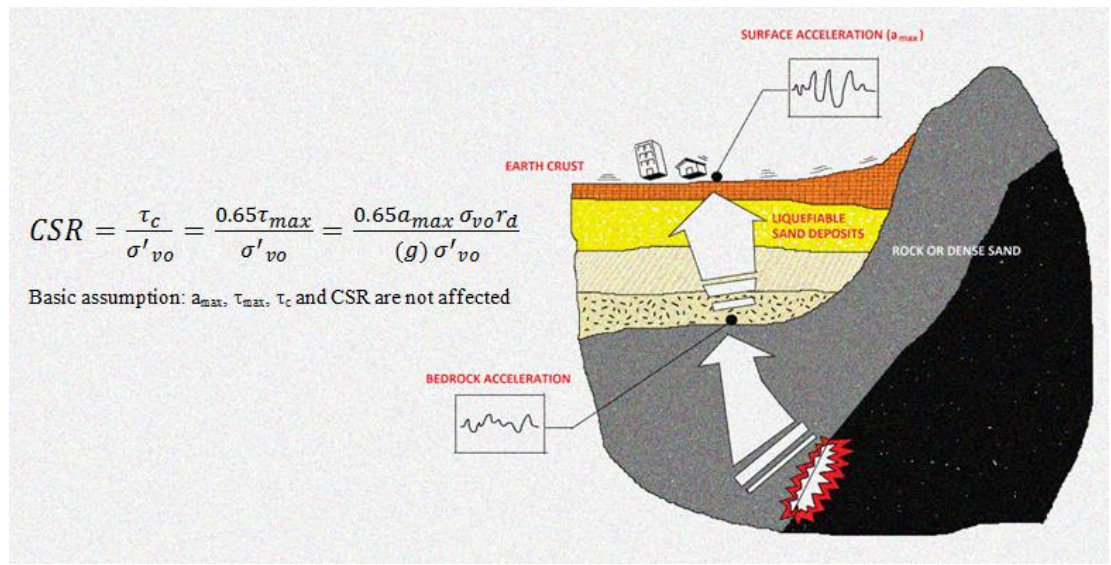


Figure 3.23: Sketch of common approach in Simplified Procedure

The factor 0.65 have been introduced in the beginning of the liquefaction study as an indicator of comparative approach between the field assessment study associated with unique time histories and laboratory measurements which in general uses uniform stress cycles. Hence, the unique time history generated by actual earthquake acting in the soil layers are represented by an equivalent number of cycles related to M_w of uniform stress acceleration. By looking back at [3-27], $\tau_c \approx 0.65 \tau_{max} \approx (0.65 a_{max}/g) \sigma_{vo} r_d$. The introduction of τ_c in [3-27] does not contribute to the development of the chart but only to relate to the laboratory measurements associated with uniform stress cycles.

Theoretical assumptions in developing [3-27] is that, a_{\max} and τ_{\max} is not related to pore pressure buildup during ground motion unlike the SOA method in laboratory in which stresses on the matter in particular. In general the parameter mentioned are generated based on actual earthquake loading mainly consisted of widely unique cycles represented by acceleration and various stresses.

The characterization of earthquake loading in liquefaction analysis can be determine by either a detailed ground response analysis or the simplified procedure. Figure 3.25 presents the equivalent cycles versus earthquake magnitude. Based on this chart τ_c can be evaluated directly. Another approach of evaluating the earthquake loading is by computing r_d and a_{\max} . Figure 3.24 presents the stress reduction factor versus depth.

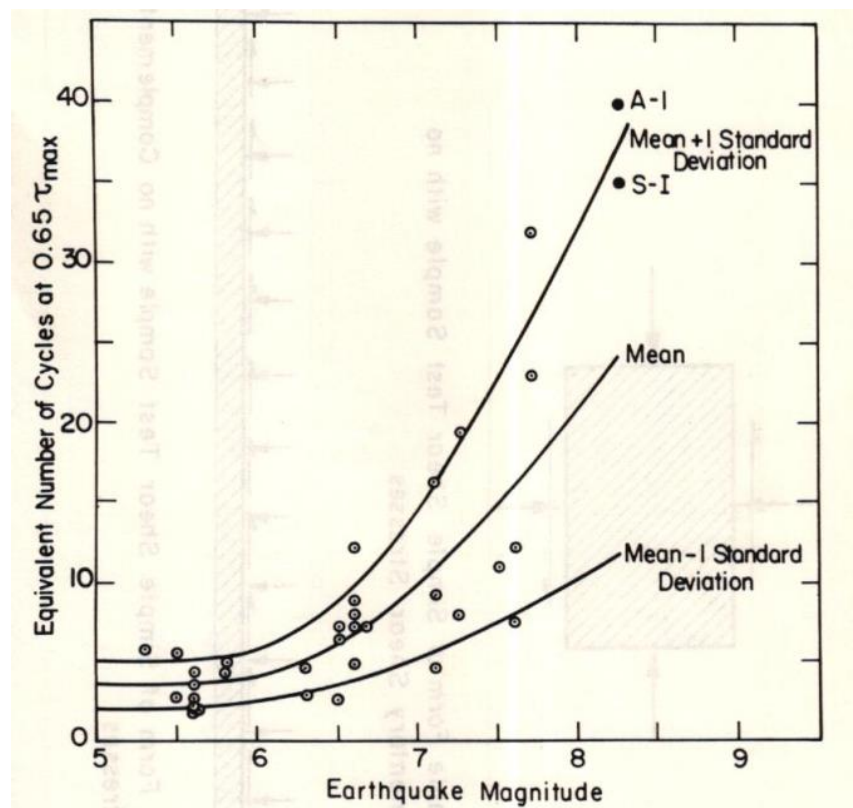


Figure 3.24: Equivalent cycles versus earthquake magnitude (Seed, 1976)

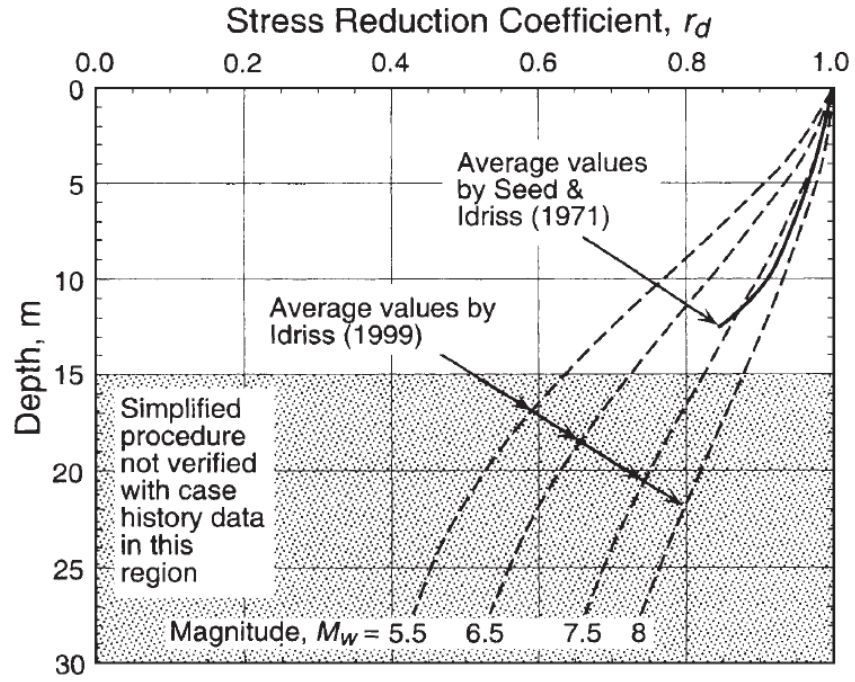


Figure 3.25: Stress reduction factor versus depth (Andrus & Stokoe II, 2000)

3.4.2 Soil Strength Measurement from SPT

A term which is suitable to describe the CRR mentioned in the previous chapter is the soil strength. According to Blake (1997) the CRR can be determined using the formula as follows:

$$CRR_{7.5} = \frac{a + cx + ex^2 + gx^3}{1 + bx + dx^2 + fx^3 + hx^4} \quad [3-28]$$

The source of these measurements for [3-28] as follows:

$$x = (N_1)60f, a = 0.048, b = -0.1248, c = -0.004721, d = 0.009578, e = 0.0006136, f = -0.0003285, g = -1.673 \times 10^{-5}, h = 3.714 \times 10^{-6}$$

As noted previously, the chart in Figure 3.20 was developed in accordance to earthquake magnitude 7.5. In order to address other magnitudes in analysis, MSF is

introduced in soil liquefaction analysis (Figure 3.26). The CRR obtained from standard chart designed for 7.5 magnitude of earthquake needs to be multiplied with MSF.

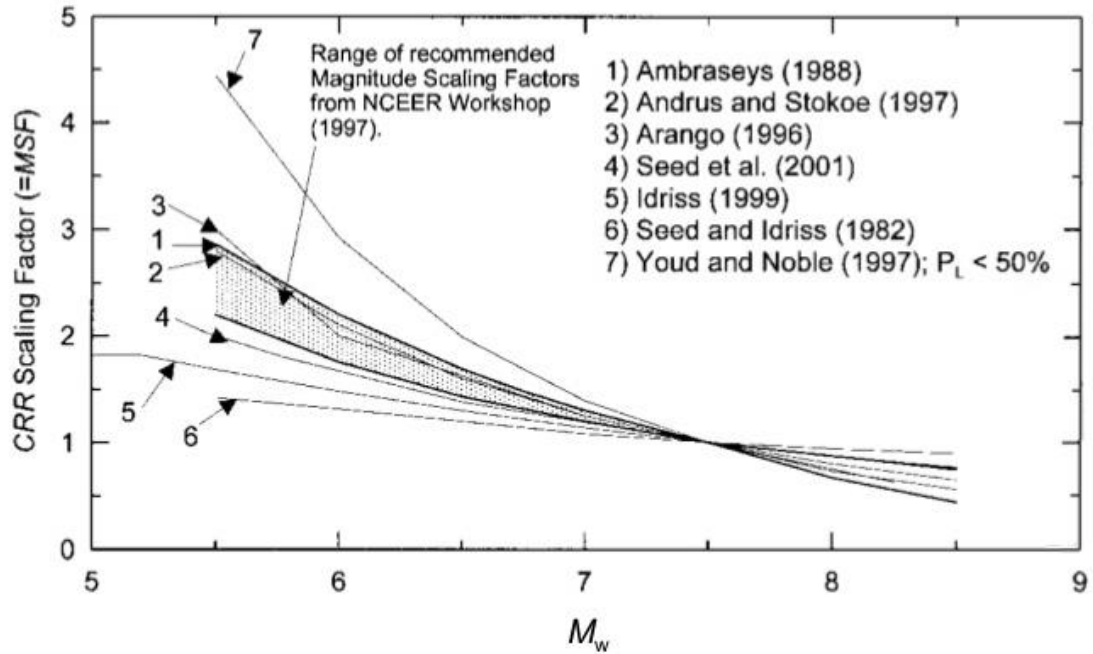


Figure 3.26: Magnitude Scaling Factor versus magnitude

The magnitude correction of CRR discussed in Robertson and Fear (1997) is given as

$$CRR_M = CRR_{7.5} \times MSF \quad [3-29]$$

The source of these measurements for [3-29] as follows:

CRR_{7.5} = Based on earthquake of magnitude 7.5, CRR_M = magnitude corrected CRR_v for a given magnitude, MSF = Magnitude scaling factor

Further discussion on result obtained from field measurement, SPT is on the number of blow counts. A correction introduced by (Soils et al., 1997) is adapted in

normalizing the blow count to an effective overburden pressure of 100 kPa. Correction factors in Table 3.5 are applied on raw data accordingly to obtain equation as follows:

$$N_{(1)60} = N_m \times C_n \times C_e \times C_b \times C_r \times C_s \quad [3-30]$$

The source of these measurements for [3-30] as follows:

N_m = number of blow counts from SPT raw data measured from field test, C_n = depth correction factor, C_e = hammer energy ratio (ER) correction factor, C_b = borehole diameter correction factor, C_r = rod length correction factor, C_s = Correction factor for samplers with or without liners

Table 3.6: Field test SPT-N corrections (Soils et al., 1997)

Term	Factor	Equipment Variable	Correction
C_n	Overburden pressure	-	$C_n = \sqrt{\left(\frac{1}{\sigma'_o}\right)}$
C_e	Energy ratio	Safety Hammer Donut Hammer Automatic Trip Hammer	$0.6 \leq C_e \leq 1.17$ $0.45 \leq C_e \leq 1.00$ $0.9 \leq C_e \leq 1.6$
C_b	Borehole diameter	$65 \text{ mm} \leq \phi \leq 115 \text{ mm.}$ $\phi = 150 \text{ mm}$ $\phi = 200 \text{ mm}$	1.00 1.05 1.15
C_r	Rod length	$3 \text{ m} \leq C_r \leq 4 \text{ m}$ $4 \text{ m} \leq C_r \leq 6 \text{ m}$ $6 \text{ m} \leq C_r \leq 10 \text{ m}$ $10 \text{ m} \leq C_r \leq 30 \text{ m}$ $C_r > 30 \text{ m}$	0.75 0.85 0.95 1.00 < 1.00
C_s	Sampling method	Standard sampler Sampler without liners	1.00 1.20

The overburden stress correction factor presented in Table 3.5 is given by:

$$C_n = \sqrt{\left(\frac{1}{\sigma'_{o'}}\right)} \quad [3-31]$$

The correction factor for the effective overburden pressure, C_n , is introduced by (Seed et al., 1983) in which the curves are valid for depths greater than 3 meters (approximately 50 kPa). A limitation to depth lower than 3 meter and limited to 2 meters in another similar concept, introduced by Liao and Whitman (1986). Curves by both findings are presented in Figure 3.27 and Figure 3.28. C_n by Liao and Whitman (1986) is indicated by:

$$C_n = 9.79 \sqrt{\left(\frac{1}{\sigma'_{o'}}\right)} \quad [3-32]$$

The source of these measurements for [3-31], [3-32] as follows:

$\sigma'_{o'}$ = the effective vertical overburden stress in kPa

The CRR developed by Youd and Idriss (2001) are based on clean sand. Adjustment to the number of blow count however is needed to cater for fines content which in the field measurement consists of silt and clay deposits. In practice, soil which contains fines are more liquefaction resistant compared to a clean sand. Hence the number of blow count from field measurement should be adjusted to the fine content in which increases its liquefaction resistance. Thus Soils et al. (1997) have developed fines content correction as follows:

$$N_{(1)60f} = \alpha + \beta N_{(1)60} \quad [3-33]$$

The source of these measurements for [3-33] as follows:

$$\alpha = 0; \beta = 1.0 \quad \text{for FC} \leq 5\%$$

$$\alpha = \exp [1.76 - (190/FC^2)] ; \beta = 0.99 + FC^{1.5}/1000 \quad \text{for } 5 \leq FC \leq 35\%$$

$$\alpha = 5.0; \beta = 1.2 \quad \text{for } FC \geq 35\%$$

$(N_1)_{60f}$ = corrected blow count, FC = fines content in %

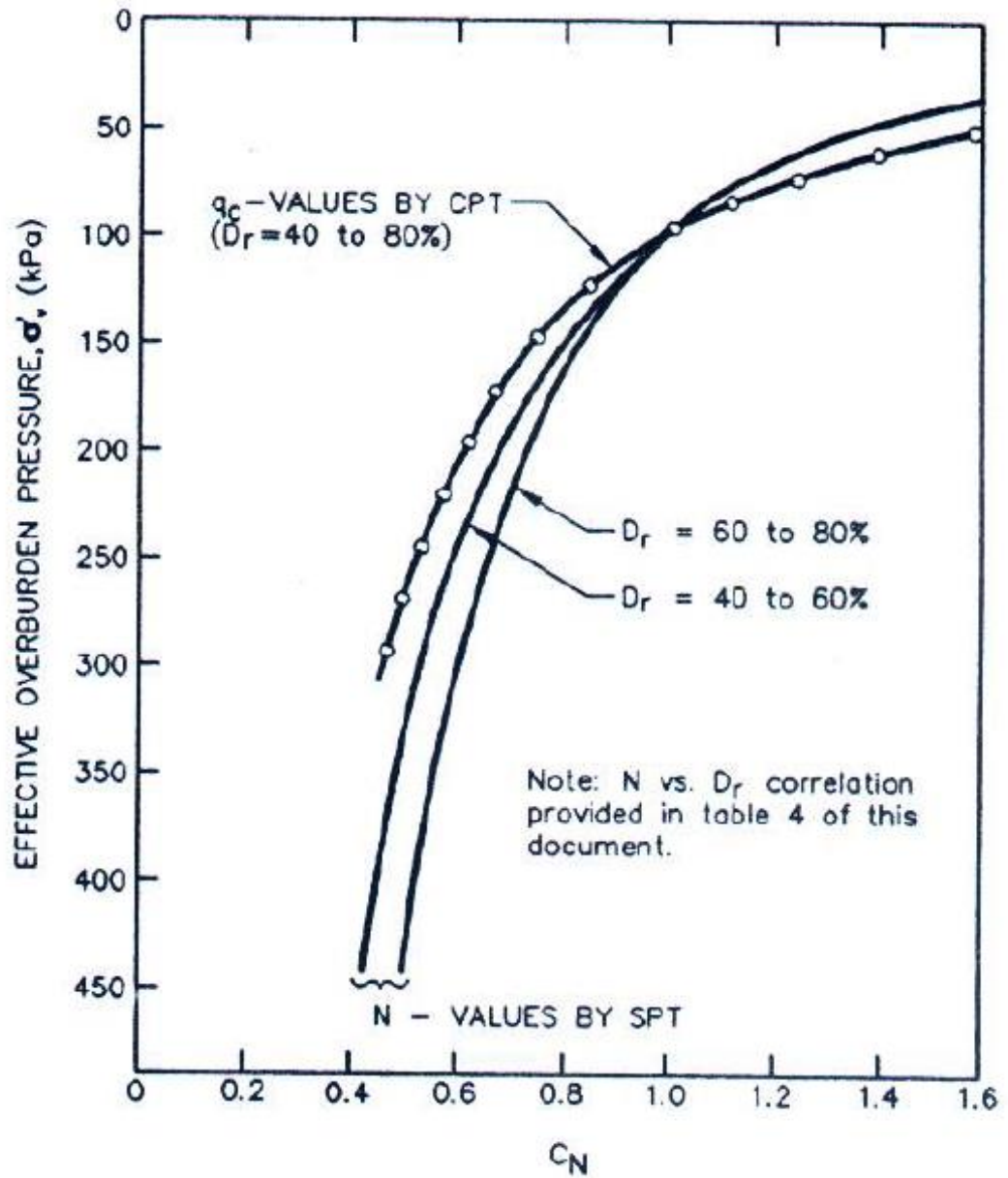


Figure 3.27: Correction factor σ'_v (Seed et al., 1983)

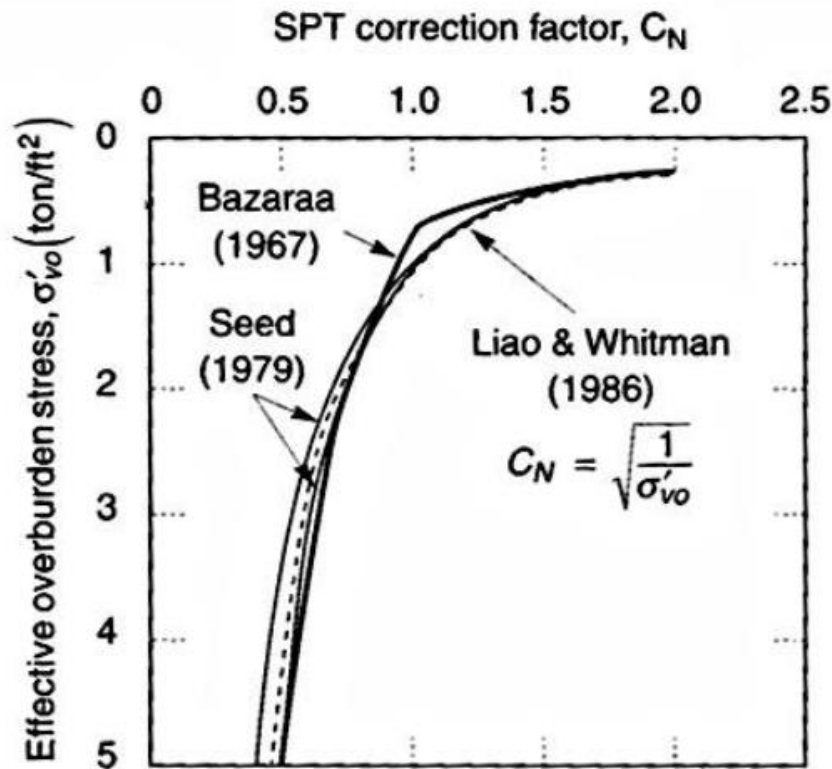


Figure 3.28: Correction factor for σ'_o (Liao & Whitman, 1986)

3.4.3 Soil Liquefaction Method Adapted in Study

The simplified techniques based on SPT are commonly used to evaluate seismic liquefaction potential. Many of the methods mentioned are developed from the liquefaction boundary using liquefaction cases. Each approach varies with each other in the aspect of calculation types, updated records of liquefaction cases, coefficients and properties introduced. In order to choose the best method and address liquefaction hazard in this study, a typical borehole from the database is presented in Figure 3.29. SI report in Kelantan has been selected since the data indicate the most vulnerable setting in the sense of liquefaction susceptibility. The sand layer reach up to 20 meter and the water table location is near surface level. In addition the size grain distribution is well graded and present very small amount of fines content in the first upper layer.

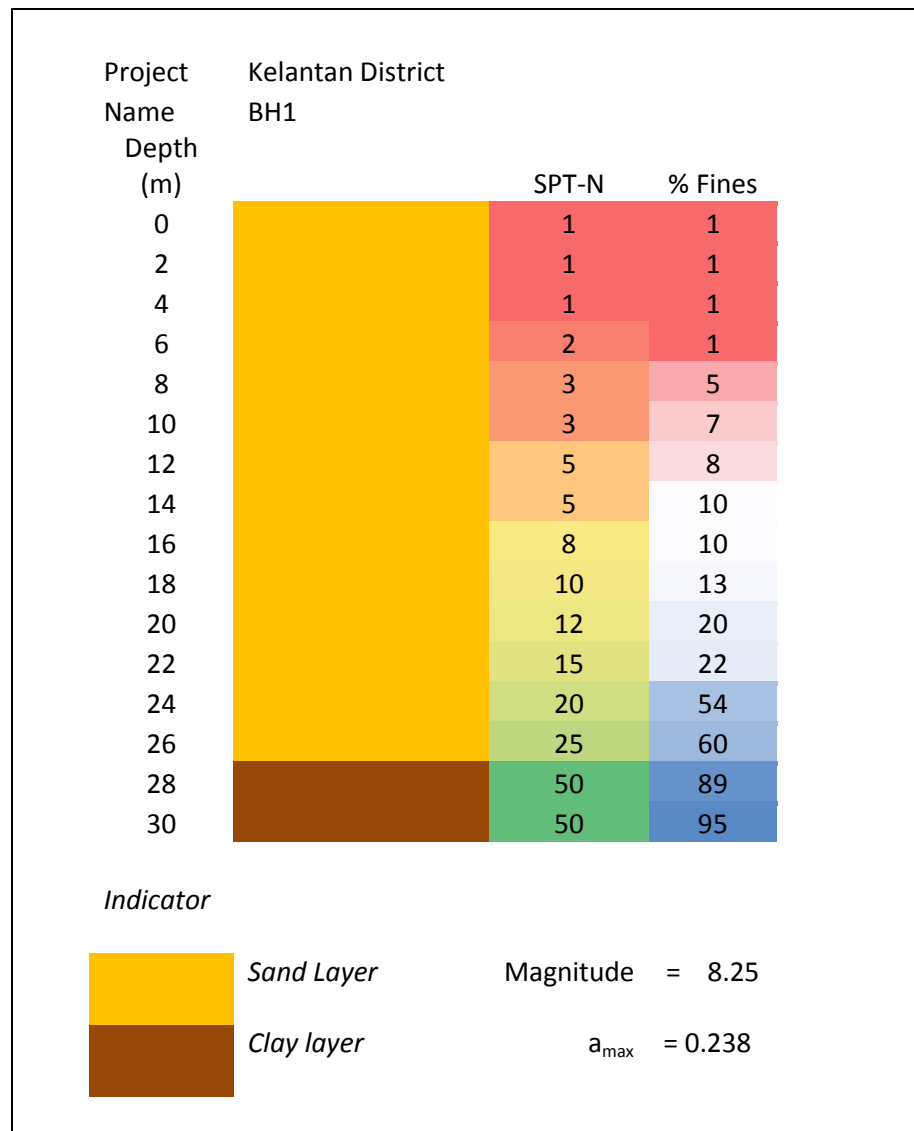


Figure 3.29: Typical borehole information in Kelantan district

The available methodology are NCEER Workshop 1997, Boulanger and Idriss 2004, Vancouver Task Force 2007, Cetin 2004, Seed 1983, Japanese Highway Bridge Code, Tokimatsu & Yoshimi 1983, Shibata 1981 and Kokusho 1983. As mentioned in the previous section, liquefaction procedure was originally developed by Harry Bolton Seed and Izzat M. Idriss using SPT-N blow counts related with a parameter representing the seismic loading of the soil, commonly termed as CSR. The CSR is compared to CRR of the soil. If the CSR exceeds CRR, the soil is likely to liquefy. The overburden stress correction factor is applied in Vancouver Task Force 2007, NCEER Workshop 1997,

Cetin 2004 and Idriss and Boulanger 2004. The particle diameter corresponding to 50 percent passing, D₅₀ in sieve analysis curve is introduced in Japanese Bridge Code.

Figure 3.30 presents the CRR_{7.5} results evaluated from available liquefaction assessment methodology. It is found that the result evaluated from all method follows a similar pattern except for Cetin 2004 method. Figure 3.31 presents the factor of safety against liquefaction using different approach. Similar findings with Figure 3.30 are obtained which clearly shows significant pattern in Cetin 2004 method.

Cetin 2004 and Seed 1983 used 201 case histories in the development of the procedures. According to Youd and Provo (2011), Idriss and Boulanger 2004 re-evaluates the Cetin 2004 and Seed 1983, using 160 case histories, introduced new datasets of 70 case histories outside Japan and deleting 40 case histories mainly from Japan. In total Idriss and Boulanger 2004 used 230 data sets consisted of highest quality field performance cases in the development of the method. Hence Idriss and Boulanger 2004 are chosen as liquefaction method in this study.

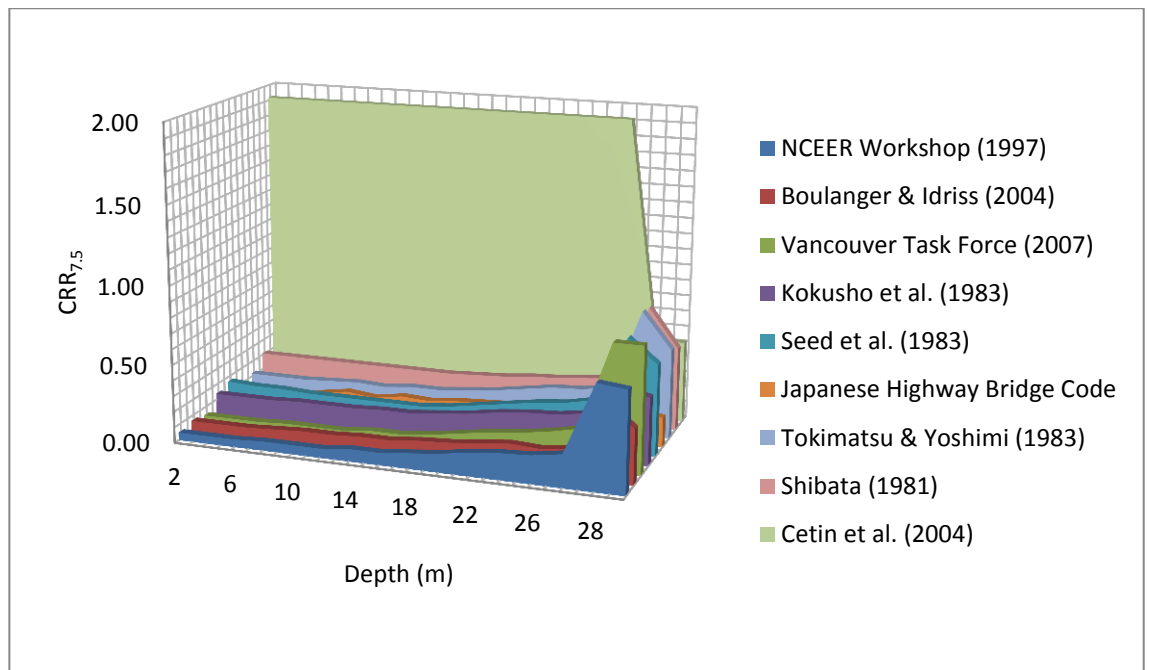


Figure 3.30: CRR_{7.5} using different approach

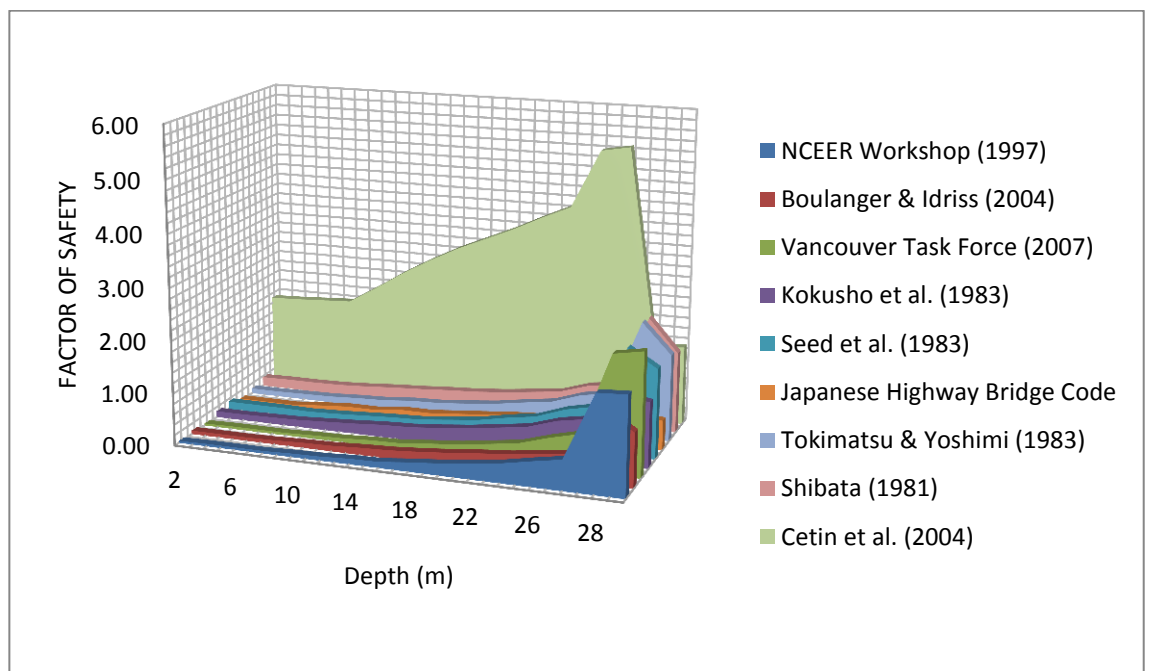


Figure 3.31: Factor of safety using different approach

3.4.4 Liquefaction Factor of Safety

The factor of safety against liquefaction, FS is the ultimate result of the liquefaction analysis and is estimated as:

$$FS = \frac{CRR}{CSR} \quad [3-34]$$

The source of these measurements for [3-34] as follows:

CRR = cyclic resistance ratio

CSR = cyclic stress ratio

FS \geq 1, there is no potential of liquefaction; If FS < 1, there is potential in liquefaction

3.4.5 Addressing Liquefaction Severity

The FS alone however does not provide sufficient indicator and parameter for evaluation of liquefaction and its damage potential at site inclusive of thickness and depth of the liquefiable layer and the FS respectively. Hence a method proposed by Iwasaki et al. (1978) namely liquefaction potential index (LPI) is adapted in study due to the inclusion of the 3 parameters mentioned as an input to summarize a site severity and is a widely used tool in liquefaction studies conducted by many researchers (Chung et al., 2014). The LPI discussed in Iwasaki et al. (1978) and Iwasaki et al. (1982) was developed in addressing foundation damage associated with liquefaction. A significant assumption of this method is that the severity of liquefaction is proportional to the thickness of liquefied soil layer, approximate depth of layer from surface and zones of which the factor of safety is less than 1. The first 20 m depth is considered to be crucial

for analysis compared to deeper depth than 20 m which cause only minor damage to surface structure. LPI is defined as

$$LPI = \int_0^{20} F(w)z dz \quad [3-35]$$

where z denotes the depth to the soil stratum and w is the depth weighting factor

For $FS < 1$; $F = 1 - FS$, For $FS \geq 1$ for $F = 0$

For $z < 20$ m, $w(z) = 10 - 0.5 z$

For $z > 20$ m, $w(z) = 0$

The liquefaction hazard is categorized using the LPI values; VERY LOW for $LPI = 0$, LOW for $0 < LPI \leq 5$, HIGH for $5 < LPI \leq 15$ and VERY HIGH for $LPI > 15$.

CHAPTER 4: RESULTS AND DISCUSSIONS

This section includes 6 main findings as presented in Table 1.2 in Chapter 1.

4.1 Soil Liquefaction Screening

4.1.1 Perlis

Relative to the size of its population, Perlis is the most diminutive state observed in the Peninsular Malaysia regional map. Perlis covers approximately 819.31 km² land area with only 20 km coastal line stretching from the northern part of the west coast of Peninsular Malaysia. The state is bordered by Satun and Songkla provinces of Thailand on the northern border and Kedah state on the south. At the present time, Kuala Perlis which overlies the coastal areas is a maritime center. A jetty located near the river mouth of Perlis river offers ferry service to Langkawi Island. Figure 4.1 presents the Kuala Perlis beach front where the jetty to Langkawi Island is located. A significant development in the soil liquefaction context observed in Kuala Perlis is its coastal road (Jalan Persisir Pantai) which connects Kuala Perlis and Kuala Sanglang approximately 18.5 km. Apart from that, development are observed at the mouth of the river with variety of building, services and fundamental facilities.



Figure 4.1: Kuala Perlis beach front

A map of Perlis state is presented in Figure 4.2. Observation being made on the 1- 2 kilometers northern shoreline areas presents concentration of abundant muddy sediments on the surface layer with a series of asymmetrical ridges running parallel to the coast and separated by shallow runnels approximately 100-200 meter wide. As for the southern region, the beach morphology changes from dissipative type of beach to a reflective type of beach. Due to high winds on wave currents, coastal degradation were observed in most of the areas on the southern part. Hence rocks of varying sizes as coastal embankment are seen in protecting the shoreline areas. A collection of 86 borehole reports at 8 locations along the shoreline made it possible in addressing the first 20 meter depth of Perlis shoreline areas. Figure 4.3 presents the grain size distribution plot in liquefaction margin of Perlis soil. Most of the silty and sandy soil is found to be positioned within the margin with possibility of liquefaction and high possibility of liquefaction. The vulnerable soil are mostly consist of silt and fine sand deposits with very small fines contents as less than 3%.

A wider visual of the soil composition under the ground are presented in Figure 4.4. Hard layer is visualized at 17 m below ground surface. The depth of sand and silt layer ranged between 10 to 18 m. Another visual of the hardness of layer in terms of SPT-N blow counts are presented in Figure 4.5. The lowest SPT blow counts are observed on the first 3 to 5 m at almost all the studied locations. At the lower depths, the SPT counts increase and consistency of the soils at these depths can be defined as dense to very dense. At deeper depths, the SPT blow counts are observed as 30-50. As a result, the SPT indicates the presence of some layers vulnerable to liquefaction in the north region and Kuala Perlis region.

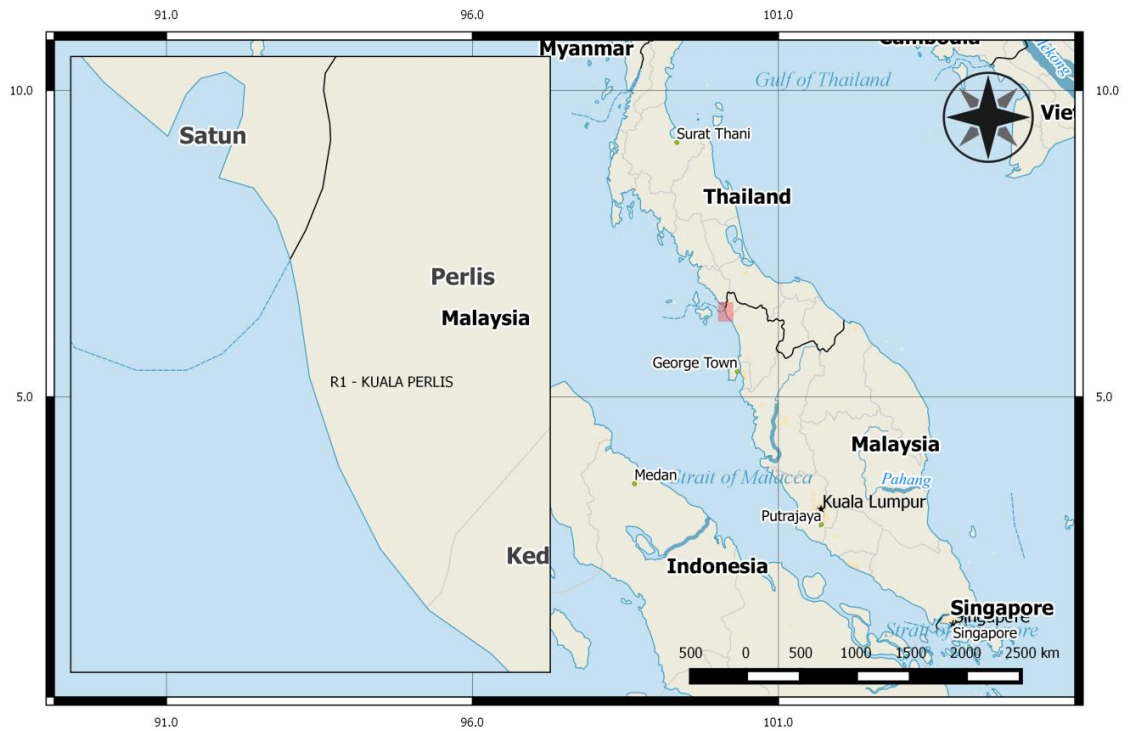


Figure 4.2: Perlis state map and study location

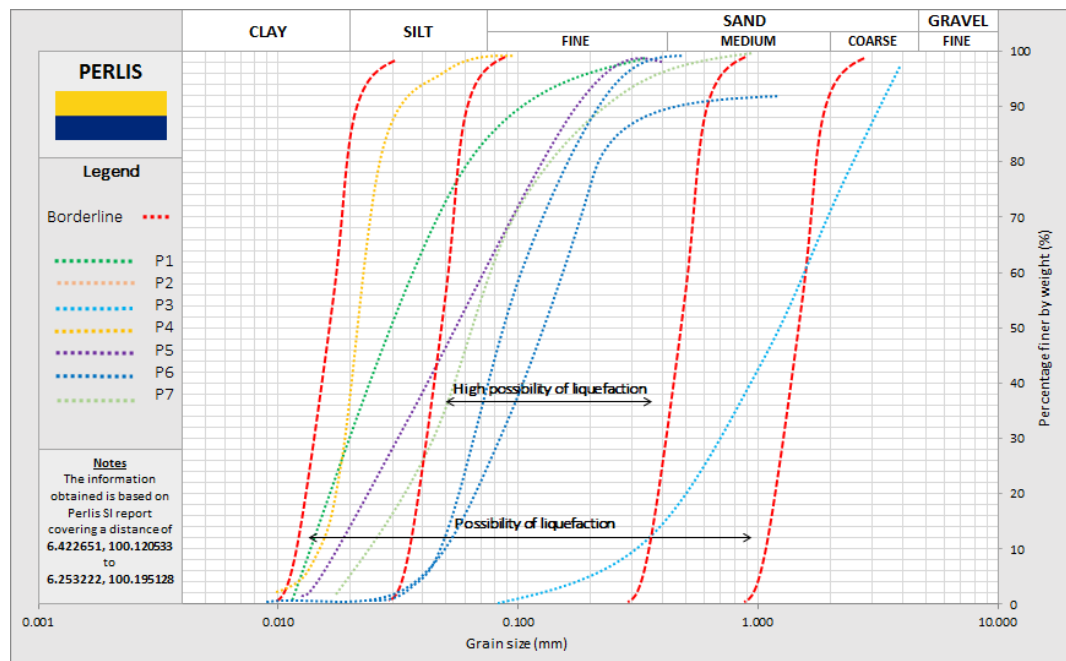


Figure 4.3: Grain size distribution plot in liquefaction margin of Perlis

The water table for each location is observed on the surface and the first 5 m below ground level (Figure 4.4). Most of the layer below water table is found to be saturated. The high population in Kuala Perlis and location in which the water table are close to the surface which underlies vulnerable deposits should be highlighted for further soil liquefaction analysis.

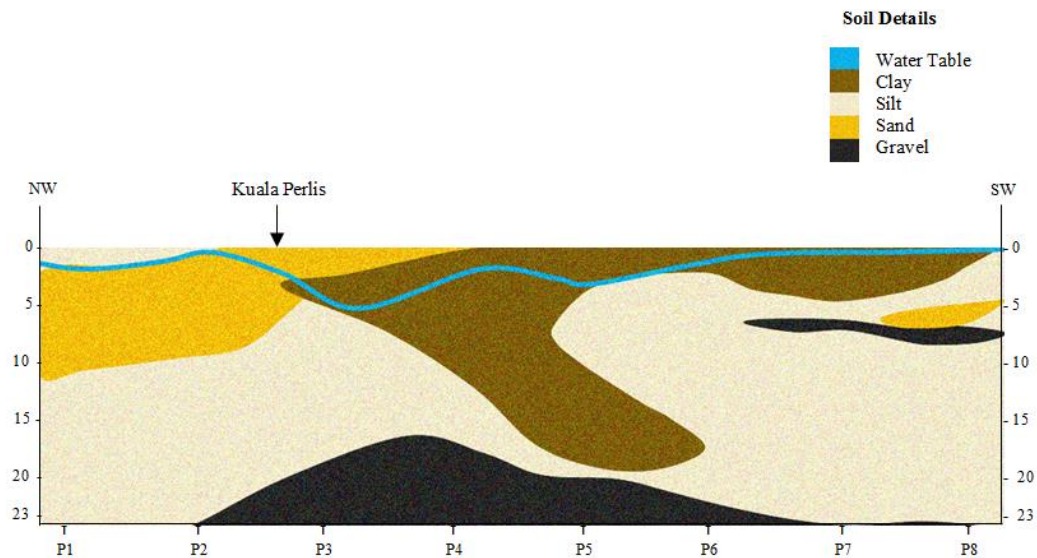


Figure 4.4: Soil layer composition of Perlis shoreline

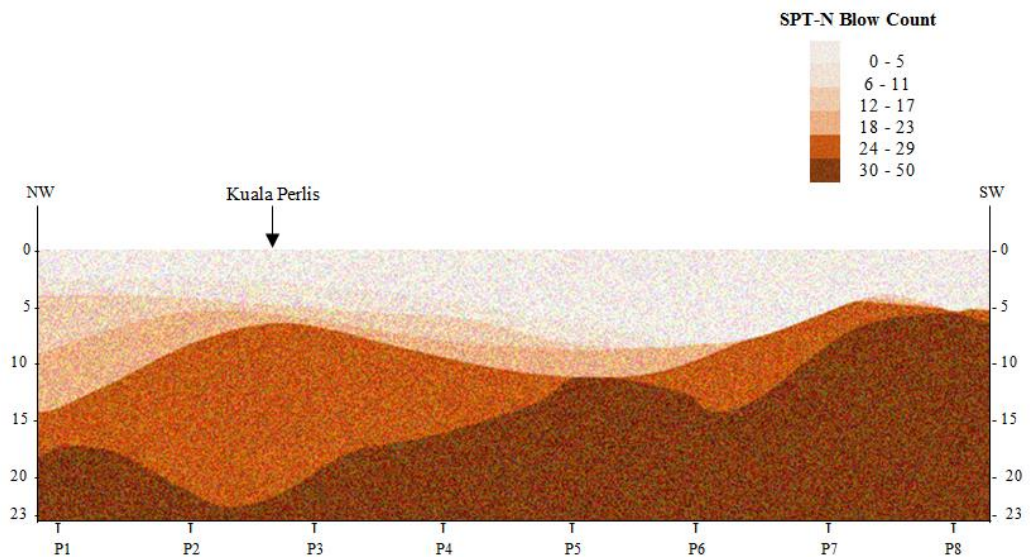


Figure 4.5: Distribution of SPT-N blow counts of Perlis shoreline

4.1.2 Kedah

Small traditional Malay rural township is observed at almost all the river mouth of Kedah state where local fishermen are located. Village houses are scattered along the shoreline areas and some areas are observed with a long stretch of coastal road. Similar to Perlis, coastal degradation were observed in most of study areas. 4 shoreline districts observed in Kedah mainland, which are Kubang Pasu, Kota Setar, Yan and Kuala Muda. Another part of Kedah is an island, Pulau Langkawi which consisted of mountains, vast paddy field and rural villages. Figure 4.6 presents Langkawi Island beach front. Figure 4.7 presents the Kedah state map and study location. Similar to Perlis, coastal degradation were observed in most of study areas in Kedah mainland which result rocks of varying sizes as coastal embankment. A collection of 104 borehole reports at various locations along the shoreline made it possible in addressing the soil exploration of Kedah mainland and Langkawi Island shoreline areas.



Figure 4.6: Distribution of SPT-N blow counts of Perlis shoreline

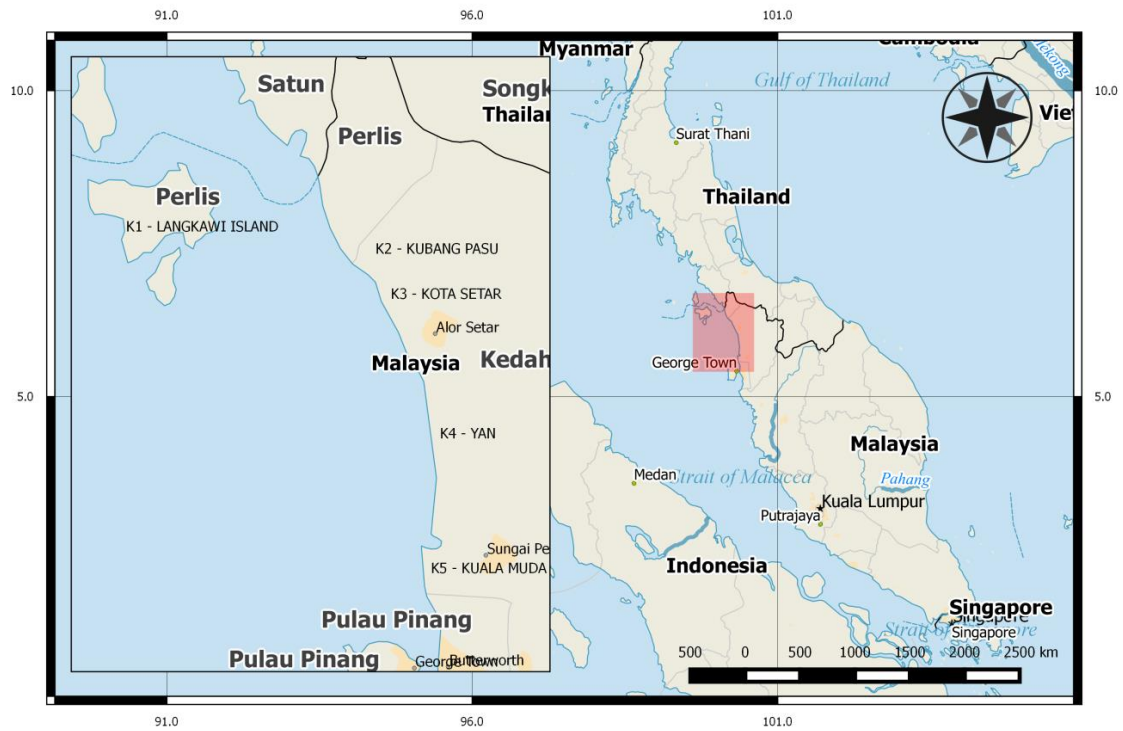


Figure 4.7: Kedah state map and study location

Throughout the study area, different soil types are observed. Figure 4.8 presents the grain size distribution plot in liquefaction margin of Kedah soil. Most of the silty and sandy soil is found to be positioned within the margin with possibility of liquefaction and high possibility of liquefaction. Sand deposits observed to be in 3 categories of fine, medium and coarse type with very little fine contents. As for the first 20 m soil visualization, 4 figures are presented to illustrate Kedah mainland and Langkawi Island shoreline soil properties (Figure 4.9 to Figure 4.12). Figure 4.9 and Figure 4.10 presents the soil layer composition and N-SPT blow counts for Langkawi Island shoreline. Almost 80% of the soil is sandy type with minor concentration of clay at few locations. Bedrock was found at near 10 m from surface at Teluk Burau. 4 significant location indicates some layers prone to liquefaction; Ulu Melaka, Teluk Burau, Pantai Chenang and Kuah. Low SPT blow counts are observed until 10 m depth at Tanjung Burau and Kuah. Ulu Melaka underlies silty soil with low blow counts for the first 5 m below

ground level. Water table near surface ranged at 0.1 m to 3.0 m was found at almost all the location. Figure 4.11 and Figure 4.12 presents the soil layer composition and N-SPT blow counts for Kedah mainland shoreline. According to the report summary, the location in which soil liquefaction should be further investigated is at Ayer Hitam and Kuala Muda district areas. Thick silty soil is found at Ayer Hitam having very low SPT blow counts on the first 2 m depth. As for Kuala Muda (Location 1), a thick 10 m sand are found to have low blow counts at first 5 m depth. At deeper depth, the SPT blow counts increase except at Yan and Kuala Muda (Location 2) which presents low blow counts at 20 m and 13 m respectively. A safe condition is found at Yan, although the blow count is low at deeper depth, the type of soil is not prone to liquefaction as presented in early literatures and in the liquefaction margin of grain size distribution plot. The water table location varies at each location with most significant location which needs to be addressed is at Kuala Muda district. The important development observed in Kedah state is the coastal road and concentrated town at river mouth with moderate buildings and basic facilities.

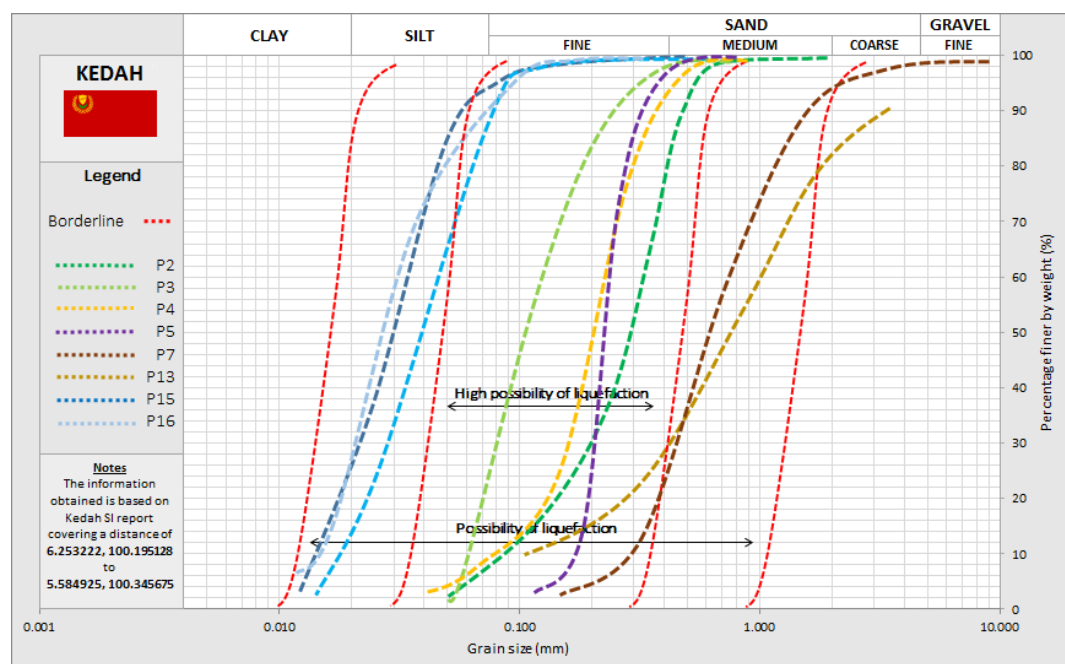


Figure 4.8: Grain size distribution plot in liquefaction margin of Kedah

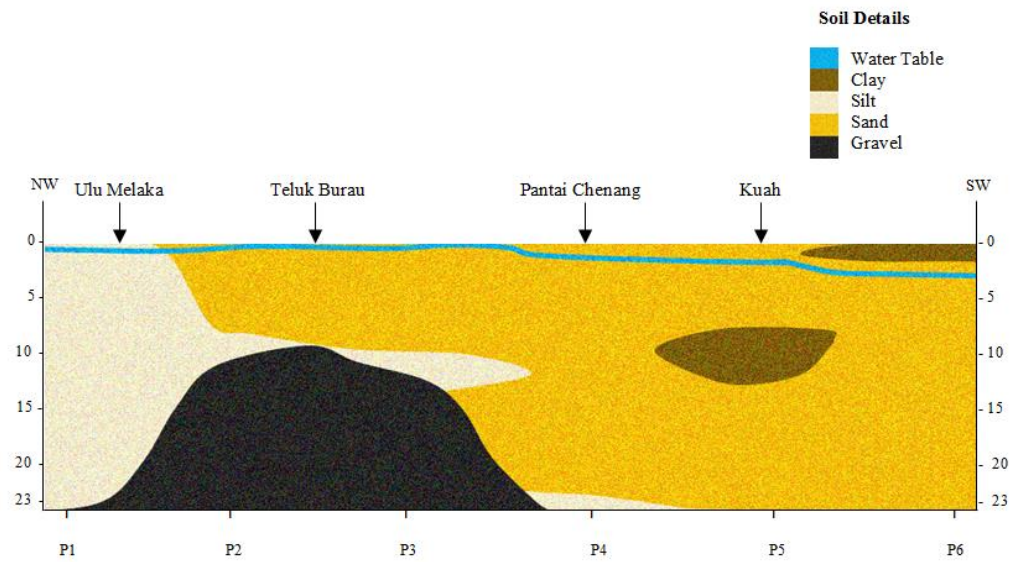


Figure 4.9: Soil layer composition of Langkawi Island shoreline

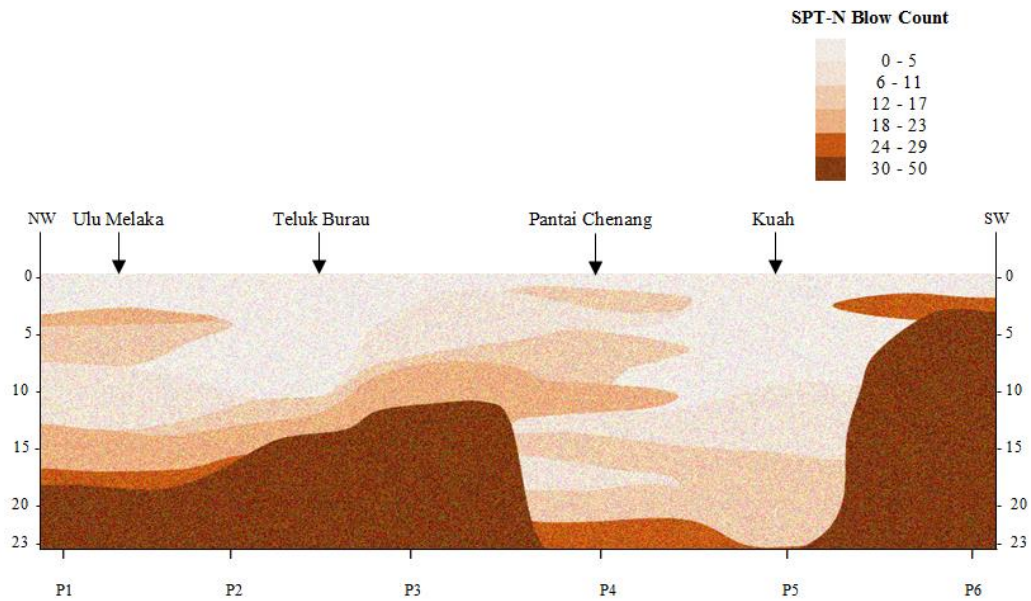


Figure 4.10: Distribution of SPT-N blow count of Langkawi Island shoreline

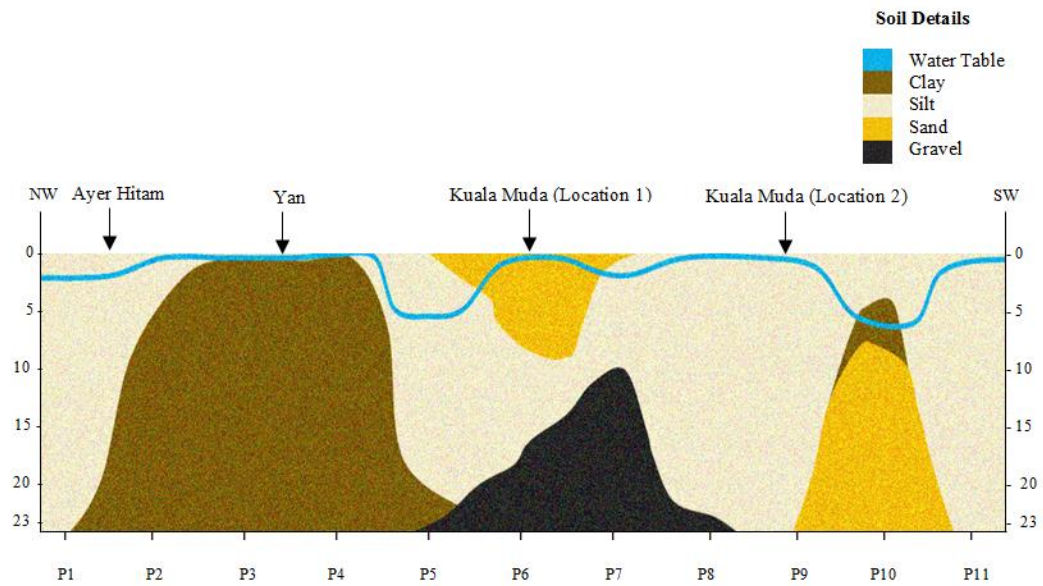


Figure 4.11: Soil layer composition of Kedah (Mainland) shoreline

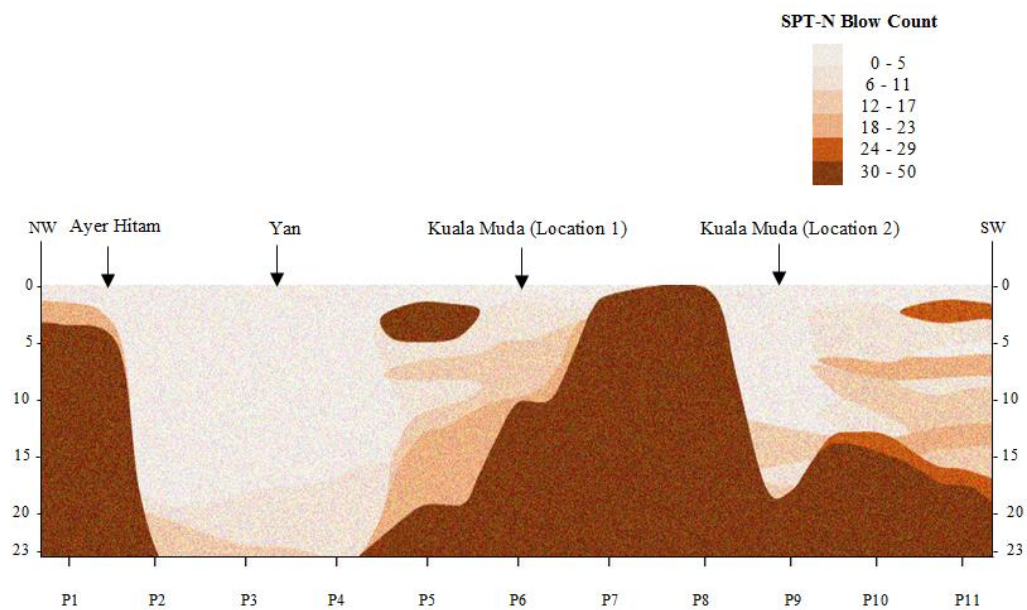


Figure 4.12: Distribution of SPT-N blow count of Kedah (Mainland) shoreline

4.1.3 Penang

Similar to Kedah state, Penang state consist of two main part which is the Penang mainland (Seberang Perai) and Penang Island. 31 locations containing 178 boreholes data of Penang were used in illustrating the soil profile and details of the state. The industrialization period in since 1972 has seen a lot of changes in the beach morphology in the present time. Penang Island is observed to be a busy city with various reclamation projects to cater residential, business hub and port areas in which generates incomes for the country (Figure 4.13). Hence the changes of natural surrounding for development have affected almost all the location in Penang result in complex behavior of the surroundings. Observation made on site reveals the shoreline area in the northern and southern region of Penang Island is of rocky type and partially sandy beach. Whereas Seberang Perai is mainly a muddy type beach with a port located in the city center. During the early years, most of the forest land and swamp land was cleared to make way for agricultural land. Figure 4.14 presents the Penang state map and study location which covers approximately 152 km of distance.



Figure 4.13: Seberang Perai beach front overlooking Penang Island

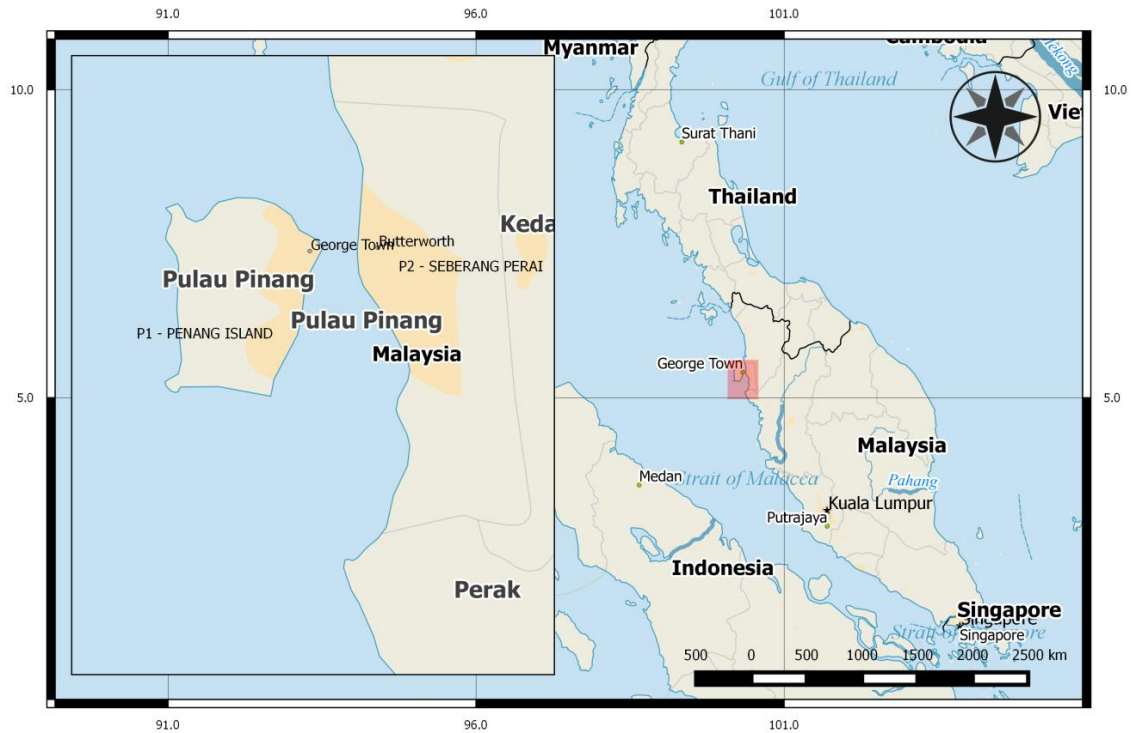


Figure 4.14: Penang state map and study location

Figure 4.15 shows the grain-size distribution curves with upper and lower bound curves for liquefaction susceptibility for both Penang Island and mainland. As observed in figure, the soils which are prone to liquefaction consist of medium to coarse type sand with very little fine contents. Medium type is found mostly in Seberang Perai whereas the coarser type of sand is mostly found in Penang Island.

A visual summary of the soil composition and distribution of SPT-N blow count of Penang shoreline is presented in Figure 4.16 to Figure 4.19. 4 important places are highlighted for the discussion as being the most significant observation in the soil liquefaction context. Thick layer of soil up to 23 m are found at Tanjung Bungah, Georgetown and Gelugor whereas in Bayan Lepas overlies 23 m silt deposits. The first 5 m depth in Tanjung Bungah and Gelugor reveals the lowest N-SPT blow count. Whereas in Georgetown and Bayan Lepas, the lowest N-SPT blow counts was found in the first 15 m depth. The water table at the highlighted location is within 0.1 m to 2.0 m.

In Seberang Perai, 3 location are highlighted which shows thick sand content ranging from 5 m to 10 m with water table near surface. The lowest SPT-N blow count are found at the first 5 meter in Butterworth and South SP areas except for Central SP, the soft layer covers up to 20 m depth. There is no rock or hard stratum defined in Seberang Perai area within the first 20 m depth area. Clay and silt deposits occupy 60% of the overall studied areas leaving 40% prone sand deposits to soil liquefaction.

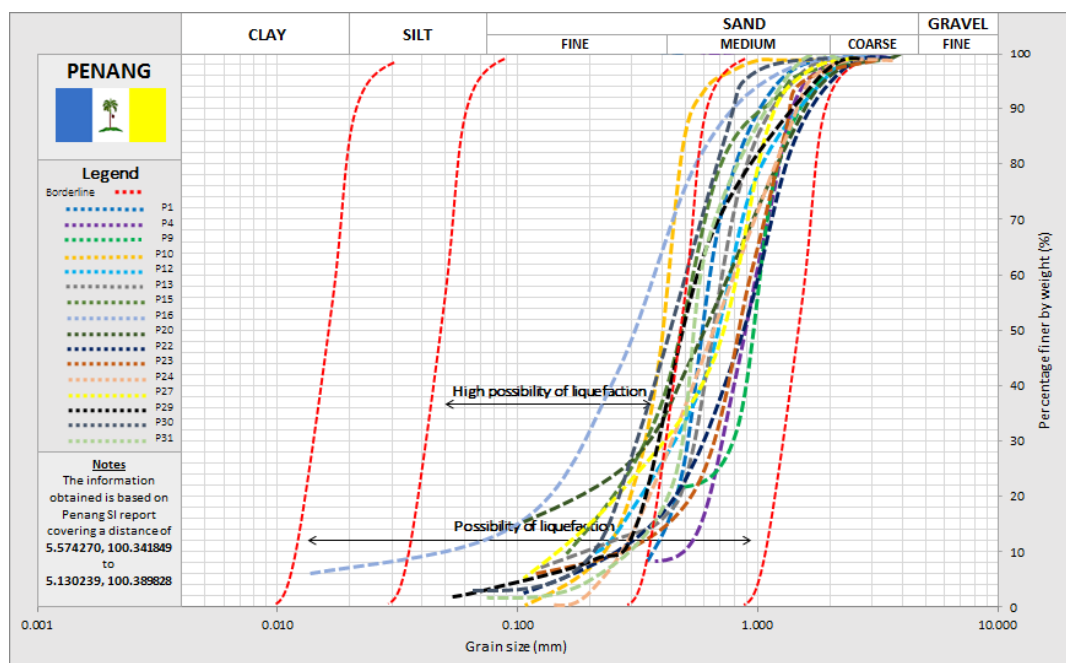


Figure 4.15: Grain size distribution plot in liquefaction margin of Penang

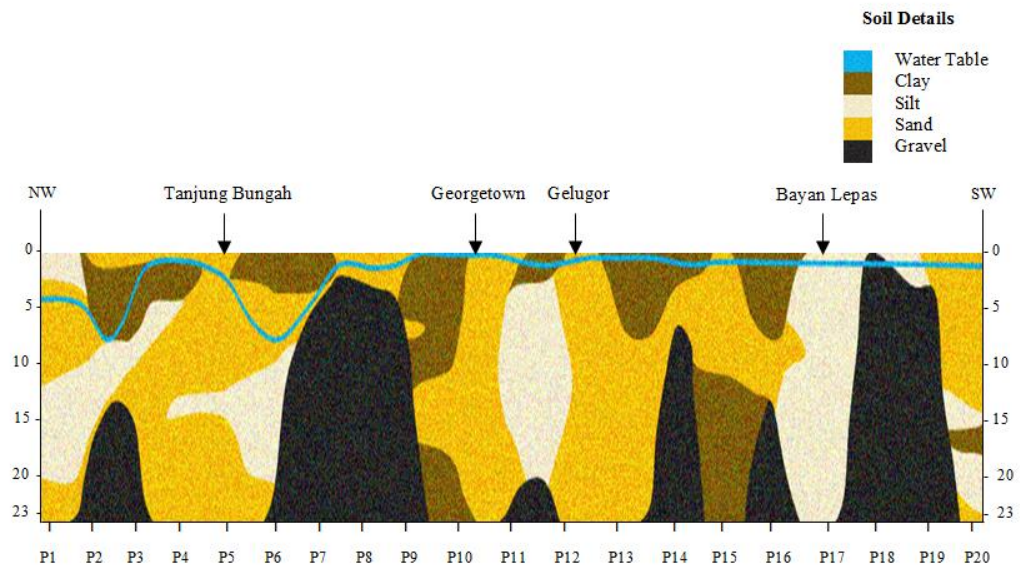


Figure 4.16: Soil layer composition of Penang (Island) shoreline

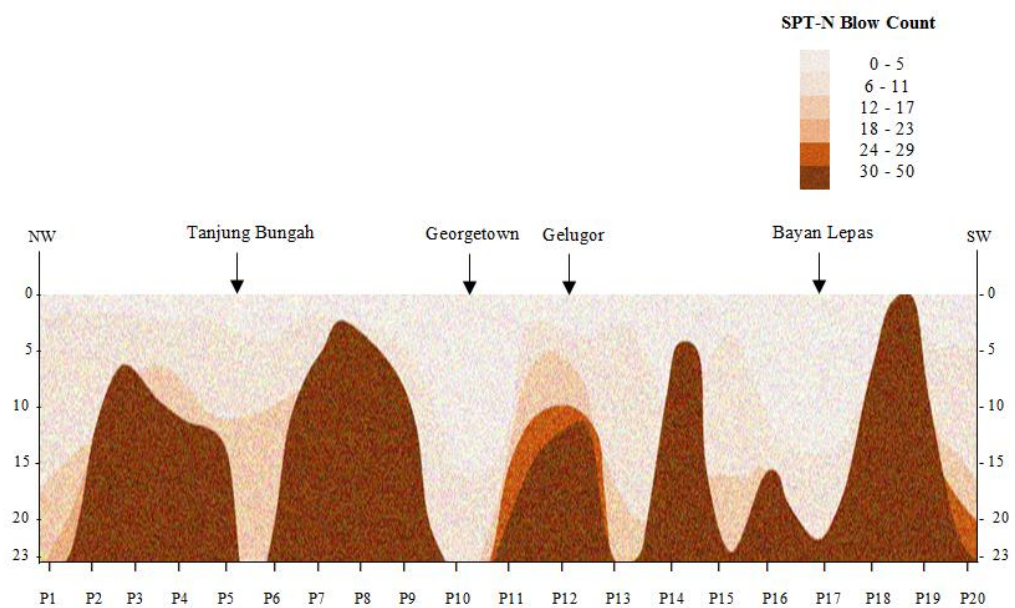


Figure 4.17: Distribution of SPT-N blow count of Penang (Island) shoreline

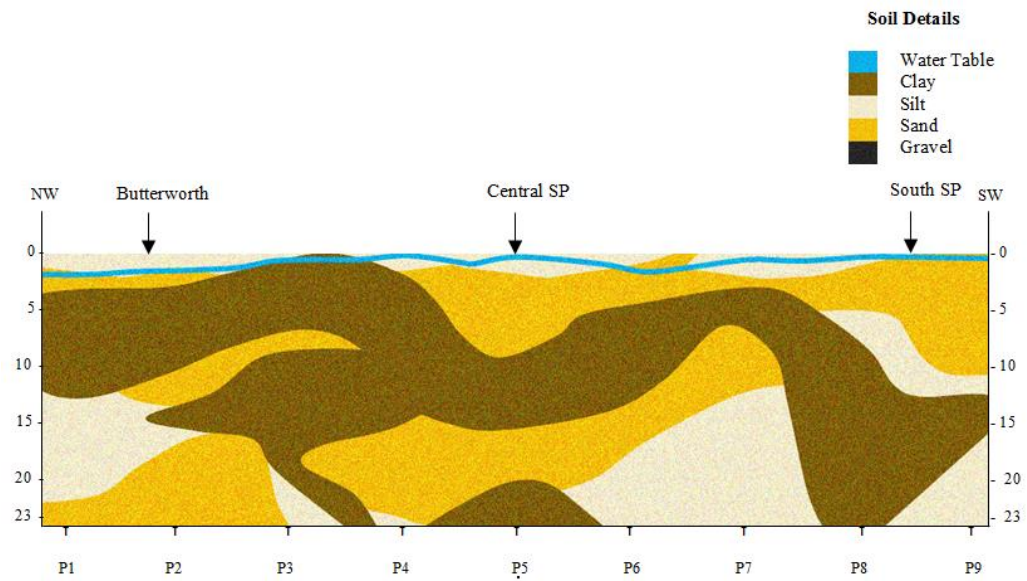


Figure 4.18: Soil layer composition of Penang (Mainland) shoreline

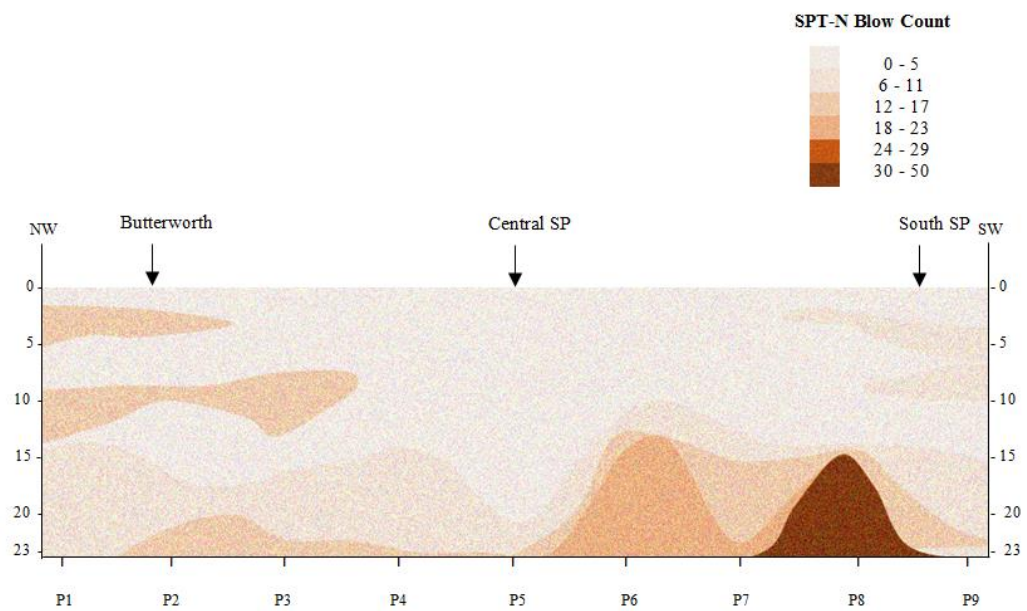


Figure 4.19: Distribution of SPT-N blow count of Penang (Mainland) shoreline

4.1.4 Perak

Perak shoreline is blessed with attractive natural environment which includes undisturbed beaches, coastal hill forest, heath forest and sea turtle nesting areas. Physical facilities, agricultural and logging activities are found scattered at various locations along the 230 km stretch shoreline. The removal of the natural environment accelerate coastal erosion as observed in some areas in Perak overload by coastal embankment running parallel to the shoreline . 42 locations with 210 boreholes made it possible for soil exploration of studied area. Wide mud shores and coastal forests rich in biodiversity are concentrated along Perak stretch due to the mild wave climate of the Straits of Malacca. Figure 4.20 shows Teluk Rubiah in Manjung district, Perak. Figure 4.21 presents the Perak state map and study location in selected district. Development is observed in location close to the river mouth where moderate buildings and basic facilities are built for the community.



Figure 4.20: Teluk Rubiah located in Manjung district, Perak

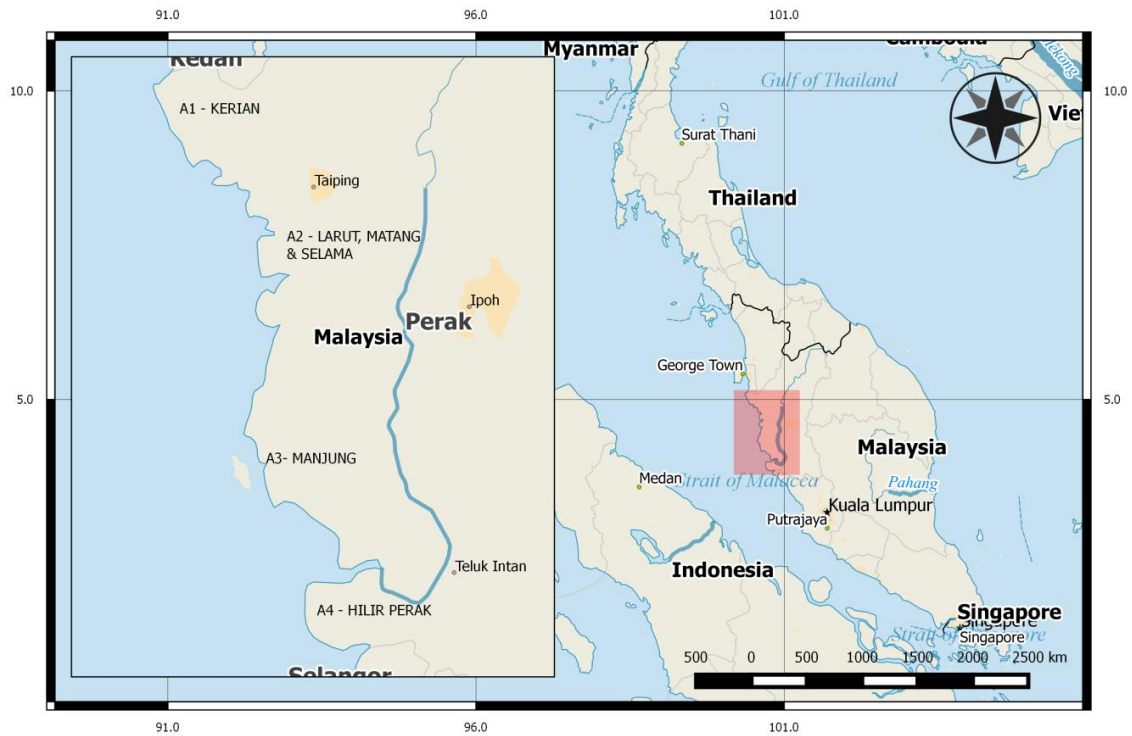


Figure 4.21: Perak state map and study location

Figure 4.22 shows the grain-size distribution curves with upper and lower bound curves for liquefaction susceptibility for Perak state. As observed in figure, the soils which are prone to liquefaction consist of silty and medium to coarse type sand with very little fine contents.

A visual summary of the soil composition and distribution of SPT-N blow count of Perak shoreline is presented in Figure 4.23 and Figure 4.24. 2 important places are highlighted for the discussion as being the most significant observation in the soil liquefaction context. Thick layer of sand up to 20 m are found at Lumut and Teluk Rubiah whereas in Bagan Datoh overlies 10 m silt deposits. Both places are reported to have low N-SPT blow count of first 10 m and 23 m below ground level. The water table at the highlighted location is within 0.1 m to 3.0 m. There is no rock or hard stratum

defined in Perak area within the first 20 m depth. Clay and silt deposits occupy 50% of the overall studied areas leaving another 50% prone sand deposits to soil liquefaction.

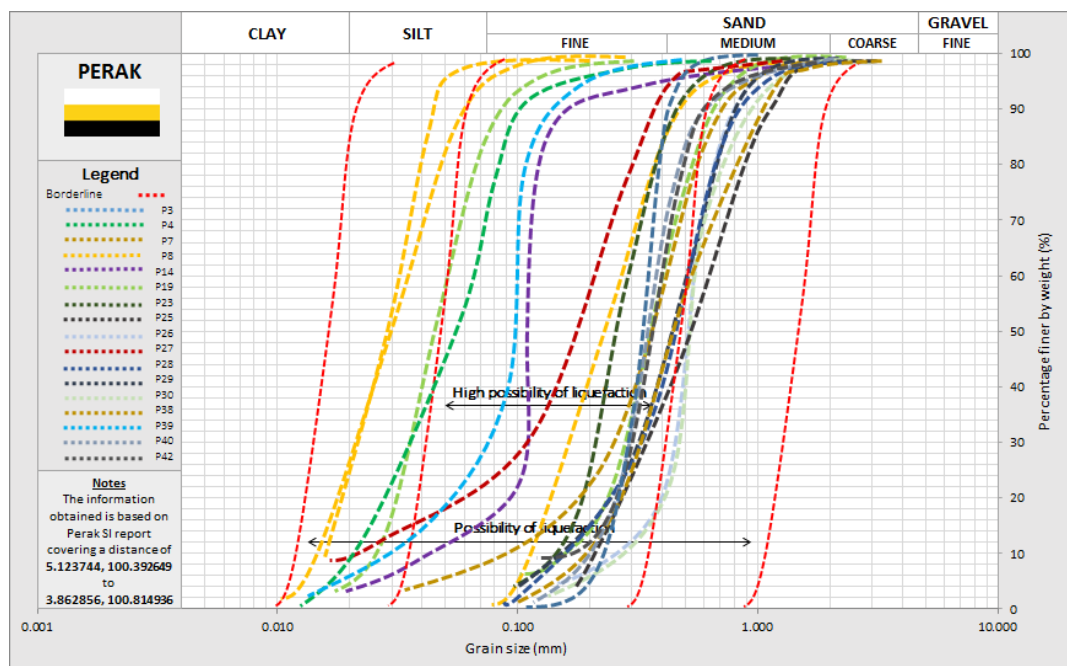


Figure 4.22: Grain size distribution plot in liquefaction margin of Perak

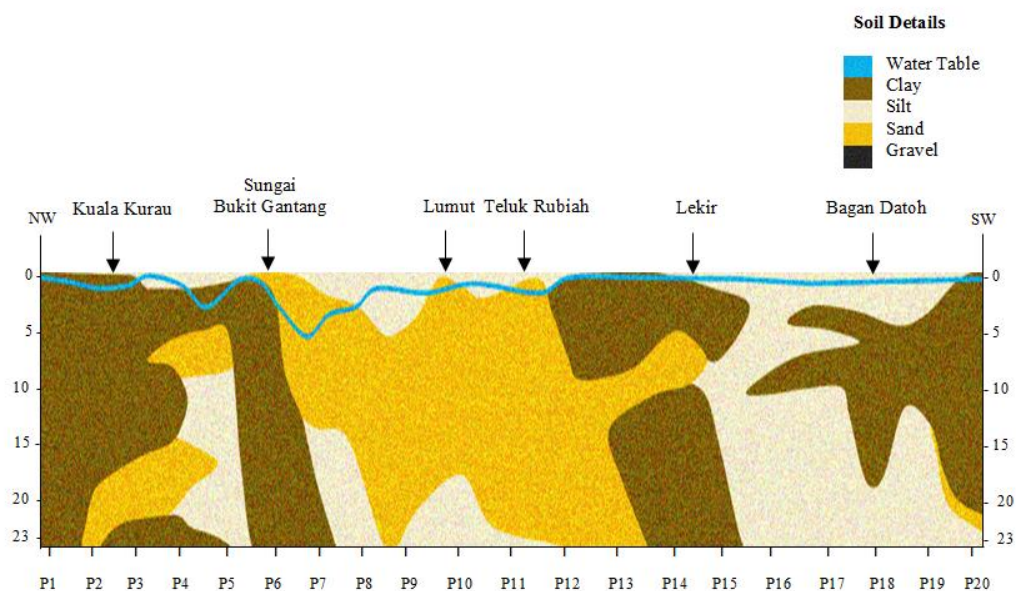


Figure 4.23: Soil layer composition of Perak shoreline

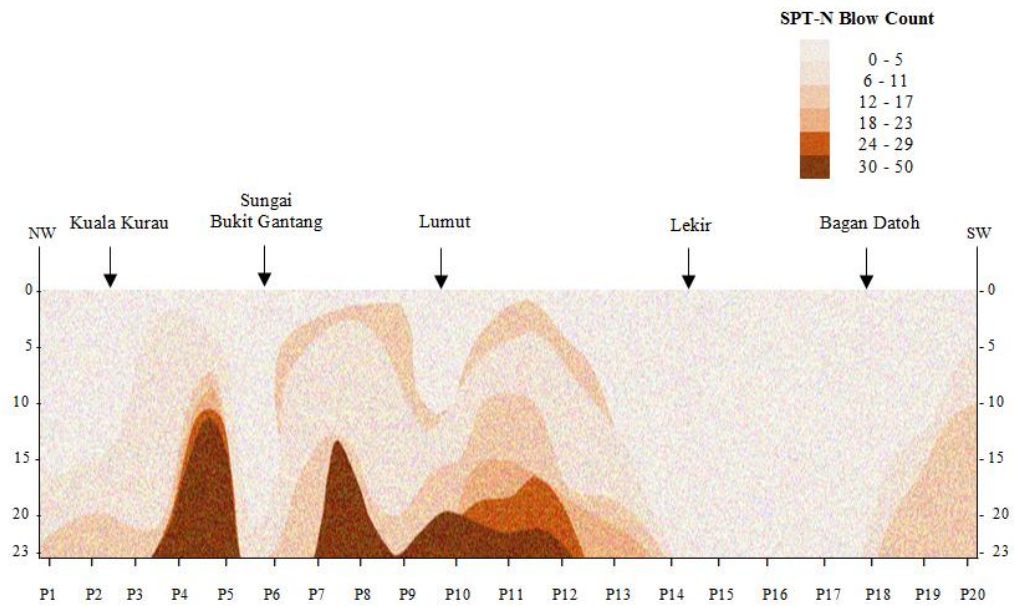


Figure 4.24: Distribution of SPT-N blow count of Perak shoreline

4.1.5 Selangor

Numerous agricultural activities are observed in the northern part of Selangor shoreline. This muddy coast is rich with soil which is suitable for vegetation and plantation. Hence along the stretch line, the clearance of mangrove areas and coastal forestation made it possible for agricultural activities. As the stretch moves south, a significant port for Malaysia is defined in which shipping activities takes place. Further south recreational spots are developed with scattered high end resorts and fishing villages. The typical type of beach in Selangor is of mudflat and silty beach. Figure 4.25 presents the beachfront at Sekinchan, Selangor. At some location where coastal erosion is critical, embankment consisted of random granite blocks are observed running parallel to the coastal road. Reflective beach are observed on the northern part whereas dissipative beach are concentrated in the southern region. Significant development is observed in the Klang district as a busy port city is defined. Reclamation project are also

observed in the southern areas. 13 locations with 79 boreholes information are used to assess the soil beneath the Selangor ground (Figure 4.26).



Figure 4.25: A small fishing village Sabak Bernam, Selangor

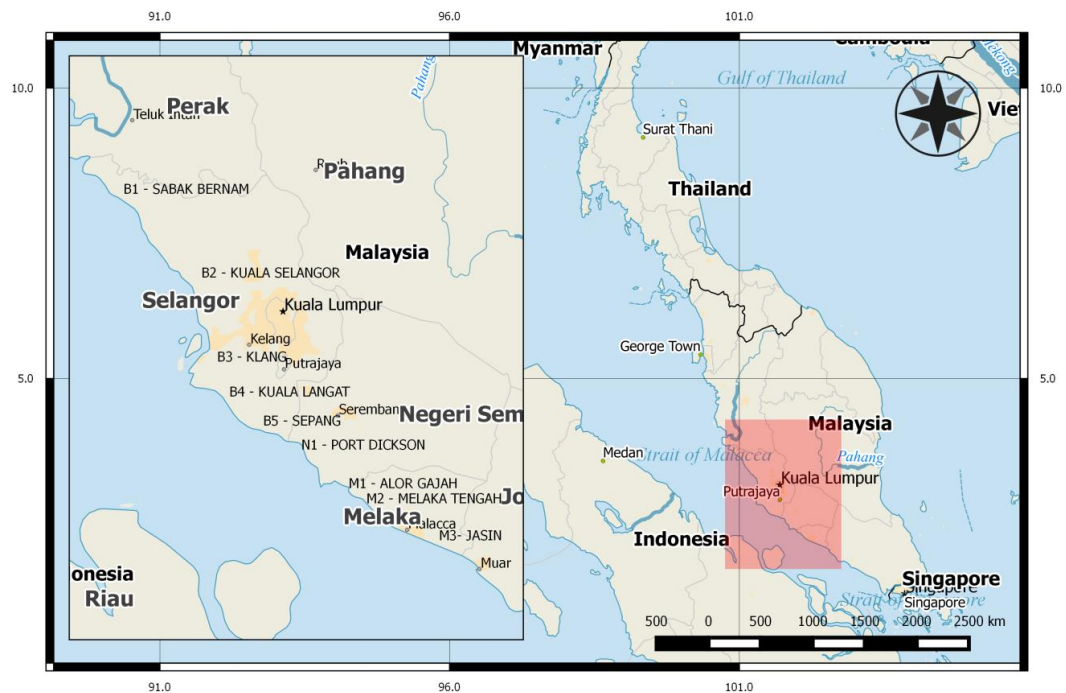


Figure 4.26: Selangor state map and study location

Figure 4.27 shows the grain-size distribution curves with upper and lower bound curves for liquefaction susceptibility for Selangor state. As observed in figure, the soils which are prone to liquefaction consist of silty and medium to coarse type sand with very little fine contents. The soil susceptibility covers both possibility and high possibility of liquefaction.

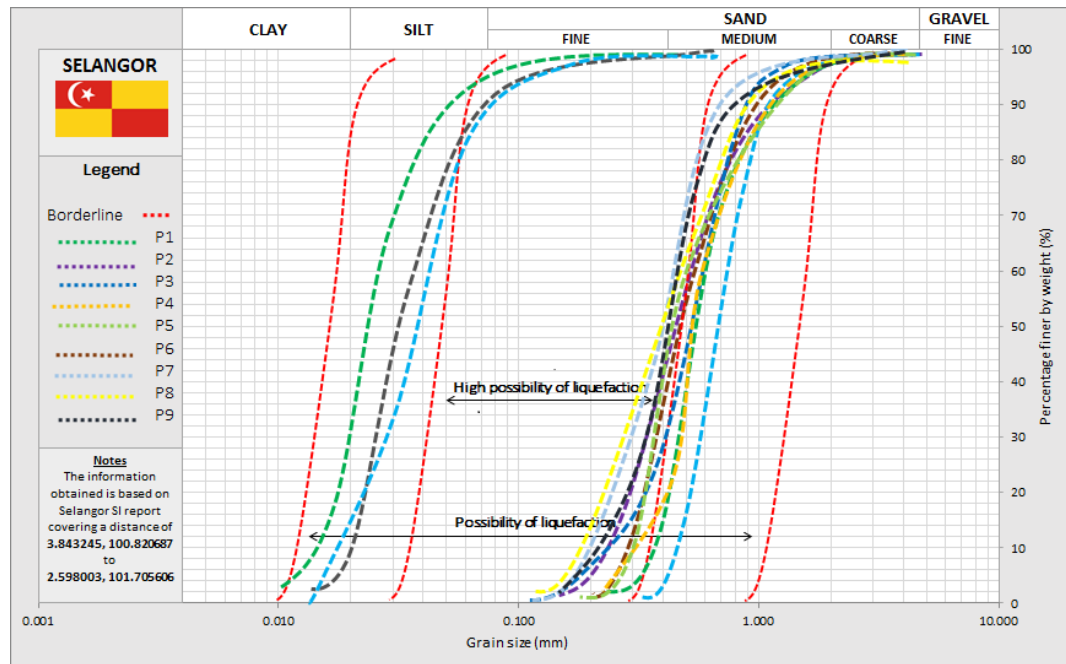


Figure 4.27: Grain size distribution plot in liquefaction margin of Selangor

A visual summary of the soil composition and distribution of SPT-N blow count of Selangor shoreline is presented in Figure 4.28 and Figure 4.29. Sungai Besar in Sabak Bernam district overlies thick soft clay deposits making it less vulnerable to soil liquefaction hazard. Thick layer of sand up to 23 m are found at Kuala Langat and Sepang areas whereas in Kuala Selangor overlies 6 m silt deposits. The first 3 m depth in all location reported low N-SPT blowcounts. A critical case is observed in Kuala Selangor, Klang and Kuala Langat district where the low N-SPT blow counts occupies a 10 m depth and more. As for the water table, the values are in ranged 0.1m – 2.0 m.

Clay and silt deposits occupy 70% of the overall studied areas leaving another 30% prone sand deposits to soil liquefaction. As development is observed heavy in Klang for port, in Kuala Langat and Sepang for agricultural and tourism sector along with reclamation project, further investigation is needed.

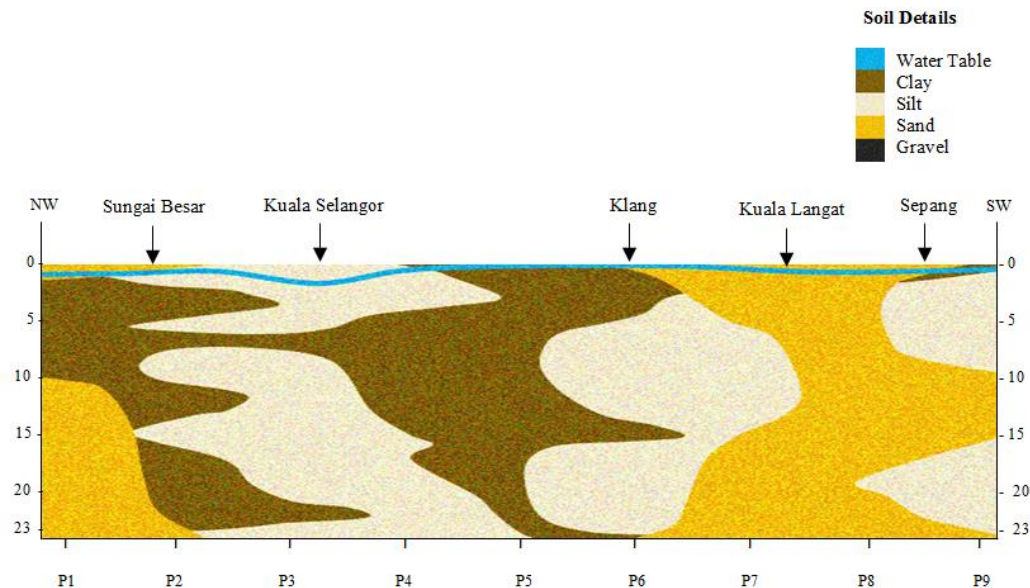


Figure 4.28: Soil layer composition of Selangor shoreline

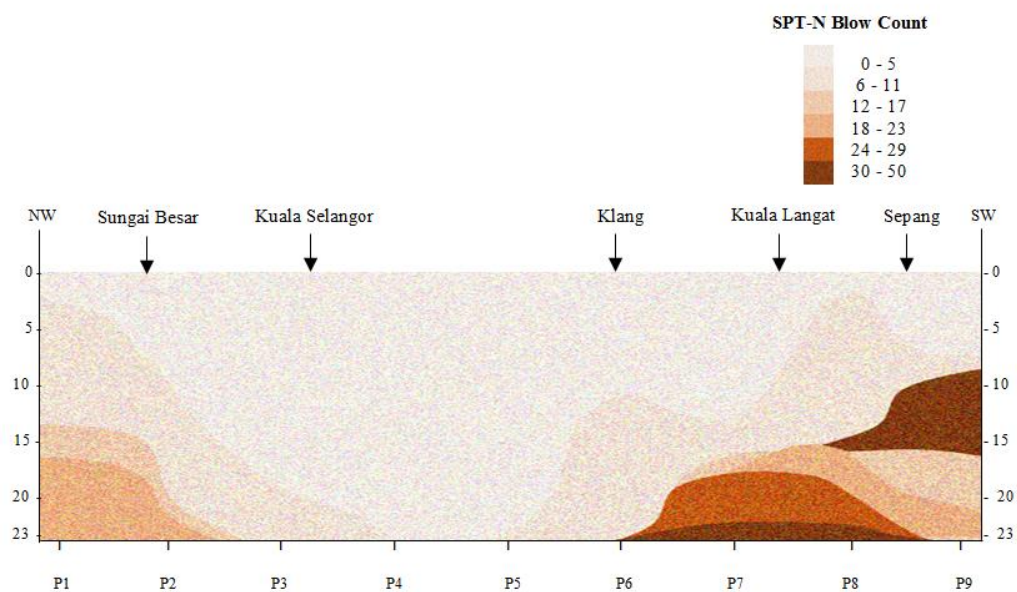


Figure 4.29: Distribution of SPT-N blow count of Selangor shoreline

4.1.6 Negeri Sembilan

Land reclamation in Port Dickson is increasing in giving way to the expansion of port and tourism industries. The northern part is developed whereas the southern part is preserved with coastal forestation in Tanjung Tuan. The type of beach observed is of reflective near the port area and dissipative in the less developed areas. This second smallest stretch covers approximately 58 km of shoreline areas. 2 locations with 20 boreholes details are observed for Negeri Sembilan shoreline district. Figure 4.30 presents the port city in Port Dickson, Negeri Sembilan where tourism areas are located neraby. In the early years, Port Dickson is well known for its flat beach but as years passed by, heavy coastal erosion takes place due to development leaving behind areas which are not safe for swimming due to the high wave current prior to the beach morphology. Figure 4.31 present the Negeri Sembilan state map and study location.



Figure 4.30: Port city in Port Dickson, Negeri Sembilan

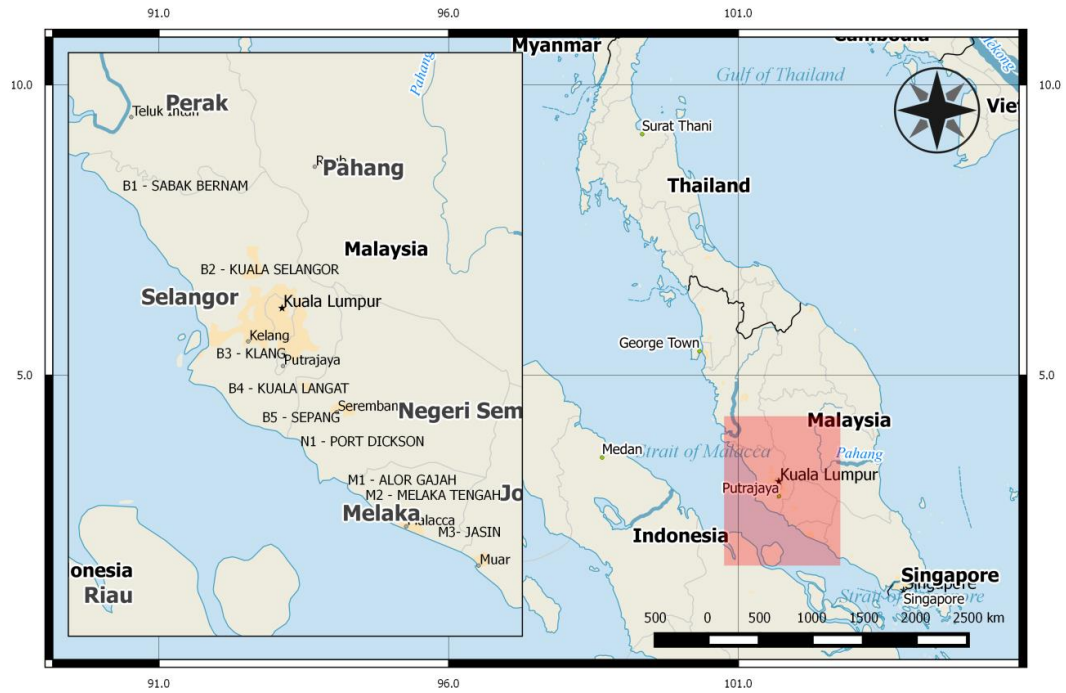


Figure 4.31: Port city in Port Dickson, Negeri Sembilan

Figure 4.32 shows the grain-size distribution curves with upper and lower bound curves for liquefaction susceptibility for Negeri Sembilan state. As observed in figure, the soils which are prone to liquefaction consist of silty to medium sand with very little fine contents. The soil susceptibility covers both possibility and high possibility of liquefaction. In general, the silt deposits show a uniformly graded soil in which there is high possibility of liquefaction potential. Similar findings are observed in the sand deposits. By observing the surface ground layer to 5 m below ground, the soil are found to be in saturated and loose state condition. The deposits in this condition are expected to have very low N-SPT blowcounts and are prone to liquefaction hazard.

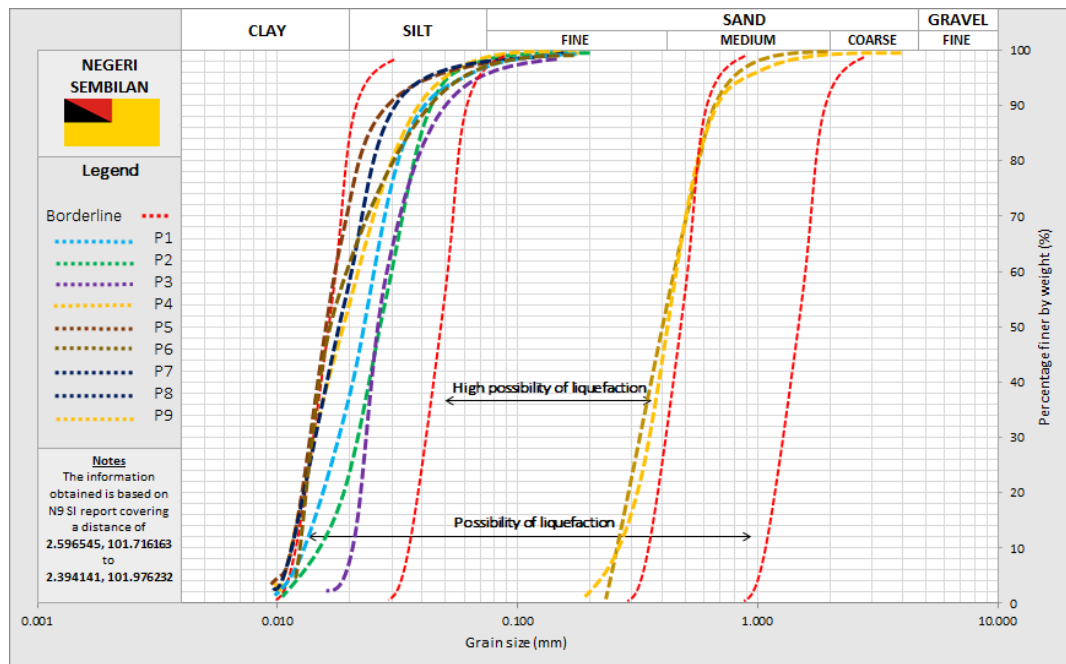


Figure 4.32: Grain size distribution plot in liquefaction margin of Negeri Sembilan

Port Dickson shoreline is likely to be made of 80% silt, 20% clay and only 10% sand. A visual summary of the soil composition and distribution of SPT-N blow count of Negeri Sembilan shoreline is presented in Figure 4.33 and Figure 4.34. The north of Port Dickson overlies thick layer of silt deposit. Similar observation was found in the most of the areas in the south except the existence of thick sand layer at few places near the Negeri Sembilan-Melaka border. Thick layer of silt up to 23 m are observed at most of the boreholes and sand thickness up to 20 m are found in few locations. In the hardness aspect, the first 5 m below ground is observed with low N-SPT blow counts which makes it most probably consist of very loose particle content. As for the water table, the values are in the range of 0.1 m – 1.0 m. There is hard stratum defined in four locations as highlighted in figure. One of which defined a rocky type beach as the stratum was found very close to the surface layer. As development is observed heavily in Port Dickson with the expansion of oil and gas industry and tourism along with reclamation project, further investigation is needed for the proper land usage of the study areas.

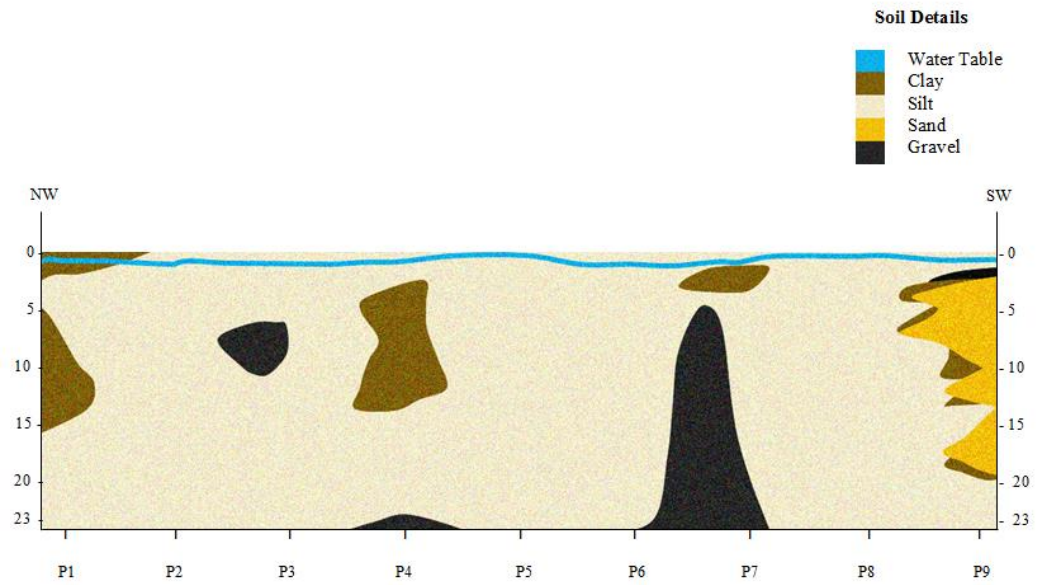


Figure 4.33: Soil layer composition of Negeri Sembilan shoreline

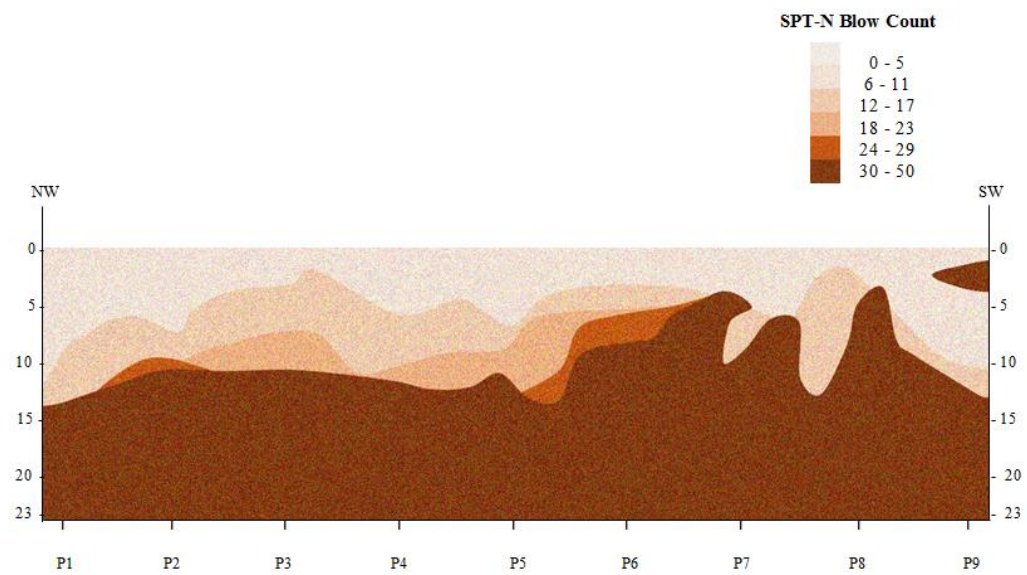


Figure 4.34: Distribution of SPT-N blow count of Negeri Sembilan shoreline

4.1.7 Melaka

The Melaka state consists of 3 main districts of which covers a total of 73 km shoreline distance makes it the fourth shortest shoreline state in Peninsular Malaysia. The middle district in which the city center is located is a busy city compared to the other 2 district. Tall residential buildings are located very close to the shoreline areas and also on reclaimed land. Two man-made island approximately 0.5 km of the coast of Melaka covers reclaimed area of 40 ha and 50 ha respectively to cater marine theme park, marina, hotels and waterfront activities. Figure 4.35 and Figure 4.36 presents a typical view of Melaka city overlooking the north and south direction. Figure 4.37 presents the Melaka state map and study location.



Figure 4.35: Melaka city overlooking south direction



Figure 4.36: Melaka city overlooking north direction

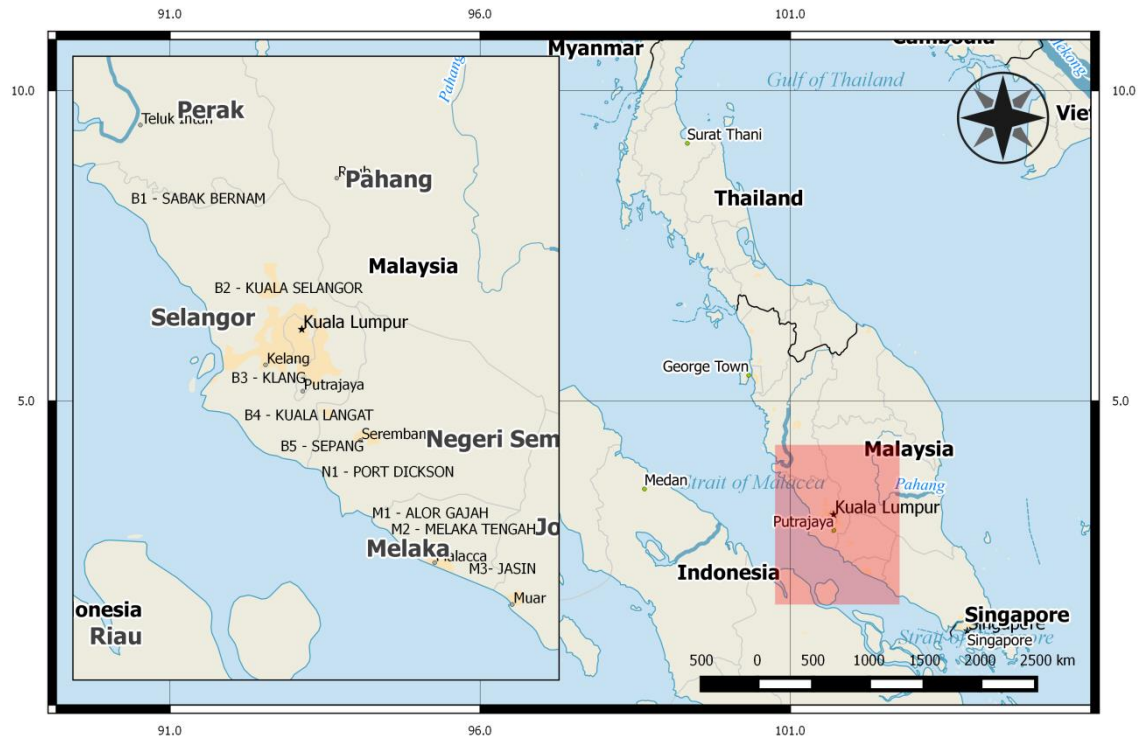


Figure 4.37: Melaka state map and study location

Throughout the study area, different soil types are observed. Figure 4.38 presents the grain size distribution plot in liquefaction margin of Melaka. Most of the silty and fine sandy soil is found to be positioned within the margin with possibility of liquefaction and high possibility of liquefaction. Sand deposits observed to be in 2 categories of silt and fine sand type with very little fine contents.

As for the first 20 m soil visualization, 2 figures are presented to illustrate Melaka shoreline soil properties. Figure 4.39 and Figure 4.40 presents the soil layer composition and N-SPT blow counts for Melaka shoreline. Almost 80% of the soil is silt with minor concentration of clay at few locations. Sand occupies 15% of the findings. Hard stratum is found at average 20 m below ground surface. 3 significant location indicates some layers prone to liquefaction; Kuala Sungai Baru, Melaka Tengah and Pantai Siring. Low SPT blow counts are observed until 7 m depth at Kuala Sungai Baru which underlies

thick silt with water table near surface ranged at 1.5 m to 2.3 m was found at almost all the location. Melaka Tengah shows similar findings with thick silt with sandy ground surface. The low SPT blow counts are up to 23 m. In addition the water table is found near surface. Whereas in Pantai Siring 4 m of thick sand occupies the surface ground with low SPT blow counts up to 7m. The water table is also near surface level.

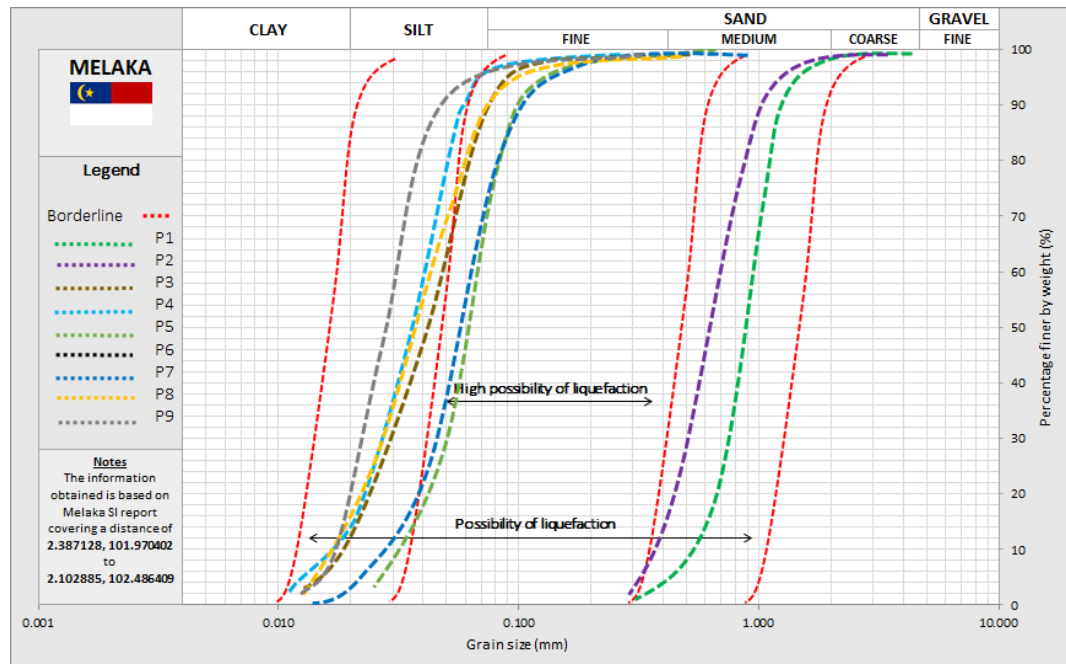


Figure 4.38: Grain size distribution plot in liquefaction margin of Melaka

The important development observed in Melaka state is the coastal road, artificial islands and land residential building development along the shoreline areas and also on reclaimed land. Prior to the increasing population and building development, the city holds significant iconic projects and holds many historic buildings as the main attraction to the state. Therefore further investigation on soil liquefaction context need to be introduced in the state of Melaka especially in the city center in optimizing the development to its full potential towards natural hazard.

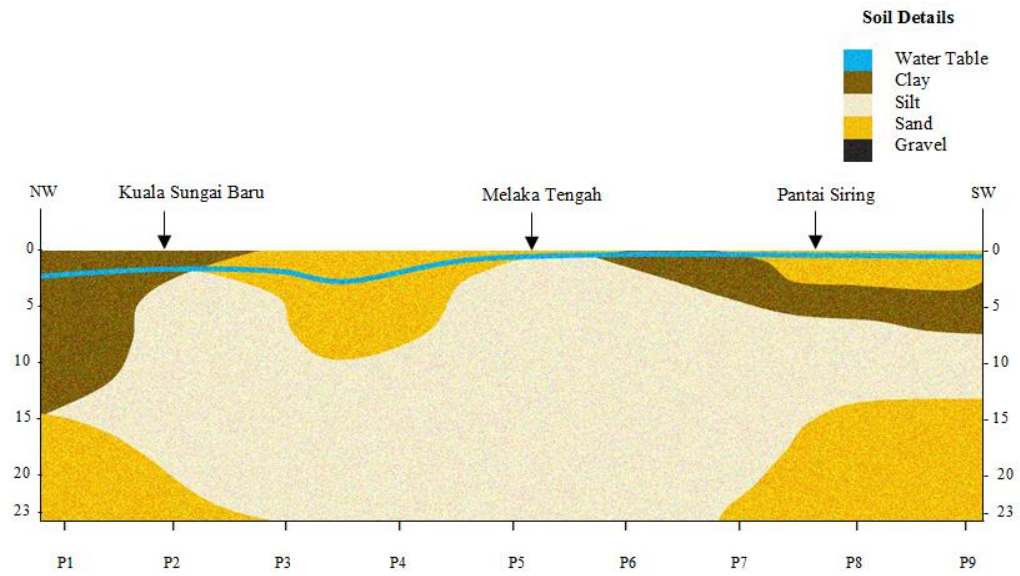


Figure 4.39: Soil layer composition of Melaka shoreline

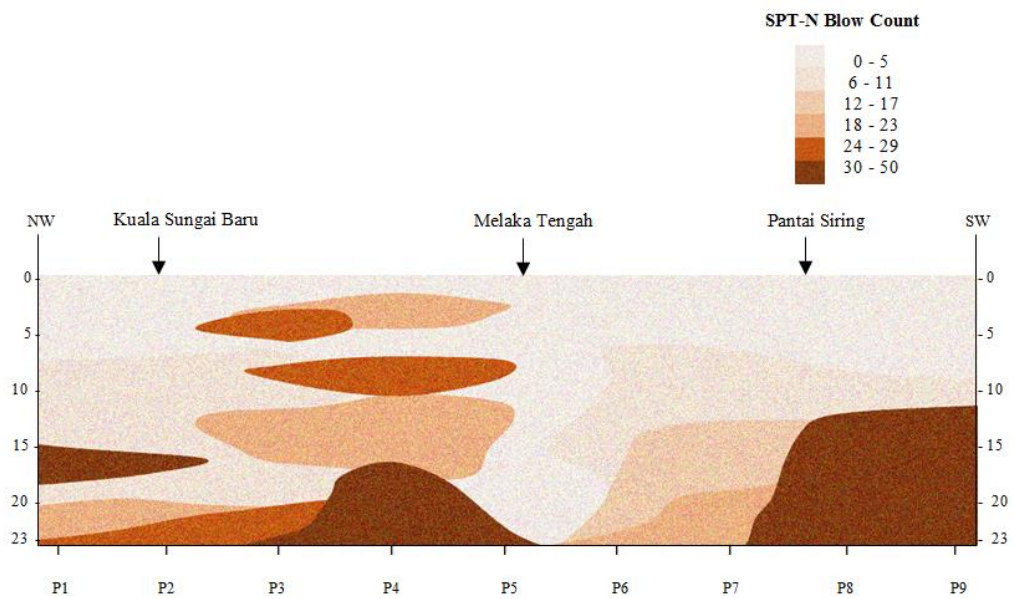


Figure 4.40: Distribution of SPT-N blow count of Melaka shoreline

4.1.8 Johor

Measuring a distance of 492 km shoreline distance, Johor state consists of 6 significant shoreline districts. The west coast area consist of 4 shoreline district; Muar, Batu Pahat, Pontian and Johor Bahru whereas the east coast consist of 2 shoreline district; Mersing and Kota Tinggi. In general, the west coast areas are made up of wetland consisted of river mouth, coastal mudflat and mangrove. The threats observed from site visit which have significant impact to the environment are severe erosion, tourism, domestic pollution, housing development and oil palm. In contrast the east coast areas features long stretch coastal sand beach with lesser threats except from port industries. Figure 4.41 presents the Johor Bahru beach front overlooking Singapore. Figure 4.42 present the Johor state map and study location. A total of 71 locations with 384 boreholes have been identified for soil assessment and visualization of Johor state.



Figure 4.41: Johor Bahru city overlooking Singapore

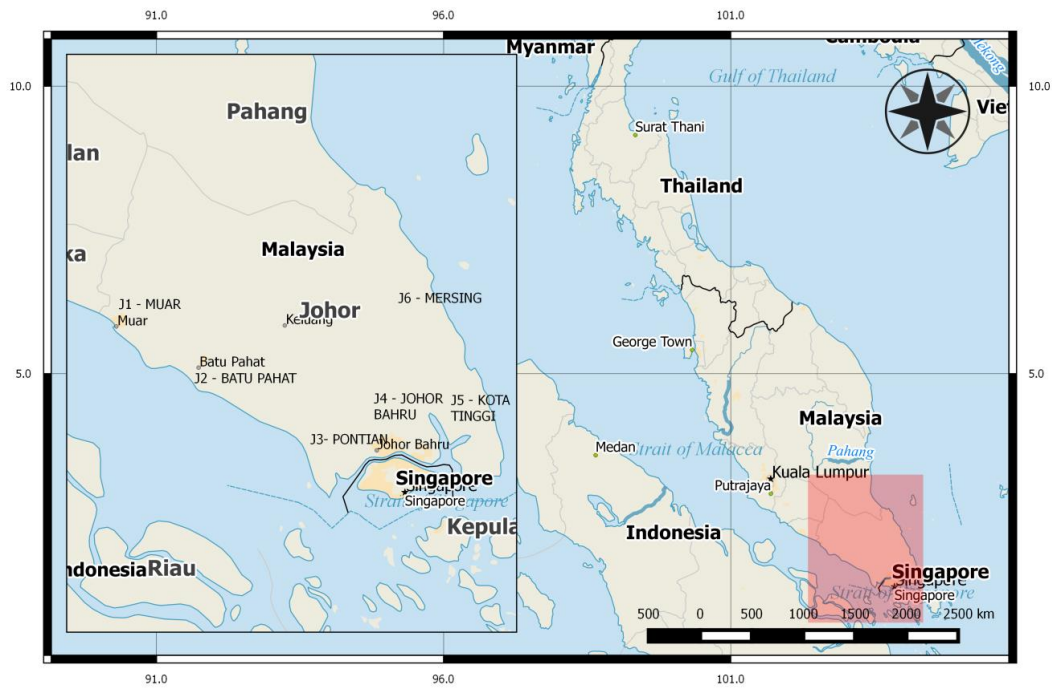


Figure 4.42: Johor state map and study location

The presentation of Johor is divided into 2 parts; the west coast Johor and east coast Johor. Figure 4.43 presents the grain size distribution plot in liquefaction margin of Johor on the west coast areas. The shoreline is found highly silt concentrated with few sand concentrated areas. About 90% of silt deposits and 40% sand of medium type are found prone to liquefaction. In contrast, Johor on the east coast areas are highly sand concentrated ranging from fine to medium type sand deposits (Figure 4.44). Both silt and sand are prone to liquefaction and found to be more than 90% of the findings, whereas only 20% of the silt is prone to liquefaction. In both findings, the gradation of deposits is found to be of uniformly graded soil in sand. Clean silt is also found in certain areas in Johor. In addition most of the prone soils are found to be located in the first 10 m depth below near ground surface.

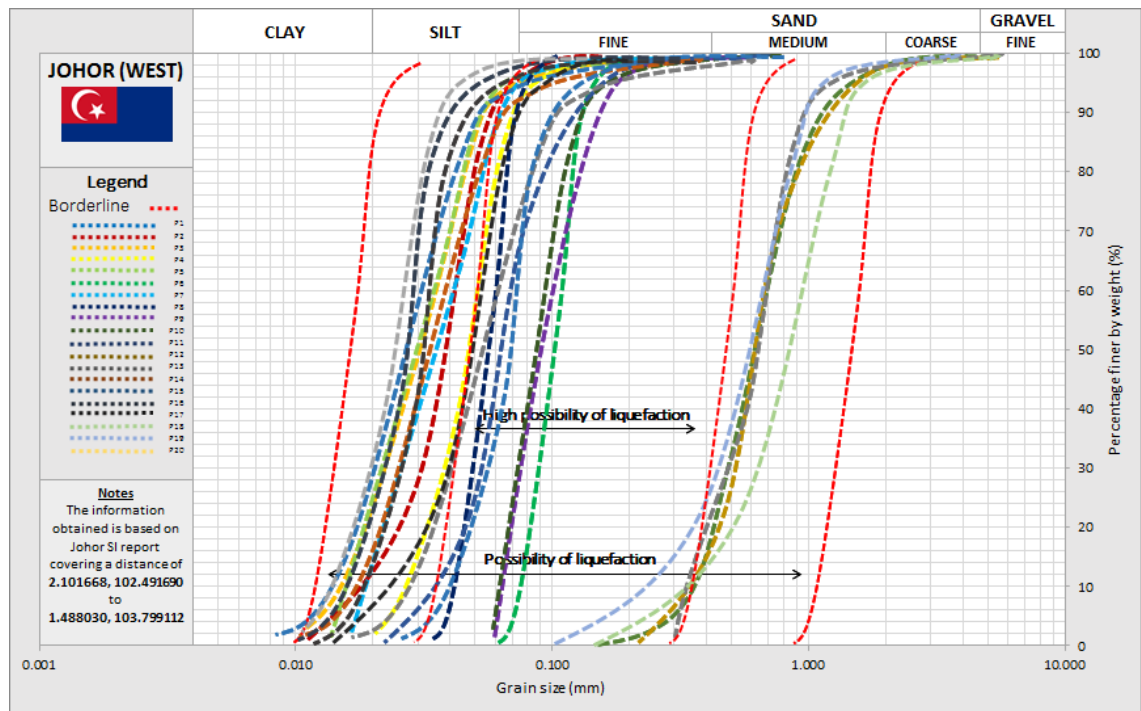


Figure 4.43: Grain size distribution plot in liquefaction margin of West Johor

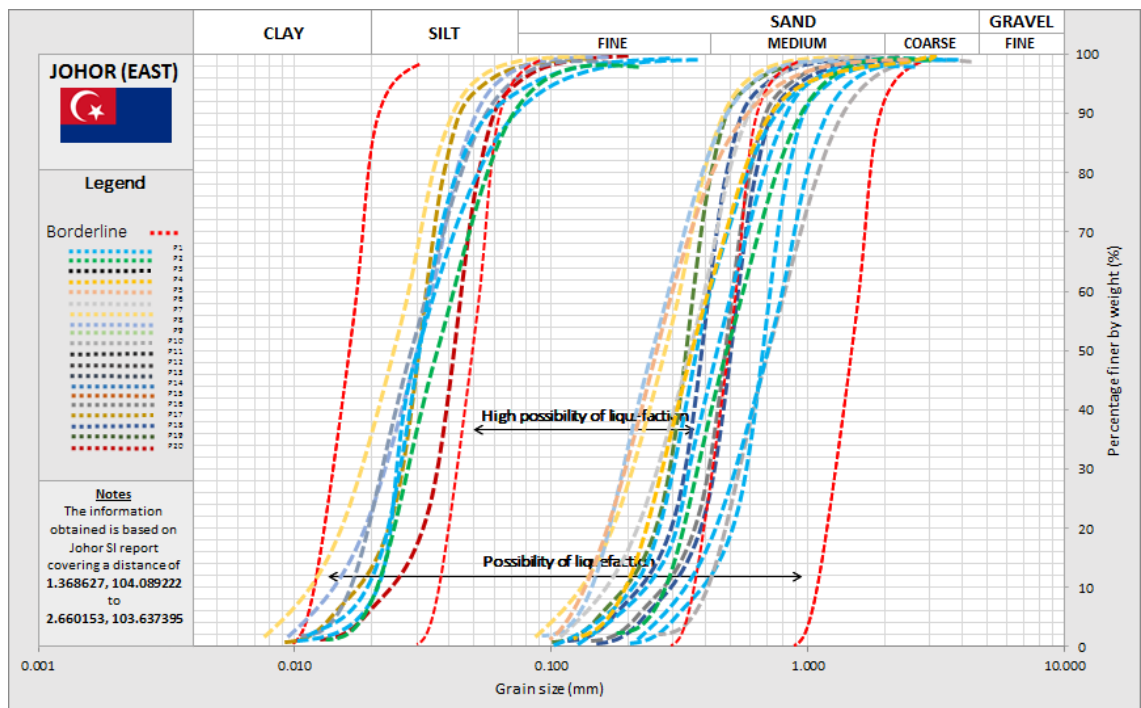


Figure 4.44: Grain size distribution plot in liquefaction margin of East Johor

The soil visualization of west Johor is presented in Figure 4.45 and Figure 4.46 in term of soil layer composition and distribution of N-SPT blow counts. In general most of the areas are not significant to liquefaction due to abundant clay deposits approximately 70% of the overall study depth except for few locations in Batu Pahat and Johor Bahru in which silt and sand are made up of the 5 m depth near ground surface level. The ground water table is in range 0.1 m – 1.5 m. The condition of soil below ground water is mostly saturated as being very close to the sea. 4 selected for discussion are Muar, Batu Pahat, Pontian and Johor Bahru. Muar are observed to be safest place in respect to liquefaction hazard as it is fully concentrated area. In Batu Pahat few areas are found to be of loose silt and sand type with very low N-SPT blow counts. Similar findings are found in Pontian as clay occupies most of the soil content. In contract Johor Bahru presents are more complicated soil composition with a mixture of 4 types of soil. The first 5 m are needed to further investigate as it shows a prone liquefaction condition. Hard stratum is defined at average 10 m depth below ground surface.

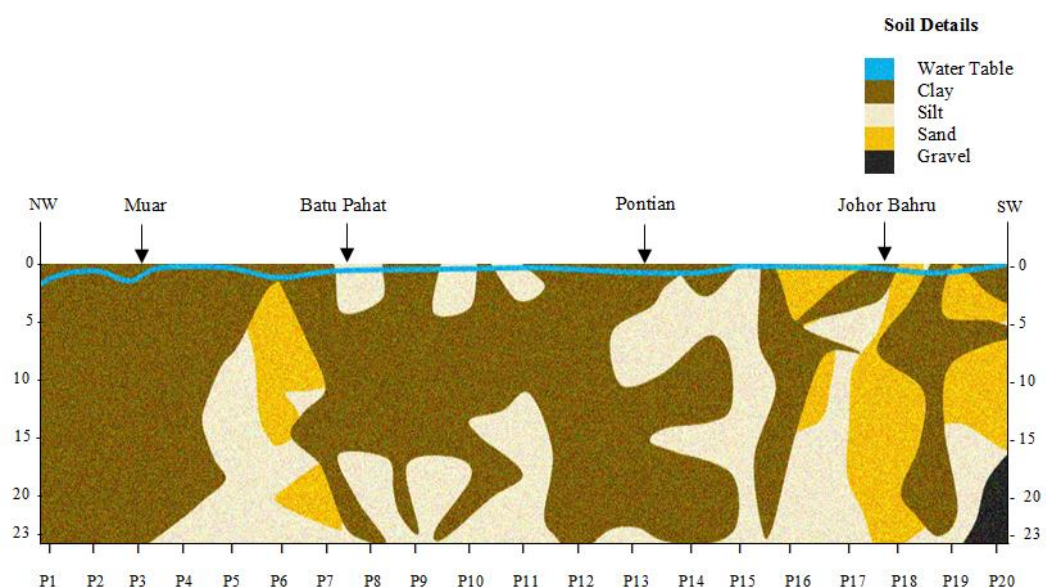


Figure 4.45: Soil layer composition of West Johor shoreline

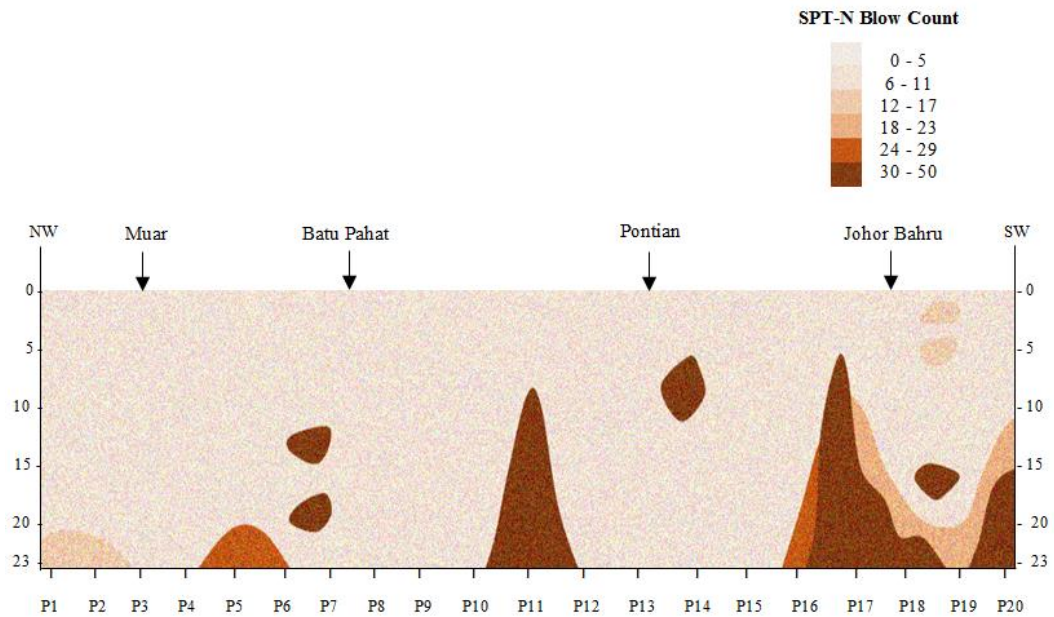


Figure 4.46: Distribution of SPT-N blow count of West Johor shoreline

Figure 4.47 and Figure 4.48 presents soil layer composition and distribution of N-SPT blow counts of east Johor consist of Kota Tinggi and Mersing. The visualization features 90% soil deposits mainly consisted of silt and sand. 5% are made out of clay and the remaining are of gravel. Water table is located near the surface are in ranged 0.1 – 2.0 m. The soil below ground water is reported to be of loose saturated particle. As the low N-SPT blow counts are found in the first 4 m below ground level, location which consist of sand and silt are observed to be prone to liquefaction. The similar information is found in Mersing except for few places, water table is found to be deeper up to 5 m below ground surface level. This condition lessens the possibility of liquefaction. Hard stratum is occupying most of the study areas with average position of 10 m below the ground. As reported earlier, port industries are being the main economy in Kota Tinggi. Proper land development of port industry is crucial as severe damage is observed in previous literatures on past earthquake-induced liquefaction events, whereas in Mersing building development is concentrated in Mersing town which is a river mouth. In

comparison with the findings for west of Johor, the hardness of soil are likely to be a major issue in the context of building development as soil improvement technique are needed in preventing from settlement in high concentrated clay areas.

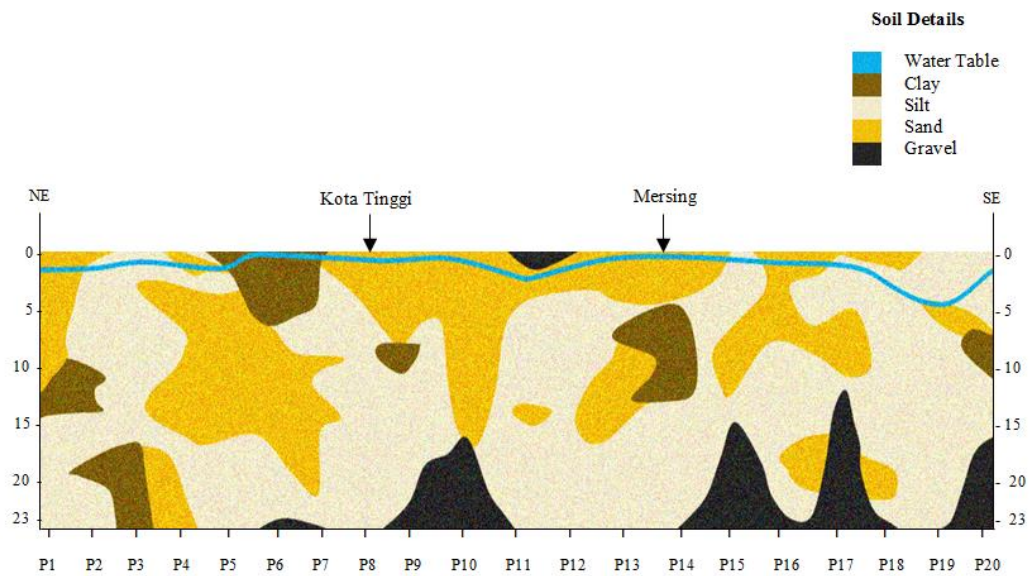


Figure 4.47: Soil layer composition of East Johor shoreline

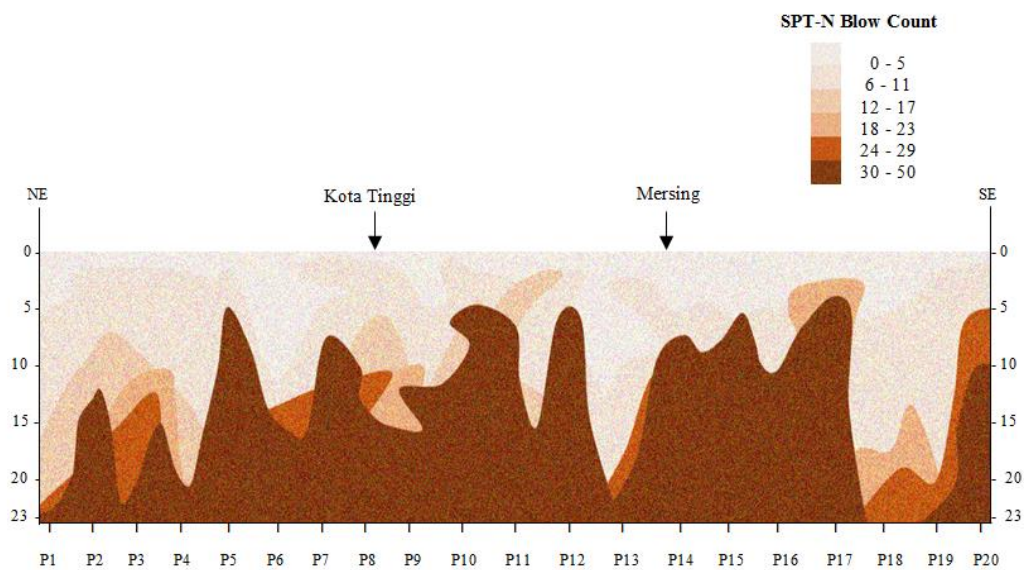


Figure 4.48: Distribution of SPT-N blow count of East Johor shoreline

4.1.9 Pahang

The 271 km shoreline is the key to the growth of its tourism and fishing industries. A multipurpose port is located 25 km to the north of Kuantan city facing the South China Sea. High population is observed at the river mouth, whereas the shoreline is dotted with resorts and scattered fishing village. Figure 4.49 presents the Pantai Cherating located in Kuantan district, Pahang.



Figure 4.49: Pantai Cherating located in Kuantan district, Pahang

Figure 4.50 presents the Pahang state map and study area. Observation being made on Kuantan shoreline areas presents concentration of sandy beach running the entire 3 main shoreline district. Due to high winds on wave currents, coastal degradation was observed in few areas in Kuantan. The natural formation due to the coastal degradation defined most of the beach area resulting in reflective and dissipative beach type of the shoreline. A collection of 103 borehole reports at 12 locations along the shoreline made it possible in addressing the first 20 meter depth of Pahang shoreline areas. Figure 4.51 presents the grain size distribution plot in liquefaction margin of Pahang soil. Most of

the sandy soil is found to be positioned within the margin with possibility of liquefaction and high possibility of liquefaction. The vulnerable soil consist mainly of fine sand deposits with very small fines contents as less than 3%.

A visual summary of the soil composition and distribution of SPT-N blow count of Pahang shoreline is presented in Figure 4.52 and Figure 4.53. Thick layer of sand up to 15 m are found at most of the shoreline district with low N-SPT blow counts whereas a thick 7 m silt are observed in Kuantan and Rompin areas. Only 10% of clay is observed in the soil content. The water table at the highlighted location is within 0.1 m to 3.0 m. There are no rocks defined in Pahang area within the first 20 m depth but a hard stratum of sand and clay are found at average 20 m below ground level. Sand deposits occupy 70% of the overall studied areas leaving another 30% silt and clay deposits. The condition of soil below water table is saturated and mostly consists of uniformly loose deposits as presented in the grain size distribution plot.

Preliminary studies conducted on Pahang shoreline areas shows significant findings in the context of soil liquefaction. The thick layer of saturated loose sand and silt deposits and near surface water table concludes the studied areas to be at high risk in liquefaction hazard. Hence the future development of shoreline areas in Pahang needs to incorporate further liquefaction assessment for proper planning of land development.

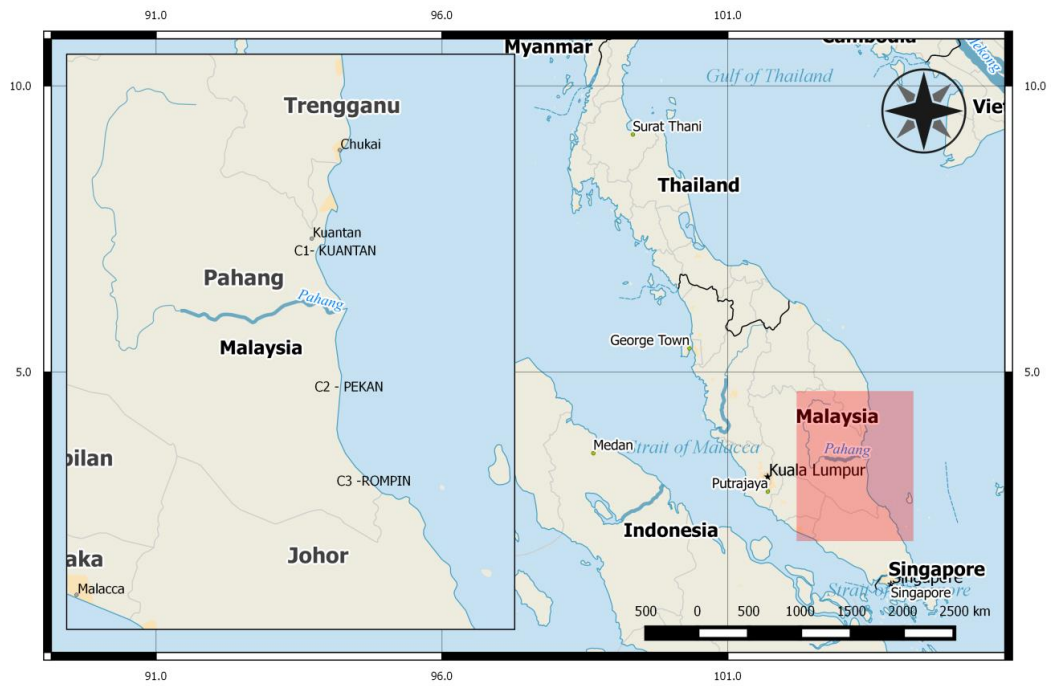


Figure 4.50: Pahang state map and study location

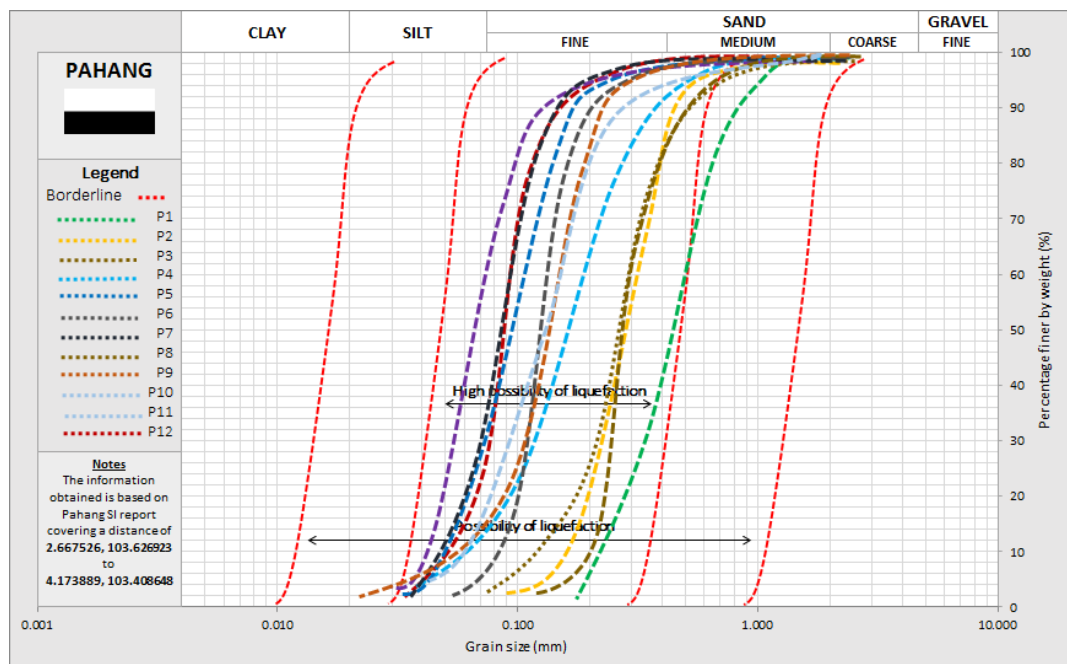


Figure 4.51: Grain size distribution plot in liquefaction margin of Pahang

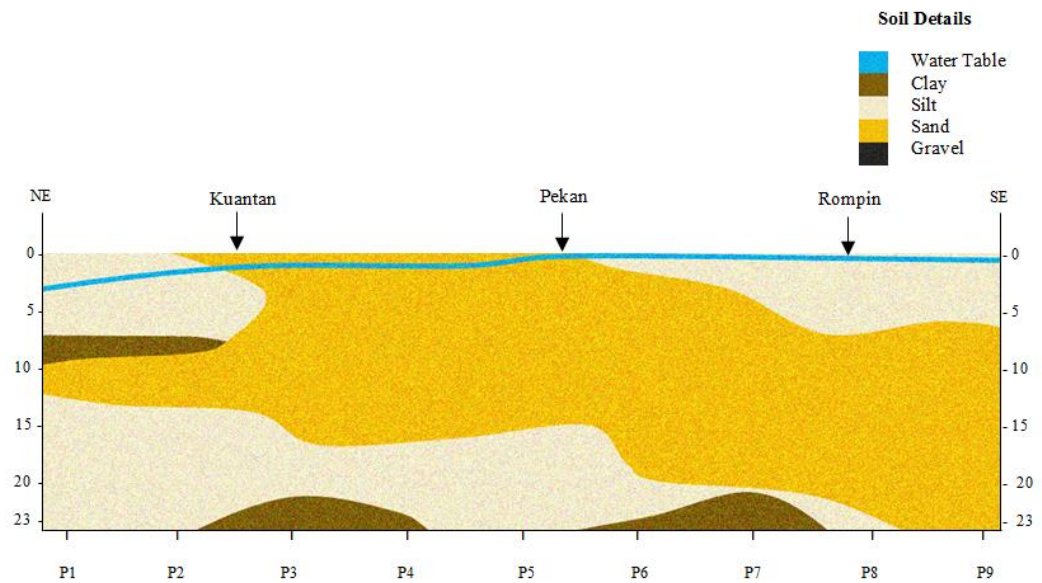


Figure 4.52: Soil layer composition of Pahang shoreline

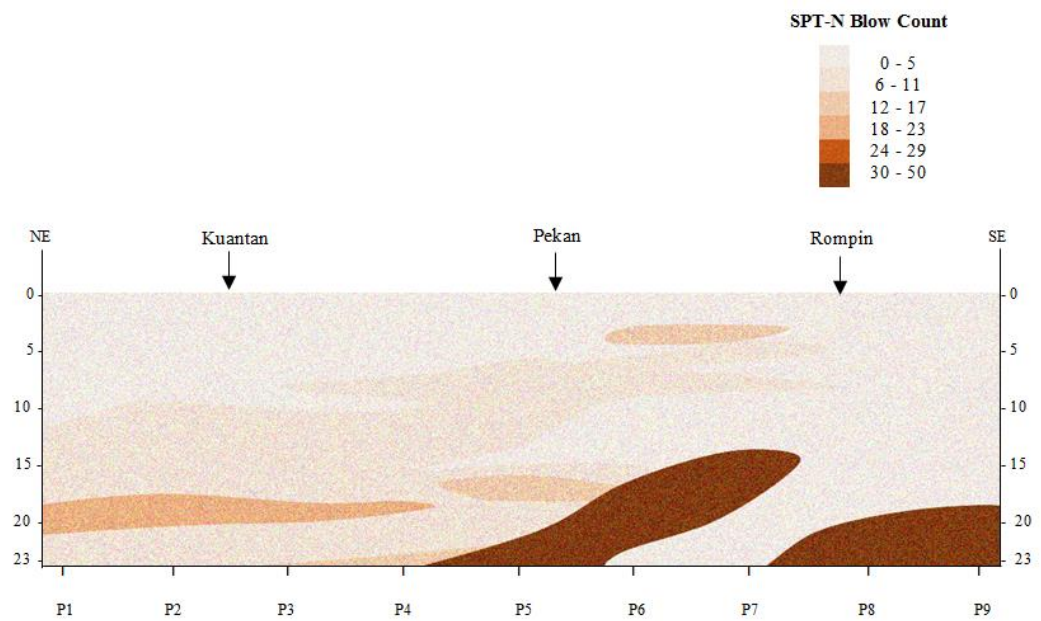


Figure 4.53: Distribution of SPT-N blow count of Pahang shoreline

4.1.10 Terengganu

Terengganu offers a wide coverage of pristine beaches stretching 244 km distance. The beach is quiet and is a home to scattering peaceful fishing village (Figure 4.54). A number of resorts located in the shoreline areas are constructed in a very simple way as to accommodate tourist and local travelers. The shoreline areas are well preserved in the northern coast districts; Besut and Setiu as there are very few development and changes in the natural environment. As the stretch line reaches the capital state of Terengganu, the beaches are no longer picture-perfect due to serious level of erosion. The erosion is caused by strong waves during monsoon season, coastal development projects and various man-made structures. Figure 4.55 present the Terengganu state map and study location.



Figure 4.54: Northern coastal area of Terengganu state

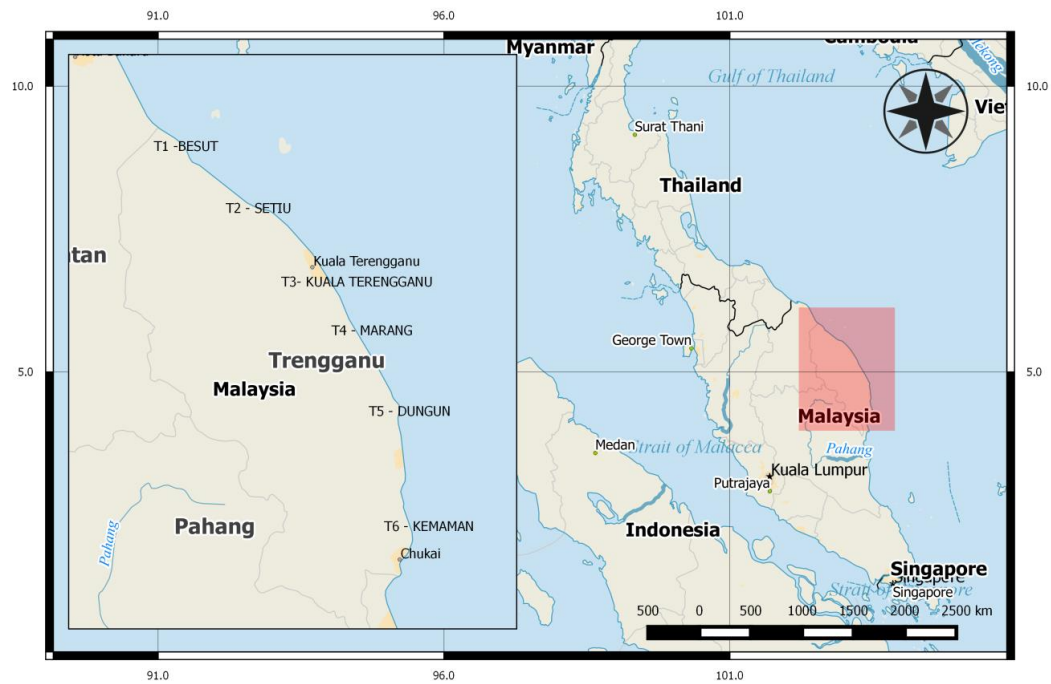


Figure 4.55: Terengganu state map and study location

A collection of 546 borehole reports at 95 locations along the shoreline made it possible in addressing the first 20 meter depth of Terengganu shoreline areas. Figure 4.56 presents the grain size distribution plot in liquefaction margin of Terengganu state. More than 95% of the soil content extracted from the soil report shows sand ranging fine to medium type prone to liquefaction. Observation made on data collection shows uniformly graded sand with very few fine contents. The size of sand is of medium type.

A visual summary of the soil composition and distribution of SPT-N blow count of Terengganu shoreline is presented in Figure 4.57 to Figure 4.58. 6 important districts are highlighted for the discussion as being the most significant observation in the soil liquefaction context. Thick layer of sand up to 20 m are found at Besut, Setiu, Marang and Kemaman. Most of the sand is of clean sand type.

Thick layer of silt up to 15 m are also observed in Marang areas. The selected areas reveal the lowest N-SPT blow count for the first 5 m depth. At the average of 20 m depth, the soil layer defined hard stratum with N-SPT blow counts more than 30. The water table at the highlighted location are within 0.1 m to 4.0 m. The beach front highlights a significant zone of saturation when observed from the SI report. This feature is one of the governing factor of soil liquefaction hazard as discussed in Chapter 2 of thesis. Clay occupies 30% of the overall studied areas leaving 70% prone condition to soil liquefaction.

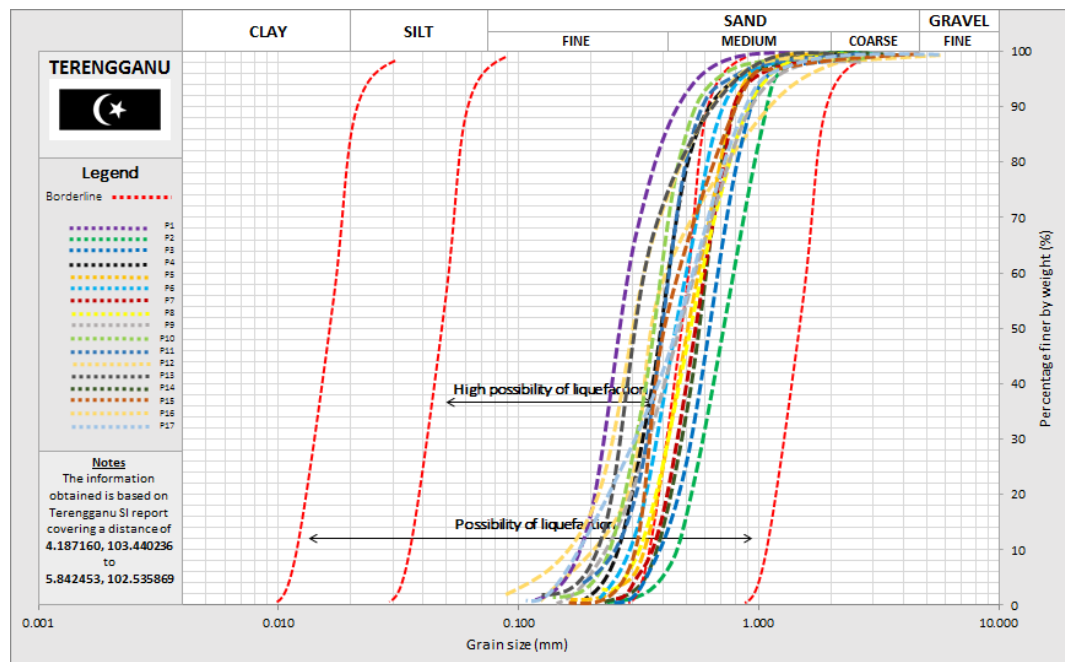


Figure 4.56: Grain size distribution plot in liquefaction margin of Terengganu

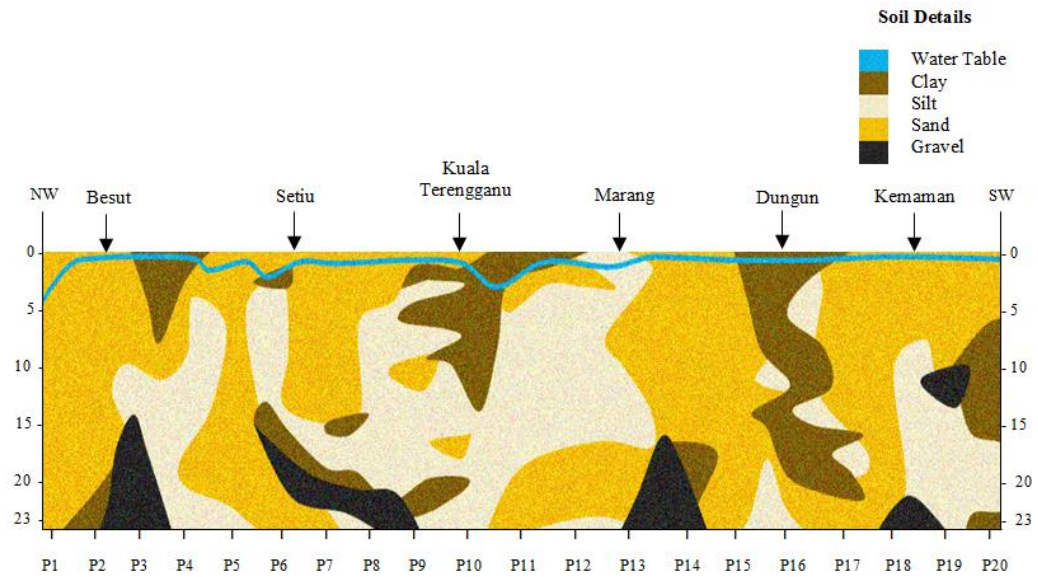


Figure 4.57: Soil layer composition of Terengganu shoreline

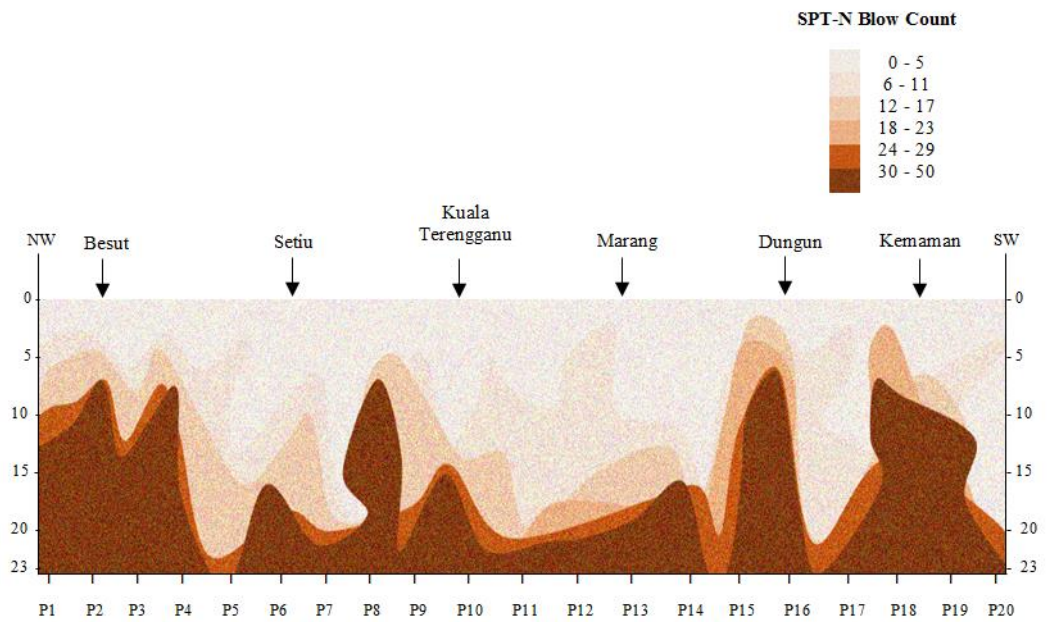


Figure 4.58: Distribution of SPT-N blow count of Terengganu shoreline

4.1.11 Kelantan

The shoreline in Kelantan state covers approximately 71 km distance and is bordered by 6 district; Tumpat, Kota Bharu, Bachok and Pasir Puteh. At the present time, a busy town overlooking the South China Sea is located in Kota Bharu. The rest of the district is in natural formation as few development observed in the areas. Due to high winds on wave currents, coastal degradation was observed in most of the studied areas. Hence rocks of varying sizes as coastal embankment are seen in protecting the shoreline areas. A collection of 341 borehole reports at 26 locations along the shoreline made it possible in addressing the first 20 meter depth of Kelantan shoreline areas. Figure 4.59 and Figure 4.60 presents the northern and southern beach location which is a picnic spot mostly to local community.



Figure 4.59: Pantai Cahaya Bulan, Tumpat district (northern area)



Figure 4.60: Pantai Irama, Bachok district (southern area)

Figure 4.61 presents the Kelantan state map and study location. Observation made on site visit shows a sandy type of beach for the entire studied shoreline district in Kelantan state.

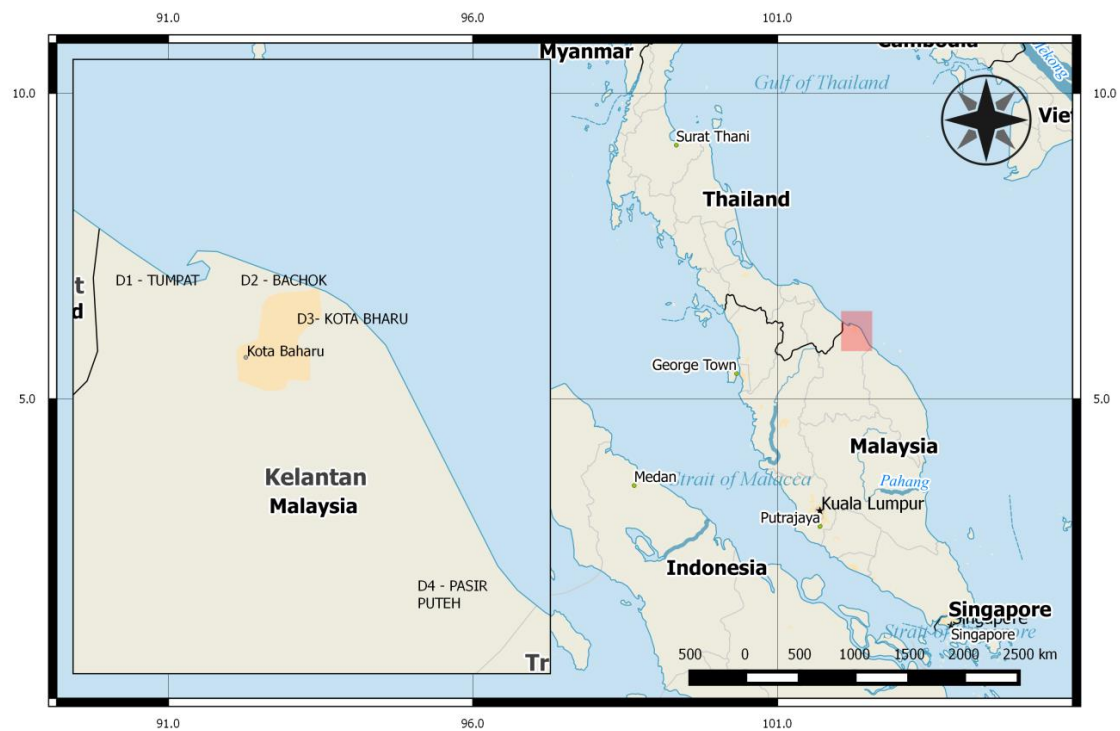


Figure 4.61: Kelantan state map and study location

Figure 4.62 presents the grain size distribution plot in liquefaction margin of Kelantan state. More than 97% of the soil content extracted from the soil report shows sand prone to liquefaction at the first 10 m depth. The type of sand are mostly consist of medium type sand similar to the findings in Terengganu state. In addition, the information obtained presents saturated loose sand deposits of uniformly graded particles near ground level in which the condition is vulnerable to soil liquefaction.

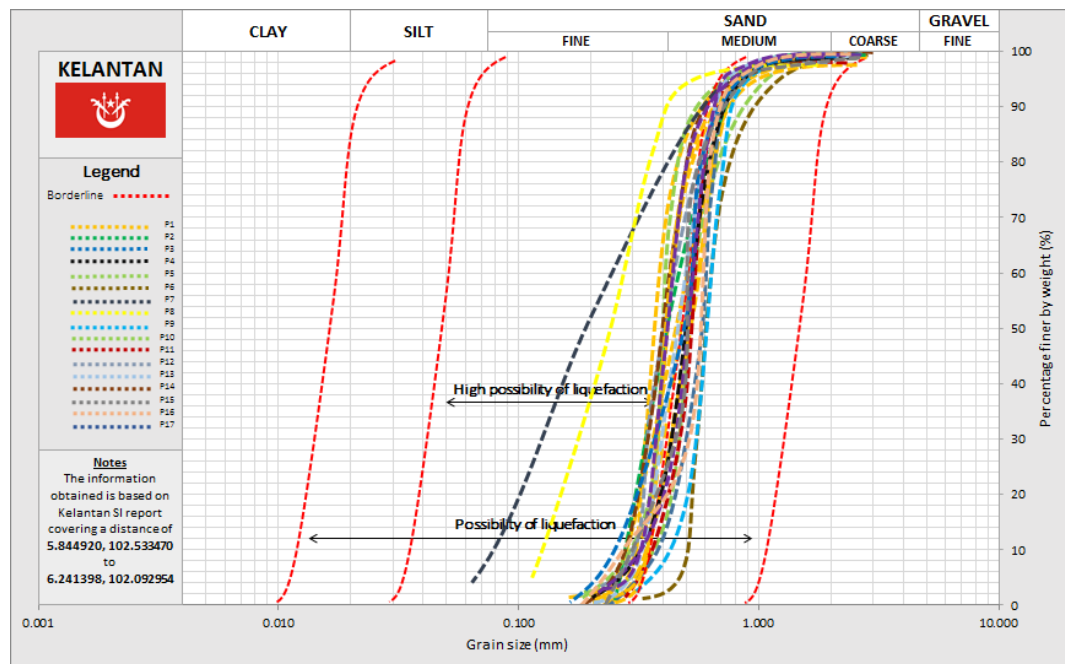


Figure 4.62: Grain size distribution plot in liquefaction margin of Kelantan

A visual summary of the soil composition and distribution of SPT-N blow count of Kelantan shoreline is presented in Figure 4.63 to Figure 4.64. 4 important districts are highlighted for the discussion as being the most significant observation in the soil liquefaction context. Thick layer of sand up to 6 m at all the shoreline district. Thick layer of silt up to 6 m are also observed in Tumpat areas. The selected areas reveal the lowest N-SPT blow count for the first 6 m depth. The water table at the highlighted

location are within 0.1 m to 2.0 m. Clay occupies 20% of the overall studied areas leaving 80% prone condition to soil liquefaction.

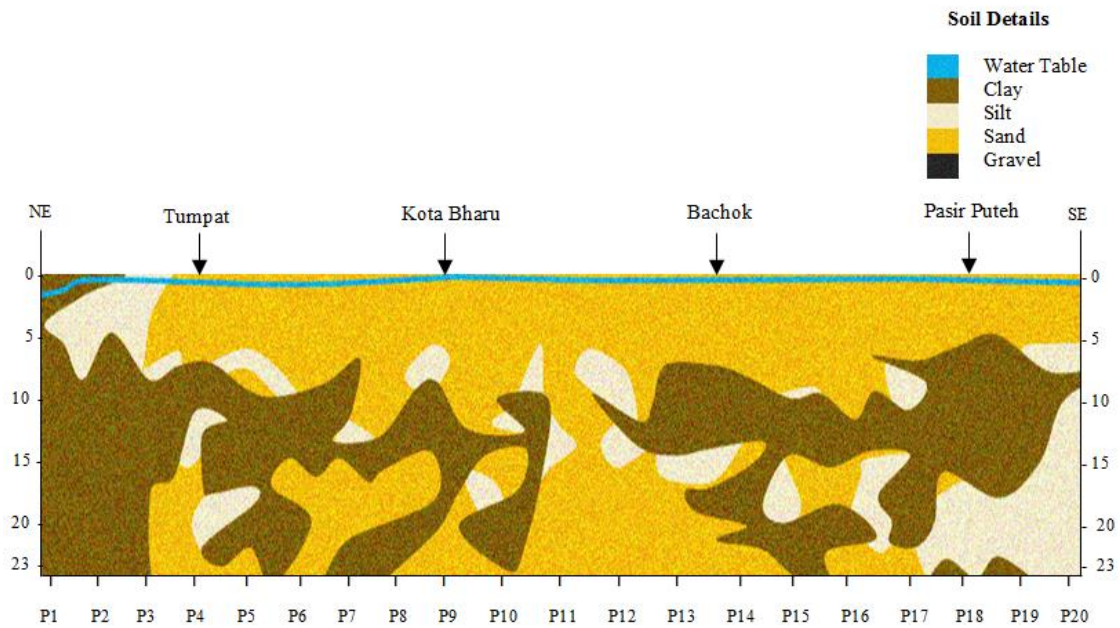


Figure 4.63: Soil layer composition of Kelantan shoreline

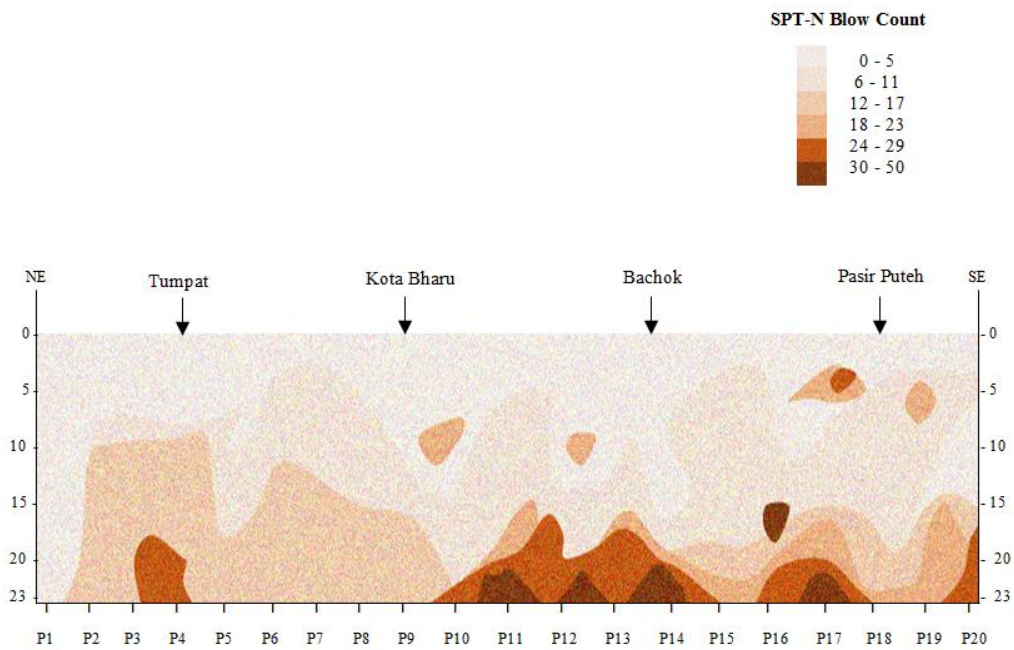


Figure 4.64: Distribution of SPT-N blow count of Kelantan shoreline

4.1.12 Susceptibility of Soil at Study Location

Based on site visit and secondary data collection, this section concludes overall findings in a table presentation. Simple tabulated approach is applied in developing this section by considering factors which likely to aid further investigation on liquefaction context in the studied areas. Hence a decision-making process is being made for studied area in whether a site needs to be evaluated for further liquefaction analysis or not. For preliminary liquefaction assessment study, 3 significant tables are presented for the decision-making process. The first tabulated findings are Table 4.1 which presents the significant contribution from general shoreline description view. The tabulated result from site visit and survey includes the selected basic parameters; type of beach, district area, district population and main economy of the studied area. The overall findings conclude the typical shoreline details of the area in providing information for further details of the areas.

The type of beach prone to liquefaction based on literatures is consisted of loose saturated deposits (Cubrinovski et al., 2011; Trifunac, 2003). Hence a sandy and muddy type beach should be highlighted as possible contributing aspect to soil liquefaction hazard. The population plays an important aspect whereby as population increase result in expansion of built environment. Reclaimed land could be motivated with demand from population (Tokimatsu & Asaka, 1998) . Lastly is the economy aspect which presents significant main activity along shoreline. The crucial economy is found to be port industries and coastal city that leads to the risk of soil liquefaction hazard (Tokimatsu et al., 2012). The increase population observed at river mouth where busy town is located motivates the land usage of nearby areas including the opening of reclaimed land in catering iconic projects and the upgrading of coastal road to cater increasing traffic found in the west coast area.

The second table is Table 4.2 presents the susceptibility of soil at studied shoreline area. The studied parameter in developing the table includes soil type, sand depth, soil grading, ground water table and fine content. As presented in earlier discussion, sand is mostly found in the east coast areas whereas silt concentration is high in the west coast area which defines most of the mud beach areas. The second table is most crucial in screening a site with preliminary findings. Concentration of high sand content in shoreline areas should be given a priority in soil liquefaction screening (Lade, 1992). The depth of loose deposits is another contributing aspect to hazard. The propagation of waves in loose deposit amplifies greatly compared to compact deposits. Depth of vulnerable soil deposit within the first 20 m from ground surface needs full attention (Arion et al., 2015). The gradation of soil which is significant is uniformly distributed or termed as 'clean sand'. The stability drastically reduced when subjected to ground motion (Aydan et al., 2012). Another aspect is the GWT. Sites having water table near surface is reported to be at risk to hazard (up to 2.0 m) (Cubrinovski et al., 2011). Moreover Kishida (1969) reported liquefaction of soils with up to 70% fines content can occur just like during Mino-Owari, Tohankai and Fukui earthquakes.

Lastly is the decision-making process presentation in Table 4.3. The parameters involves is the existing development, MMI, future development and remarks. The development aspect noted some significant changes in the land usage which can be a risk to hazard (Ashford et al., 2011; Aydan et al., 2012). The uncertainties in the changing environment enhanced the risk hence MMI scale with more than III level defines an important aspect in the factors leading to soil liquefaction (Papathanassiou et al., 2012). The remarks in Table 4.3 relates back to all 3 tables presented. The more significant aspect is fulfilled result in priority in the liquefaction analysis. Figure 4.65 and Figure 4.66 presents the compiled graphical illustration of the ground water table measurement.

Table 4.1: General information of shoreline areas

Code Area	Type of beach	District Area (km²)	District Population	Economy
R1	sandy	810	225 630	Main port
K1	sandy	479	92 784	Tourism
K2	muddy/sandy	946	214 479	Prawn Farming
K3	muddy/sandy	665	357 176	Main Jetty
K4	muddy/sandy	246	66 606	Fishery
K5	muddy/sandy	923	443 488	Fishery
P1	sandy	295	510 996	Main City/Tourism
P2	muddy/sandy	755	818 197	Industrial/Commercial Hub
A1	muddy/sandy	958	120 192	Agricultural
A2	muddy/sandy	2095	245 015	Agricultural
A3	muddy/sandy	1168	211 113	Tourism/Fishery
A4	muddy/sandy	1752	128 143	Agricultural/Fishery
B1	muddy/sandy	1056	46 354	Fishery
B2	muddy/sandy	1195	205 257	Tourism/Fishery
B3	muddy/sandy	573	744 062	Main port
B4	muddy/sandy	885	220 214	Tourism/Fishery
B5	muddy/sandy	612	207 354	Tourism
N1	sandy	6686	110 991	Tourism
M1	sandy	660	173 712	Tourism/Fishery
M2	sandy	314	484 885	Industrial/Commercial Hub
M3	sandy	679	131 539	Tourism/Fishery
J1	muddy	1376	239 027	Tourism/Fishery
J2	muddy	1873	401 902	Tourism/Fishery
J3	muddy	907	149 938	Tourism/Fishery
J4	sandy	1816	1 334 188	Tourism/Fishery
J5	sandy	3489	187 824	Tourism/Fishery
J6	sandy	2836	69 028	Tourism/Fishery
C1	sandy	3805	105 587	Tourism/Fishery
C2	sandy	2960	443 796	Tourism/Fishery
C3	sandy	5296	109 848	Tourism/Fishery
T1	sandy	243	136 563	Tourism/Fishery
T2	sandy	1360	54 563	Tourism/Fishery
T3	sandy	605	337 553	Tourism/Fishery
T4	sandy	666	95 283	Tourism/Fishery
T5	sandy	2735	149 851	Tourism/Fishery
T6	sandy	2536	166 750	Main port
D1	sandy	170	147 179	Fishery
D2	sandy	403	468 438	Fishery
D3	sandy	280	126 350	Fishery
D4	sandy	434	113 191	Fishery

Table 4.2: The susceptibility of soil at studied area

Code Area	Soil Type	Sand/Silt Depth (m)	Soil Grading	Ground Water Table (m)	Fine content %
R1	Sand/Silt	> 20	uniform	Full	1
K1	Sand/Silt	< 10	uniform	Full	1
K2	Sand/Silt	< 10	uniform	Full	12
K3	Sand/Silt	< 10	uniform	Full	20
K4	Sand/Silt	< 10	uniform	Full	2
K5	Sand/Silt	< 10	uniform	1.35	11
P1	Sand	> 20	uniform	0.40	1
P2	Sand	> 20	uniform	1.70	1
A1	Sand/Silt	> 20	uniform	0.50	9
A2	Sand/Silt	15-20	uniform	Full	11
A3	Sand/Silt	> 20	uniform	0.12	2
A4	Sand/Silt	15-20	uniform	0.09	3
B1	Sand/Silt	> 20	uniform	0.47	1
B2	Sand/Silt	> 20	uniform	2.20	4
B3	Sand/Silt	> 20	uniform	0.44	3
B4	Sand/Silt	15-20	uniform	Full	3
B5	Sand/Silt	> 20	uniform	Full	7
N1	Sand /Silt	< 10	uniform	2.00	9
M1	Sand/Silt	< 10	uniform	1.00	11
M2	Sand/Silt	< 10	uniform	Full	2
M3	Sand/Silt	< 10	uniform	Full	19
J1	Silt	< 10	uniform	0.60	1
J2	Silt	15-20	uniform	Full	5
J3	Silt	< 10	uniform	Full	2
J4	Sand /Silt	15-20	uniform	Full	1
J5	Sand /Silt	< 10	uniform	Full	1
J6	Sand /Silt	15-20	uniform	Full	2
C1	Sand	> 20	uniform	Full	4
C2	Sand	< 10	uniform	1.12	6
C3	Sand	> 20	uniform	0.20	1
T1	Sand	> 20	uniform	Full	5
T2	Sand	> 20	uniform	Full	1
T3	Sand	> 20	uniform	Full	6
T4	Sand	> 20	uniform	Full	1
T5	Sand	> 20	uniform	Full	1
T6	Sand	> 20	uniform	Full	1
D1	Sand	15-20	uniform	Full	1
D2	Sand	15-20	uniform	Full	1
D3	Sand	> 20	uniform	Full	1
D4	Sand	15-20	uniform	0.20	2

Table 4.3: Decision making process for soil liquefaction screening

Code Area	Existing Development	Future Development	MMI Scale	Remarks on Liquefaction Evaluation
R1	town/remote	Port Expansion	V	Further Analysis
K1	town/remote	Tourism	V	Further Analysis
K2	town/remote	Coastal Road	V	Further Analysis
K3	city	Coastal Road	V	Further Analysis
K4	town/remote	Coastal Road	V	Further Analysis
K5	town/remote	Coastal Road	V	Further Analysis
P1	city	Reclaimed Land	VI	Further Analysis
P2	town/remote	Coastal Road	VI	Further Analysis
A1	town/remote	Coastal Road	VI	Further Analysis
A2	town/remote	Coastal Road	VI	Further Analysis
A3	town/remote	Coastal Road/Tourism	VI	Further Analysis
A4	town/remote	Coastal Road	VI	Further Analysis
B1	town/remote	Coastal Road	VI	Further Analysis
B2	town/remote	Coastal Road	VI	Further Analysis
B3	city	Port Expansion	VI	Further Analysis
B4	town/remote	Coastal Road	VI	Further Analysis
B5	town/remote	Coastal Road/Tourism	VI	Further Analysis
N1	town/remote	Coastal Road/Tourism	V	Further Analysis
M1	town/remote	Coastal Road	V	Further Analysis
M2	city	Reclaimed Land	V	Further Analysis
M3	town/remote	Coastal Road	V	Further Analysis
J1	town/remote	Coastal Road	VI	Further Analysis
J2	city	Coastal Road	VI	Further Analysis
J3	town/remote	Coastal Road	VI	Further Analysis
J4	city	Reclaimed Land	VI	Further Analysis
J5	town/remote	Port Expansion	VI	Further Analysis
J6	town/remote	Tourism	VI	Further Analysis
C1	town/remote	Coastal Road	III	Further Analysis
C2	city	Reclaimed Land	III	Further Analysis
C3	town/remote	Coastal Road	IV	Further Analysis
T1	town/remote	Coastal Road	IV	Further Analysis
T2	town/remote	Coastal Road	IV	Further Analysis
T3	city	Reclaimed Land	IV	Further Analysis
T4	town/remote	Coastal Road /Tourism	IV	Further Analysis
T5	town/remote	Port Expansion	IV	Further Analysis
T6	town/remote	Port Expansion	IV	Further Analysis
D1	town/remote	Coastal Road	IV	Further Analysis
D2	city	Coastal Road	IV	Further Analysis
D3	town/remote	Coastal Road	IV	Further Analysis
D4	town/remote	Coastal Road	IV	Further Analysis

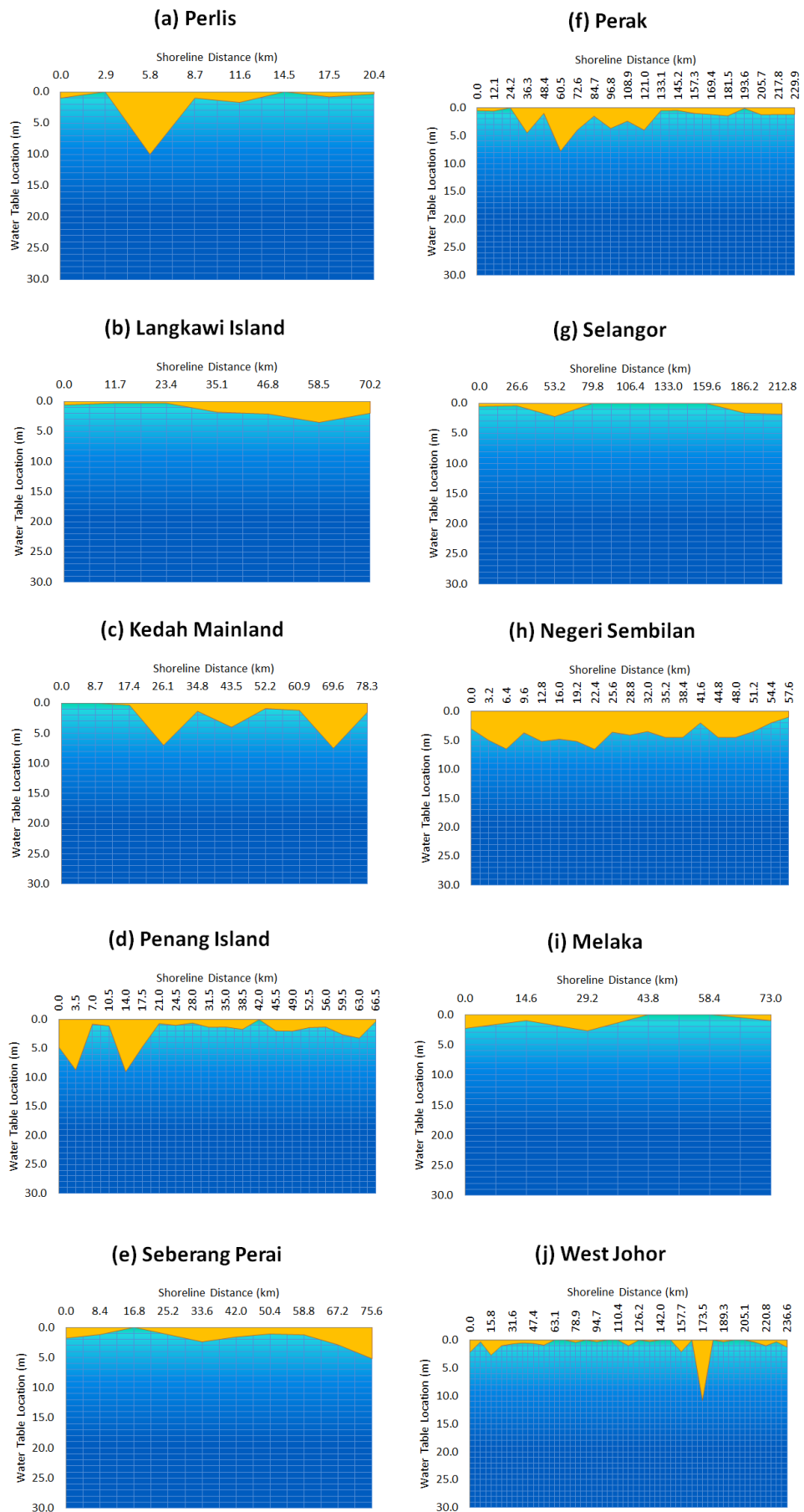


Figure 4.65: Ground water table location for west coast areas

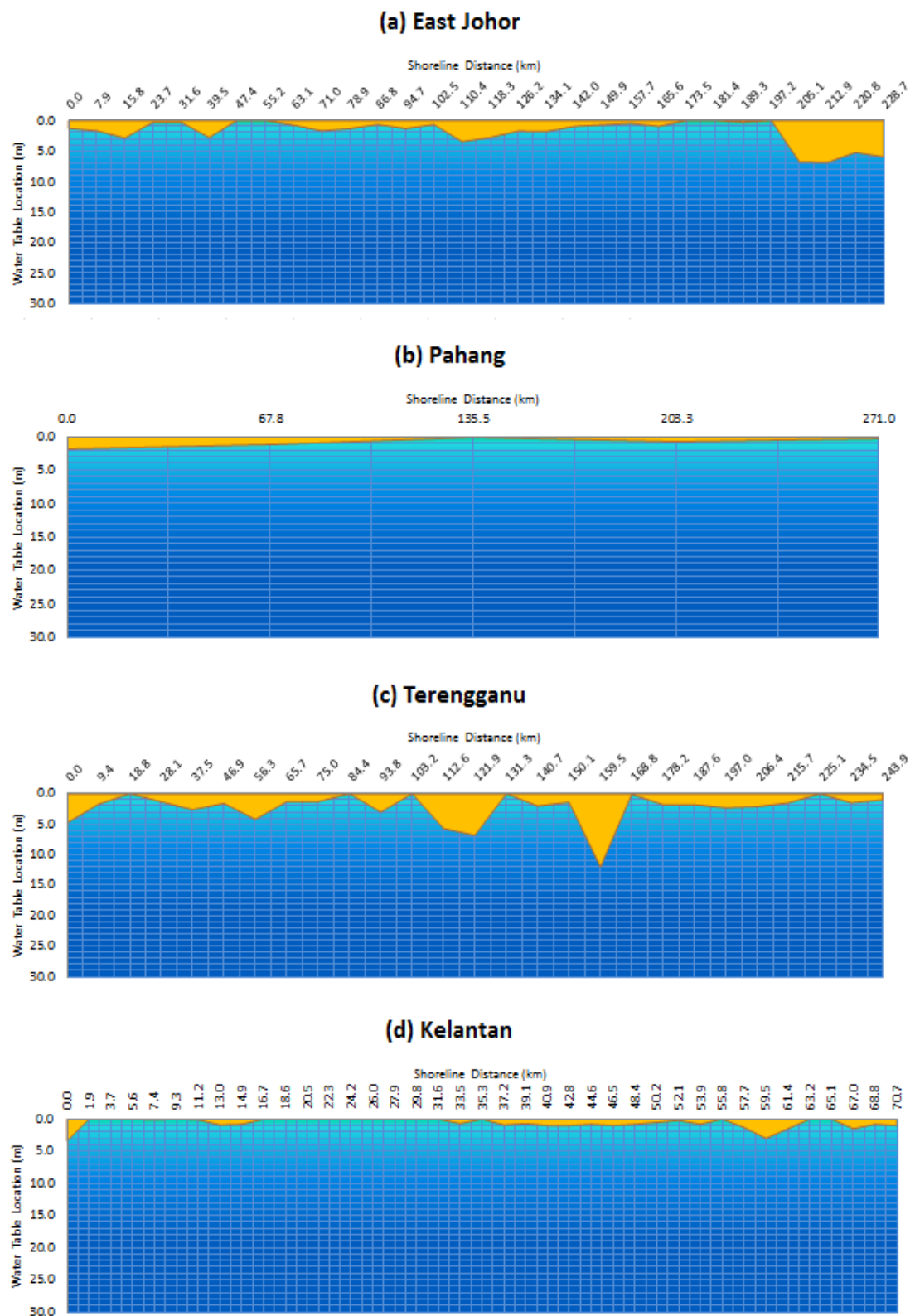


Figure 4.66: Ground water table location for east coast areas

4.1.13 Summary

The initiation of liquefaction hazard in Peninsular Malaysia is affected by a number of parameters. A comprehensive investigation was undertaken to determine the findings of liquefaction susceptibility factors; soil details and ground water table of shoreline districts in Peninsular Malaysia. The conclusion is highlighted in point form as follows:

1. Sandy type beaches occupy almost 90% of east shoreline areas whereas muddy type beaches are found on the west shoreline areas. The soil deposit which is vulnerable to soil liquefaction is found highly concentrated at almost all the studied location near surface ground level.
2. Sand with very little fine content in the particle gradation study are found in 90% study location which in general define a uniformly graded material vulnerable to soil liquefaction hazard.
3. Clean sand and silt found from site investigation report increase the risk of hazard and enhance further investigation to be carried out in the selected areas.
4. The location of ground water table near surface at studied location makes a wider coverage of the hazard as most of the deposit underlying the water table is in saturated condition

5. The expansion and increasing of reclaimed land observed in selected state shows significant changes in the natural environment which will lead to more uncertainties in the surrounding areas.
6. In the present condition, the east coast areas are less significant to hazard in general due to few developments compared to the west coast areas with iconic project built on reclaimed land although the east coast are highly sand concentrated. Without proper consideration on the soil liquefaction hazard effect in the development design, future development and valuable assets are at stake with the uncertainties from the environment.
7. Proper management of the shoreline areas are needed in providing safe environment for the community. Hence guideline on hazard information needs to be reached out to local authorities and community of the ground condition.
8. All the studied areas along the shoreline areas of Peninsular Malaysia shows significant indicator for further liquefaction evaluation.

4.2 Cyclic Triaxial Test

The soil performance is observed from cyclic triaxial test. The main result is to obtain the dynamic properties of sample mainly the modulus reduction and damping ratio curve.

4.2.1 Soil Liquefaction Observation

Figure 4.67 to Figure 4.70 shows the dynamic response of regional sand. The cyclic deviator stress was applied with a frequency of 1 Hz and amplitude value of 0.5. An approximation of 0.5 kN continuous axial force is observed. For the test, the initial cell pressure and backpressure were 350 kPa and 250 kPa respectively. The confining pressure is calibrated to 100 kPa. Based on 400 cycles of applied axial stress, Figure 4.67 presents the plot of deviator stress versus number of cycle of load application. Due to the loading applied, a continuous deviator stress is observed until the setup reaches 400 cycles. The nature of axial strain, pore pressure and axial deformation due to the loading is shown in Figure 4.68 to Figure 4.70. By using the Terzaghi's principle, when the pore pressure equals to the confining pressure which will result in zero effective confining pressure, this notes one of the termination criteria in soil liquefaction. Another criteria is when the axial strain exceeded 20% which is a condition of a liquefy state. In Figure 4.68, after about 387 cycles, the axial strain exceeded 20%. However the pore pressure becomes equal to the confining pressure at 233 cycles (Figure 4.69). The pore pressure is observed constant after reaching the confining pressure. This condition can be explained with the remaining resistance of the soil to deform and also to the fact that the soil dilates. During dilation the pore pressure is reduces and helps stabilization of soil under loading as mentioned in Seed (1979) and commonly known as cyclic mobility. Figure 4.70 present the plot of axial displacement versus number of cycle of load application. As the stress continuously applied on sand, the deformation of soil is observed in linear behavior similar to the plot of axial strain (Figure 4.68). As the axial

strain reaches 20%, the deformation of soil reaches more than 10 mm. Hence the termination criteria for this result are based on the 20% axial strain.

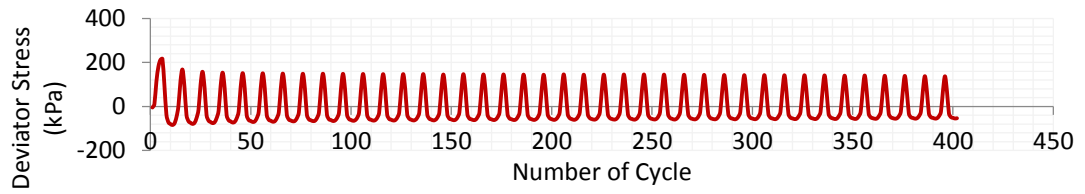


Figure 4.67: Plot of deviator stress vs number of cycle of load application (sand)

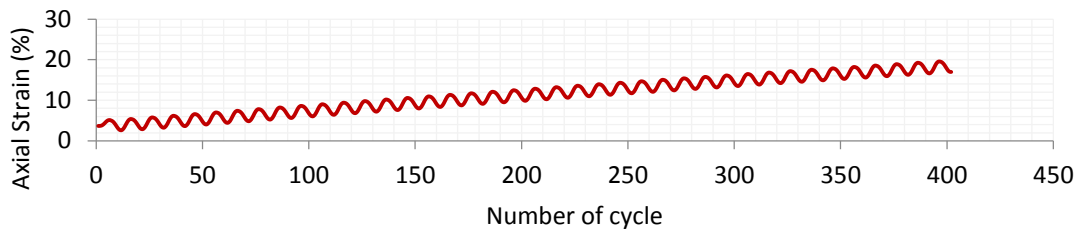


Figure 4.68: Plot of axial strain vs number of cycle (sand)

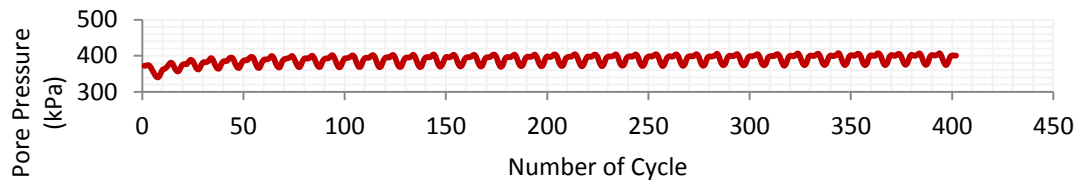


Figure 4.69: Plot of pore pressure vs number of cycle (sand)

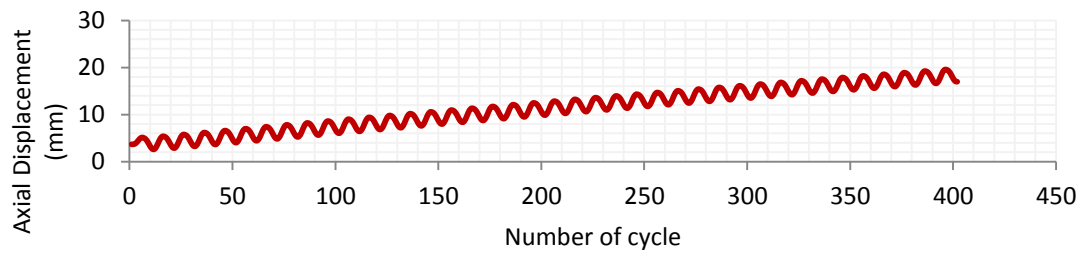


Figure 4.70: Plot of axial displacement vs number of cycle (sand)

Another similar test setup is conducted using clay samples. Figure 4.71 to Figure 4.73 presents the plots of clay behavior towards cyclic loading. The deviator stress plot is similar as presented in Figure 4.67. In contrast, clay presents insignificant findings in the soil liquefaction context. The axial strain and axial displacement is very small compared to the findings in sand samples. As for the pore pressure, there is only a slight increase as the cycle reaches 400. Moreover the pore pressure is very low. The nature of clay with high fine particles makes it not susceptible to soil liquefaction.

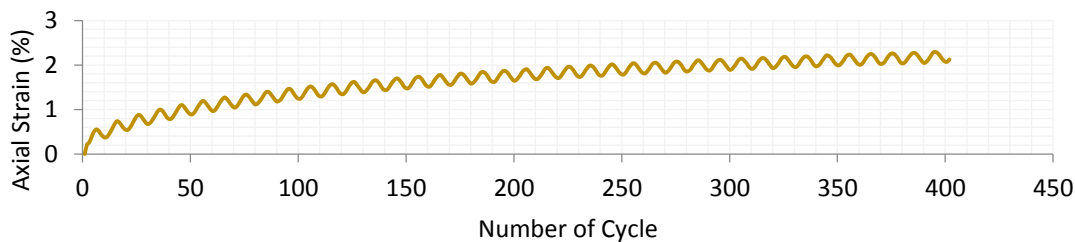


Figure 4.71: Plot of axial strain vs number of cycle (clay)

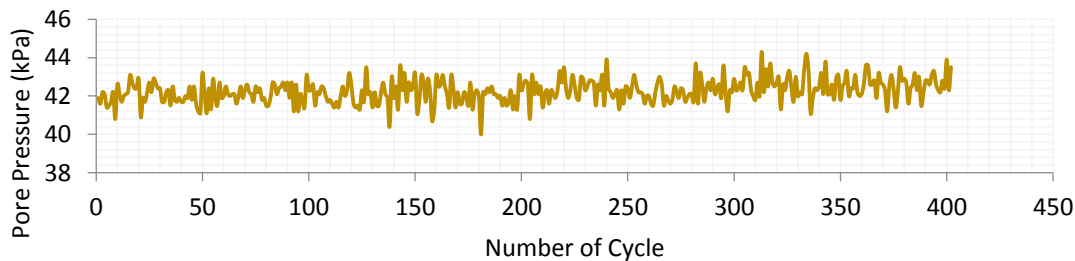


Figure 4.72: Plot of pore pressure vs number of cycle (clay)

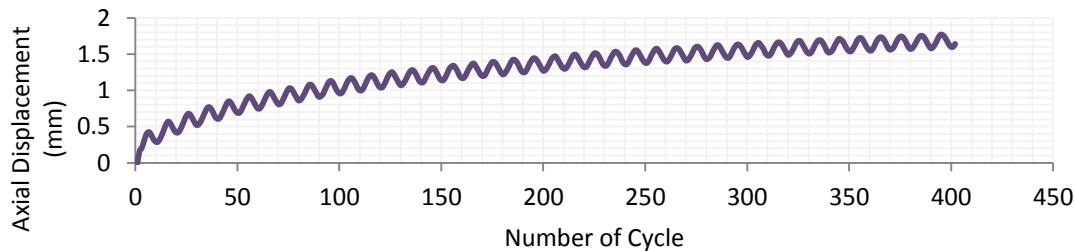


Figure 4.73: Plot of axial displacement vs number of cycle (clay)

4.2.2 Stress-Strain Behavior

The stress-strain behavior of sand and clay subjected to control loading is presented in Figure 4.74 and Figure 4.75 respectively. In general, it can be observed that an increase in the cyclic stress leads to an increase in the axial strain. From the figures, a decrease in the modulus and increase in the hysteresis loop area indicates material degradation. The degradation is faster in sand with observed increased area of hysteresis loop compared to clay samples. This emphasized the significant features of sand as a deposit which is highly susceptible to soil liquefaction.

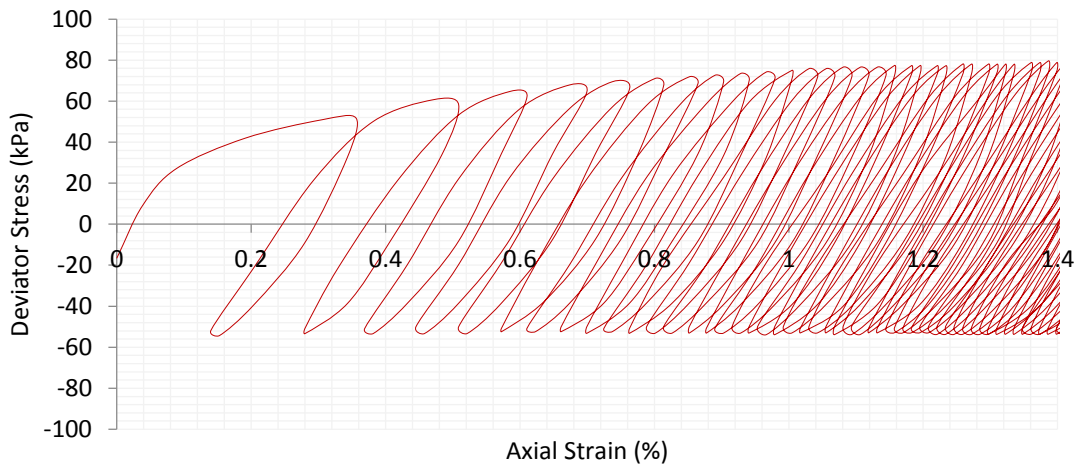


Figure 4.74: Stress-strain behavior of sand subjected to controlled loading

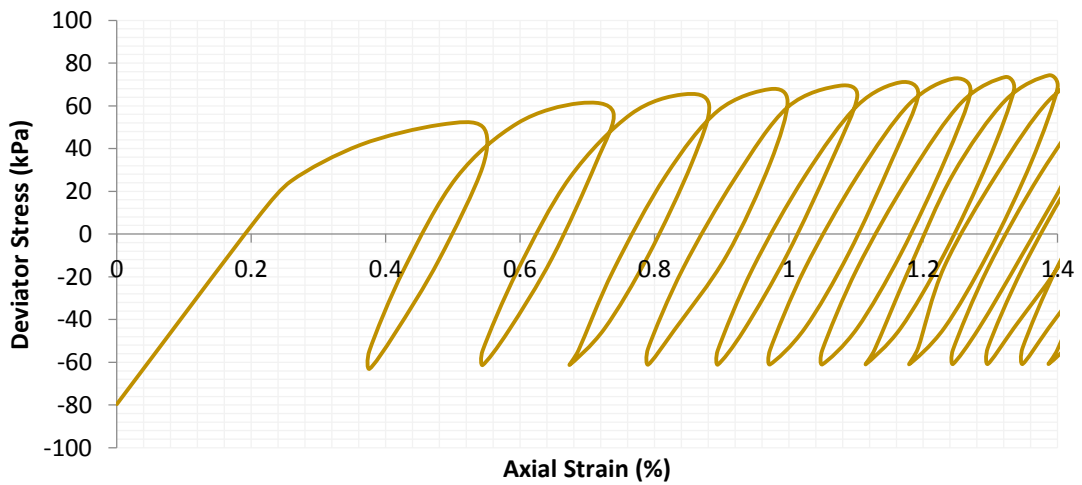


Figure 4.75: Stress-strain behavior of clay subjected to controlled loading

4.2.3 Shear Modulus Reduction and Damping Ratio Curves

Based on the hysteresis loop in Figure 4.74 and Figure 4.75, the shear modulus reduction and damping ratio curves are developed. Figure 4.76 and Figure 4.77 presents the shear modulus reduction curves of sand and clay respectively. The shear modulus reduction curve for sand obtained has shown good agreement with the previous published work. Both sand and clay are greatly depends on shear strain. The shear modulus was found decreasing with the increasing shear strain. As the strain increases, the material indicates loss of stiffness. At any level of strain, the shear modulus of sand is lesser than the shear modulus of clay.

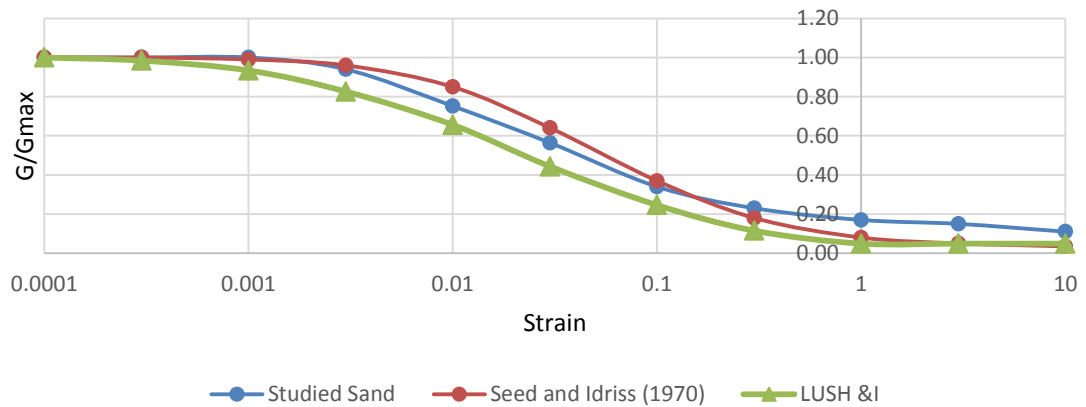


Figure 4.76: Shear modulus reduction curve for sand

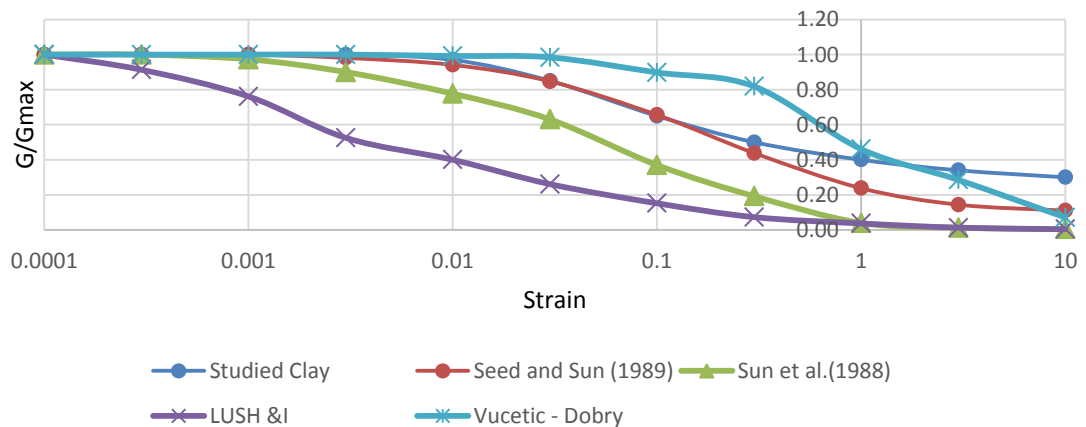


Figure 4.77: Shear modulus reduction curve for clay

Figure 4.78 and Figure 4.79 presents the damping ratio curves of sand and clay respectively. At smaller cyclic shear strains, the damping ratio of clay is higher than the damping ratio in sand, while at larger shear strains, the damping ratio of clay is lower than the damping ratio in sand. This behavior is close to a study conducted by Idriss (1990).

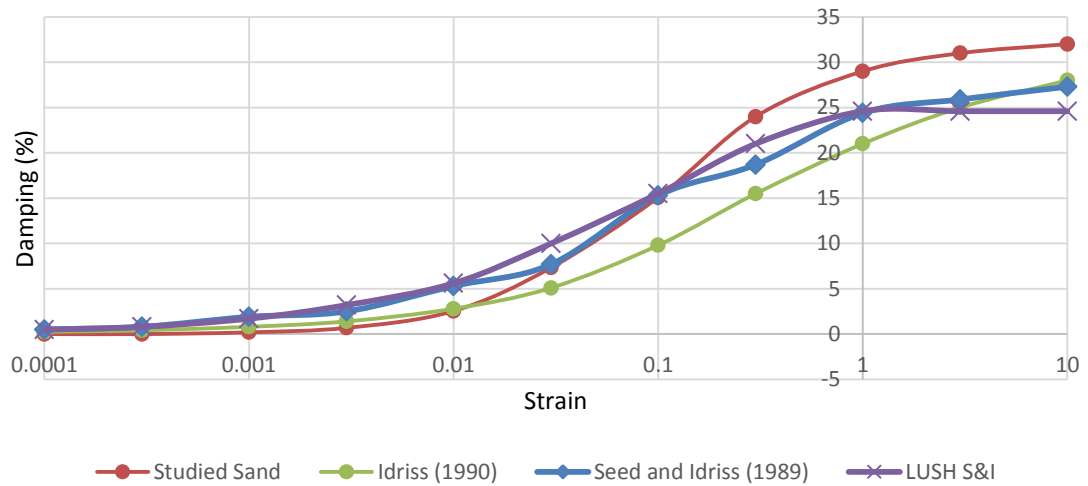


Figure 4.78: Damping ratio curve for sand

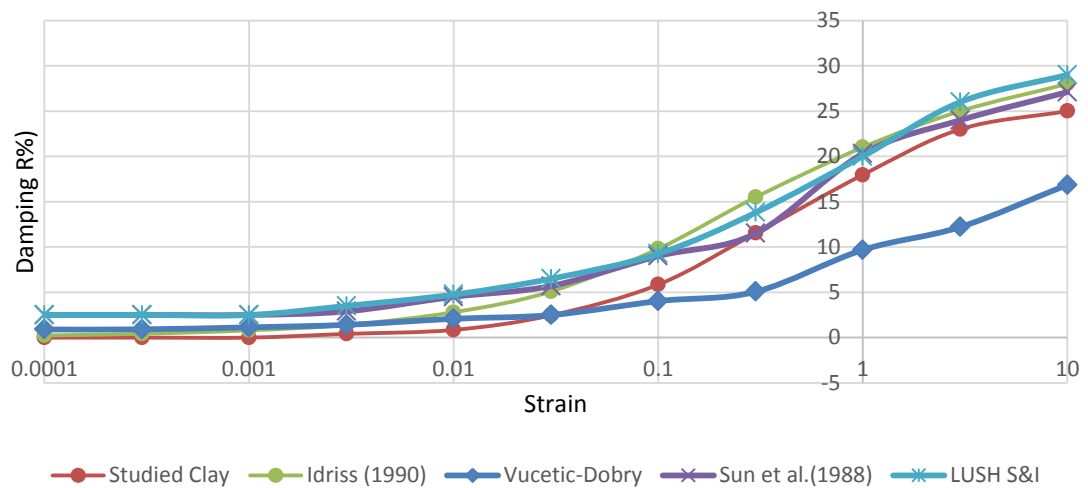


Figure 4.79: Damping ratio curve for clay

4.2.4 Summary

In this study, a series of the cyclic triaxial tests were conducted on 2 types of soil deposits which consists of sand and clay. The shear modulus reduction and damping ratios curves versus cyclic shear strain were analyzed under different soil type. Then the estimated shear modulus and damping ratio curves are compared with existing published work. The following conclusions can be drawn:

1. The regional sand tested is susceptible to soil liquefaction whereas the clay are not susceptible to soil liquefaction. This have been presented in the compiled reports in Chapter 2 of thesis study where most of the reports are consisted of sand and silt deposits vulnerable to soil liquefaction.
2. Sand degrades faster during cyclic loading compared to clay. The study emphasized the important characteristics that sand poses which makes significant contribution to stress application.
3. In both test samples, when the strain increases, the shear modulus decreases, whereas damping ratio increases. In general, the behavior is similar to published work used for comparative study. The stiffness in clay is higher compared to sand when the stress is applied repeatedly under cyclic loading.
4. In general different soil samples produce unique behavior towards any stress application. Hence the result obtained is most valid for liquefaction assessment of regional site condition where the samples are collected.

4.3 Earthquake Study

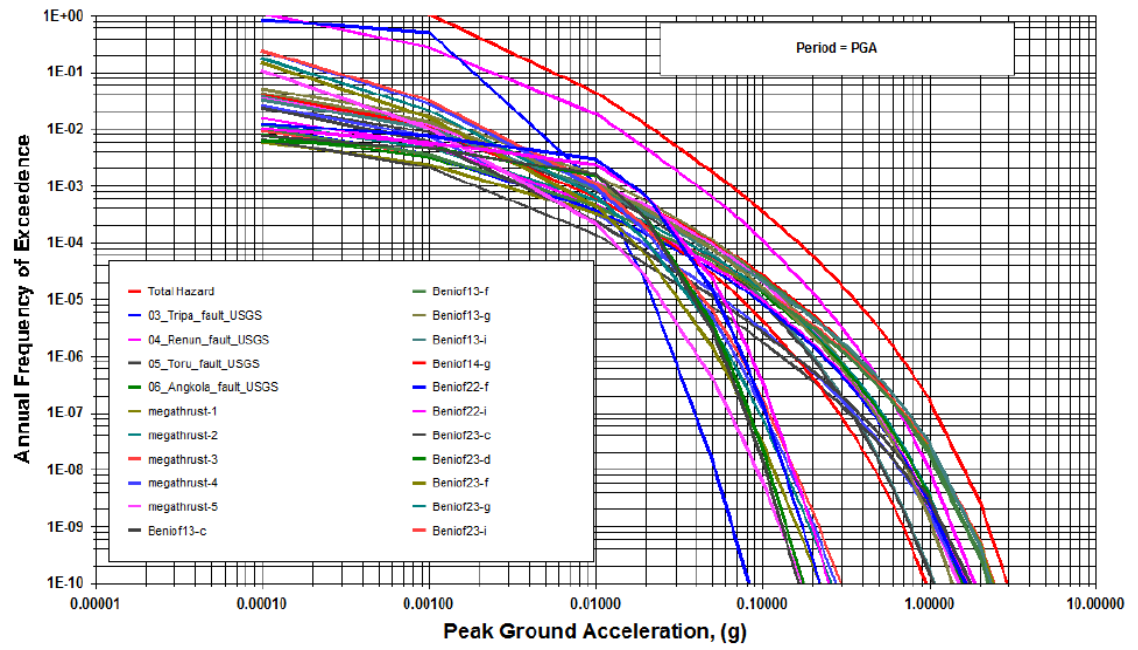
4.3.1 Probabilistic Seismic Hazard Assessment (PSHA)

Based on PSHA, 3 main outputs of studied area are presented under this section mainly the probabilistic hazard, de-aggregation hazard and scaled spectrum. The characterization of earthquake loading in liquefaction analysis of this study is evaluated using a detailed ground response analysis due to different ground condition and geotechnical setting of the shoreline.

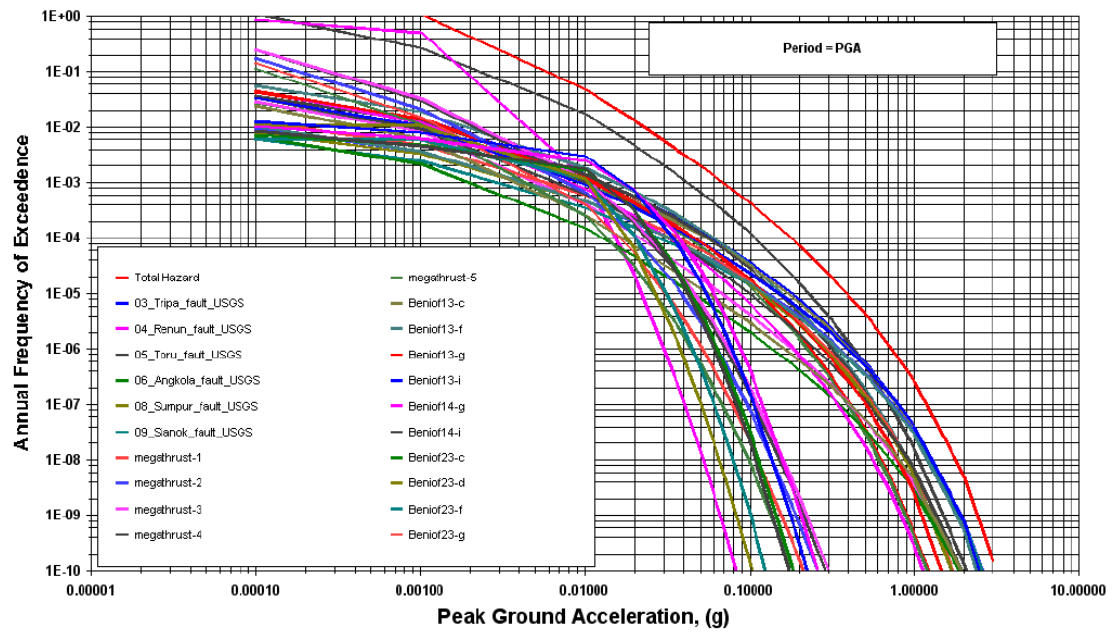
4.3.1.1 Generation and Simulation of Synthetic Ground Motion

Hazard curves developed presents the contribution from various earthquake sources. In this study a total of 21 earthquake sources consists of far field and nearby faults were carefully selected for the development of hazard curves. The type of seismic source controls hazard at various spectral accelerations. The typical probabilistic hazard in the west coast areas and the east coast areas which consists of 9 site location of studied state from PGA source is shown in Figure 4.80 and Figure 4.81. The plot of annual frequency of exceedance versus the peak ground acceleration presents constant decreasing of graph results as the earthquake sources distance from site.

The Peninsular Malaysia experienced tremors, some of which caused damage to both buildings and infrastructures. Hence the evaluation of the probabilistic hazard consists of nearby faults which have significant contribution to the earthquake hazard. The hazard curves from nearby moderate magnitude are observed to be different from that large-magnitude subduction zone earthquake. The most significant to the studied area are seismic source from far field earthquake namely the Tripa fault segment. Other far field seismic source such as Renun, Toru and Angkora are less significant to the studied areas follow by the remaining benioff type seismic source.

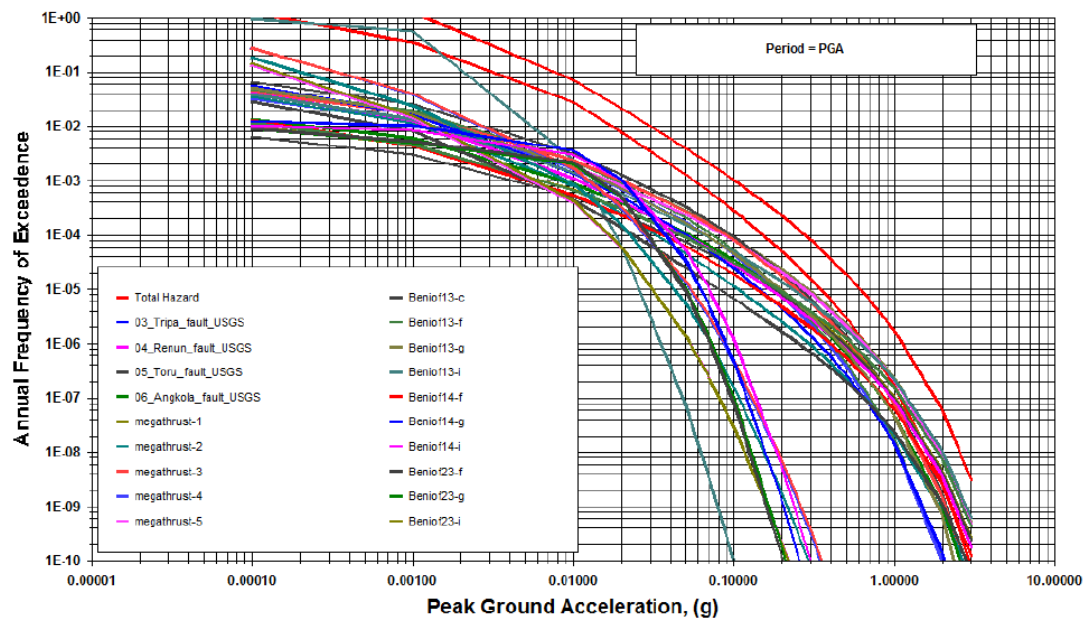


(a) Perlis

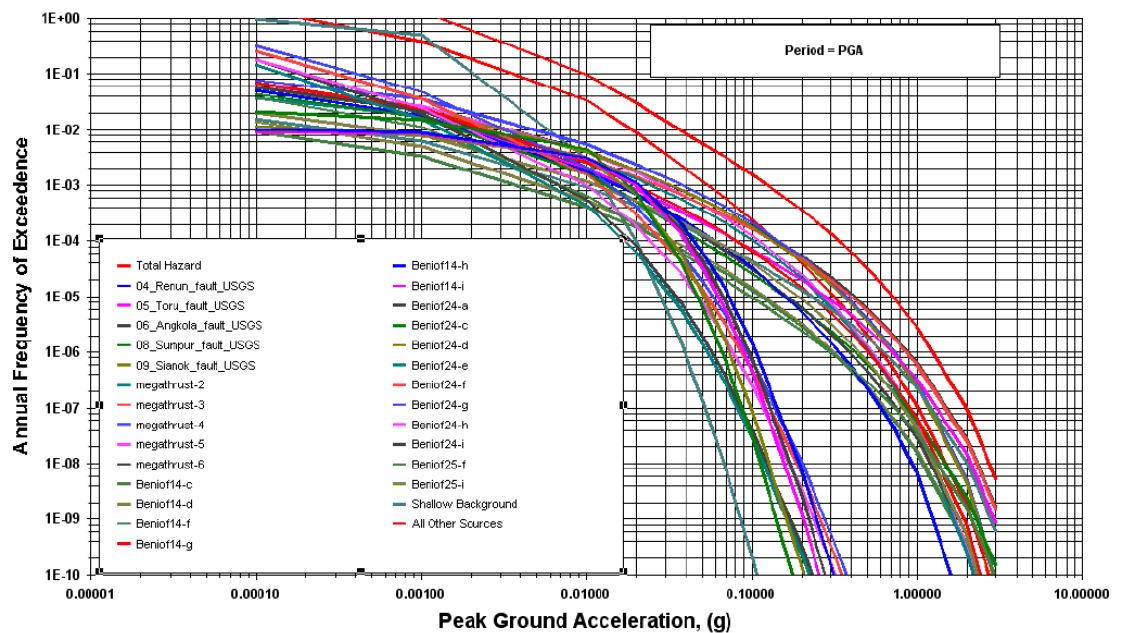


(b) Kedah

‘Figure 4.80, continued’

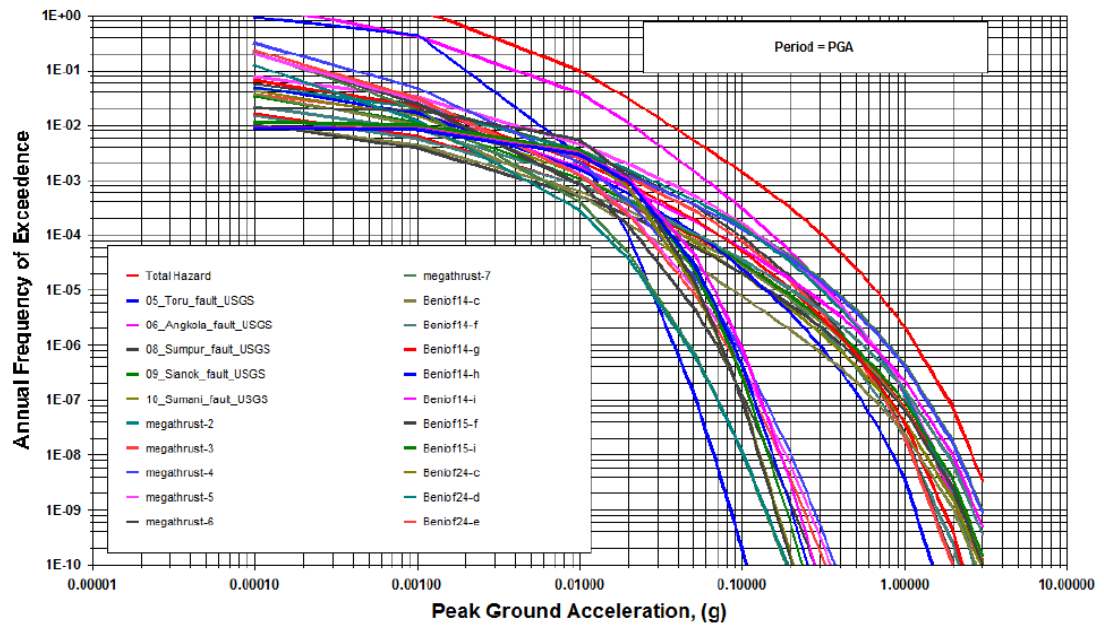


(c) Penang



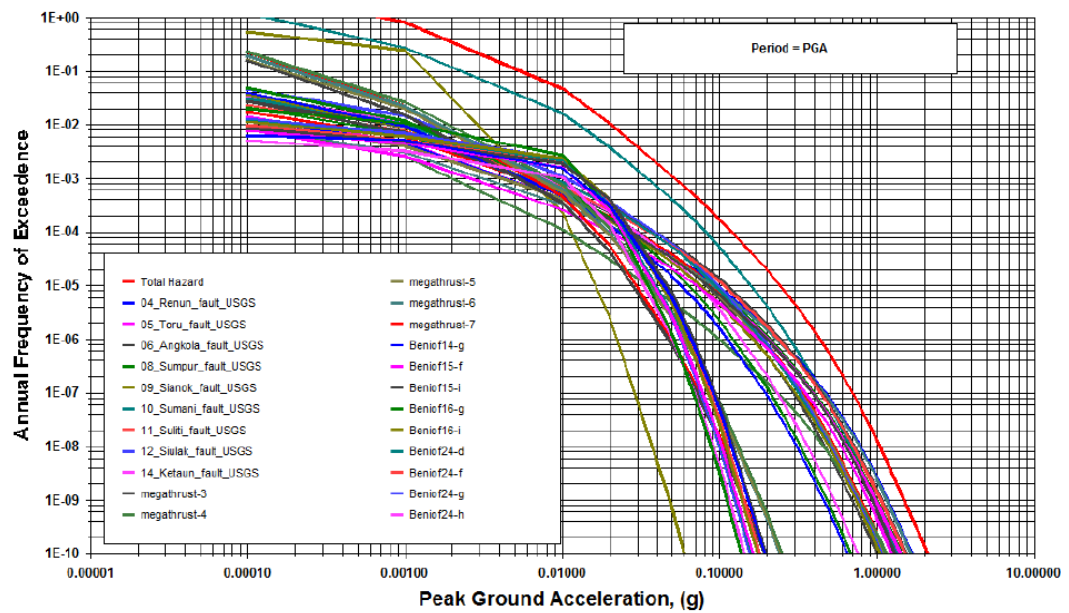
(d) Selangor

‘Figure 4.80, continued’



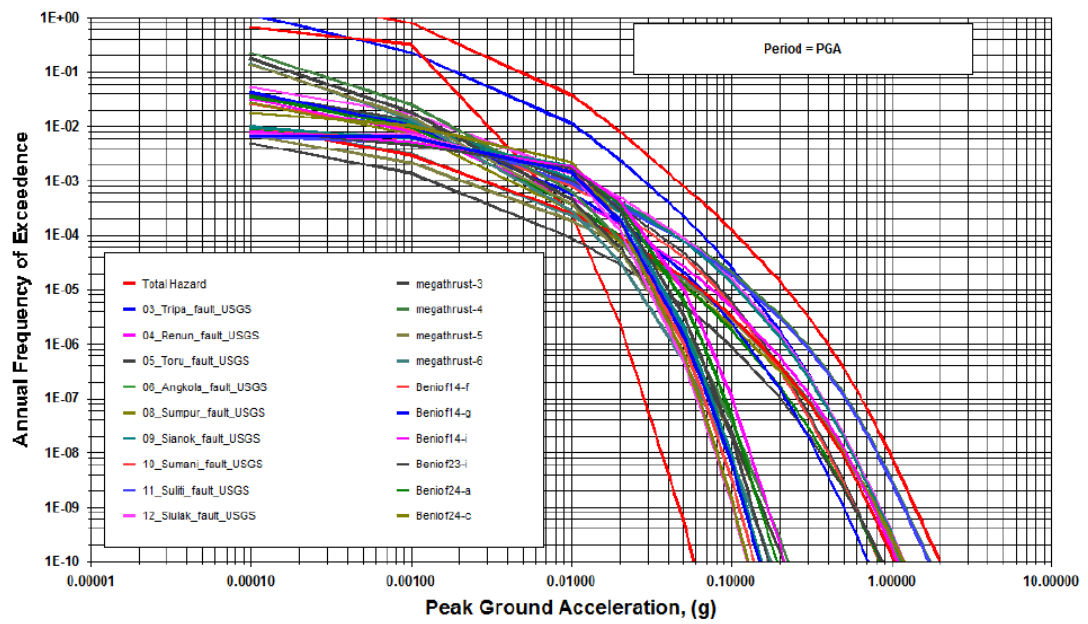
(e) Melaka

Figure 4.80: Typical probabilistic hazard at west coast areas for PGA

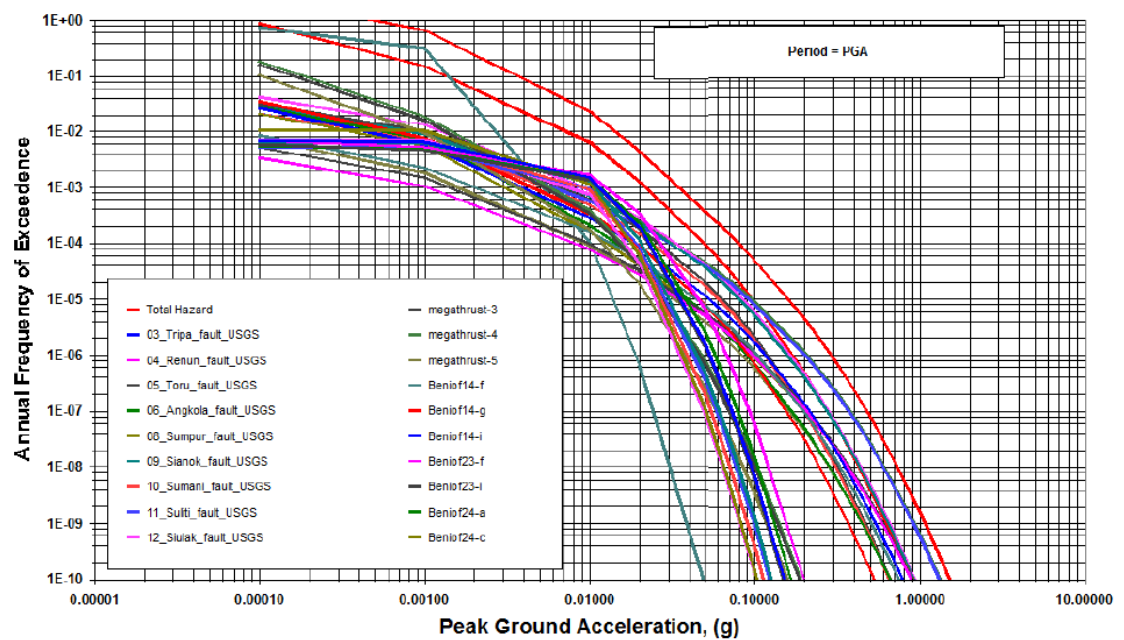


(a) East Johor

‘Figure 4.81, continued’

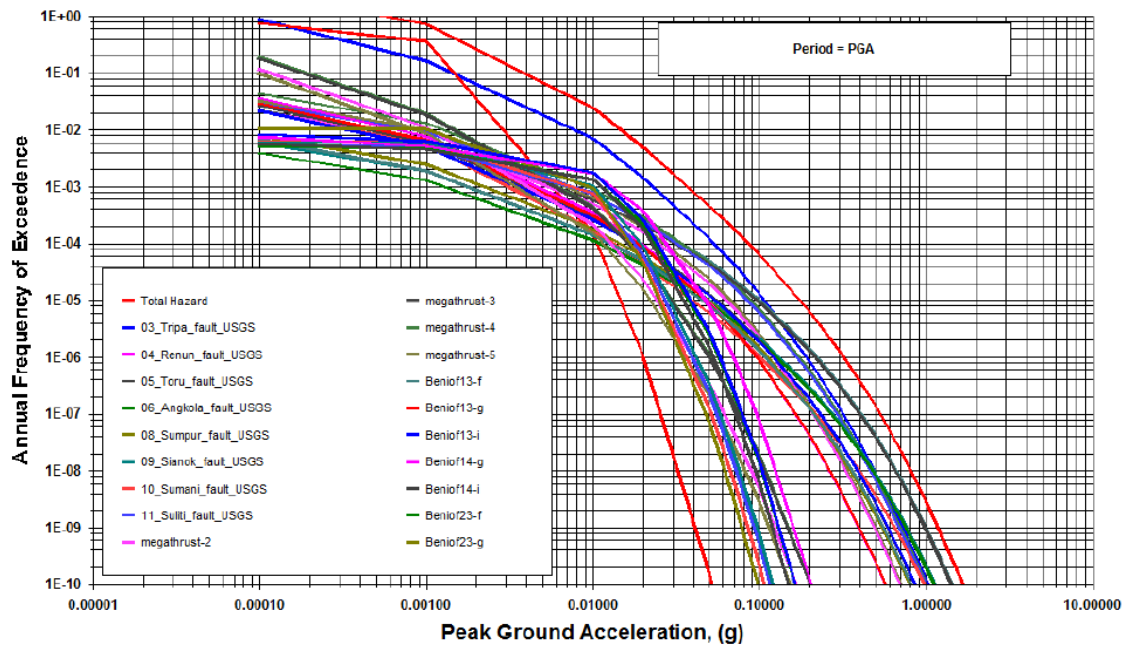


(b) Pahang



(c) Terengganu

‘Figure 4.81, continued’



(d) Kelantan

Figure 4.81: Typical probabilistic hazard at east coast areas for PGA

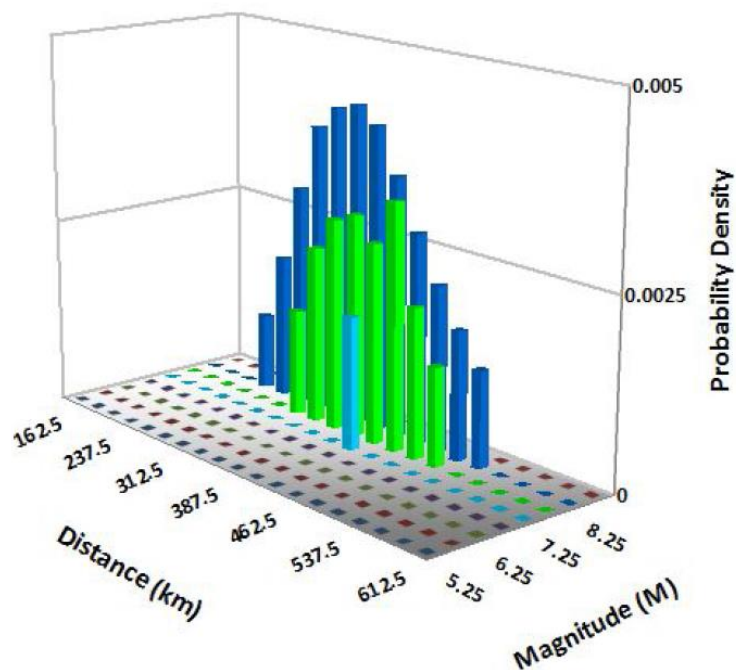
4.3.1.2 De-Aggregation Hazard

Based on hazard curve presented in 4.3.1.1 which combines all the sources, magnitudes and distances, the intuitive understanding about controlling hazard sources are difficulty hence hazard de-aggregation plot is needed (Kim & Hashash, 2013). The hazard de-aggregation plot identify likely major contributor to seismic hazard. It helps to identify the magnitudes and distances of controlling seismic sources. De-aggregation generates the relative contributions to ground motion from seismic sources in terms of ground motion magnitude and source-to-site distance.

The typical de-aggregation hazards for the studied state consist of west coast areas and east coast areas are shown in Figure 4.82 to Figure 4.83 respectively. Typical

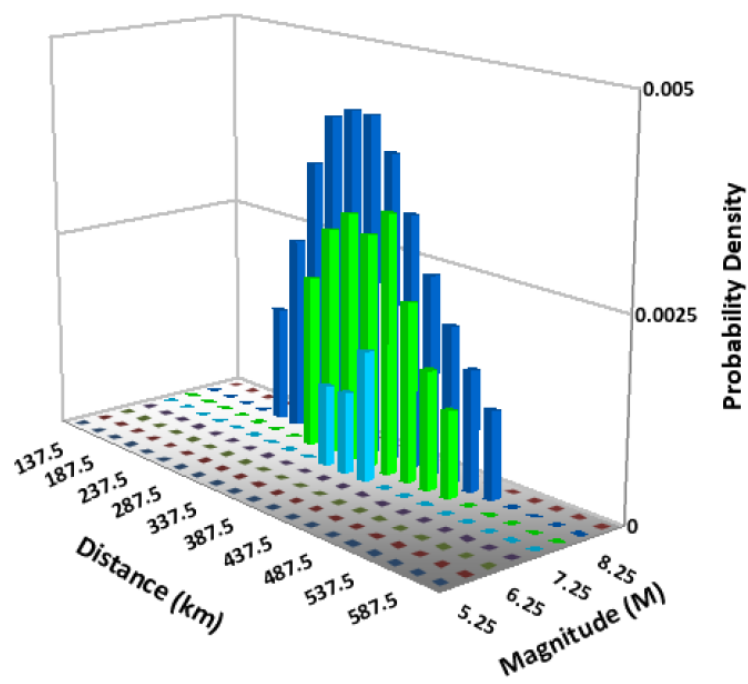
simple de-aggregation has a unimodal distribution with one clear peak or most frequent value. The result for most state highlights increasing value at first, rising to a single peak where it then decreases. The peak presents nearby earthquakes whereas the tail includes a larger and more distance earthquakes. For location in Kelantan and Terengganu, a broader peak of hazard contributions is observed. This is due to the low activity and remote location from high activity zones. The hazard contributions are consists mainly of wide range of magnitudes and earthquakes.

For the studied west coast site, the primary contributors to hazard are at a distance of 237.5 km with a magnitude of 8.25 whereas the east coast areas are at a distance of 587.5 km with a magnitude of 8.25. The west coast is closer to the seismic source as to compare to the east coast area which is further from the fault. However the magnitude remains same with a value of 8.25 for both findings.

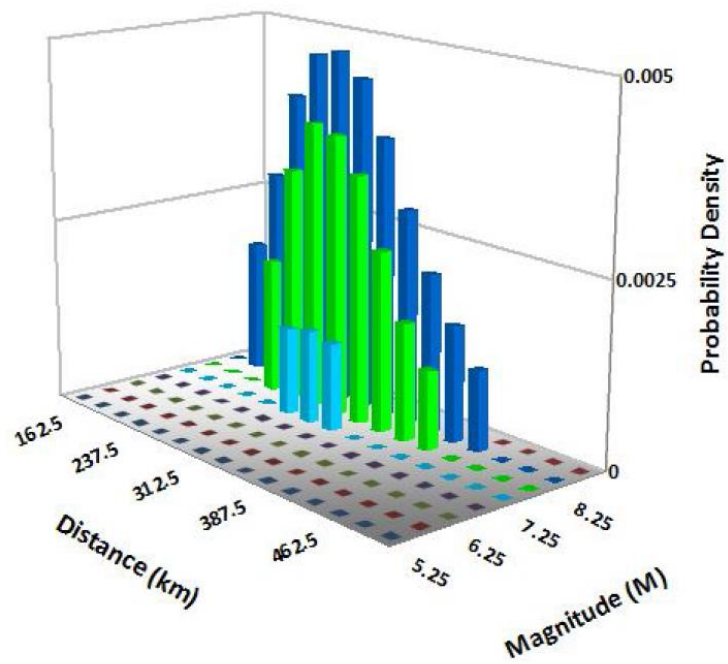


(a) Kangar

‘Figure 4.82, continued’

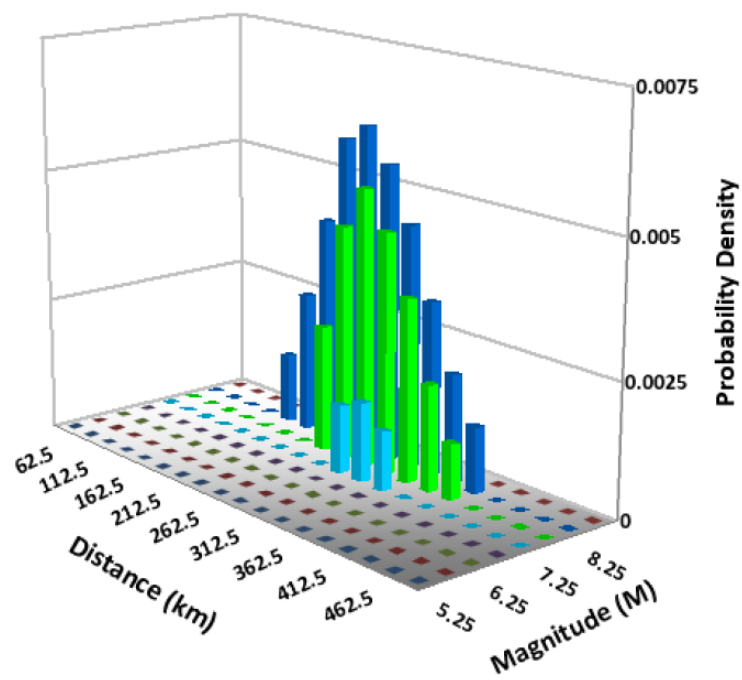


(b) Kedah

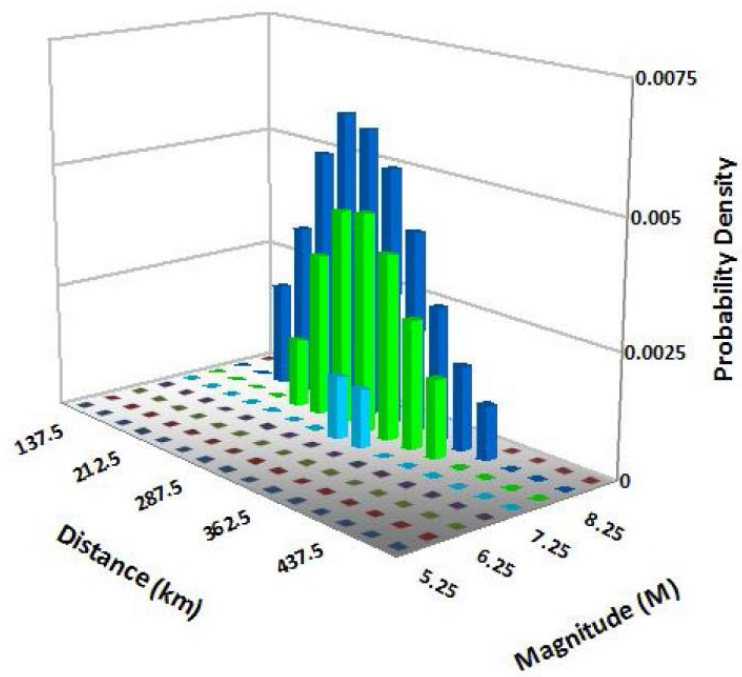


(c) Penang

‘Figure 4.82, continued’

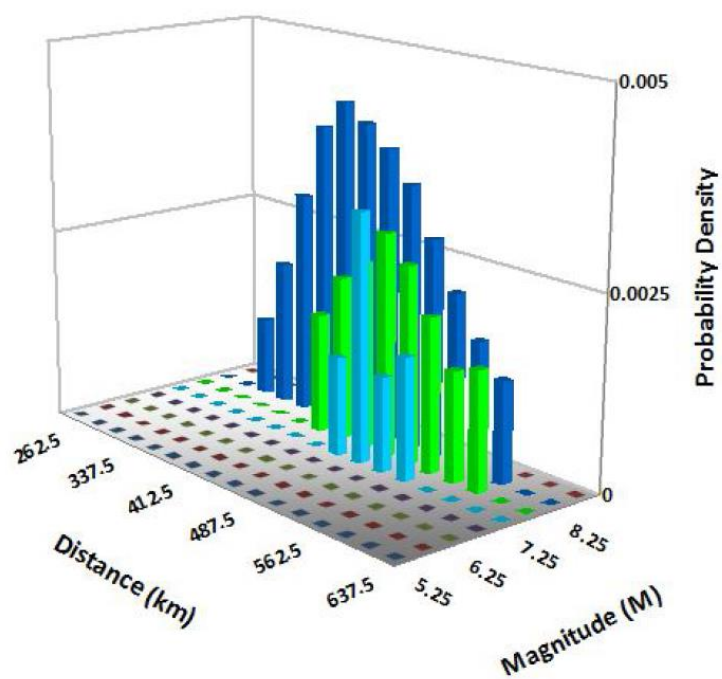


(d) Selangor



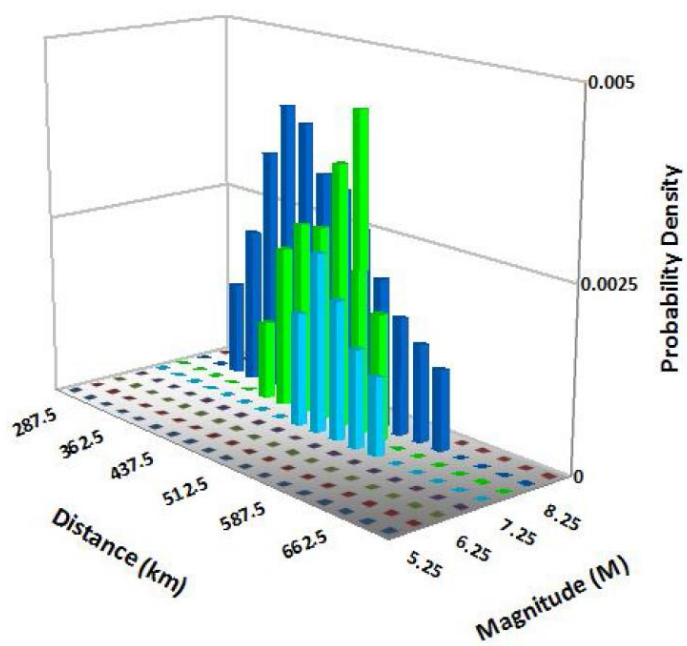
(e) Melaka

‘Figure 4.82, continued’



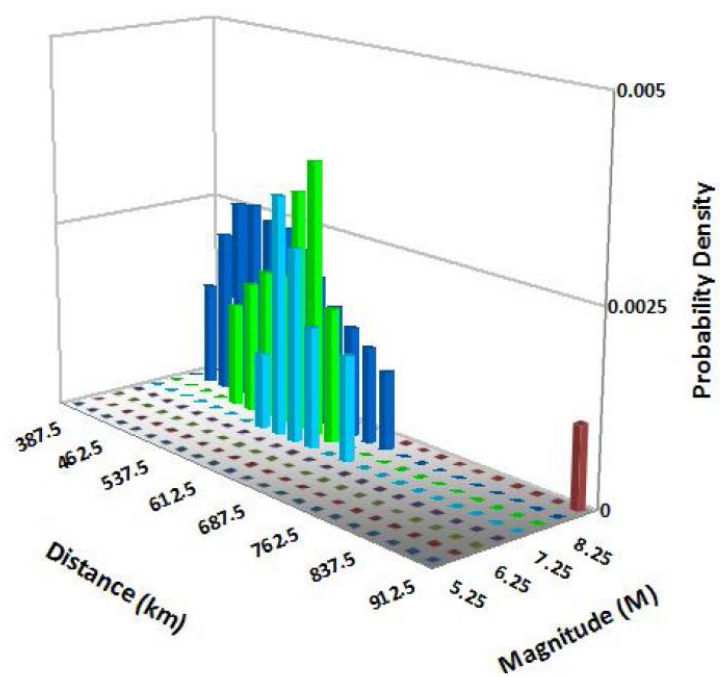
(f) West Johor

Figure 4.82: De-aggregation hazard of 500 year return period for west coast

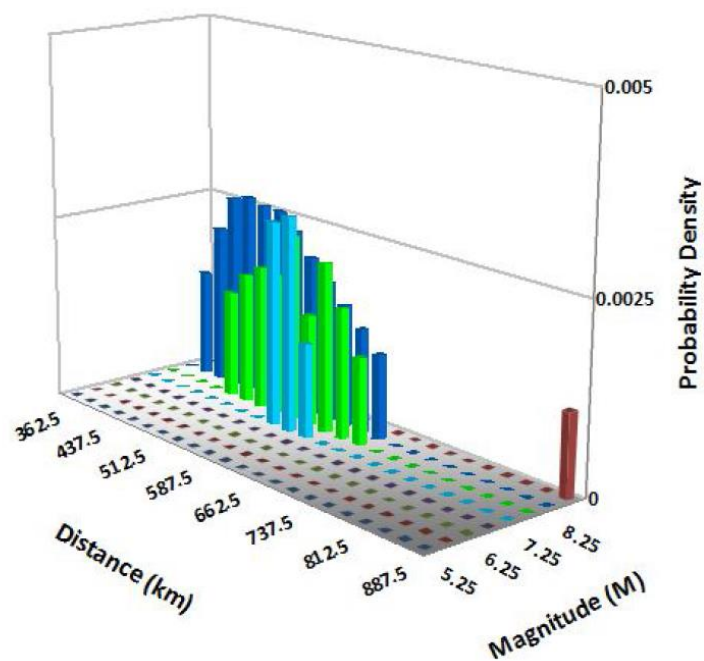


(a) Pahang

‘Figure 4.83, continued’



(b) Terengganu



(c) Kelantan

Figure 4.83: De-aggregation hazard of 500 year return period for east coast

Table 4.4 presents the deaggregation hazard of 500 year return period for selected states. The main indicator which will later be used to select the ground motion in the spectral matching procedure extracted from this chart is the distance and magnitude.

Table 4.4: The deaggregation hazard of 500 year return period for 11 states

Shoreline State	Distance (m)	Magnitude (M)
Perlis	312.5	8.25
Kedah	287.5	8.25
Pulau Pinang	237.5	8.25
Perak	237.5	8.25
Selangor	262.5	8.25
Seremban	262.5	8.25
Melaka	212.5	8.25
West Johor	337.5	8.25
East Johor	587.5	8.25
Pahang	587.5	8.25
Terengganu	612.5	8.25
Kelantan	437.5	8.25

4.3.1.3 Scaled Spectrum

The scaled spectrums for 11 state of Peninsular Malaysia for return period of 500 and 2500 years are shown from Figure 4.84 and Figure 4.85. It has been observed that for selected sources, as the distance from the fault increases, the value of spectral acceleration reduces. Hence, the east coast of Peninsular Malaysia (Kelantan, Terengganu, Pahang, and East Johor) presents lower value of spectral acceleration. As the period increases, the result of scaled spectrum tends to become asymptotic. These results will be useful in carrying out the spectral matching procedure to obtain the ground motion at bedrock.

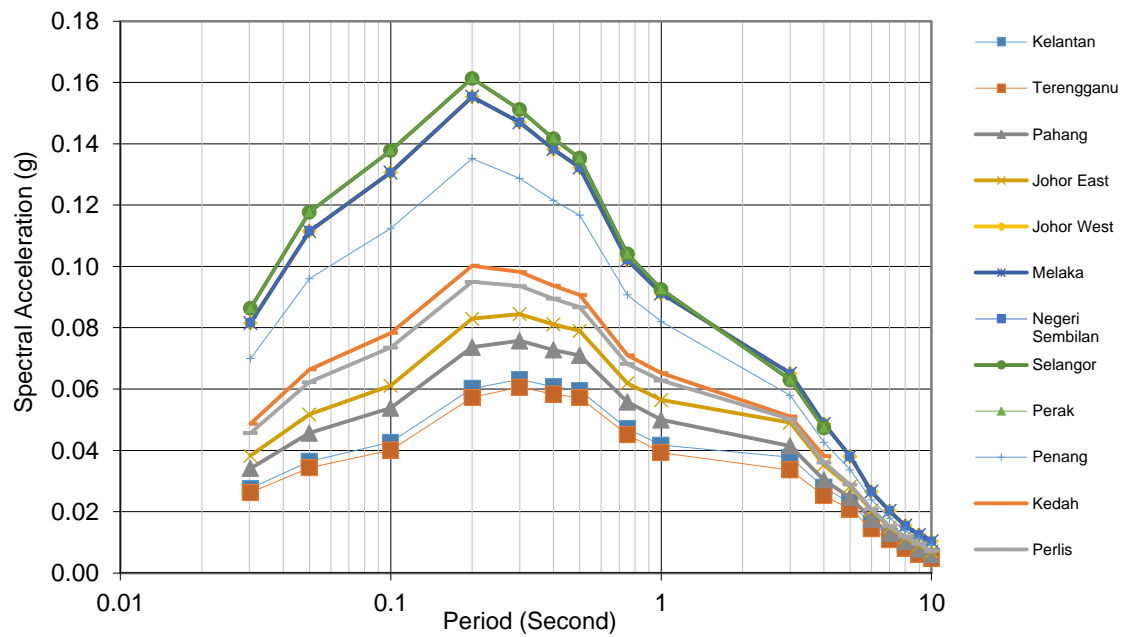


Figure 4.84: Bedrock spectrum with 500 year return period of hazard

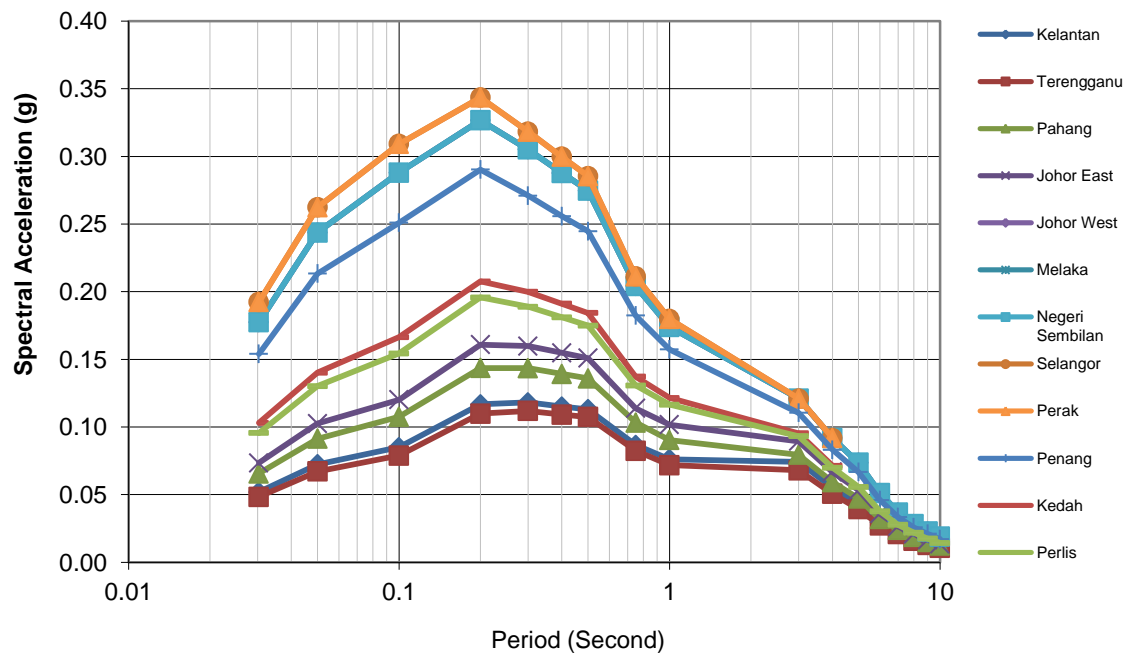
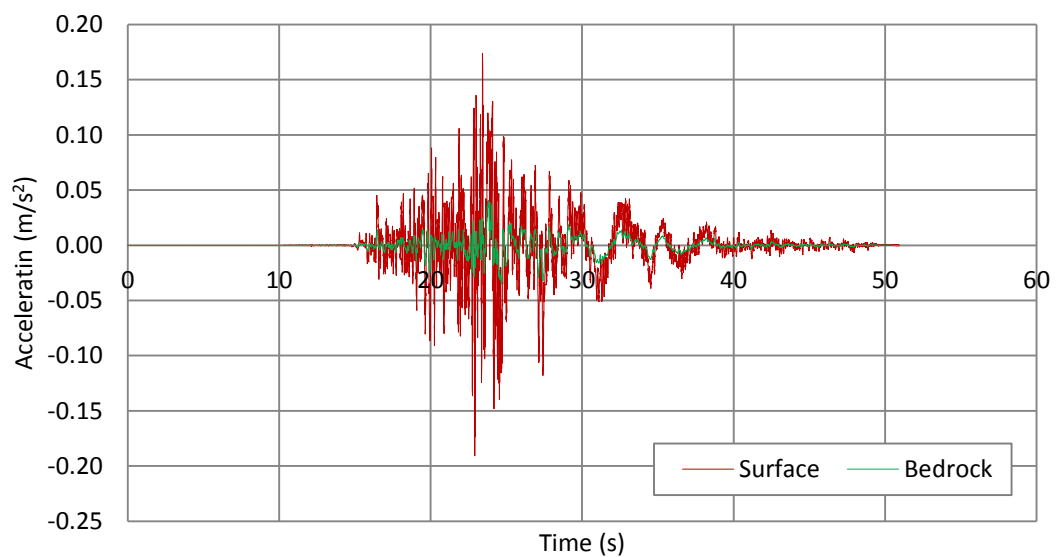


Figure 4.85: Bedrock spectrum with 2500 year return period of hazard

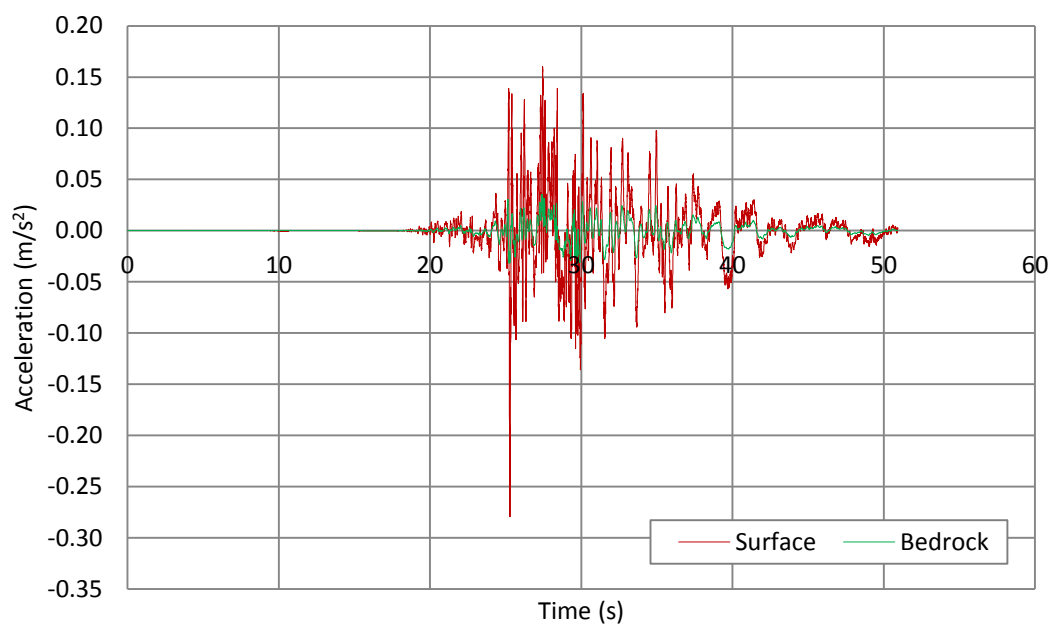
4.3.2 Generation and Simulation of Synthetic Ground Motion

This study analyzed nearly 2074 SPT samples from over 325 locations that were drilled along the shoreline area of Peninsular Malaysia, to access the characteristics of wave behavior propagating through different layer of soils. These data allowed a subsurface investigation and evaluation of peak surface acceleration to be assigned in the liquefaction analysis. Figure 4.86 and 4.87 presents the result simulation of bedrock (PGA) bedrock and also surface (PSA) for all the studied states. The variety of color represents ground motion at different shoreline state of Peninsular Malaysia. The maximum PGA is observed at the west coast areas. Lower PGA is defined in most of places in the east coast region. The longest period of which the ground motion ends was found to be located in Seremban. However the development of PSA shows significant effect in most of the region in the east coast region. The propagation of seismic waves in soil varies with different setting of soil strata. Bedrock propagates direct dispersion of energy whereas when seismic waves pass through loose deposits the energy is released in a complex way that it tends to show increment of energy (Holzer et al., 1989).

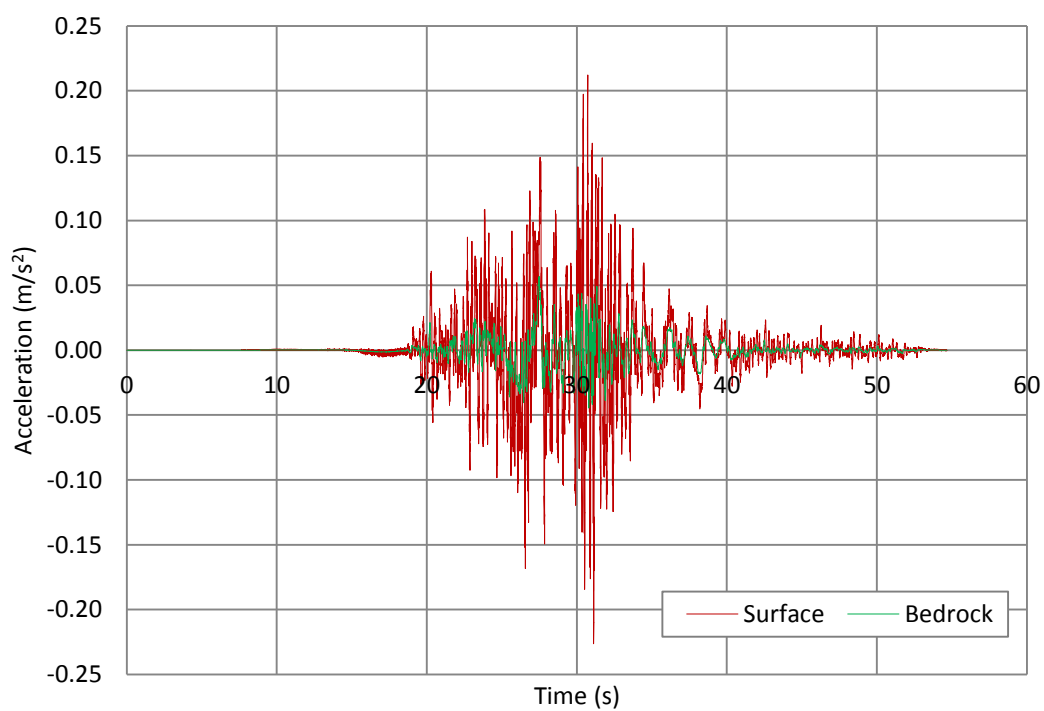


(a) Perlis

‘Figure 4.86, continued’

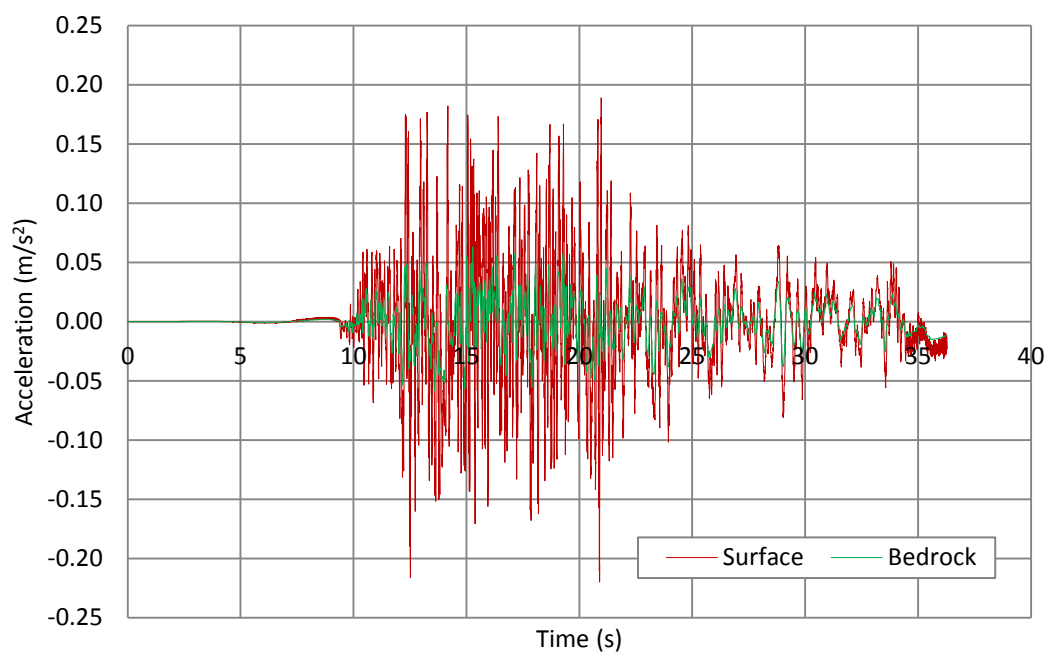


(b) Kedah

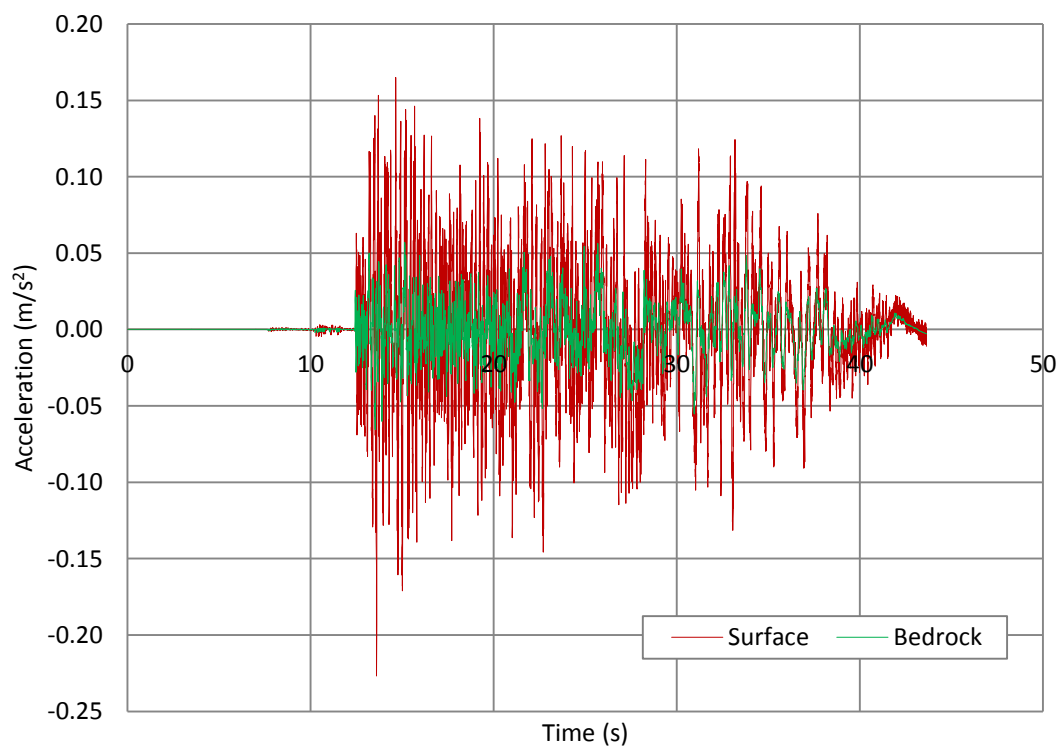


(c) Penang

‘Figure 4.86, continued’

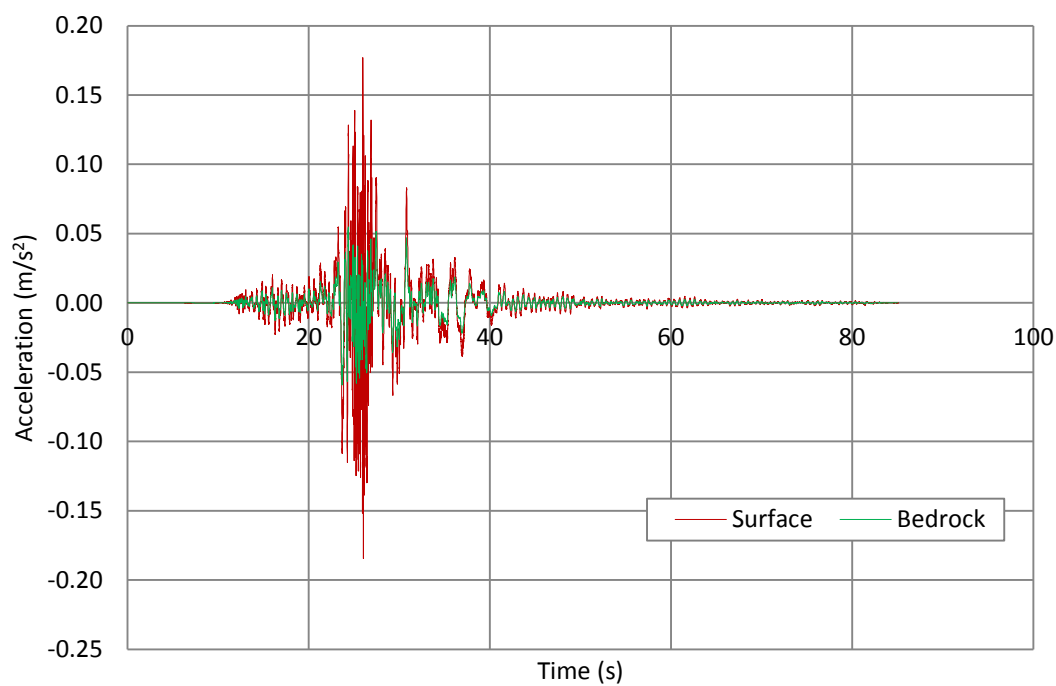


(d) Perak

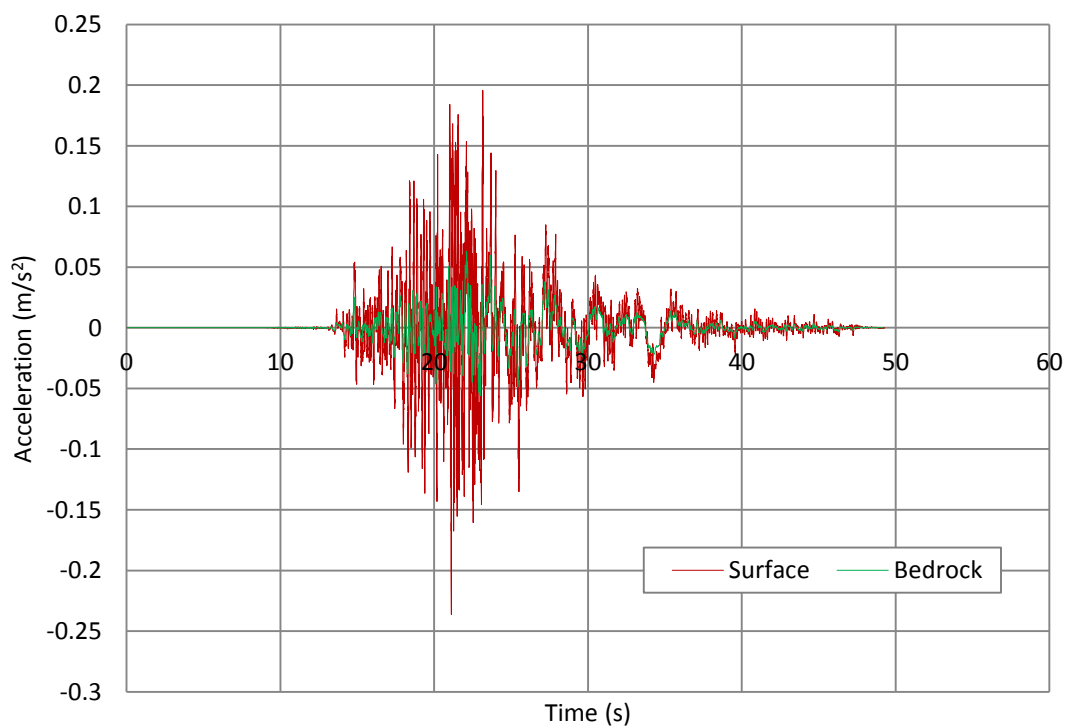


(e) Selangor

‘Figure 4.86, continued’

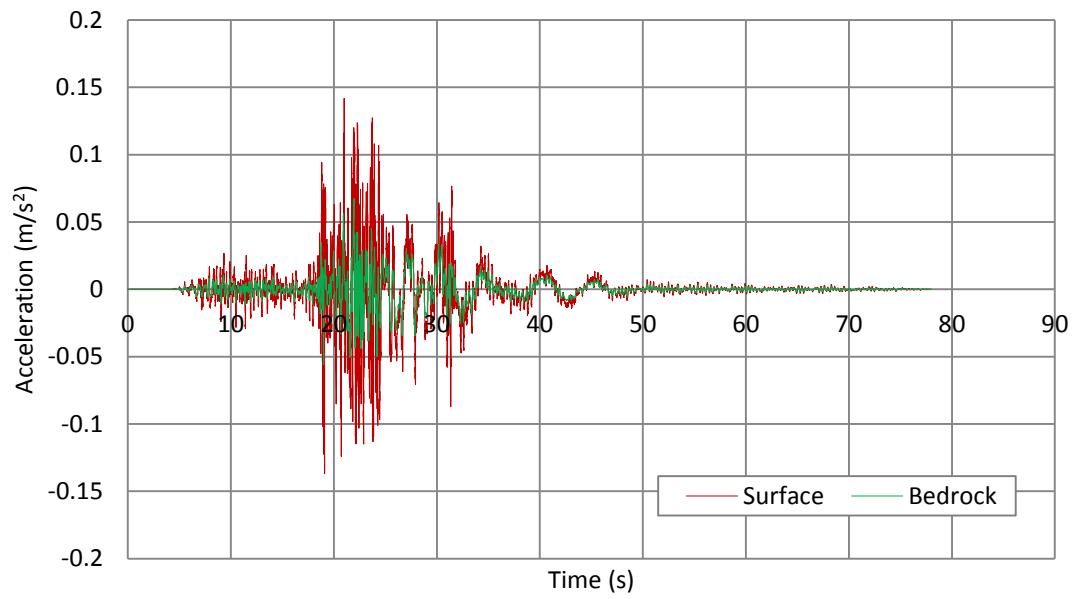


(f) Negeri Sembilan



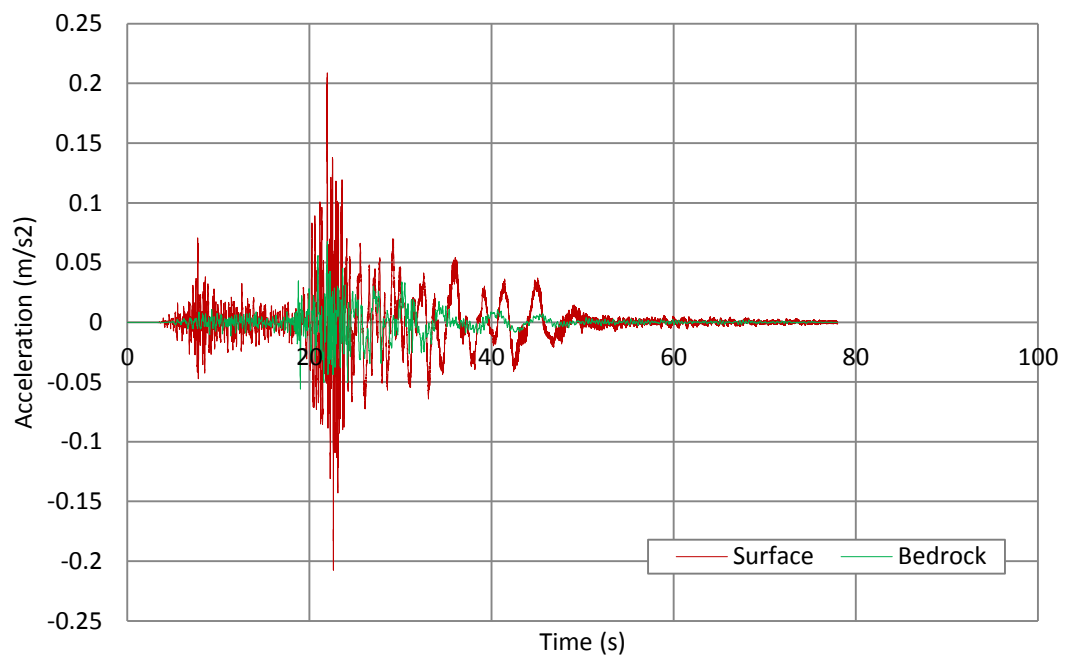
(g) Melaka

‘Figure 4.86, continued’



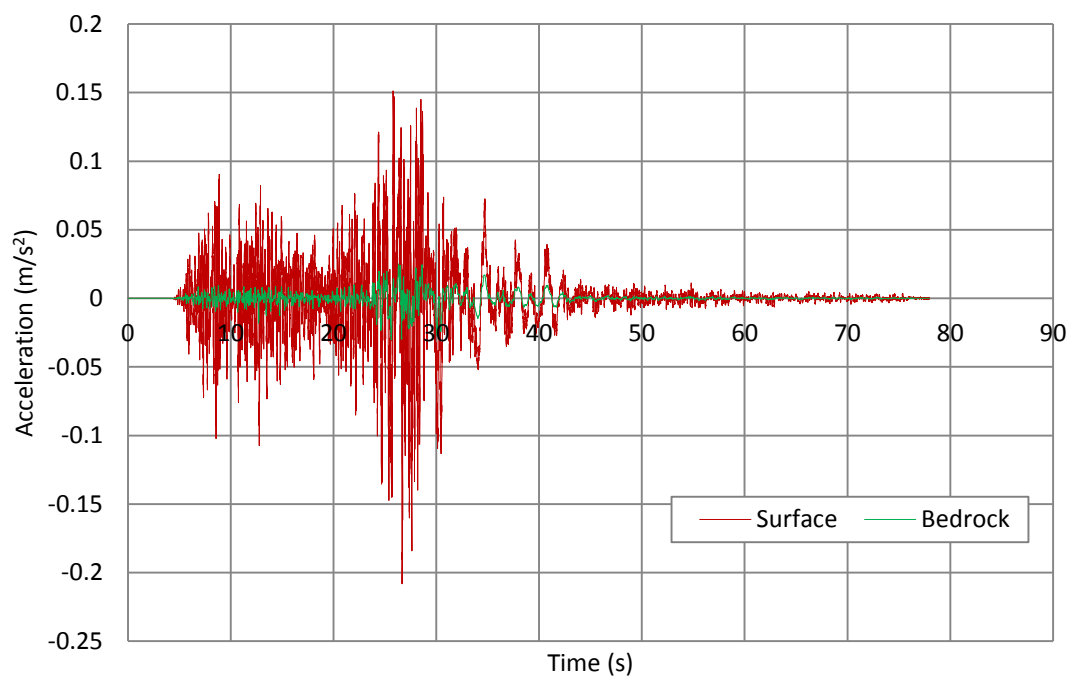
(h) West Johor

Figure 4.86: Simulation from bedrock (PGA) to surface (PSA) of west coast region

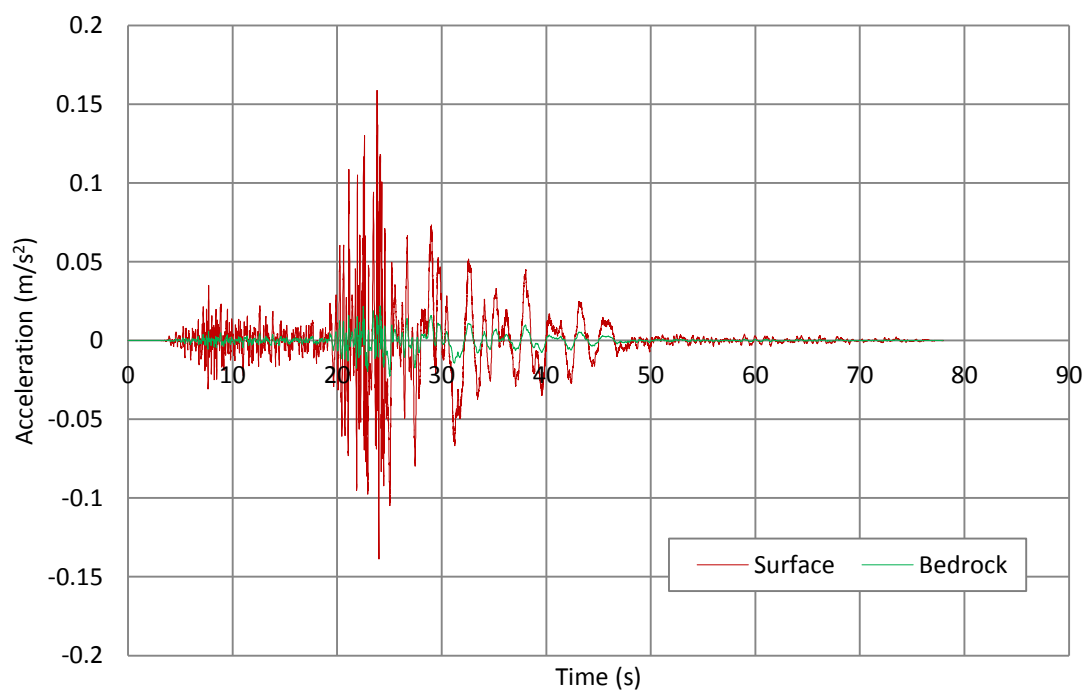


(a) East Johor

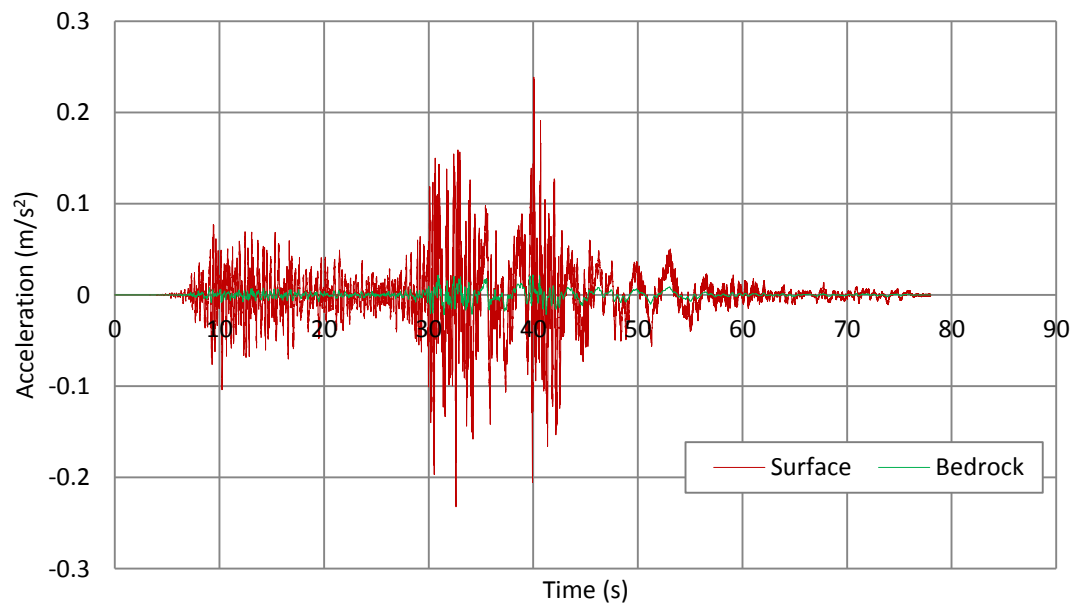
‘Figure 4.87, continued’



(b) Pahang



(c) Terengganu



(d) Kelantan

Figure 4.87: Simulation from bedrock (PGA) to surface (PSA) of east coast region

Table 4.5 presents the summary of significant values extracted from the ground motion simulation from the bedrock to the surface for all the studied area. The high amplification values are demonstrated at Kelantan and Terengganu mainly due to the high concentration of deep loose soil layer which enhanced the propagation of wave through the soil layers (Ishac & Heidebrecht, 1982).

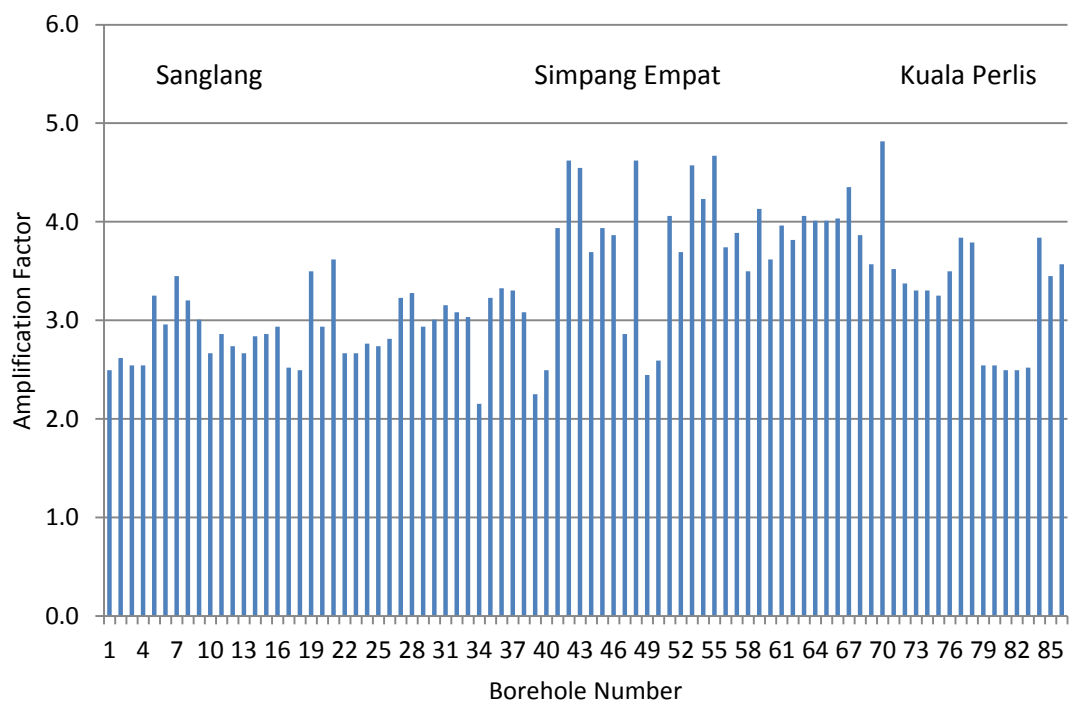
Table 4.5: Amplification factor of 11 studied states for 500 years return period

Shoreline State	PGA	PSA	Max. Amplification Factor
Perlis	0.04	0.19	4.62
Kedah	0.04	0.24	6.67
Pulau Pinang	0.06	0.23	3.99
Perak	0.06	0.23	3.65
Selangor	0.07	0.23	3.49
Seremban	0.06	0.14	2.35
Melaka	0.06	0.24	3.74
West Johor	0.07	0.24	3.49
East Johor	0.03	0.21	6.43
Pahang	0.03	0.18	6.01
Terengganu	0.02	0.20	8.72
Kelantan	0.02	0.24	11.02

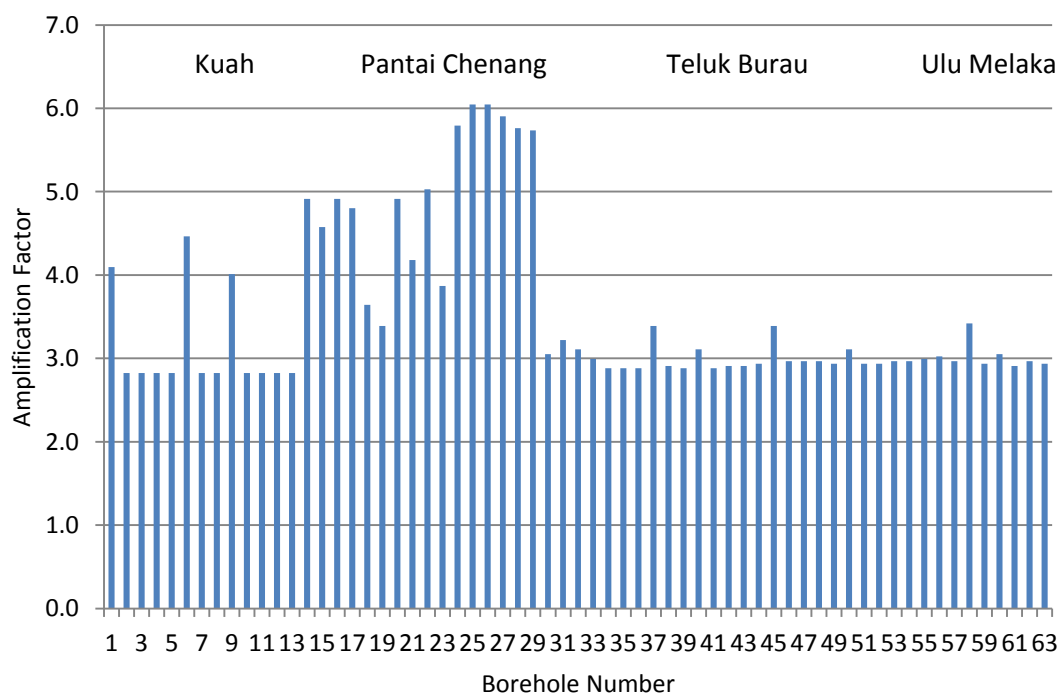
4.3.3 Microzonation Line (Amplification Factor)

The amplification factor generated from the seismological data through the PSHA has been applied in microzonation chart line of 1972 km shoreline. Figure 4.88 presents the amplification factor of 11 states along shoreline. By observing the chart, maximum amplification factor in west coast region was found in Kedah state with a value of 7.8 factors. The rest of the state in west coast region shows constant amplification factor in the range of 2 to 5 factor. A closer look of high amplification factor is concentrated in major cities mainly due to the strategic location and natural formation such as lagoon, river mouth and long beach (Bhuiyan et al., 2013; Yasuda et al., 2012). Hence the risk is high at highly populated area which defines heavily congested built environment. Reclaimed land in parts of west coast region especially in Penang Island and Melaka is also at risk based on the amplification factor generated for this study. Sudden peak in Penang Island is mainly due to formation of loose deposits concentration in the area. Proper management, earthquake resistant design and preparation plan is recommended at specific area with high amplification factor (Adalier & Elgamal, 2004).

On the other hand east coast region define a much higher amplification factor significantly in Terengganu and Kelantan region. Ports, power plant and harbor facilities are at high risk during ground motion which scattered in most of the shoreline district of Terengganu. The highest amplification factor was found in Tumpat district, Kelantan follow by Pasir Puteh district with a factor of 14.7 and 11 respectively. Terengganu shows constant factor of nearing 8 at most of the shoreline district. At the moment the Kelantan shoreline is not heavily developed hence the risk is low. The future development of the areas needs critical attention as the amplification is found the highest among the other states of the west coast region.

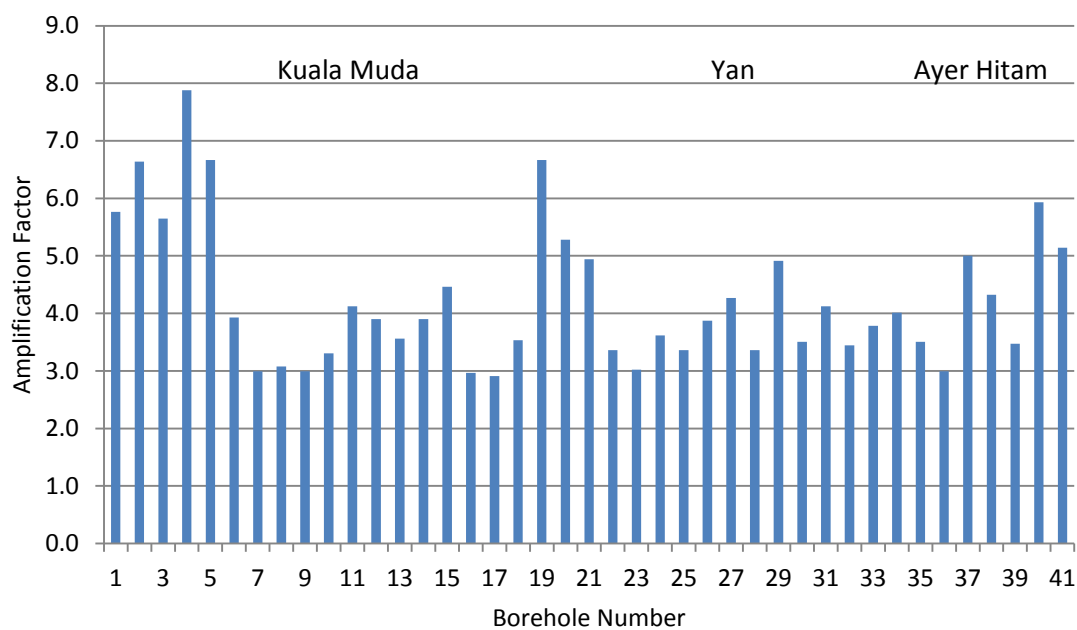


(a) Perlis

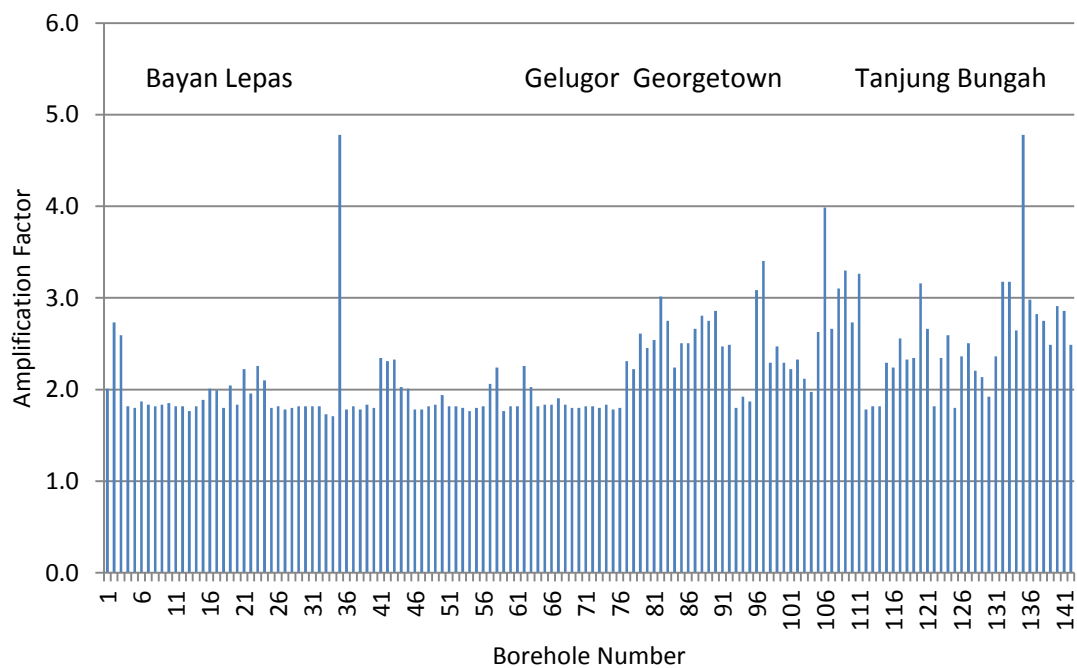


(b) Langkawi Island

‘Figure 4.88, continued’

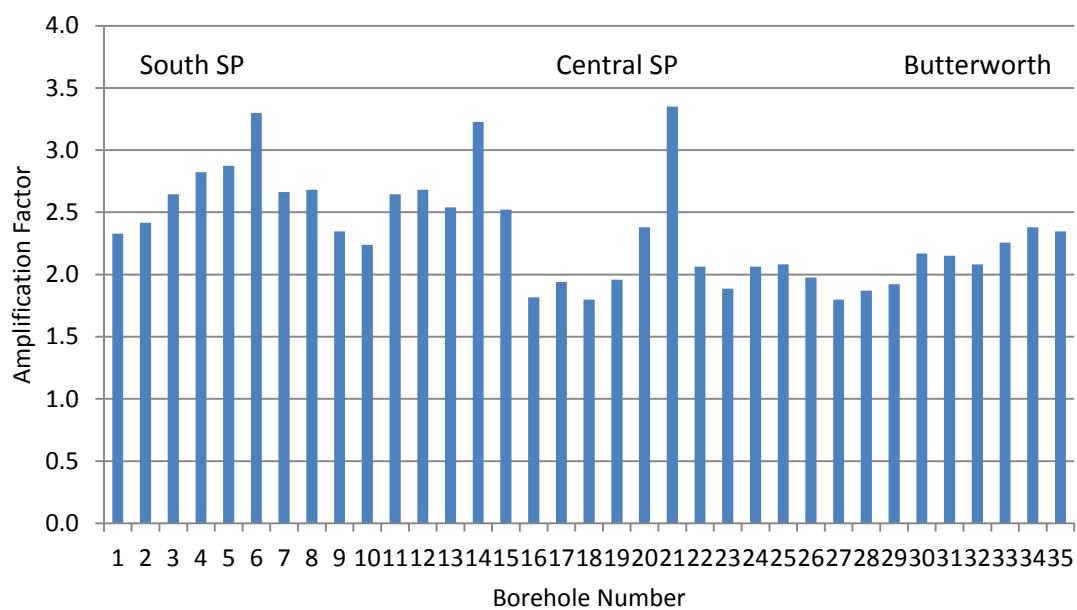


(c) Kedah Mainland

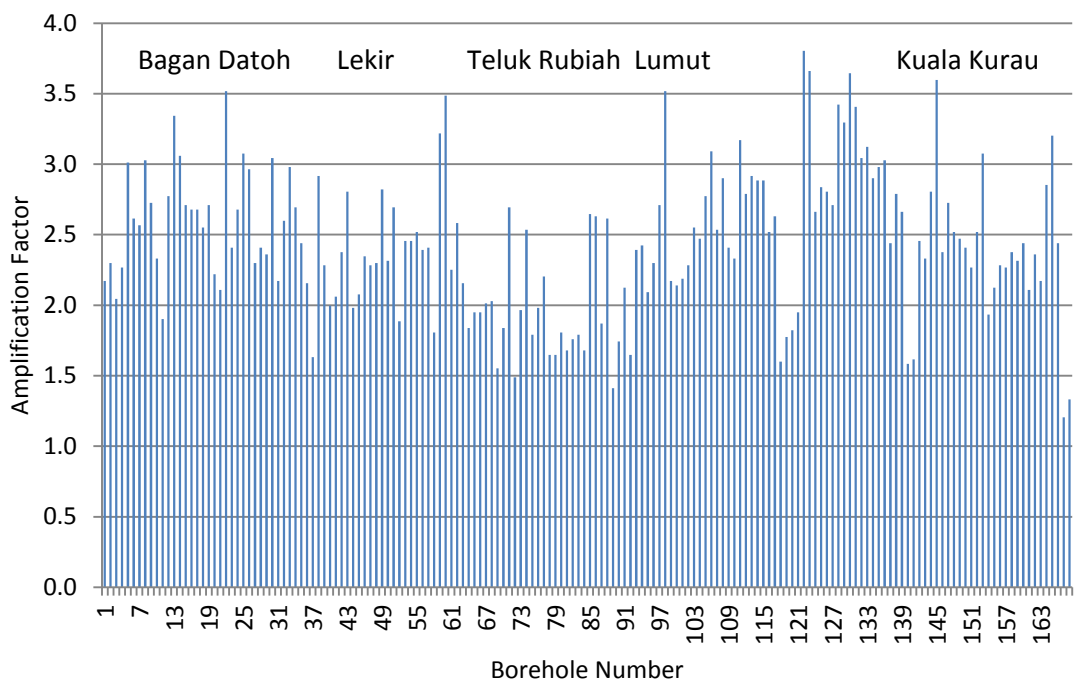


(d) Penang Island

‘Figure 4.88, continued’

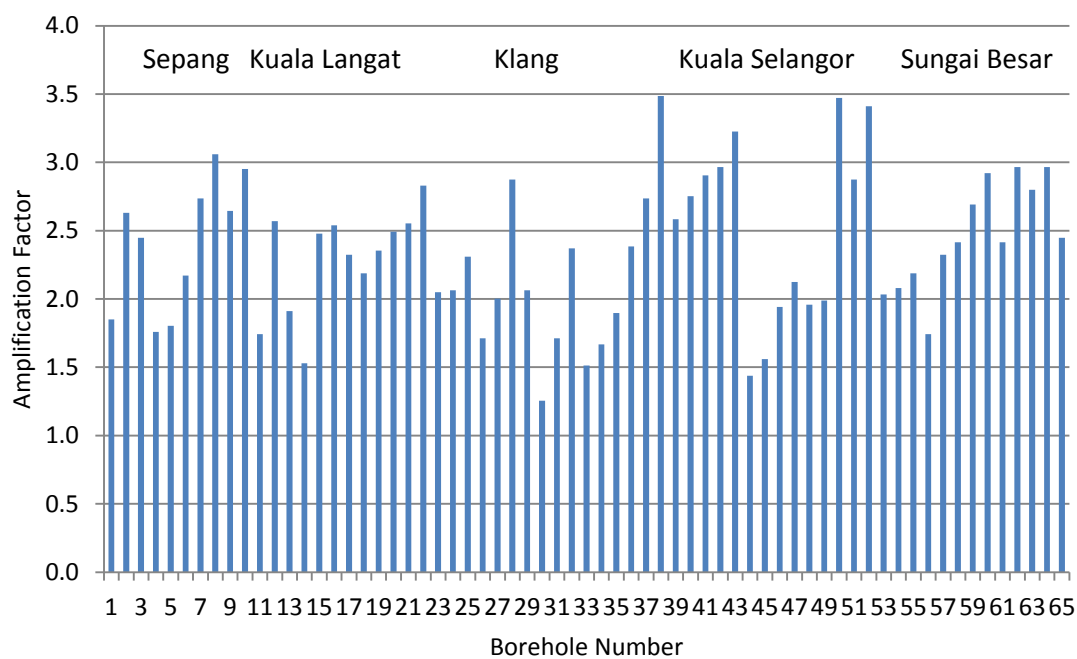


(e) Seberang Perai

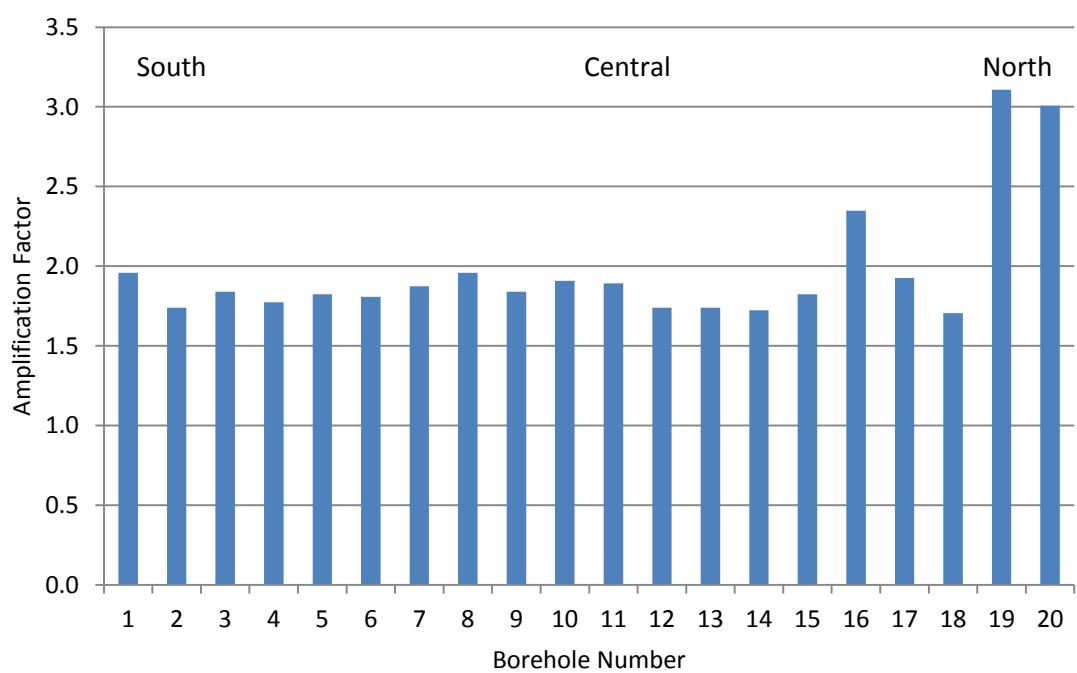


(f) Perak

‘Figure 4.88, continued’

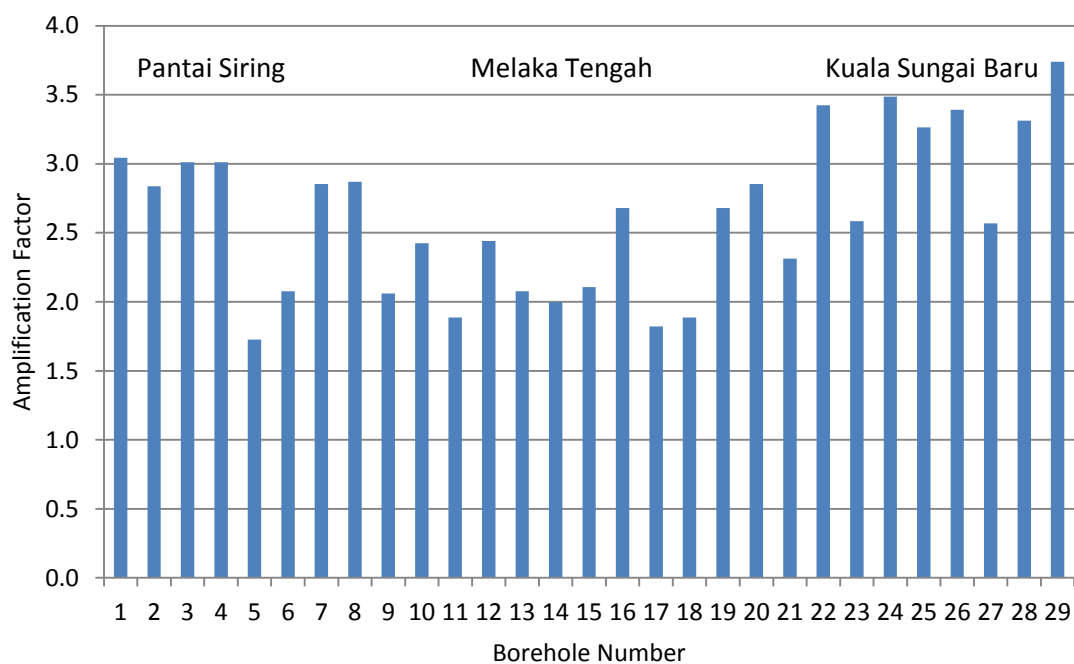


(g) Selangor

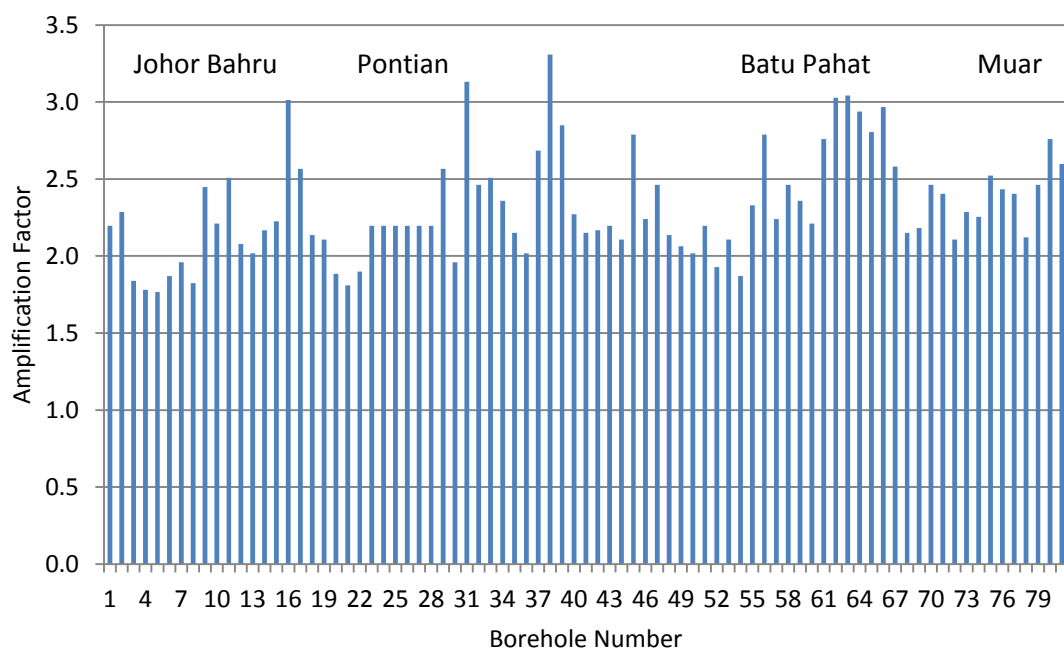


(h) Negeri Sembilan

‘Figure 4.88, continued’

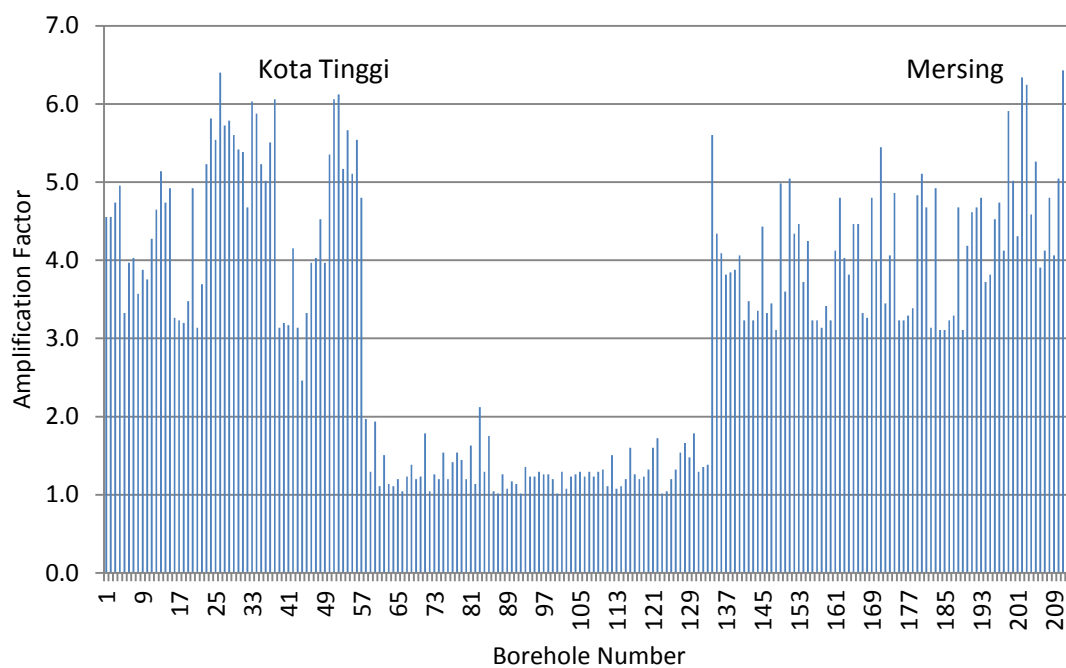


(i) Melaka

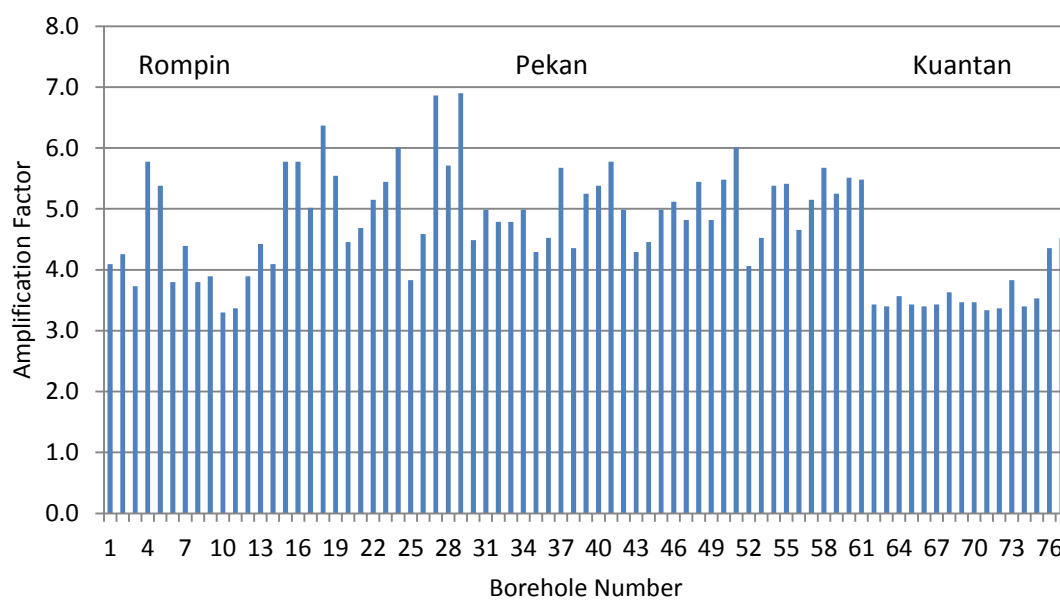


(j) West Johor

‘Figure 4.88, continued’

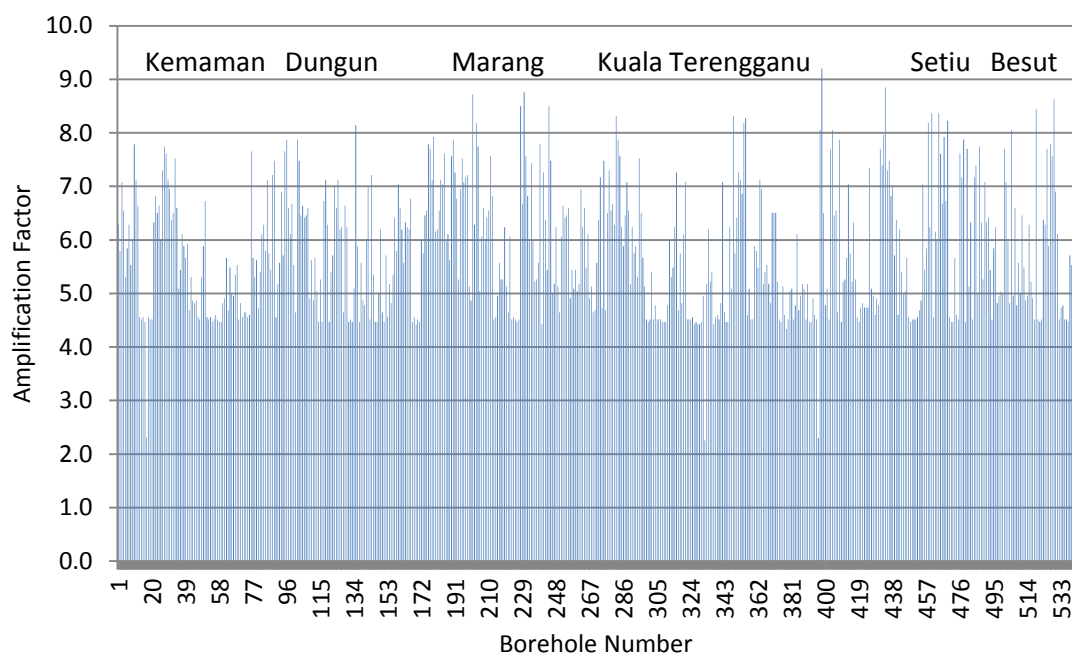


(k) East Johor

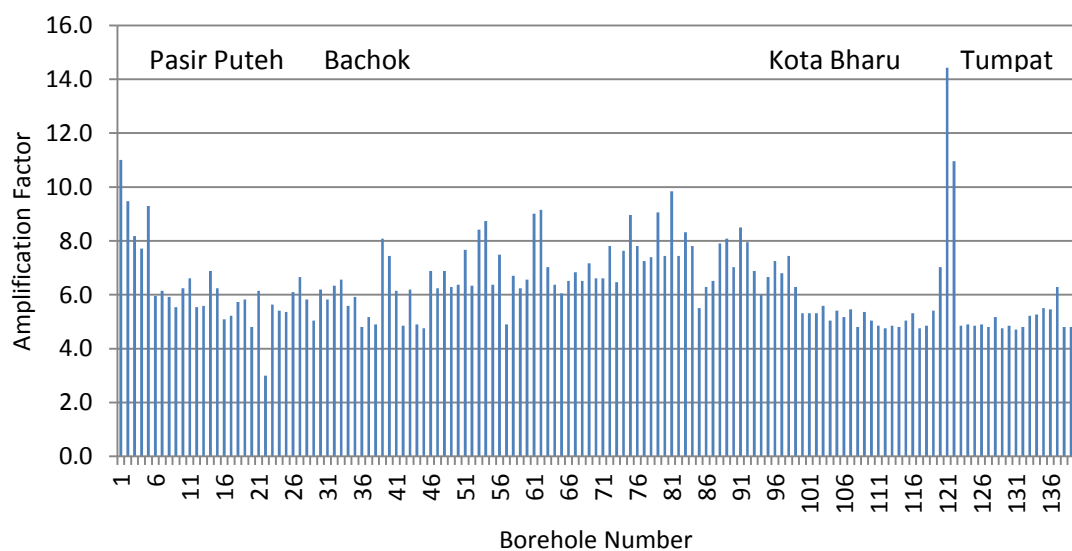


(l) Pahang

‘Figure 4.88, continued’



(m) Terengganu



(n) Kelantan

Figure 4.88: Microzonation line of 11 states in Peninsular Malaysia

4.3.4 Comparative Study of Recent Findings to Previous Works

Different sources of seismic information is selected and tabulated in Table 4.6. 3 works which was previously documented in the last 8 years are compiled for comparative study on the PGA value at bedrock. The works are Petersen et al. (2008), Adnan et al. (2005) and Azmi et al. (2013). This study consists of 7359 working file of the earthquake catalog from 1 May 1900 to 31 December 2009. Petersen et al. (2008) introduced earthquake catalog which contains 6710 records from 1964 to 2006 and presents close value of PGA at bedrock with the recent study. In contrast Adnan et al. (2005) presents low value of PGA compared to recent study. On the other hand, Azmi et al. (2013) introduced higher range of PGA values with more than 60% increase for Pulau Pinang.

The earthquake data from Adnan et al. (2005) are obtained from USGS, International Seismological Center (ISC) and MMD. The working file is 12149 with dated earthquake events between 27 February 1903 and 30 December 2000. The earthquake catalogs from Azmi et al. (2013) are acquired from USGS and Indonesian Meteorology Agency (BMG) with earthquake records compiled from 1871 to 2011. The different aspect of seismicity properties and considerations adapted in each works contribute to the different PGA values at bedrock in Peninsular Malaysia. The presentation of PGA differs due to the seismic parameters applied in the main seismic analysis. A site specific is also another contribution of differences in the findings. Hence the value is best represented with latest and updated content of the seismic parameters introduced in the main seismic analysis.

Table 4.6: Comparative study of PGA for 500 years return period

Shoreline State	Recent study PGA at bedrock 2016	PGA at bedrock (M. Petersen et al., 2008)	PGA at bedrock (Adnan et al., 2005)	PGA at bedrock (Azmi et al., 2013)
Perlis	0.04	0.05	0.01 - 0.02	-
Kedah	0.04	0.05	0.01 - 0.02	-
Pulau Pinang	0.06	0.05	0.01 - 0.02	0.09 - 0.10
Perak	0.06	0.06	0.01 - 0.02	-
Selangor	0.07	0.06	0.02 - 0.03	-
Negeri Sembilan	0.06	0.06	0.02 - 0.03	-
Melaka	0.06	0.05	0.02 - 0.03	-
West Johor	0.07	0.05	> 0.03	-
East Johor	0.03	0.05	0.02 - 0.03	-
Pahang	0.03	0.04	0.02 - 0.03	-
Terengganu	0.02	0.04	< 0.01	-
Kelantan	0.02	0.04	< 0.01	-

4.3.5 Summary

The microzonation study has summarized the output from PSHA, SMP and SRA in modelling the seismicity in the regional settings and in generating the microzonation line. The following conclusions can be drawn:

1. In PSHA, the aggregation of hazard model of 500 years return earthquake period design presents wide magnitude and distance of the earthquakes that contribution most of the hazard at selected states in Peninsular Malaysia. The results indicate that very near seismic sources of relative higher magnitudes are the dominating sources of hazard for the selected states of Peninsular Malaysia generally the west coast areas. The contributions from distance sources are

relatively low but cannot be neglected due to intrinsic uncertainties and limited seismic catalogues.

2. The SMP conducted presents unique ground motion at bedrock for each of the studied location. Similar to the PSHA, the west coast areas presents a stronger ground motion at bedrock in compared to the east coast areas.
3. In SRA, the east coast areas present stronger ground motion on the surface compared to the west coast areas. High amplification values are achieved in states such as Kelantan and Terengganu ($AF > 8$). Kedah, Pahang and East Johor simulate AF between 6 and 7, where the rest of the state presents $AF < 5$. This is due to the composition of concentrated loose and soft soil which enhanced the amplification of wave propagating through the soil layer. Thick layer of sand and silt as presented in section 4.1 have found generating the stronger ground motion in the seismicity study.

4.4 Liquefaction Hazard Assessment and Mapping

4.4.1 Graphical Illustration of Liquefaction Zones

Based on simplified procedure, a presentation of liquefaction layer in each of the studied area is presented in Figure 4.89 to Figure 4.102. The liquefaction layer illustrations are developed for shoreline areas of Peninsular Malaysia corresponding to ground motion developed from PSHA for annual probability of exceedance equal to 10% in 50 years (equal to return periods of 500 years) provide screening aid to assess liquefy layer at studied site. Figure 4.89 illustrates the liquefaction layer of Perlis. It appears as though the whole shoreline areas are exposed to liquefaction threat for the first 5 meter below ground level as indicated by the red zone of potentially liquefied zone. Major concern of findings is the coastal roads that stretch along these areas which are a significant asset for the state in providing mobility for goods and services. In summary, the combination of high groundwater within loose sandy sediments constitutes a significant liquefy layer beneath Perlis. Hence it is recommended for future developments located in designated liquefaction hazard zones to adapt procedures and guidelines for improvement of the existing built environment along the shoreline areas as to provide safety and minimized effect from liquefaction hazard.

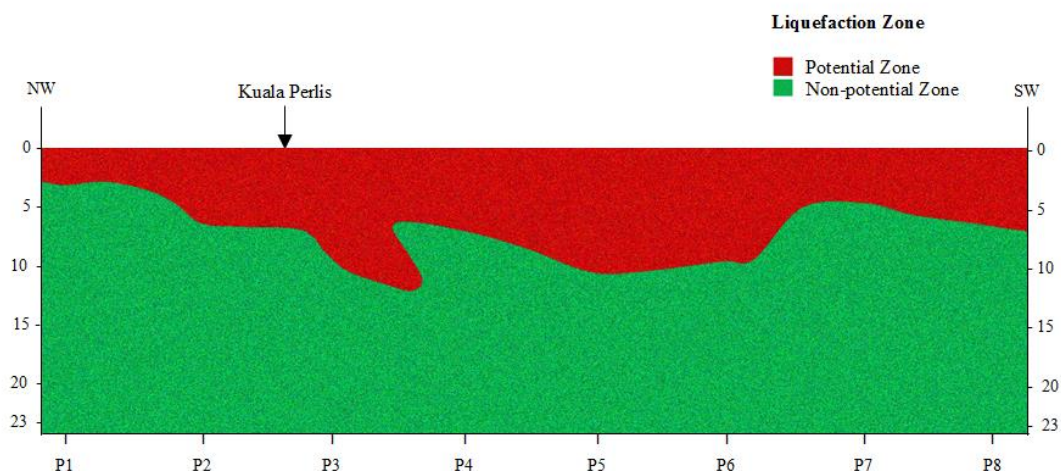


Figure 4.89: Liquefaction layer of Perlis

Similar findings are observed in the state of Langkawi and the mainland of Kedah which is a tourist spot and business hub of the country illustrated in Figure 4.90 and Figure 4.91. The loose sandy sediments with high groundwater have defined danger zoned for the entire studied areas. The major concern is sites which presents liquefied layer for the whole 20 m observed in Ulu Melaka, Pantai Chenang, Ayer Hitam and Yan.

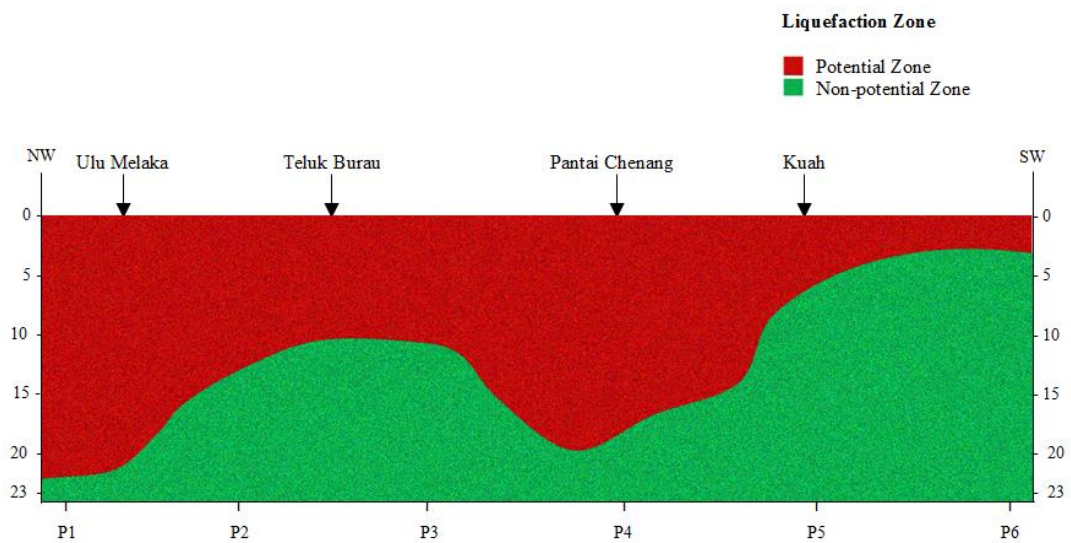


Figure 4.90: Liquefaction layer of Langkawi

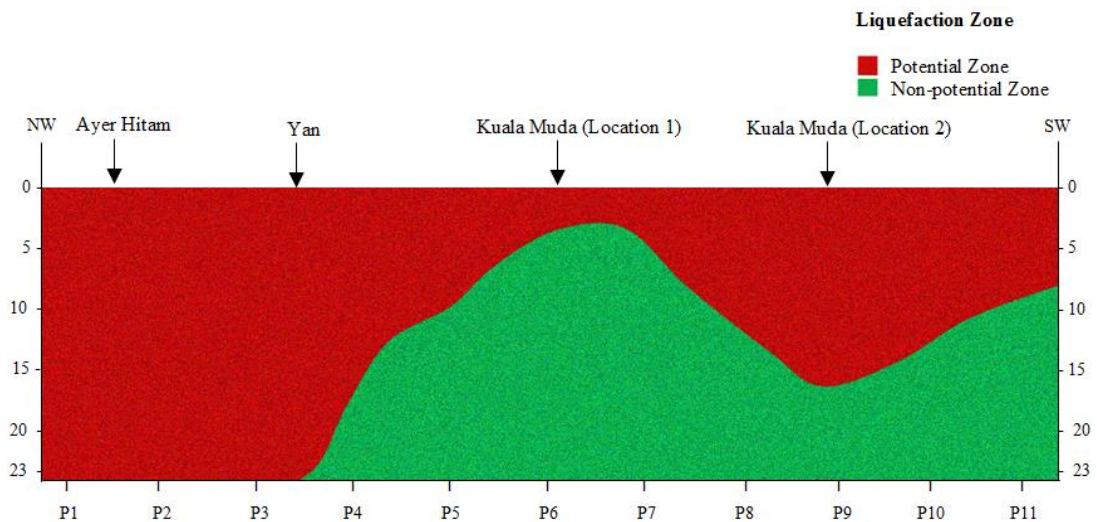


Figure 4.91: Liquefaction layer of Kedah

Figure 4.92 and Figure 4.93 illustrated the liquefaction layer of Penang state. The mainland of Penang presents a denser zone of liquefied soil compared to the island. Approximately 40% of the Penang Island is developed along the shoreline area and the remaining is in its natural state. The spreading liquefy zones in the first 5 m below surface is supporting built environment consist of multiple high rise buildings, residential units and town city. All of which is densely populated area.

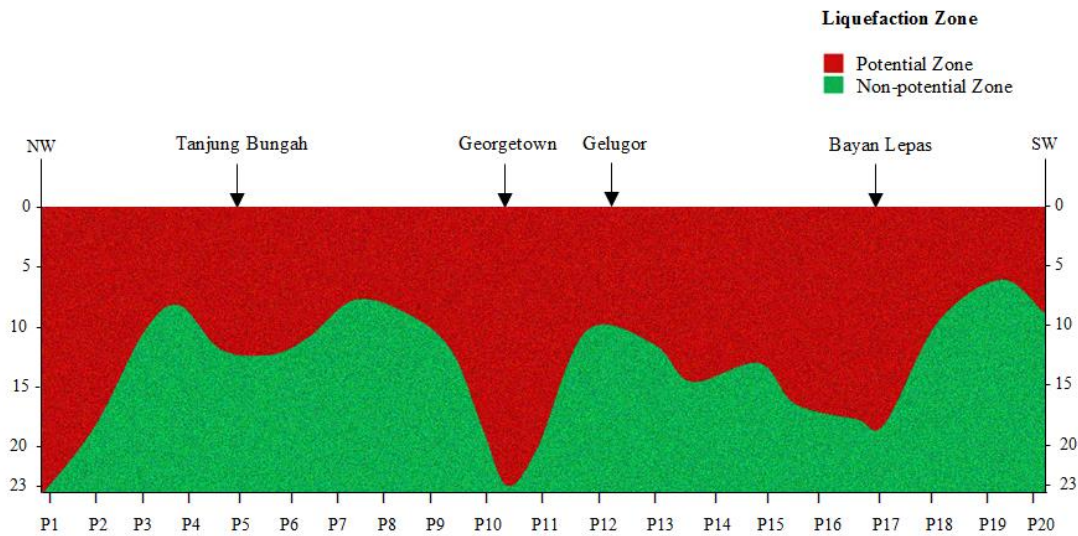


Figure 4.92: Liquefaction layer of Penang Island

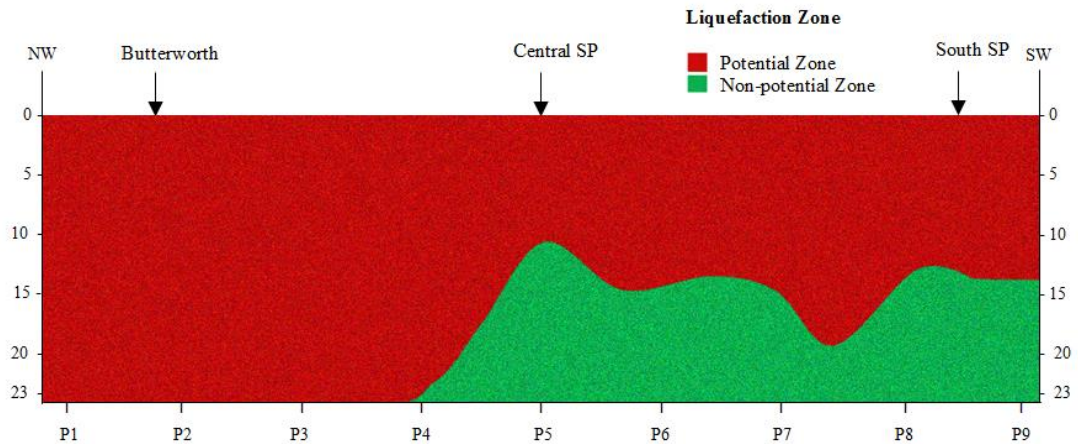


Figure 4.93: Liquefaction layer of Seberang Perai

Figure 4.94 illustrates the liquefaction layer of Perak. As there are no significant development observed in Perak, existing infrastructures should take cautious measures in as it presents liquefy layer for more than 70% of the overall studied layer.

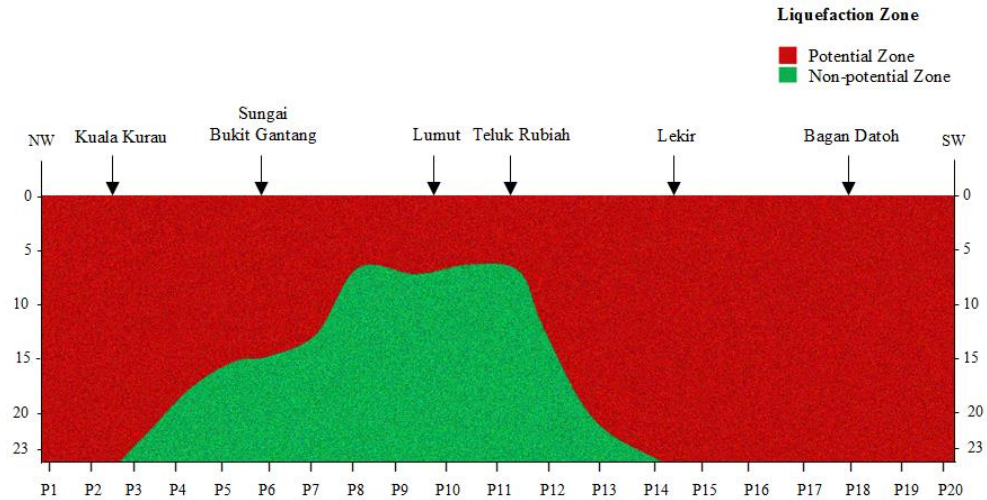


Figure 4.94: Liquefaction layer of Perak

Figure 4.95 presents the liquefaction layer of Selangor. The liquefy zone are found to be in random distribution. Some areas such as Kuala Langat present significant threat to liquefaction hazard.

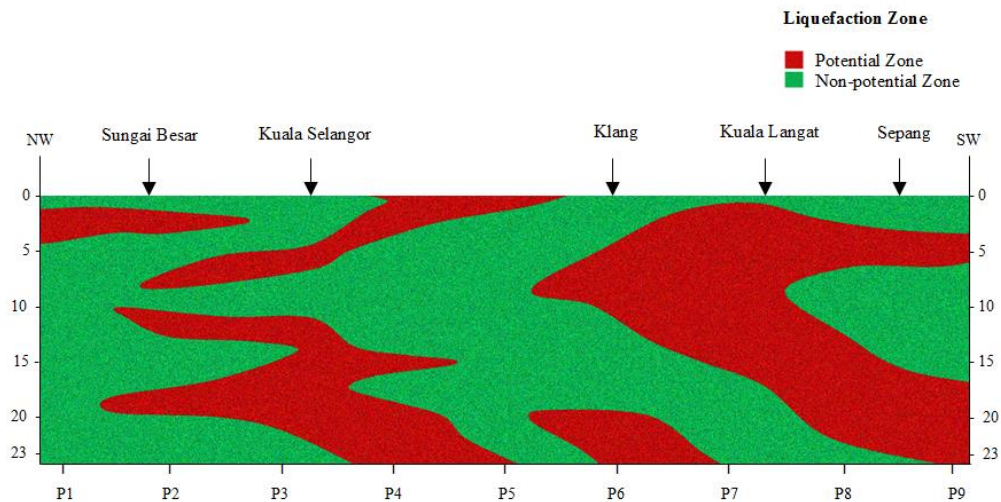


Figure 4.95: Liquefaction layer of Selangor

Only 5% of areas in the southern portion of Port Dickson presents liquefy zone, whereas other shows no threat to the hazard (Figure 4.96). In contrast Melaka presents 2 locations which are vulnerable to the threat; Melaka Tengah and Pantai Siring, both of which a town city and a tourist spot (Figure 4.97). The expansion of land through reclamation method should be investigated further with special design for substructure in countering the liquefaction hazard.

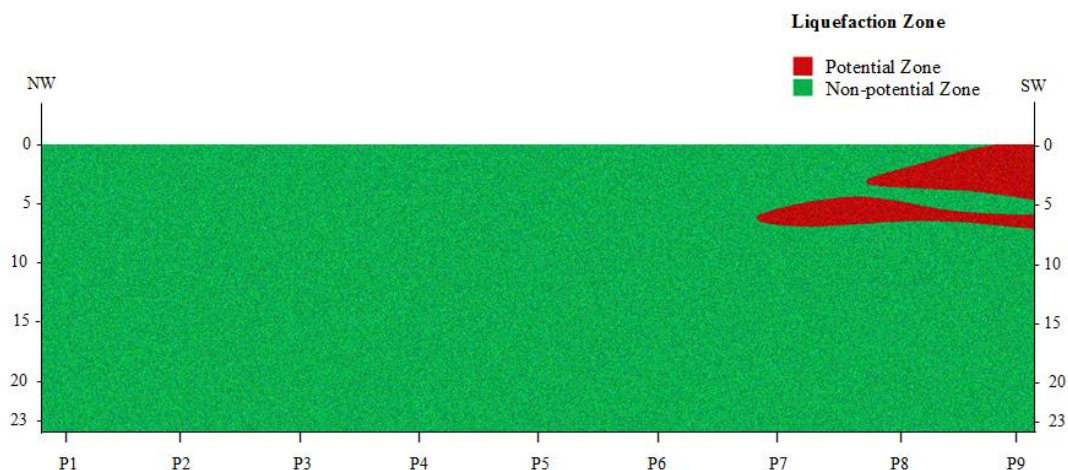


Figure 4.96: Liquefaction layer of Negeri Sembilan

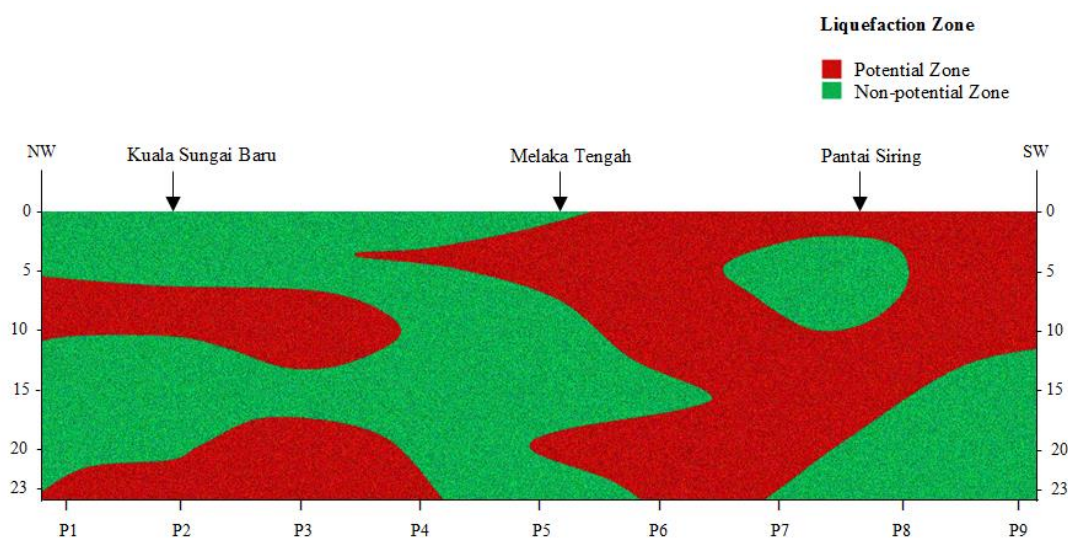


Figure 4.97: Liquefaction layer of Melaka

Figure 4.98 and Figure 4.99 present the Johor result of the west coast areas and east coast areas. The distribution of liquefy zone does not present constant pattern as it is more observed as a scattered data. Significant areas in the west coast are Batu Pahat and Pontian as the liquefy zones exist on the surface level. Similar findings are found in the east coast areas in few areas in Kota Tinggi and Mersing. In defining an ideal design of built environment, areas with liquefy zone close to the surface should be abandoned and preserved in its natural state as to prevent for disaster during liquefaction hazard.

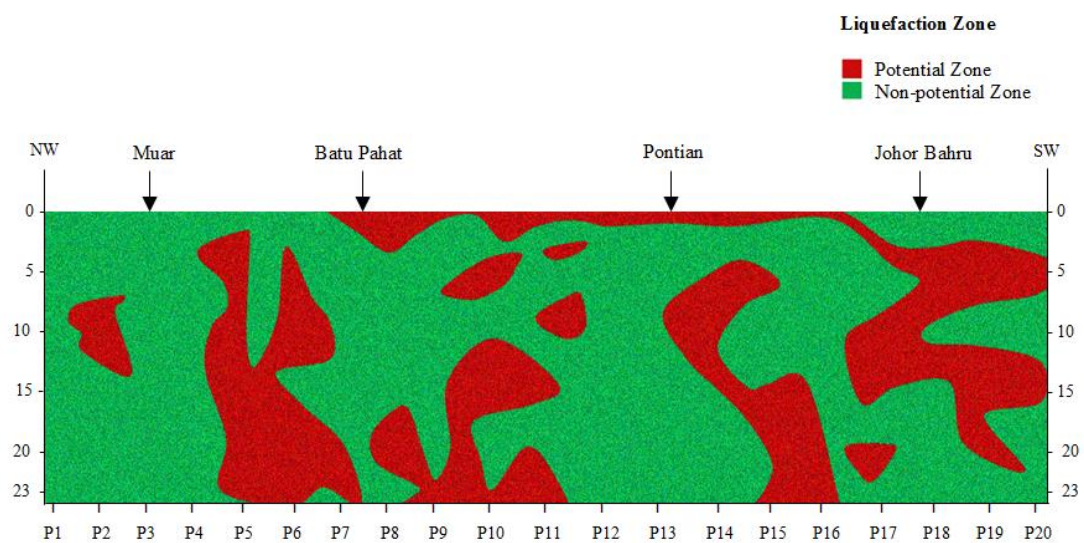


Figure 4.98: Liquefaction layer of West Johor

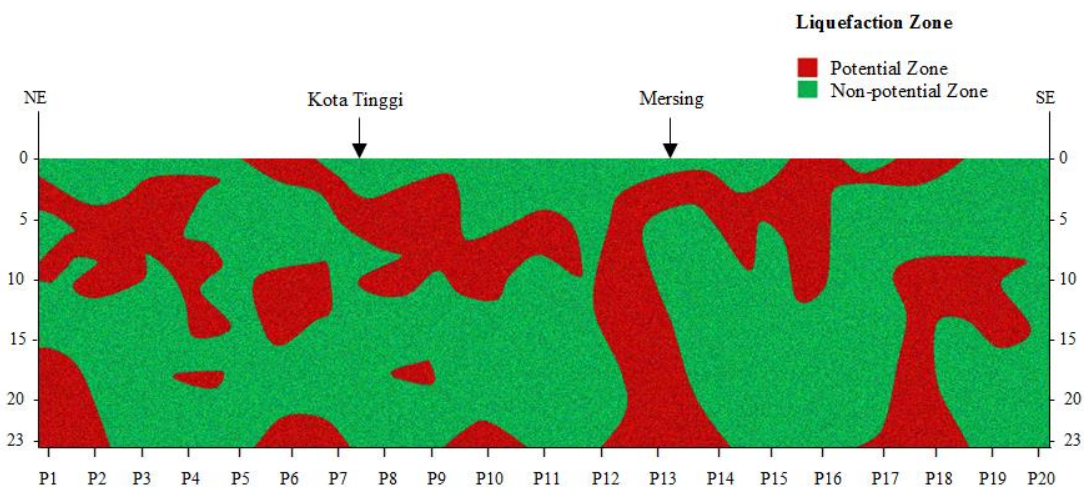


Figure 4.99: Liquefaction layer of East Johor

Pahang state presents liquefy zone of 60% of overall studied layer (Figure 4.100). The existing of liquefy layer after 2 m below ground surface denotes the importance of special design for substructure penetrating into the soil especially in Kuantan areas. Pekan and Rompin are less developed compared to Kuantan shows advantage of lesser effect during earthquake hazard. The existing of port in Kuantan presents the importance of adapting soil improvement method and special subsurface design in minimizing the liquefaction hazard. A vulnerable place in Pekan should enhanced awareness of future development as the layer of liquefy zone at most of the areas can reach up to 23 meters below ground surface. As safer location defined in Rompin, the place could be a shelter to accommodate victims from the earthquake hazard provided the road are in good performance after the disaster to transfer people, foods and services.

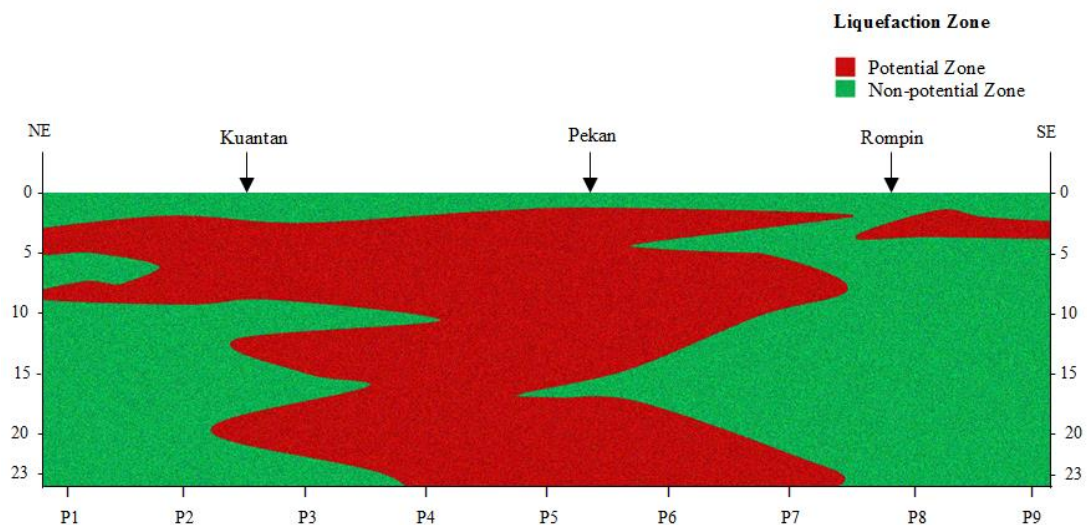


Figure 4.100: Liquefaction layer of Pahang

Figure 4.101 and Figure 4.102 presents liquefaction layer of Terengganu and Kelantan. Approximately 50% of the areas in Terengganu are affected with liquefaction where more than 60% affected areas are found in Kelantan. Major concern should be provided in Kuala Terengganu as it is the main concentration of built environment. The

northern areas are less develop; Besut and Setiu. Hence the liquefaction context shows no significant contribution to the place unless future development with heavily built environment is constructed at the place. Dungun and Kemaman also need further investigation as main ports are located at these locations. Similar findings are observed in Kelantan where the concentration of population is located in Kota Bharu. The liquefaction definition is made significant when the location is developed unlike a location in natural state where the surroundings presents lesser damaging effect after earthquake disaster.

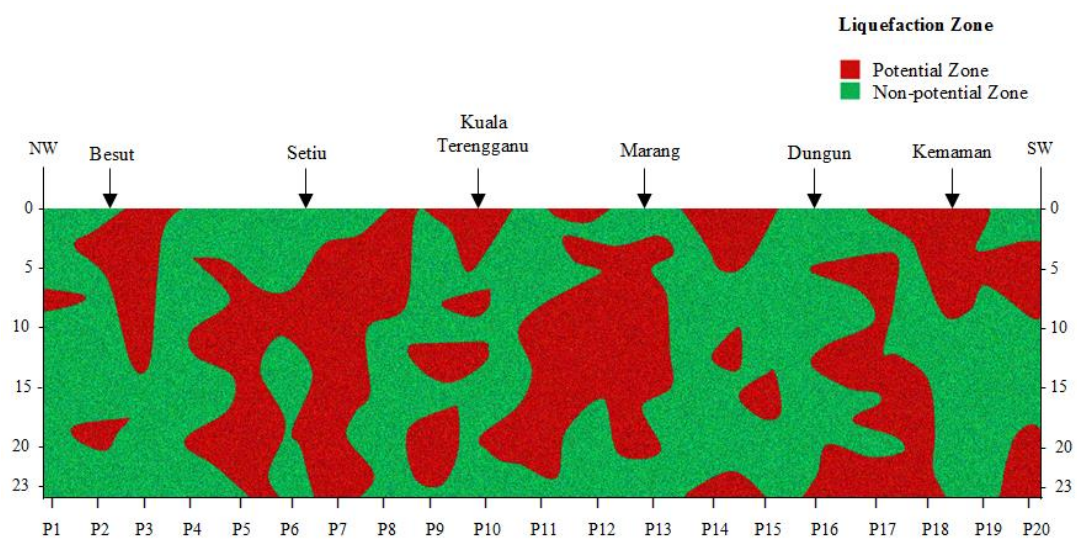


Figure 4.101: Liquefaction layer of Terengganu

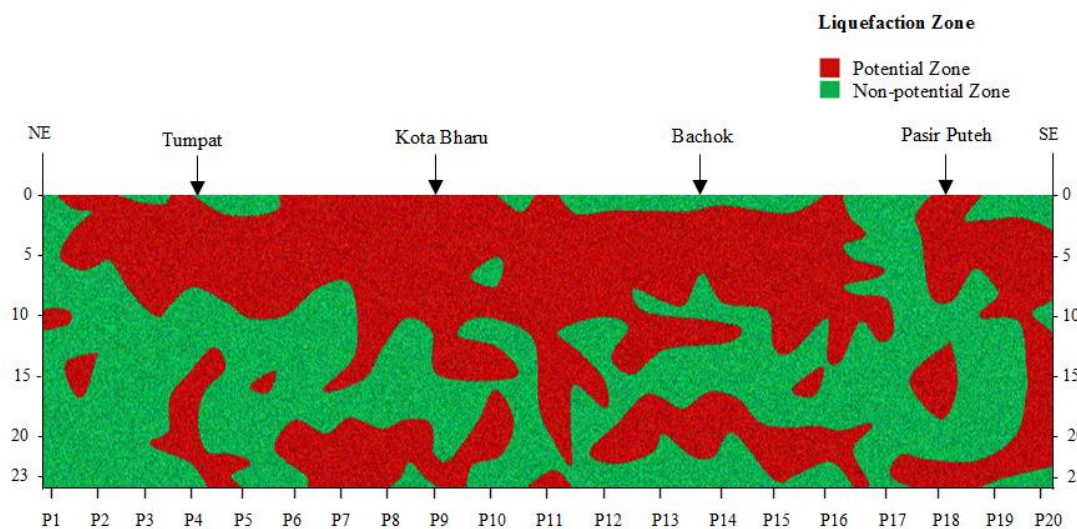


Figure 4.102: Liquefaction layer of Kelantan

4.4.2 Liquefaction Hazard Map

By using LPI to summarize the studied area, a map of liquefaction hazard along the shoreline areas of Peninsular Malaysia is plotted in Figure 4.103. The east coast areas present multiple higher intensity of liquefaction hazard compared to the areas in the west coast. This is due to the high concentration of vulnerable loose deposits in east coast region. The Kelantan and Terengganu state are at high risk based on the hazard intensity due to the 'clean sand' observed in the soil composition figure generated in section 4.1.10 and section 4.1.11. Although the PGA generated for east coast region is less significant compared to the west coast region however the PSA generated shows high propagation in the east coast region compared to the west coast region. The findings is similar with the one found in Christchurch and Tokyo Bay Japan where soil liquefaction was found to be critical at sites with similar settings (Yasuda et al., 2012). The existing development along the shoreline are recommended for further study to introduced proper mitigation method against soil liquefaction on existing structures.

On the other hand vulnerable silt which exists more than 60% in the west coast areas contributes to the high hazard intensity in the areas. The shallow ground water table in all the studied location also makes most areas vulnerable to hazard. The northern part of west coast region shows higher hazard intensity compared to the southern part. Seismic source from long distance earthquake presented in section 4.3.1.1 plays significant role in defining the severity of the specific site. Reclaimed land is recommended to be continuously monitored as to provide safe built environment towards sudden changes in the environment. A proper planning for preparedness and mitigation towards hazard is crucial as the region is moving at very fast pace in the development context. Lesson learnt from previous soil liquefaction induced ground motion are a motivation and a step forward in benefiting the regional ground and natural formation of the geological setting of Peninsular Malaysi.

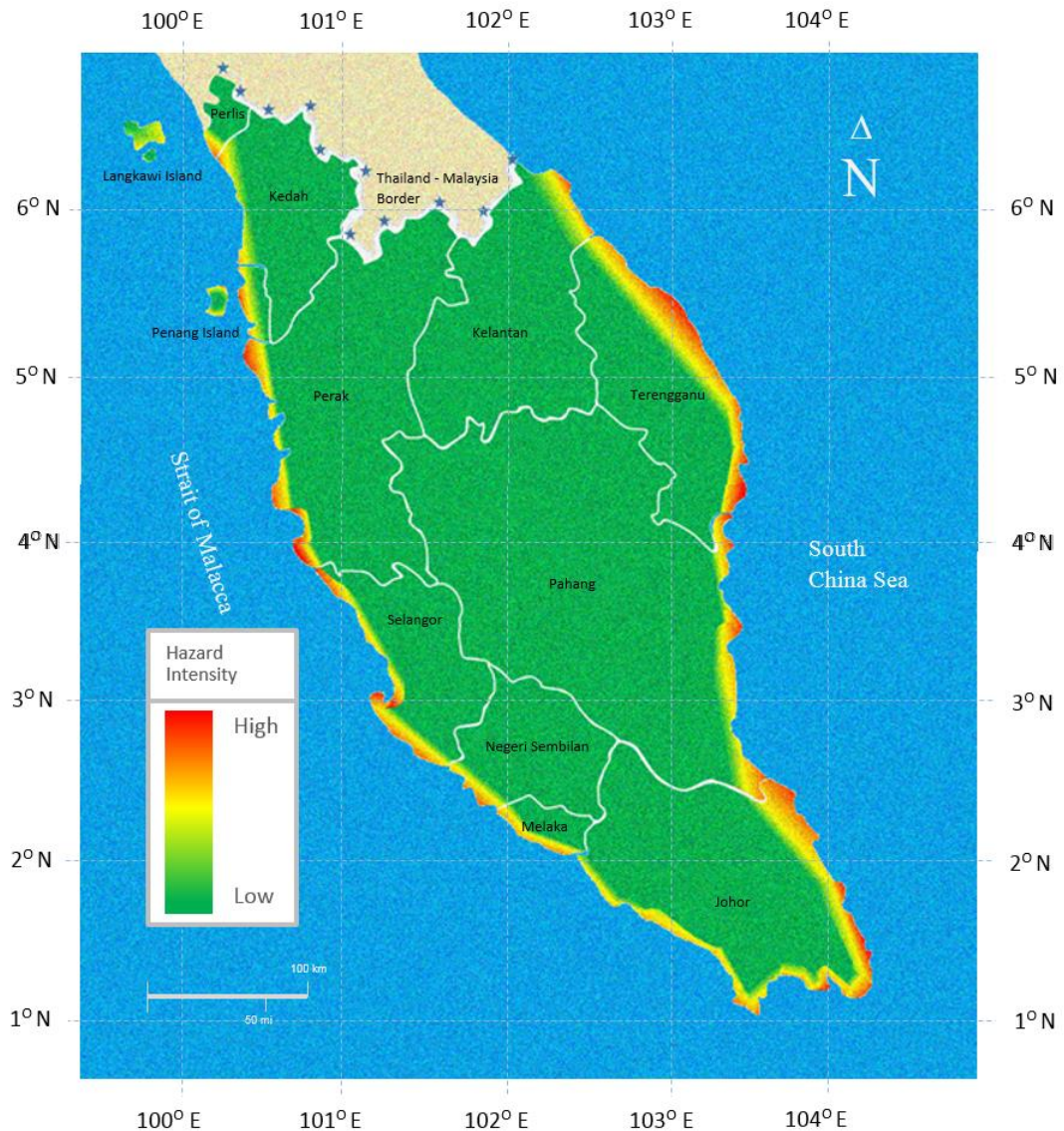


Figure 4.103: Liquefaction hazard map of shoreline areas of Peninsular Malaysia

4.4.3 Mitigation Zoning

The general procedure in making hazard-informed evaluation is to highlight potential hazard zones along the shoreline areas in addressing authorities and local councils about soil liquefaction threat for future improvement, mitigation and remediation works. The quantification is subjected to contributing factors of hazard. Observation from available

data which was made in section 4.1 on the decision making process result in addressing high possibility and uncertain situations in the most optimized manner in the context of Peninsular Malaysia. The wide use of resources is to ensure that appropriate action is taken quickly and efficiently in reducing unknown hazard in the location. Limited resources are prioritized accordingly in generating Table 4.7 to Table 4.8 for soil liquefaction hazard quantification (Law & Ling, 1992; Tokimatsu & Asaka, 1998; Wang, 1979). The tables are summarized with a summation of the scores for the driving effect of hazard which is then concluded under respected zones and categories of hazard level. The zones are presented with a description of severity level ranging from low to high level. By using available mitigation in the wide scope of the present research, each category of hazard level is related to the mitigation aspect respectively (Ashford et al., 2000; El Mohtar et al., 2012; Mitchell, 2008; Porbaha et al., 1999; Shenthana et al., 2004; Yegian et al., 2007).

Table 4.9 and Table 4.10 summarize the hazard level at each studied locations along with the hazard category in providing the mitigation information according to existing literature (Chávez et al., 2017; MacAskill & Guthrie, 2017; Tokimatsu et al., 2012; Wotherspoon et al., 2015). This approach is to acknowledge individuals as well as the community about hazard information in the areas which could lead them in making safe decisions and effective planning of their surroundings (Bouziou & O'Rourke, 2017; Bretherton, 2017; Wang & Guldman, 2016). This information could trigger more detail research to be carried out by local and also international governing bodies from research institution as well as engineering firms in shaping good measures in the near development of Peninsular Malaysia (Bhuiyan et al., 2013).

Table 4.7: Input for score

SL-INPUT-01	
LPI Index	Score
> 30	100
15	75
10	50
5	25
0	0

Table 4.8: Output 1 for the shoreline zoning and soil liquefaction category

SL-OUTPUT-01						
Score	Shoreline Zone	Soil Liquefaction Category				
		SL-0	SL-1	SL-2	SL-3	SL-4
76 - 100	Z-5	20	40	60	80	100
51 - 75	Z-4	16	32	48	64	80
26 - 50	Z-3	12	24	36	48	60
21 - 25	Z-2	8	16	24	32	40
0 - 20	Z-1	4	8	12	16	20

Table 4.9: Output 2 for the severity level, action and mitigation

SL-OUTPUT-02		SL-OUTPUT-03		
Zone	Severity Level	Category	Action	Mitigation
Z-5	Critical impact	SL-4	Forest restoration and rehabilitation	Abandon site
Z-4	Important impact	SL-3	Conduct site specific investigation	Special Analysis for Structure
Z-3	Moderate impact	SL-2	Further Analysis	Ground Improvement Techniques
Z-2	Low impact	SL-1	Monitor	No Action
Z-1	Insignificant impact	SL-0	No Action	No Action

Table 4.10: Liquefaction zone for 40 shoreline districts of Peninsular Malaysia

Area	SL- INPUT- 01	SL- INPUT- 02	SL- INPUT- 03	SL- INPUT- 04	Total INPUT	SL- OUTPUT- 01	SL- OUTPUT- 03
R1	25	25	25	25	100	Z-5	SL-4
L1	15	10	25	25	75	Z-4	SL-4
K1	15	5	25	15	60	Z-4	SL-3
K2	25	5	25	10	65	Z-4	SL-3
K3	25	10	25	25	85	Z-5	SL-3
K4	25	10	25	15	75	Z-5	SL-3
P1	25	25	25	25	100	Z-5	SL-4
P2	15	25	25	25	90	Z-5	SL-4
A1	15	25	25	25	90	Z-5	SL-4
A2	15	15	25	15	70	Z-4	SL-3
A3	25	25	25	25	100	Z-5	SL-4
A4	25	25	25	25	100	Z-5	SL-4
B1	25	25	25	25	100	Z-5	SL-4
B2	25	25	15	25	90	Z-5	SL-4
B3	25	25	25	25	100	Z-5	SL-4
B4	25	25	25	25	100	Z-5	SL-4
B5	25	25	25	25	100	Z-5	SL-4
N1	15	5	15	25	60	Z-4	SL-2
M1	15	10	25	15	65	Z-4	SL-2
M2	25	5	25	25	80	Z-5	SL-3
M3	25	10	25	15	75	Z-5	SL-3
J1	25	10	25	25	85	Z-5	SL-3
J2	25	15	25	25	90	Z-5	SL-4
J3	25	5	25	25	80	Z-5	SL-4
J4	25	25	25	25	100	Z-5	SL-4
J5	25	10	25	25	85	Z-5	SL-4
J6	25	25	25	25	100	Z-5	SL-4
C1	25	25	25	25	100	Z-5	SL-4
C2	25	10	25	25	85	Z-5	SL-4
C3	25	25	25	25	100	Z-5	SL-4
T1	15	25	25	25	90	Z-5	SL-4
T2	25	25	25	25	100	Z-5	SL-4
T3	15	25	25	25	90	Z-5	SL-4
T4	15	25	25	25	90	Z-5	SL-4
T5	15	25	25	25	90	Z-5	SL-4
T6	25	25	25	25	100	Z-5	SL-4
D1	25	15	25	25	90	Z-5	SL-4
D2	25	15	25	25	90	Z-5	SL-4
D3	15	25	25	25	90	Z-5	SL-4
D4	15	15	25	25	80	Z-5	SL-4

4.4.4 Summary

The illustration of graphical contents of liquefaction zone and the liquefaction hazard map presents significant awareness in regional settings. The information presents more than 90% of studied areas are prone to liquefaction hazard. The following conclusions can be drawn:

1. East coast areas present higher intensity of liquefaction hazard compared to the west coast areas. This put future development at stake if to be constructed at site located on the shoreline areas.
2. More than 60% of shoreline areas in east coast region are in natural state. Less development is observed makes the region much safer in the context of earthquake disaster.
3. Vulnerable silt deposit exists in most of the studied location in west coast region. Hence the existing built environment are at stake as there has not been designed to cater the earthquake loading and liquefaction effect. Reclaimed projects in Penang, Selangor and Melaka are advised to adapt to earthquake resisting design as some of the areas are prone to liquefaction hazard. This scene is demonstrated in most of the built environment in Tokyo Bay, Japan as presented in the literature review of thesis study.

CHAPTER 5: CONCLUSION AND RECOMMENDATION

5.1 Conclusions

The conclusions are as follows:

- i. The liquefaction assessment study presents condition of Peninsular Malaysia in the context of soil liquefaction hazard. It was found that most of the areas are prone to liquefaction hazard and needs further liquefaction assessment in evaluating the level of severity.
- ii. Modulus reduction curves and damping ratio curves extracted from cyclic triaxial testing presents unique behavior of soil when subjected to cyclic loading. The sand sample tested shows vulnerability towards cyclic loading whereas the clay sample tested shows good resistance towards cyclic loading.
- iii. The ground motion generated from earthquake study presents unique amplification factor for studied site. The highest amplification factor occurs in the east coast region whereas the west coast region shows much lower amplification factor due soil layers which affect the propagation of waves.
- iv. Soil liquefaction hazard map developed in study provides the severity of hazard at studied sites. Most of shoreline areas present significant vulnerability towards hazard. The mitigation chart developed in study shows most of areas need special design of foundation for the construction of structures along the shoreline of Peninsular Malaysia.

5.2 Recommendation for Future Work

The future works are as follows:

- i. The graphical illustrations presented can be further updated with more borehole data collection and present general description.
- ii. Soil samples from site specific can be tested. Hence unique findings of the regional soil performance can be observed
- iii. Recent earthquake can be included in the earthquake study.
- iv. Recent procedure of liquefaction assessment can be implemented.

5.3 Implication and Application of Study

The study can be an eye-opener for Malaysian to observe the natural surroundings around them which can lead to natural disaster when not managed in proper way. Development should be led by team of expertise that provides concrete evidence on impact when it comes to land development and usage. As for the application of study, any building development along the shorelines can adapt this thesis as reference or guideline in exploring the soil underneath and evaluate its performance in the context of soil liquefaction hazard.

REFERENCES

- Adalier, K., & Elgamal, A. (2004). Mitigation of liquefaction and associated ground deformations by stone columns. *Engineering Geology*, 72(3), 275-291.
- Adnan, A., Hendriyawan, A. M., & Irsyam, M. (2006). *Development of seismic hazard map for peninsular malaysia*. Paper presented at the Proceeding on Malaysian Science and Technology Congress.
- Adnan, A., Hendriyawan, H., Marto, A., & Irsyam, M. (2005). Seismic hazard assessment for Peninsular Malaysia using gumbel distribution method.
- Akçal, A. N., Acar, M. H., & Budak, G. (2015). Research on the Liquefaction Potential of the Yamansaz Region in Antalya, Turkey. *Procedia Earth and Planetary Science*, 15, 271-277.
- Al Atik, L., & Abrahamson, N. (2010). An improved method for nonstationary spectral matching. *Earthquake Spectra*, 26(3), 601-617.
- Andrews, D. C., & Martin, G. R. (2000). *Criteria for liquefaction of silty soils*. Paper presented at the Proc., 12th World Conf. on Earthquake Engineering.
- Andrus, R. D., & Stokoe II, K. H. (2000). Liquefaction resistance of soils from shear-wave velocity. *Journal of geotechnical and geoenvironmental engineering*, 126(11), 1015-1025.
- Arion, C., Calarasu, E., & Neagu, C. (2015). Evaluation of Bucharest soil liquefaction potential. *Math Model Civil Eng*, 11(1), 5-12.
- Ashford, S., Rollins, K., Bradford V, S., Weaver, T., & Baez, J. (2000). Liquefaction mitigation using stone columns around deep foundations: Full-scale test results. *Transportation Research Record: Journal of the Transportation Research Board*(1736), 110-118.
- Ashford, S. A., Boulanger, R. W., Donahue, J. L., & Stewart, J. P. (2011). Geotechnical quick report on the Kanto Plain region during the March 11, 2011, Off Pacific Coast of Tohoku earthquake, Japan. *GEER Association Report No GEER-025a, Geotechnical Extreme Events Reconnaissance (GEER)*.
- Aydan, Ö., Ulusay, R., Hamada, M., & Beetham, D. (2012). Geotechnical aspects of the 2010 Darfield and 2011 Christchurch earthquakes, New Zealand, and geotechnical damage to structures and lifelines. *Bulletin of Engineering Geology and the Environment*, 71(4), 637-662.
- Azmi, M., Kiyono, J., & Furukawa, A. (2013). Development of probabilistic seismic hazard map of Penang Island, Malaysia. *歴史都市防災論文集*, 7, 153-160.
- Baker, J. W., & Jayaram, N. (2008). Correlation of spectral acceleration values from NGA ground motion models. *Earthquake Spectra*, 24(1), 299-317.

- Balendra, T., & Li, Z. (2008). Seismic hazard of Singapore and Malaysia. *EJSE special issue: earthquake engineering in the low and moderate seismic regions of Southeast Asia and Australia*.
- Bardet, J., & Tobita, T. (2001). A Computer Program for Non-linear Earthquake Response Analyses of Layered Soil Deposits. *Department of Civil Engineering, University of Southern California*.
- Bhattacharya, S., Tokimatsu, K., Goda, K., Sarkar, R., Shadlou, M., & Rouholamin, M. (2014). Collapse of Showa Bridge during 1964 Niigata earthquake: A quantitative reappraisal on the failure mechanisms. *Soil Dynamics and Earthquake Engineering*, 65, 55-71.
- Bhuiyan, M. A. H., Siwar, C., & Ismail, S. M. (2013). Tourism development in Malaysia from the perspective of development plans. *Asian Social Science*, 9(9), 11.
- Blake, T. (1997). Summary Report of Proceedings of the NCEER Workshop on Evaluation of Liquefaction Resistance of Soils. Youd TL, and Idriss IM: eds., Technical Report NCEER 97-0022.
- Boulanger, R. W., & Idriss, I. (2008). Soil liquefaction during earthquake. *Engineering monograph, EERI, California, USA*, 266.
- Bouziou, D., & O'Rourke, T. D. (2017). Response of the Christchurch water distribution system to the 22 February 2011 earthquake. *Soil Dynamics and Earthquake Engineering*, 97, 14-24.
- Brackley, H. (2012). *Review of liquefaction hazard information in eastern Canterbury, including Christchurch City and parts of Selwyn, Waimakariri and Hurunui Districts*: Environment Canterbury Regional Council.
- Bray, J. D., Markham, C. S., & Cubrinovski, M. (2016). Reprint of Liquefaction assessments at shallow foundation building sites in the Central Business District of Christchurch, New Zealand. *Soil Dynamics and Earthquake Engineering*, 91, 234-245.
- Bray, J. D., Markham, C. S., & Cubrinovski, M. (2017). Liquefaction assessments at shallow foundation building sites in the Central Business District of Christchurch, New Zealand. *Soil Dynamics and Earthquake Engineering*, 92, 153-164.
- Bretherton, J. (2017). Christchurch's High Performance Rebuild. *Procedia Engineering*, 180, 1044-1055.
- Chang, S. E. (2000). Disasters and transport systems: loss, recovery and competition at the Port of Kobe after the 1995 earthquake. *Journal of transport geography*, 8(1), 53-65.
- Chang, S. E., & Nojima, N. (2001). Measuring post-disaster transportation system performance: the 1995 Kobe earthquake in comparative perspective. *Transportation research part A: policy and practice*, 35(6), 475-494.

- Chávez, V., Mendoza, E., Silva, R., Silva, A., & Losada, M. A. (2017). An experimental method to verify the failure of coastal structures by wave induced liquefaction of clayey soils. *Coastal Engineering*, 123, 1-10.
- Chong, F. S., & Pfeiffer, D. (1975). *Hydrogeological Map of Peninsular Malaysia: Peta Hidrogeologi Semenanjung Malaysia*: Director General of Geological Survey, Malaysia.
- Chung, C.-K., Kim, H.-S., & Sun, C.-G. (2014). Real-time assessment framework of spatial liquefaction hazard in port areas considering site-specific seismic response. *Computers and Geotechnics*, 61, 241-253.
- Cornell, C. A. (1968). Engineering seismic risk analysis. *Bulletin of the seismological society of America*, 58(5), 1583-1606.
- Cubrinovski, M., Bray, J. D., Taylor, M., Giorgini, S., Bradley, B., Wotherspoon, L., & Zupan, J. (2011). Soil liquefaction effects in the central business district during the February 2011 Christchurch earthquake. *Seismological Research Letters*, 82(6), 893-904.
- Cubrinovski, M., & Robinson, K. (2016). Lateral spreading: Evidence and interpretation from the 2010–2011 Christchurch earthquakes. *Soil Dynamics and Earthquake Engineering*, 91, 187-201.
- Davis, R., & Berrill, J. (1996). Liquefaction susceptibility based on dissipated energy: A consistent design methodology. *Bulletin of the New Zealand National Society for Earthquake Engineering*, 29(2), 83-91.
- Day, R. W. (2002). *Geotechnical earthquake engineering handbook*: McGraw-Hill.
- DeMets, C., Gordon, R. G., & Argus, D. F. (2010). Geologically current plate motions. *Geophysical journal international*, 181(1), 1-80.
- El Mohtar, C., Bobet, A., Santagata, M., Drnevich, V., & Johnston, C. (2012). Liquefaction mitigation using bentonite suspensions. *Journal of geotechnical and geoenvironmental engineering*, 139(8), 1369-1380.
- Gao, X., Ma, X., & Li, X. (2011). The great triangular seismic region in eastern Asia: Thoughts on its dynamic context. *Geoscience Frontiers*, 2(1), 57-65.
- Ghani, A. A., Azirun, M. S., Ramli, R., & Hashim, R. (2008). Geochemical contrast between Beroga (Kuala Kelawang pluton) and Semenyih (Kuala Lumpur pluton) granites in Kuala Kelawang area, Negeri Sembilan. *Bulletin of the Geological Society of Malaysia*, 54, 71-47.
- Green, R. A., Maurer, B. W., Bradley, B. A., Wotherspoon, L., & Cubrinovski, M. (2013). Implications from liquefaction observations in New Zealand for interpreting paleoliquefaction data in the central eastern United States (CEUS). *US Geological Society Final Technical Report County of San Diego low impact development handbook (2009). Geotechnical consideration.*

- Grundy, P. (2010). *The padang earthquake 2009—lessons and recovery*. Paper presented at the Australian Earthquake Engineering Society 2010 Conference.
- Gutenberg, B., & Richter, C. F. (1956). Earthquake magnitude, intensity, energy, and acceleration (second paper). *Bulletin of the seismological society of America*, 46(2), 105-145.
- Hakam, A., & Suhelmidawati, E. (2013). Liquefaction Due to September 30th 2009 Earthquake in Padang. *Procedia Engineering*, 54, 140-146.
- Hansen, W. R. (1965). *Effects of the earthquake of March 27, 1964, at Anchorage, Alaska*: US Government Printing Office.
- Harun, Z. (2002). Late mesozoic-early tertiary faults of Peninsular Malaysia. *Geological Society of Malaysia Bulletin*, 45, 117-120.
- Hatmoko, J. T., & Suryadharma, H. (2015). Prediction of Liquefaction Potential Study at Bantul Regency the Province of Special Region of Yogyakarta Indonesia. *Procedia Engineering*, 125, 311-316.
- Holtz, R. D., & Kovacs, W. D. (1981). *An introduction to geotechnical engineering*.
- Holzer, T., Youd, T., & Hanks, T. (1989). Dynamics of liquefaction during the 1987 Superstition Hills, California, earthquake. *Science*, 244(4900), 56-59.
- Huang, Y., & Yu, M. (2013). Review of soil liquefaction characteristics during major earthquakes of the twenty-first century. *Natural hazards*, 65(3), 2375-2384.
- Hutchison, C. S. (1989). *Geological evolution of South-east Asia* (Vol. 13): Clarendon Press Oxford.
- Idriss, I. (1990). *Response of soft soil sites during earthquakes*. Paper presented at the Proc. H. Bolton Seed Memorial Symposium.
- Idriss, I., & Boulanger, R. W. (2008). *Soil liquefaction during earthquakes*: Earthquake Engineering Research Institute.
- Irsyam, M., Dangkoa, D. T., Hoedajanto, D., Hutapea, B. M., Kertapati, E. K., Boen, T., & Petersen, M. D. (2008). Proposed seismic hazard maps of Sumatra and Java islands and microzonation study of Jakarta city, Indonesia. *Journal of earth system science*, 117(2), 865-878.
- Ishac, M. F., & Heidebrecht, A. C. (1982). Energy dissipation and seismic liquefaction in sands. *Earthquake Engineering & Structural Dynamics*, 10(1), 59-68.
- Isobe, K., Ohtsuka, S., & Nunokawa, H. (2014). Field investigation and model tests on differential settlement of houses due to liquefaction in the Niigata-ken Chuetsu-Oki earthquake of 2007. *Soils and Foundations*, 54(4), 675-686.
- Iwasaki, T., Tatsuoka, F., Tokida, K.-i., & Yasuda, S. (1978). *A practical method for assessing soil liquefaction potential based on case studies at various sites in Japan*. Paper presented at the Proc., 2nd Int. Conf. on Microzonation.

- Iwasaki, T., & Tokida, K.-i. (1980). *Studies on Soil Liquefaction Observed During the Miyagi-Ken Oki Earthquake of June 12, 1978*: publisher not identified.
- Iwasaki, T., Tokida, K., Tatsuoka, F., Watanabe, S., Yasuda, S., & Sato, H. (1982). *Microzonation for soil liquefaction potential using simplified methods*. Paper presented at the Proceedings of the 3rd international conference on microzonation, Seattle.
- Kang, G.-C., Chung, J.-W., & Rogers, J. D. (2014). Re-calibrating the thresholds for the classification of liquefaction potential index based on the 2004 Niigata-ken Chuetsu earthquake. *Engineering Geology*, 169, 30-40.
- Kawakami, F., & Asada, A. (1966). Damage to the ground and earth structures by the Niigata earthquake of June 16, 1964. *Soils and Foundations*, 6(1), 14-30.
- Kawamura, M., & Chen, C.-c. (2013). Precursory change in seismicity revealed by the Epidemic-Type Aftershock-Sequences model: A case study of the 1999 Chi-Chi, Taiwan earthquake. *Tectonophysics*, 592, 141-149.
- Kawasumi, H. (1968). *General report on the Niigata Earthquake of 1964*: Electrical Engineering College Press.
- Kaya, Z., & Erken, A. (2015). Cyclic and post-cyclic monotonic behavior of Adapazari soils. *Soil Dynamics and Earthquake Engineering*, 77, 83-96.
- Kim, B., & Hashash, Y. M. (2013). Site response analysis using downhole array recordings during the March 2011 Tohoku-Oki earthquake and the effect of long-duration ground motions. *Earthquake Spectra*, 29(s1), S37-S54.
- Kishida, H. (1969). Characteristics of liquefied sands during Mino-Owari, Tohankai and Fukui earthquakes. *Soils and Foundations*, 9(1), 75-92.
- Koester, J., & Tsuchida, T. (1988). Earthquake-induced liquefaction of fine-grained soils-considerations from Japanese research. Final report, October 1986-September 1988: Army Engineer Waterways Experiment Station, Vicksburg, MS (USA). Geotechnical Lab.
- Kramer, S. L., Sideras, S. S., & Greenfield, M. W. (2016). The timing of liquefaction and its utility in liquefaction hazard evaluation. *Soil Dynamics and Earthquake Engineering*, 91, 133-146.
- Kulkarni, R., Youngs, R., & Coppersmith, K. (1984). *Assessment of confidence intervals for results of seismic hazard analysis*. Paper presented at the Proceedings of the Eighth World Conference on Earthquake Engineering.
- Kumar, S. S., Krishna, A. M., & Dey, A. (2017). Evaluation of dynamic properties of sandy soil at high cyclic strains. *Soil Dynamics and Earthquake Engineering*, 99, 157-167.
- Lade, P. V. (1992). Static instability and liquefaction of loose fine sandy slopes. *Journal of Geotechnical Engineering*, 118(1), 51-71.

- Lat, C. N., & Ibrahim, A. T. (2009). Bukit Tinggi earthquakes: November 2007–January 2008. *Bulletin of Geological Society of Malaysia*, 55, 82-86.
- Law, K., & Ling, Y. (1992). *Liquefaction of granular soils with non-cohesive and cohesive fines*. Paper presented at the Proc., 10th World Conf. on Earthquake Engineering.
- Liao, S. S., & Whitman, R. V. (1986). Overburden correction factors for SPT in sand. *Journal of Geotechnical Engineering*, 112(3), 373-377.
- Liu, L., & Li, Y. (2001). Identification of liquefaction and deformation features using ground penetrating radar in the New Madrid seismic zone, USA. *Journal of Applied Geophysics*, 47(3), 199-215.
- Liyanapathirana, D., & Poulos, H. (2004). Assessment of soil liquefaction incorporating earthquake characteristics. *Soil Dynamics and Earthquake Engineering*, 24(11), 867-875.
- MacAskill, K., & Guthrie, P. (2017). Organisational complexity in infrastructure reconstruction – A case study of recovering land drainage functions in Christchurch. *International Journal of Project Management*, 35(5), 864-874.
- Malaysia, T. (2007). About Tourism Malaysia. *Malaysia Truly Asia*.
- Marzuki, A. (2010). Tourism development in Malaysia. A review on federal government policies. *Theoretical and Empirical Researches in Urban Management*, 5(8 (17), 85-97.
- Maurer, B. W., Green, R. A., Cubrinovski, M., & Bradley, B. A. (2015). Fines-content effects on liquefaction hazard evaluation for infrastructure in Christchurch, New Zealand. *Soil Dynamics and Earthquake Engineering*, 76, 58-68.
- McCulloch, D. S., & Bonilla, M. G. (1970). *Effects of the earthquake of March 27, 1964, on the Alaska Railroad*: US Government Printing Office.
- McGuire, R. (1976). EQRISK: Evaluation of earthquake risk to site. *US Geol. Surv. Open-File Rep*, 76-67.
- McGuire, R. K. (2004). *Seismic hazard and risk analysis*: Earthquake Engineering Research Institute.
- Melnick, D., Cisternas, M., Moreno, M., & Norambuena, R. (2012). Estimating coseismic coastal uplift with an intertidal mussel: calibration for the 2010 Maule Chile earthquake (Mw = 8.8). *Quaternary Science Reviews*, 42, 29-42.
- Menoni, S. (2001). Chains of damages and failures in a metropolitan environment: some observations on the Kobe earthquake in 1995. *Journal of Hazardous Materials*, 86(1), 101-119.
- Mitchell, J. K. (2008). Mitigation of liquefaction potential of silty sands *From research to practice in geotechnical engineering* (pp. 433-451).

- Muntohar, A. S. (2014). Research on Earthquake Induced Liquefaction in Padang City and Yogyakarta Area. *Jurnal Geoteknik HATTI IX (1)*, ISSN, 0853-4810.
- Nabilah, A., & Balendra, T. (2012). Seismic hazard analysis for Kuala Lumpur, Malaysia. *Journal of Earthquake Engineering*, 16(7), 1076-1094.
- Ngah, K., Madon, M., & Tjia, H. (1996). Role of pre-Tertiary fractures in formation and development of the Malay and Penyu basins. *Geological Society, London, Special Publications*, 106(1), 281-289.
- Ohsaki, Y. (1966). Niigata earthquakes, 1964 building damage and soil condition. *Soils and Foundations*, 6(2), 14-37.
- Orense, Kiyota, T., Yamada, S., Cubrinovski, M., Hosono, Y., Okamura, M., & Yasuda, S. (2011). Comparison of liquefaction features observed during the 2010 and 2011 Canterbury earthquakes. *Seismological Research Letters*, 82(6), 905-918.
- Ornthammarath, T., Warnitchai, P., Worakanchana, K., Zaman, S., Sigbjörnsson, R., & Lai, C. G. (2011). Probabilistic seismic hazard assessment for Thailand. *Bulletin of Earthquake Engineering*, 9(2), 367-394.
- Pailoplee, S., Sugiyama, Y., & Charusiri, P. (2010). Probabilistic seismic hazard analysis in Thailand and adjacent areas by using regional seismic source zones. *Terrestrial, Atmospheric and Oceanic Sciences*, 21(5), 757-766.
- Papathanassiou, G., Caputo, R., & Rapti-Caputo, D. (2012). Liquefaction phenomena along the paleo-Reno River caused by the May 20, 2012, Emilia (northern Italy) earthquake. *Annals of Geophysics*, 55(4).
- Petersen, M., Harmsen, S., Mueller, C., Haller, K., Dewey, J., Luco, N., . . . Lidke, D. (2008). *New USGS Southeast Asia seismic hazard maps*. Paper presented at the The 14th World Conf. Earthquake Engineering.
- Petersen, M. D., Dewey, J., Hartzell, S., Mueller, C., Harmsen, S., Frankel, A., & Rukstales, K. (2004). Probabilistic seismic hazard analysis for Sumatra, Indonesia and across the Southern Malaysian Peninsula. *Tectonophysics*, 390(1), 141-158.
- Pollitz, F. F., & Sacks, I. S. (1997). The 1995 Kobe, Japan, earthquake: A long-delayed aftershock of the offshore 1944 Tonankai and 1946 Nankaido earthquakes. *Bulletin of the Seismological Society of America*, 87(1), 1-10.
- Porbaha, A., Zen, K., & Kobayashi, M. (1999). Deep mixing technology for liquefaction mitigation. *Journal of infrastructure systems*, 5(1), 21-34.
- Ramli, M. Z., & Adnan, A. (2004). *Earthquake engineering education plan for low intensity Eearthquake region*. Paper presented at the Conference On Engineering Education.
- Robertson, & Fear. (1997). Cyclic liquefaction and its evaluation based on the SPT and CPT *Technical report NCEER* (Vol. 97, pp. 41-87): US National Center for Earthquake Engineering Research (NCEER).

- Robertson, P. K., Wride, C. E., List, B. R., Atukorala, U., Biggar, K. W., Byrne, P. M., . . . Zavodni, Z. (2000). The Canadian Liquefaction Experiment: an overview. *Canadian Geotechnical Journal*, 37(3), 499-504.
- Seed, H. B. (1976). Evaluation of soil liquefaction effects on level ground during earthquakes. *Liquefaction problems in geotechnical engineering*, 2752, 1-104.
- Seed, H. B. (1979). Considerations in the earthquake-resistant design of earth and rockfill dams. *Geotechnique*, 29(3), 215-263.
- Seed, H. B., Idriss, I., & Arango, I. (1983). Evaluation of liquefaction potential using field performance data. *Journal of Geotechnical Engineering*, 109(3), 458-482.
- Seed, H. B., & Idriss, I. M. (1971). Simplified procedure for evaluating soil liquefaction potential. *Journal of Soil Mechanics & Foundations Div.*
- Shenthan, T., Nashed, R., Thevanayagam, S., & Martin, G. R. (2004). Liquefaction mitigation in silty soils using composite stone columns and dynamic compaction. *Earthquake Engineering and Engineering Vibration*, 3(1), 39.
- Shuib, M. K. (2009). The recent Bukit Tinggi earthquakes and their relationship to major geological structures. *Bulletin of Geological Society of Malaysia*, 55, 67-72.
- Soils, N. W. o. E. o. L. R. o., Youd, T. L., & Idriss, I. M. (1997). *Proceedings of the NCCER Workshop on Evaluation of Liquefaction Resistance of Soils*: National Center for Earthquake Engineering Research.
- Sonoda, K., & Kobayashi, H. (1997). On impact-like failure of reinforced concrete structures by Hyogo-ken Nanbu Earthquake (Kobe, 1995). *Publication of: Computational Mechanics Publications*.
- Srbulov, M. (2014). Geo-testing *Practical Guide to Geo-Engineering* (pp. 15-55): Springer.
- Tate, R., Tan, D., & Ng, T. (2008). Geological Map of Peninsular Malaysia. *Scale*, 1(1), 000.
- Thevanayagam, S., & Martin, G. (2002). Liquefaction in silty soils—screening and remediation issues. *Soil Dynamics and Earthquake Engineering*, 22(9), 1035-1042.
- Tokimatsu, K., & Asaka, Y. (1998). Effects of liquefaction-induced ground displacements on pile performance in the 1995 Hyogoken-Nambu earthquake. *Soils and Foundations*, 38(Special), 163-177.
- Tokimatsu, K., Tamura, S., Suzuki, H., & Katsumata, K. (2012). Building damage associated with geotechnical problems in the 2011 Tohoku Pacific Earthquake. *Soils and Foundations*, 52(5), 956-974.

- Trifunac, M. (2003). Nonlinear soil response as a natural passive isolation mechanism. Paper II. The 1933, Long Beach, California earthquake. *Soil Dynamics and Earthquake Engineering*, 23(7), 549-562.
- Tsai, C.-C., & Hashash, Y. M. A. (2008). A novel framework integrating downhole array data and site response analysis to extract dynamic soil behavior. *Soil Dynamics and Earthquake Engineering*, 28(3), 181-197.
- Tsuchida, H. (1970). *Evaluation of liquefaction potential of sandy deposits and measures against liquefaction induced damage*. Paper presented at the Proceedings of the Annual Seminar of the Port and Harbour Research Institute, pp.(3-1)-(3-33)(in Japanese).
- Tsukamoto, Y., Kawabe, S., & Kokusho, T. (2012). Soil liquefaction observed at the lower stream of Tonegawa river during the 2011 off the Pacific Coast of Tohoku Earthquake. *Soils and Foundations*, 52(5), 987-999.
- Unjoh, S., Kaneko, M., Kataoka, S., Nagaya, K., & Matsuoka, K. (2012). Effect of earthquake ground motions on soil liquefaction. *Soils and Foundations*, 52(5), 830-841.
- Van Ballegooy, S., Malan, P., Lacrosse, V., Jacka, M., Cubrinovski, M., Bray, J., . . . Cowan, H. (2014). Assessment of liquefaction-induced land damage for residential Christchurch. *Earthquake Spectra*, 30(1), 31-55.
- Vigny, C., Simons, W., Abu, S., & Bamphenyu, R. (2005). Insight into the 2004 Sumatra-Andaman earthquake from GPS measurements in southeast Asia. *Nature*, 436(7048), 201.
- Villemure, M., Wilson, T., Bristow, D., Gallagher, M., Giovinazzi, S., & Brown, C. (2012). Liquefaction ejecta clean-up in Christchurch during the 2010-2011 earthquake sequence.
- Wang, C.-H., & Guldmann, J.-M. (2016). A spatial panel approach to the statistical assessment of seismic impacts and building damages: Case study of Taichung, Taiwan. *Computers, Environment and Urban Systems*, 57, 178-188.
- Wang, W. (1979). *Some findings in soil liquefaction*: Earthquake Engineering Department, Water Conservancy and Hydroelectric Power Scientific Research Institute.
- Wilkinson, S., Grant, D., Williams, E., Paganoni, S., Fraser, S., Boon, D., . . . Free, M. (2013). Observations and implications of damage from the magnitude M w 6.3 Christchurch, New Zealand earthquake of 22 February 2011. *Bulletin of Earthquake Engineering*, 1-34.
- Wotherspoon, Pender, & Orense. (2012). Relationship between observed liquefaction at Kaiapoi following the 2010 Darfield earthquake and former channels of the Waimakariri River. *Engineering Geology*, 125(0), 45-55.
- Wotherspoon, L. M., Orense, R. P., Green, R. A., Bradley, B. A., Cox, B. R., & Wood, C. M. (2015). Assessment of liquefaction evaluation procedures and severity

- index frameworks at Christchurch strong motion stations. *Soil Dynamics and Earthquake Engineering*, 79, Part B, 335-346.
- Xu, L.-Y., Cai, F., Wang, G.-X., Ugai, K., Wakai, A., Yang, Q.-Q., & Onoue, A. (2013). Numerical assessment of liquefaction mitigation effects on residential houses: Case histories of the 2007 Niigata Chuetsu-offshore earthquake. *Soil Dynamics and Earthquake Engineering*, 53, 196-209.
- Yamaguchi, A., Mori, T., Kazama, M., & Yoshida, N. (2012). Liquefaction in Tohoku district during the 2011 off the Pacific Coast of Tohoku Earthquake. *Soils and Foundations*, 52(5), 811-829.
- Yasuda, S., Harada, K., Ishikawa, K., & Kanemaru, Y. (2012). Characteristics of liquefaction in Tokyo Bay area by the 2011 Great East Japan earthquake. *Soils and Foundations*, 52(5), 793-810.
- Yasuda, S., Verdugo, R., Konagai, K., Sugano, T., Villalobos, F., Okamura, M., . . . Towhata, I. (2010). Geotechnical damage caused by the 2010 Maule, Chile earthquake. *ISSMGE Bulletin*, 4(2), 16-27.
- Yegian, M., Eseller-Bayat, E., Alshawabkeh, A., & Ali, S. (2007). Induced-partial saturation for liquefaction mitigation: experimental investigation. *Journal of geotechnical and geoenvironmental engineering*, 133(4), 372-380.
- Yoshida, N., & Kudo, K. (2000). Geotechnical re-evaluation of liquefaction at Kawagishi-cho site during 1964 Niigata earthquake, Summaries of the Technical Papers of Annual Meeting of AIJ, Tohoku. *Structure II*, 293-294.
- Youd, & Bartlett, S. F. (1989). *Case histories of lateral spreads from the 1964 Alaskan earthquake*. Paper presented at the Proceedings, Third Japan-US Workshop on Earthquake Resistant Design of Lifeline Facilities and Countermeasures for Soil Liquefaction.
- Youd, T., & Idriss, I. (2001). Liquefaction resistance of soils: summary report from the 1996 NCEER and 1998 NCEER/NSF workshops on evaluation of liquefaction resistance of soils. *Journal of geotechnical and geoenvironmental engineering*, 127(4), 297-313.
- Youd, T. L., & Provo, U. (2011). *A look inside the debate over EERI Monograph MNO 12*. Paper presented at the The California Geotechnical Engineering Association (CalGeo), 2011 Annual Conference.
- Youngs, R. R., & Coppersmith, K. J. (1985). Implications of fault slip rates and earthquake recurrence models to probabilistic seismic hazard estimates. *Bulletin of the seismological society of America*, 75(4), 939-964.

LIST OF PUBLICATIONS AND PAPERS PRESENTED

Hashim, H., Suhatri, M., & Hashim, R. (2017, June). Preliminary study of soil liquefaction hazard at Terengganu shoreline, Peninsular Malaysia. In *Materials Science and Engineering Conference Series* (Vol. 210, No. 1, p. 012020).